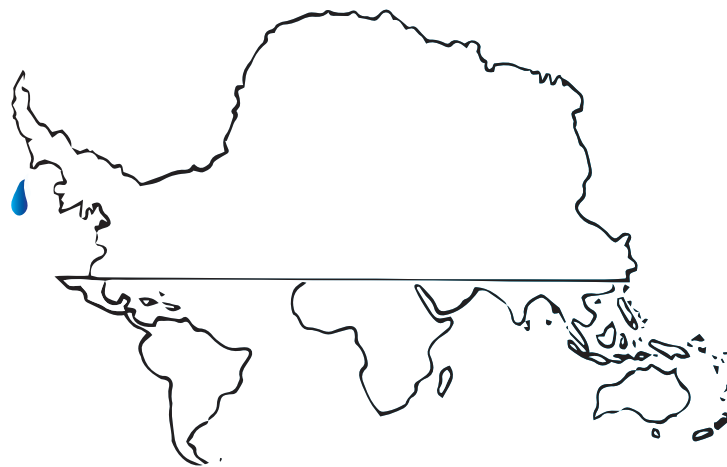


Quaternary Antarctic Ice Sheet Dynamics

Johannes Sutter

Dissertation zur Erlangung des akademischen Grades
Doktor der Naturwissenschaften (Dr. rer. nat.)



Universität Bremen, Fakultät Physik  Universität Bremen

Alfred Wegener Institut 

Betreuer & 1. Gutachter: Prof. Dr. Gerrit Lohmann

2. Gutachter: Prof. Dr. Peter Lemke

Abstract

Quaternary Antarctic Ice Sheet Dynamics

The Antarctic Ice Sheet (AIS) plays a major role in the evolution of Quaternary glacial-interglacial cycles and in the global climate system in general. By a variety of ice-ocean and ice-atmosphere feedback processes, changes in the dynamics of the southern ice giant are felt throughout the globe. Ice cores drilled down to the bedrock of the East Antarctic Ice Sheet provide a glimpse into the climate history of the past one million years via water stable isotopes and trapped gasses conserved in the slow flowing ice (climate proxies). Dramatic changes in ice volume and extent characterize the evolution of the AIS during the last 130.000 years, affecting both Southern Hemisphere and global climate. A central protagonist in this history of the AIS is the West Antarctic Ice Sheet (WAIS), due to its unique setting extending into several ocean basins and thus being prone to destabilization triggered by warming of the Southern Ocean.

The objective of this thesis is to shed light on the glacial-interglacial dynamics of the AIS by means of 3D ice sheet modeling. The dynamic evolution of the WAIS during the Last Interglacial (LIG) and in the future is investigated and potential climate thresholds for an marine ice sheet collapse identified. Special attention is given to the role of basal melting underneath the ice shelves in the growth and decay of the WAIS. An ocean warming range of 2 – 3°C is found to be sufficient to trigger an irreversible retreat of the marine ice sheet culminating in its complete collapse and a global Antarctic sea level contribution of up to 5m during the last interglacial as well as within the next millennia. It is found that the collapse depends on a complex interplay of precipitation patterns, bedrock topography, ocean bathymetry and ultimately Southern Ocean warming. Intrinsic timescales defined by the topographic features of the WAIS are found leading to a characteristic two phase collapse of the ice sheet. This thesis, for the first time, provides an estimate of LIG climate conditions required for a WAIS collapse within the range of proxy data for LIG Southern Ocean temperatures on the basis of 3D ice sheet modeling. Peak LIG sea levels of 7 – 9m are corroborated and the Antarctic contribution to the latter identified. Future Southern Hemisphere warming as projected by the IPCC would set the WAIS on a path of long term retreat culminating in several meter sea level rise during the next millennia. Rapid warming however, triggering a fast collapse of the Antarctic ice shelves within centuries, would set the stage for a multi-centennial collapse of the WAIS with grave consequences for low lying coastal settlements.

The full last glacial cycle is simulated with a transient climate forcing incorporating proxy data as well as results from a global circulation model. The processes behind the timing and extent of the last glaciation in Antarctica are investigated in sensitivity studies, illuminating the role of ice shelf-ocean dynamics en route to the Last Glacial Maximum. Flat grounded ice sheets are found to have covered the Weddell and Ross Sea at least partially, while grounding lines advanced considerably in the Bellinghausen- and Amundsen-Sea as well as around the Antarctic Peninsula. Strong sensitivities of this ice sheet advance with respect to small changes in basal shelf melting are found, as well as teleconnections between dynamics in geographically separated ocean basins. Further, the ultimate retreat leading to the Holocene AIS, is simulated focussing specifically on marine ice sheet dynamics as well. A passive tracer advection scheme is utilized to simulate ice cores which are then compared to the deep Antarctic ice cores (e.g. Dome C, EDML, Vostok), providing valuable insights and constraints into ice evolution and the hydrological cycle during the last interglacial. Finally, ice sheet modeling excursions into the Pliocene and Miocene provide

a broader context of the AIS behavior in the deeper past. This thesis extends the current knowledge of Antarctic Ice Sheet dynamics during the last glacial cycle and beyond as well as shedding light on potential future contributions to global sea level.

Zusammenfassung

Dynamik des Antarktischen Eisschildes im Quartär

Das Antarktische Eisschild spielt eine zentrale Rolle im Kommen und Gehen von Glazialen und Interglazialen während des Quartärs sowie für das globale Klimasystem. Durch eine Vielzahl von Wechselwirkungen zwischen Eis, Ozean und Atmosphäre, haben Veränderungen des Eisgiganten weltweite Auswirkungen. Eiskerne, die bis zur Basis des Ostantarktischen Eisschildes gebohrt wurden, geben durch die in ihnen konservierten Wasserstoff- und Sauerstoff-Isotopen und eingeschlossenen Gase einen einmaligen Einblick in die Klimageschichte unseres Planeten während der letzten eine Million Jahre. Dramatische Fluktuationen der Ausdehnung und der Masse des Antarktischen Eisschildes charakterisieren die Entwicklung desselben während der letzten 130.000 Jahre, was Konsequenzen sowohl für das Klima der Südhalbkugel als auch nördlich des Äquators hat. Durch die einmalige Konstellation an der Grenze zwischen Luft, Eis und Wasser, stand das Westantarktische Eisschild im Zentrum der vergangenen Entwicklungen. Warme Ozeanströmungen, welche die Eisschelfe der Westantarktis unterspülen, können das gesamte Westantarktische Eisschild destabilisieren und dadurch zu einem Meeresspiegelanstieg von mehreren Metern führen.

Das primäre Ziel dieser Dissertation ist die Untersuchung der Entwicklung des Antarktischen Eisschildes während des letzten Glazial-Interglazialen Zyklus. Die Dynamik des Westantarktischen Eisschildes im letzten Interglazial (Eem) und in der Zukunft wird beleuchtet und potentielle Klimakippunkte, welche einen Kollaps des Westantarktischen Eisschildes bewirken, identifiziert. Besonderes Augenmerk liegt auf den Effekten des Schmelzens unter den Antarktischen Eisschelfen und deren Auswirkungen auf die Stabilität des marinen Eisschildes. Die Ergebnisse zeigen eine Temperaturleitplanke von 2°C , deren Überschreitung einen irreversiblen Rückgang der Gründungslinie des Westantarktischen Eisschildes nach sich zieht. Dies führt zu einem Meeresspiegelanstieg von bis zu 5 Metern während der nächsten Jahrtausende. Der Kollaps des Westantarktischen Eisschildes wird mithin beeinflusst von mehreren Faktoren, darunter die Bathymetrie der Ozeanbecken, die Eisschildtopographie, Niederschlagsmuster und insbesondere die Erwärmung des südlichen Ozeans. Weiterhin führt die Topographie der Westantarktis zu einem charakteristischen zweiphasigen Rückzug des Eisschildes, welcher eine Rolle im kolportierten zweigeteilten Meeresspiegelmaximum im Eem gespielt haben könnte. Diese Dissertation zeigt, dass ein Kollaps des Westantarktischen Eisschildes im Eem durch die von Proxydaten suggerierte Ozeanerwärmung durchaus im Bereich des Möglichen liegt. Dadurch werden die Hinweise auf einen Meeresspiegelanstieg von 7 – 9 Metern im Eem bestärkt und die Rolle der Antarktis ausdifferenziert. Die Modellergebnisse zeigen, dass die durch einige Szenarien des Intergovernmental Panel on Climate Change (IPCC) prognostizierte zukünftige Erwärmung der Südhemisphäre zu einem irreversiblen Rückzug der Westantarktis führen könnte, verbunden mit einem Meeresspiegelanstieg von mehreren Metern während der nächsten Jahrtausende. Sollten die Antarktischen Eisschelfe im Laufe weniger Jahrzehnte kollabieren (getrieben von Schmelzen und Kalben), könnte dies sogar zu einem Kollaps binnen weniger Jahrhunderte führen. Dies hätte drastische Konsequenzen für die Bevölkerung von niedrig liegenden Küstengebieten.

Weiterhin wird der letzte glaziale Zyklus simuliert. Ein aus Proxydaten und Klimamodellen gespeister transienter Klimaantrieb wird genutzt, um die Treiber und Prozesse, welche der Dynamik des Antarktischen Eisschildes im letzten Glazial zugrundeliegen, zu identifizieren. Die Ergebnisse zeigen eine, zumindest partielle, Bedeckung des Ross und Weddellmeeres mit flachen Eisschilden. Die Eisgründungslinie in der

Amundsen, der Bellinghausen See und der Antarktischen Halbinsel war weit vorangeschritten, teilweise bis an den Rand des Kontinentalschelfs. Die Modellergebnisse zeigen eine hohe Sensitivität der Ausbreitung der marinen Eisschilde gegenüber kleinen Veränderungen im basalen Schmelzen der Schelfeise. Wechselwirkungen zwischen Eisschelfdynamiken in geographisch getrennten marinen Becken werden in den Simulationen gezeigt. Weiterhin wird der postglaziale Rückzug des Antarktischen Eisschildes in Sensitivitätsstudien mit Fokus auf die Massenbilanz antarktischer Eisschelfe untersucht. Abschliessend wird die Entwicklung eines Tracermoduls dokumentiert, welches die Berechnung der Stratigraphie des Antarktischen Eisschildes ermöglicht. Erste Ergebnisse zur Altersverteilung in tiefen antarktischen Eiskernen (z.b. die Kerne Dome C, EDML und Vostok) werden vorgestellt. Abschliessend wird die Dynamik des Antarktischen Eisschildes in der tieferen Vergangenheit, spezifisch des Pliozäns und des Miozäns, untersucht.

Die vorliegende Dissertation erweitert das aktuellen Wissensstand der Forschung bezüglich vergangener Dynamiken des Antarktischen Eisschildes und bietet einen Ausblick auf mögliche zukünftige Beiträge der Antarktis zum globalen Meeresspiegelanstieg.

Acknowledgments

This work was made possible by the unfaltering support of many people. First and foremost, I would like to express my gratitude to Gerrit Lohmann, for his support, his insight into the intricacies of climate interactions, as well as his excellent sensor for interesting scientific challenges, and, last but not least, for providing me with all the freedom I needed to conclude this PhD successfully. Further, I want to thank Malte Thoma, who introduced me to ice sheet modeling and taught me much about programming. I would like to thank Klaus Grosfeld for the inspirational discussions on glaciology as well as managing ones PhD, not to forget his never ending investment in the Earth System Research School (ESSReS) which I had the privilege of being part of. Thanks to Helge Meggers for coordinating ESSReS and always having an open door. Many thanks to Stefanie Klebe, who was an invaluable support when it came to organizing funding money, solving tricky bureaucratic problems and her general positive spirit in the Paleoclimate Dynamics Group. I'm truly grateful to Peter Lemke for giving me the opportunity to explore the world of scientific policy think tanks as a research analyst in the German Advisory Council on Global Change. I would like to thank Gerd Rohardt, Gerrit Lohmann and Peter Lemke for giving me the opportunity to join an Antarctic expedition onboard Polarstern. Also, I would like to extend my thanks to all my colleagues for the endless hours spent during lunch breaks (and making it through years of Hochschulmensa food), coffee breaks and the pilgrimage from Bremen to Bremerhaven and back. Special thanks go out to Mischa Ungermann for post-lunch break Ultimate Frisbee breaks and shared PhD-sarcasm, and to Paul Gierz for exchanging "professional" Pythonia. Greatly acknowledged are the people which made my Polarsternexpedition unforgettable, Fritsche, Schnittchen, Sabinemeda, CDDD, Priska, Majo & den Unseriösen. For the moral as well as lectoral support in the critical phase of the PhD I am deeply grateful to Angela (as well as for creating the artwork on the title). I want to conclude my acknowledgements by expressing my gratitude to my Family. Without them, all this would not have been possible.

List of Abbreviations

AIS Antarctic Ice Sheet	IPCC Intergovernmental Panel on Climate Change
AMOC Atlantic Meridional Overturning Circulation	kyr(s) kilo-year(s)
AOGCM Atmosphere-Ocean General Circulation Model	LGM Last Glacial Maximum
BP Before Present	LIG Last Interglacial
CDW Circumpolar Deep Water	MIS Marine Isotope Stage
CE Common Era	MISI Marine Ice Sheet instability
COSMOS Community Earth System Models	MMCT mid-Miocene Climate Transition
EDML Epica Dronning Maud Land	PD Present Day
EISMINT European Ice Sheet Modeling Initiative	P-E Precipitation minus Evaporation
EPICA European Project for Ice Coring in Antarctica	PLISMIP Pliocene Ice Sheet Model Intercomparison Project
EOT Eocene-Oligocene Transition	PRISM Pliocene Research, Interpretation and Synoptic Mapping
FRIS Filchner-Ronne Ice Shelf	RIMBAY Revised Ice sheet Model BAseD on pat-tYn
GCM General Circulation Model	RS Ross Schelf
GIS Greenland Ice Sheet	SAT Surface Air Temperature
GRIP Greenland Ice Core Project	SST Sea Surface Temperature
IRD Ice Rafted Debris	SIA Shallow Ice Approximation
ISM Ice Sheet Model	SSA Shallow Shelf Approximation
	WAIS West Antarctic Ice Sheet
	WOA World Ocean Atlas

Contents

Acknowledgments	9
Preface	15
1 Introduction	19
2 Methods	31
2.1 The Ice Sheet Model	31
2.2 Ice Shelf Mass Balance	33
2.3 Present Day Control Run	36
2.4 COSMOS	37
2.5 Passive Tracer Modeling	37
2.5.1 A Paleothermometer	38
2.5.2 Passive Tracer Advection	38
2.6 Feasibility of Tracer Studies	41
3 Last Interglacial Antarctic Ice Sheet Dynamics	43
3.1 Last Interglacial West Antarctic Ice Sheet Collapse	43
3.1.1 Setting the Stage	43
3.2 Experimental Setup	44
3.3 Stable West Antarctic Ice Sheet under COSMOS Forcing	45
3.4 Ocean Temperature Thresholds for West Antarctic Ice Sheet Collapse	47
3.4.1 Twin Peak Sea Level Rise	47
3.4.2 Further Climatological Driving Forces	49
3.5 Reconciling LIG Sea Level Highstand	49
4 Future Antarctic Dynamics	51
5 Constraining Antarctic Ice Sheet Volume in the Late-Pliocene	57
5.1 Experimental Boundary Conditions and Participating Ice Sheet Models	57
5.2 The Present Day Control Simulations	61
5.3 Pliocene Antarctic Ice Sheet Equilibrium Simulations	63
5.4 Contribution to Late-Pliocene Sea Level	64
5.5 PLISMIP Inconclusive	65

6	Glaciation and the Last Glacial Maximum	67
6.1	Antarctic Ice Sheet Advance Following the Last Interglacial	68
6.2	Glacial COSMOS Forcing	69
6.3	The Role of Parametrizations and their Implication on Sea Level Evolution	71
6.4	A Wide Range of Potential Last Glacial Maximum Ice Sheet Configurations	73
6.5	Drivers of Antarctic Ice Sheet Glaciation	74
6.6	Proxy and Modeling Constraints on the Last Glacial Maximum Antarctic Ice Sheet	75
7	Post-Glacial Retreat of the Antarctic Ice Sheet	77
7.1	Ice Shelf Dynamics Key to Antarctic Ice Sheet Retreat	79
7.2	The Effects of Fast Ice Shelf Collapse and Bathymetry	82
7.3	The Deglaciation Puzzle	84
8	Unraveling the Past: a Model-Data Intercomparison of Ice Cores	87
8.1	Caveats of Ice Core Modeling	88
8.2	Experimental Setup	89
8.3	Present Day Equilibrium Results	91
9	Antarctic Ice Sheet Evolution in the Miocene	97
9.1	Experimental Design	97
9.2	Bedrock vs. Climate	101
9.3	Mid-Miocene AIS Dynamics Driven by Bedrock Configuration and Precipitation	104
10	Conclusions	105
10.1	Antarctic Ice Sheet Dynamics and Sea Level Contribution in the Last Interglacial	106
10.2	Future Antarctic Sea Level Contribution	108
10.3	The Antarctic Ice Sheet in the Pliocene	109
10.4	The Antarctic Ice Sheet in the Last Glacial Maximum	110
10.5	Antarctic Deglaciation: Towards a Holocene Antarctic Ice Sheet	111
10.6	Unlocking the Antarctic Climate Archive: Ice Core Simulations	112
10.7	The Mid-Miocene Antarctic Ice Sheet	113
10.8	Using Ice Sheet Models to Reconstruct Past and Predict Future Ice Sheet Dynamics, a Cautionary Tale	114
11	Appendix	117
11.1	Ice Sheet Processes	117
11.2	Present Day Climate Forcing	118
11.3	COSMOS Last Interglacial Climate	118
11.4	Glacial-Interglacial Simulations	123
11.5	West Antarctic Ice Sheet Bathymetry	124
11.6	Model Behavior in the "Pollard 2009" Setting	125
11.7	Transient Evolution of the AIS	126
11.8	LGM Grounding Line Positions	126
11.9	List of Publications	132

List of Figures

1.1	Paleo proxy data compilation	21
1.2	Map of Antarctica	22
1.3	Thesis overview	24
2.1	RIMBAY components	31
2.2	SSH-SIA	32
2.3	Basal shelf mass balance [Pritchard et al., 2012]	33
2.4	Basal shelf melting schematic	34
2.5	Sea surface temperatures (WOA)	35
2.6	Ocean temperatures underneath Antarctic ice shelves (modeled)	35
2.7	Present day control run (ISM)	36
2.8	COSMOS	37
2.9	EISMINT ice sheet topography	39
2.10	Eismint ice age	40
3.1	LIG proxy data	45
3.2	LIG sea level changes derived from ice sheet modeling	46
3.3	Transient transect across the simulated LIG AIS	48
4.1	Future precipitation-temperature relationship (from [Frieler et al., 2015])	51
4.2	Snapshots of simulated Future AIS surface elevations	52
4.3	Simulated future AIS evolution	53
4.4	Probabilistic projections of AIS sea level contribution [Ritz et al., 2015]	54
4.5	Projections of AIS sea level contribution [Golledge et al., 2015]	54
5.1	PlioMIP ensemble results	59
5.2	Climate forcings used in PLISMIP [de Boer et al., 2015]	60
5.3	PLISMIP grounded AIS volume in the RIMBAY PD ctrl simulations	61
5.4	PLISMIP present day control simulations	62
5.5	PLISMIP grounded AIS volume in the control simulations	62
5.6	PLISMIP grounded AIS volume in the RIMBAY Pliocene simulations	63
5.7	PLISMIP grounded AIS volume in the Pliocene control simulation	63
5.8	PLISMIP grounded AIS volume in the PRISM-3 simulations	64
6.1	Last glaciation proxies	67

6.2	LGM model and data reconstructions	68
6.3	Initial boundary conditions for the LGM simulations	68
6.4	LGM COSMOS forcing ocean	69
6.5	LGM COSMOS forcing surface temperature	70
6.6	LGM COSMOS forcing precipitation	70
6.7	Last glaciation 1	71
6.8	Last glaciation 2	72
6.9	Last glaciation 3	72
6.10	Last glaciation 4	73
6.11	AIS LGM surface elevations	74
6.12	AIS LGM grounding line positions	76
7.1	Deglacial proxies	77
7.2	Deglaciation 1	78
7.3	Deglaciation 2	80
7.4	Deglaciation 3	81
7.5	Deglaciation 4	81
7.6	Deglaciation 5	82
7.7	Antarctic Ice Sheet surface elevation after deglaciation	83
7.8	Weddell Sea bathymetry at the LGM	84
8.1	Antarctic hydrologic cycle schematic	87
8.2	EDML backtracing study [Huybrechts et al., 2007]	89
8.3	Greenland & Antarctic isotopic distribution [Goelles et al., 2014]	89
8.4	Antarctic deep ice core locations	90
8.5	Lagrangian tracer schematic	90
8.6	Simulated ice ages in the present day control simulation	91
8.7	Transect through the AIS at WAIS and Dome C ice cores	93
8.8	Transect through the AIS at EDML and Vostok ice core	94
8.9	Deep ice core age depth relationship derived from the present day control simulation	95
9.1	Miocene COSMOS ocean forcing	99
9.2	Miocene COSMOS atmospheric forcing	100
9.3	Miocene bedrock reconstructions	101
9.4	Miocene AIS volume 1	102
9.5	Miocene AIS volume 2	103
9.6	Miocene AIS volume 3	103
9.7	Miocene AIS volume 4	103
11.1	Ice sheet processes	117
11.2	Observed present day shelf melt rates	118
11.3	Southern Ocean temperatures (World Ocean Atlas)	119
11.4	ALBMAP v1	120
11.5	LIG climate anomalies	121

11.6 LIG climate anomalies (Ocean)	122
11.7 Dome C deuterium depletion	123
11.8 WAIS bathymetry	124
11.9 Extreme interglacial AIS evolution	125
11.10LIG Eg1 AIS evolution	126
11.11LIG Eg2 AIS evolution	127
11.12LIG Eg3 AIS evolution	128
11.13LIG E1 AIS evolution	129
11.14LIG E2 AIS evolution	130
11.15LIG E3 AIS evolution	131
11.16AIS LGM grounding line positions 2	132

Preface

Ever tried. Ever failed. No matter. Try again. Fail again. Fail better.
Samuel Beckett

The human civilization has reached such an unprecedented state of influence on the planet Earth that the time we live in is fittingly coined Anthropocene (anthropos - human, kainos - new). A carbon based economy and the everlasting human pursuit of wealth and happiness intensify the pressure on the environment and the global climate system. Men is en route to break through several planetary boundaries leaving the safe operating space of a sustainable civilization. Already now, the climate impacts of our resource mongering lifestyles can be observed in many places, but especially in the polar regions where climate feedback processes aggravate global warming, melt sea ice and glaciers and thin the gigantic ice sheets of Greenland and Antarctica. These formerly remote barren landscapes, only admired and feared by a handful adventurers, whalers and explorers, are now at the centre of interest for climate scientists and policy makers alike.

Introduction

Everybody talks about the weather, but nobody does anything about it.

Unknown

The climate system will undergo unprecedented changes in this and the coming centuries. Before the industrial revolution and the large scale combustion of fossil fuels, the oscillatory changes of global climate were paced by the sun's irradiation, the atmospheric composition of greenhouse gases, such as carbon dioxide and methane, tectonic changes and the odd volcanic eruption covering the globe in a cooling blanket. However, humans capacity to transform fossilized organic matter into energy and blowing their remains into the atmosphere in the form of climate active gasses, has pushed the climate into an alternate future trajectory [Stocker et al., 2013]. Human society has stumbled into the role of an actor, shaping the future climate for millennia to come. Consequently public interest in Earth's climate has been growing in the late 20th century and has been greatly heightened in recent decades. This is due to the realization of the potentially devastating consequences which human-caused climate change implies for the well being of future generations. A major focus of this interest concerns the polar Ice Sheets of Greenland and Antarctica due to their potential impact on global sea level and their general role in the climate system¹. As of yet many aspects of ice sheet dynamics and their interactions with the climate system are still poorly understood². To improve predictions of future climate and ice sheet changes it is invaluable to take a close up look into the past. This thesis investigates the dramatic evolution of the Antarctic Ice Sheet (AIS) during the last 130.000 years and beyond, in order to shed light on the stability of the West Antarctic Ice Sheet (WAIS) in warm climates, Antarctica's contribution to sea level variations in the past and in the future, and to improve the understanding of the climate archive conserved in Antarctic ice cores.

The Ongoing Ice Age

In relation to the larger periods of Earth's existence we live in an ongoing ice age only interrupted by short bursts of warm periods, so called interglacials, the present one called Holocene [Jouzel et al.,

¹Ice sheets affect the climate in multiple ways, most prominent is their cooling influence on the atmosphere via the highly reflective properties of ice and snow compared to e.g. liquid water, stoney surfaces or forests.

²See for example the review of Hannah et. al 2013 [Hanna et al., 2013] or the news report in Nature 2015 "*gains in antarctic ice might offset losses*".

2007]. This may appear surprising since the majority of Earth's surface is ice free, but on geological time scales we live in relatively cold times. Earth underwent a series of monumental transitions - being ice free (e.g. in the Cretaceous³), and possibly almost fully covered by ice and snow (Snowball Earth hypothesis⁴). The present Ice Age began ca. 40 million years ago (the late Cenozoic glaciation) with the glaciation of Antarctica. Global atmospheric CO₂ concentrations and temperatures have been generally decreasing since then (see Figure 1.1). At about 1.2 million years ago, the beginning of the Quaternary, a rhythmical cycle of glaciations (ca. 90.000 years) and shorter interglacials (ca 10.000 years) dominated Earth's climate and the Cryosphere⁵. The Serbian Astronomer Milutin Milankovitch proposed that variations in the Earth's orbit around the Sun⁶, influencing the amount of solar radiation received on the planets surface, were the cause for the glacial-interglacial cycles. However, a comprehensive theory for the succession and timing of cold and warm times is still to be put forth - its formulation one of the central motives of paleoclimate research.

The Past as a Key to the Future

The investigation of the paleoclimate, in particular with respect to the alternation of cold and warm periods in Earth's history, provides a fascinating framework for approaching an understanding of the multifactorial interconnected processes which have and will alter the face of the planet. The examination of the planet's history is a pivotal key⁷, particularly with respect to understanding the dynamics of the Antarctic Ice Shield (AIS) with changing climate.

The evolution of the AIS throughout Earth's climate, its paleoclimate dynamics, includes the enigmas of a drastically reduced ice sheet (e.g in the Miocene and Pliocene see chapters 9 & 5) as well as ice sheets extending to the continental shelf during the large glaciations⁸. Hence the present day AIS is but a snapshot in its transient evolution. Variations in the Earth's orbit influencing the energy balance on its surface appear to be the major driver behind the glacial interglacial cycles in the Quaternary (from about 2.6 ml years ago until to date). About 1.2 Million years ago a shift from the obliquity signal 40kyr cycles to an eccentricity signal of 100kyr cycles occurred [Raymo and Ruddiman, 1992]. This shift's cause has remained one of the big unanswered questions in paleoclimate science. The Milankovitch cycles are conserved within water stable isotopes⁹ precipitated with snow on the polar ice sheets; thereby leaving an echo of past climatic conditions [Jouzel et al., 1997]. The analyses of ice cores thus opens the gate to a rich climate archive containing invaluable information for the reconstruction of Earth's climate history (see chapters 2 and 8).

³Ca. 145-60 million years ago being the final geological period closing with the extinction of the Dinosaurs. It was characterized by CO₂ levels about six times higher than today, warm polar regions and temperature gradients between the pole and the equator of less than 30°C (compared to 100°C today for the Southern Hemisphere).

⁴Proponents of this theory claim that glacial sedimentary deposits found in tropical latitudes support the Snowball Earth Hypothesis.

⁵The term Cryosphere summarized all regions covered by snow, permafrost and ice.

⁶Earth's orbit around the Sun changes with ca. 100.000 years periodicity, the axial tilt with ca. 41.000 years and the axis of rotation with ca. 23.000 years.

⁷Of course the reverse also holds and is an important insight for science in general, expressed in the words by the 19th century geologist Charles Lyell *The present is the key to the past*.

⁸E.g. the last glacial maximum (LGM) ca 21.000 yr ago, see chapter 6 and [Bentley et al., 2014].

⁹Heavy water, Deuterium, and the oxygen isotope ¹⁸O are used to reconstruct past temperature variations, see chapters 2 and 8.

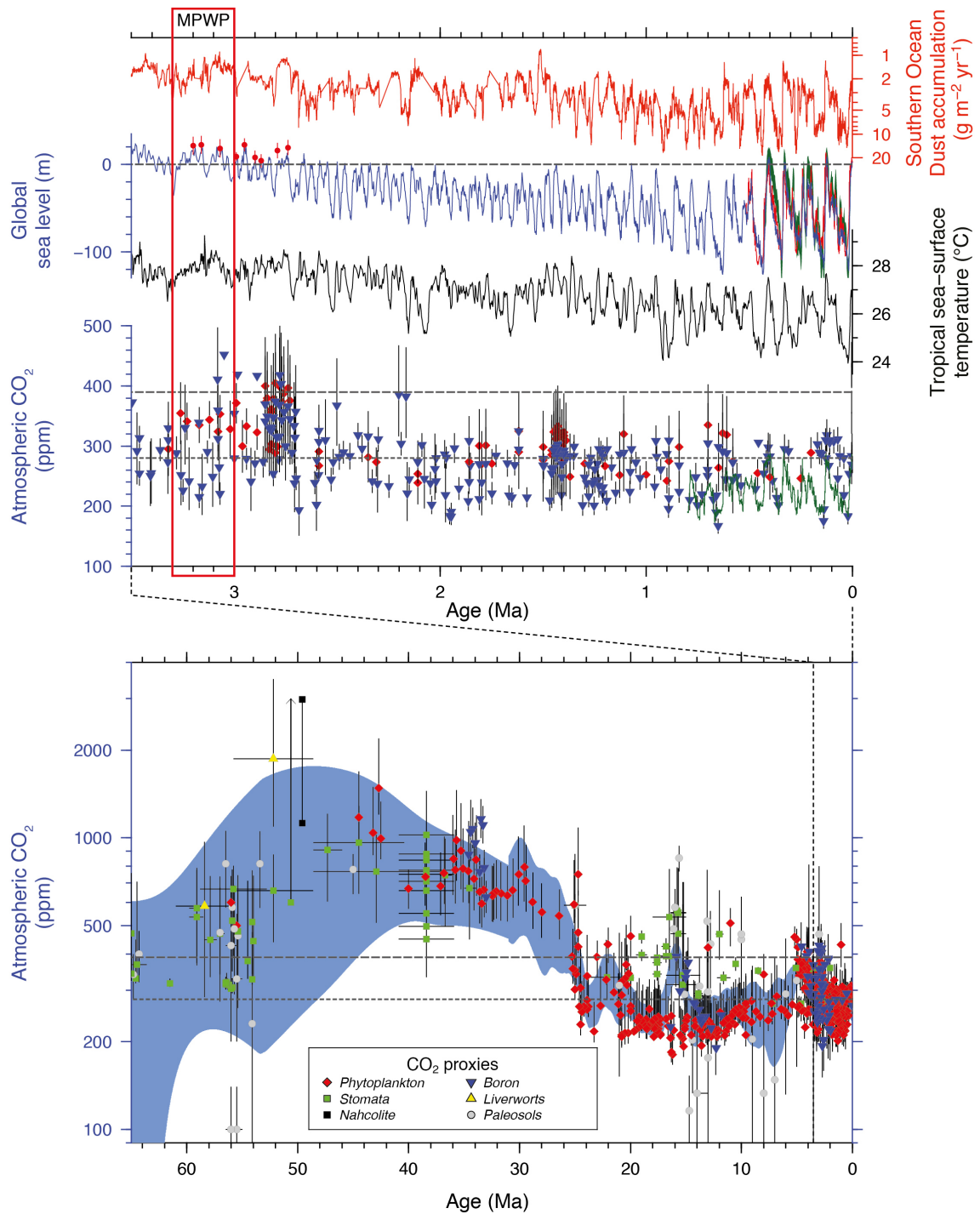


Figure 1.1: Compilation of paleo data spanning the last 60 million years (from [Stocker et al., 2013].)

Why Antarctica

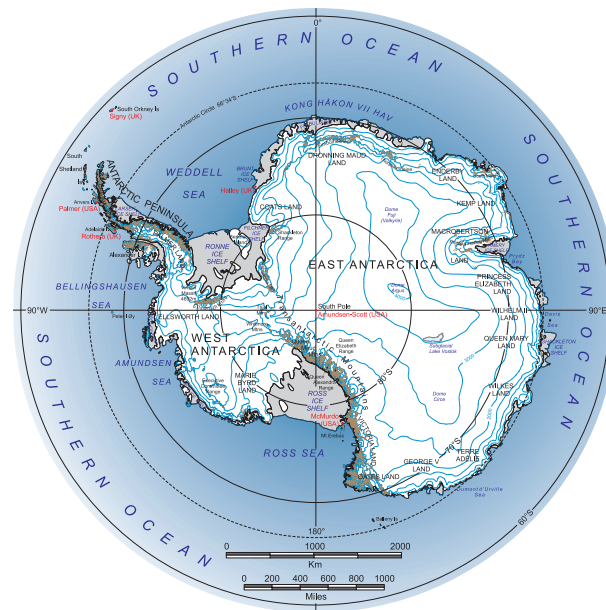


Figure 1.2: Antarctica and its regions. While the West Antarctic Ice Sheet is mostly based below sea level, and fringed by large (Filchner Ronne & Ross) and smaller ice shelves (e.g. Getz Ice Shelf), most of the ice is stored in the ice domes of East Antarctica. Map from United States Geological Survey (see lima.usgs.gov).

Antarctica is a continent of superlatives; the highest, coldest and windiest place on Earth. It conserves enough frozen water to raise global sea level by about 58 m [Fretwell et al., 2013]. Covering the South Pole its icy realms extend to a staggering 63° S (the northernmost region of the Antarctic peninsula). The enormous size of the AIS makes it a truly global player in the climate system. It feeds the global ocean conveyor belt with meltwater from its ice shelves and its enormous seasonal sea ice cycle. It cools the atmosphere by its high albedo and elevations¹⁰.

For human civilization the undoubtedly largest impact of the Antarctic continent is its potential influence on global sea level. In the 1970's, scientific revelations uncovered a weak spot in the south polar ice blanket [Mercer, 1978], previously thought eternal, which was famously coined the "weak underbelly" [Hughes, 1981] of the AIS. Mainly based below sea level, the WAIS (see Figure 1.2) extends its reach out into the ocean where it forms floating ice shelves. Only a few regions are resting on bedrock above sea level. These structural conditions pertain a significant susceptibility to warming of Southern Ocean temperatures [Rignot et al., 2014, Joughin et al., 2014]. It has been proposed that climate change, as a consequence of unabated greenhouse gas emissions [Stocker et al., 2013] could heat up the polar regions enough to trigger a catastrophic collapse of the WAIS [Mercer, 1978], raising sea levels by more than 3m [Bamber et al., 2009] and threatening coastal populations, infrastructure, agriculture and vulnerable ecosystems [Field et al., 2014, Nicholls and Cazenave, 2010, Neumann et al., 2015]. To predict the future behavior of the AIS as accurately as possible is vital for policymakers and the public alike, considering the consequences of unabated greenhouse gas emissions for the slowly awakening ice giant.

¹⁰For a graphical depiction of ice sheet climate interactions, see Figure 11.1 in chapter 11.

Future and Past Antarctic Ice Sheet Dynamics

Many facets of the intricate dynamics governing the waxing and waning of the AIS are still elusive, but large strides in glaciological observations and ice sheet modeling in the last decades have uncovered many previously unknown mechanisms controlling ice flow patterns, ice sheet-shelf advance, retreat and collapse. Facing considerable warming during this century, the stability of the WAIS is under increased scrutiny. Recent observations and ice sheet modeling studies suggest that the WAIS might be en route to a widespread retreat, potentially unlocking rapid sea level rise in the next centuries and beyond [Rignot et al., 2014, Joughin et al., 2014, Pollard et al., 2015, Winkelmann et al., 2015, Feldmann and Levermann, 2015, Sutter et al., 2015a]. However, since many aspects of ice sheet dynamics are still poorly understood, "medium confidence" - results of ice sheet modeling (as termed by the most recent Intergovernmental Panel on Climate Change [Stocker et al., 2013]¹¹) have to be conceded. For example, a recent study has claimed, that the Antarctic Ice Sheet is actually growing [Zwally et al., 2015], which is contradictory to previous publications stating a slightly negative mass balance through the last decades [Ivins et al., 2013, Zammit-Mangion et al., 2015, Harig and Simons, 2015]. A growing body of glaciologists and ice sheet modelers are bent on improving observations and the physical representation of ice sheet dynamics in complex models. High resolution, complex ice sheet models are investigating grounding line dynamics [Favier et al., 2014, Cornford et al., 2015] and ocean models are being developed to simulate the complex ocean circulation patterns and heat transport underneath the Antarctic ice shelves [Hellmer et al., 2012, Hattermann et al., 2014, Nakayama et al., 2014, Stewart and Thompson, 2015]. However, computational constraints and technical difficulties (e.g. re-gridding the land-sea mask online during a simulation) still prevent the application of sophisticated modeling schemes in long term paleo-ice sheet model simulations. It is thus necessary at present to fall back to simple parameterizations of ice physics in modeling paleoclimate ice sheet dynamics [Stocker et al., 2013]¹² and chapter 2).

Currently, the past stability of the WAIS in a warming world and the grand evolution of the AIS is poorly constraint, since observational data from proxy reconstructions are sparse¹³, and ice sheet models only begin to produce more reliable fore- and hindcasts. Central research foci presently address the future mass balance of the AIS and its impact on sea level in the centuries and millennia to come [Ritz et al., 2015, Golledge et al., 2015, Mengel et al., 2015, Winkelmann et al., 2015, Sutter et al., 2015a], the advance and retreat of the ice sheets' grounding line [Favier et al., 2014, Cornford et al., 2015], the ice-ocean interactions underneath the vast Antarctic ice shelves [Hellmer et al., 2012, Pritchard et al., 2012, Depoorter et al., 2013], as well as the past influence of the large paleo ice sheets on timing and extent of glacial-interglacial cycles [Abe-Ouchi et al., 2013] and the effects of a warming or cooling climate on the long term ice sheet dynamics [Wilson et al., 2013, Knorr and Lohmann, 2014]. All these topics are intertwined and mutually dependent, illustrating both the difficulties and the fascination of the complex science covering AIS dynamics.

In the following chapters these topics are addressed, with the goal of improving the understanding of

¹¹See chapter 13 of the WG1: "There is high confidence in projections of thermal expansion and Greenland surface mass balance, and medium confidence in projections of glacier mass loss and Antarctic surface mass balance".

¹²See chapter 3 of the WG1: "continental-scale ice sheet models currently rely on improved parameterisations (Alley et al., 2008; Pollard and DeConto, 2009; Levermann et al., 2012)".

¹³Both in space and time, see for example the review of the AIS evolution following the last glacial maximum [Bentley et al., 2014].

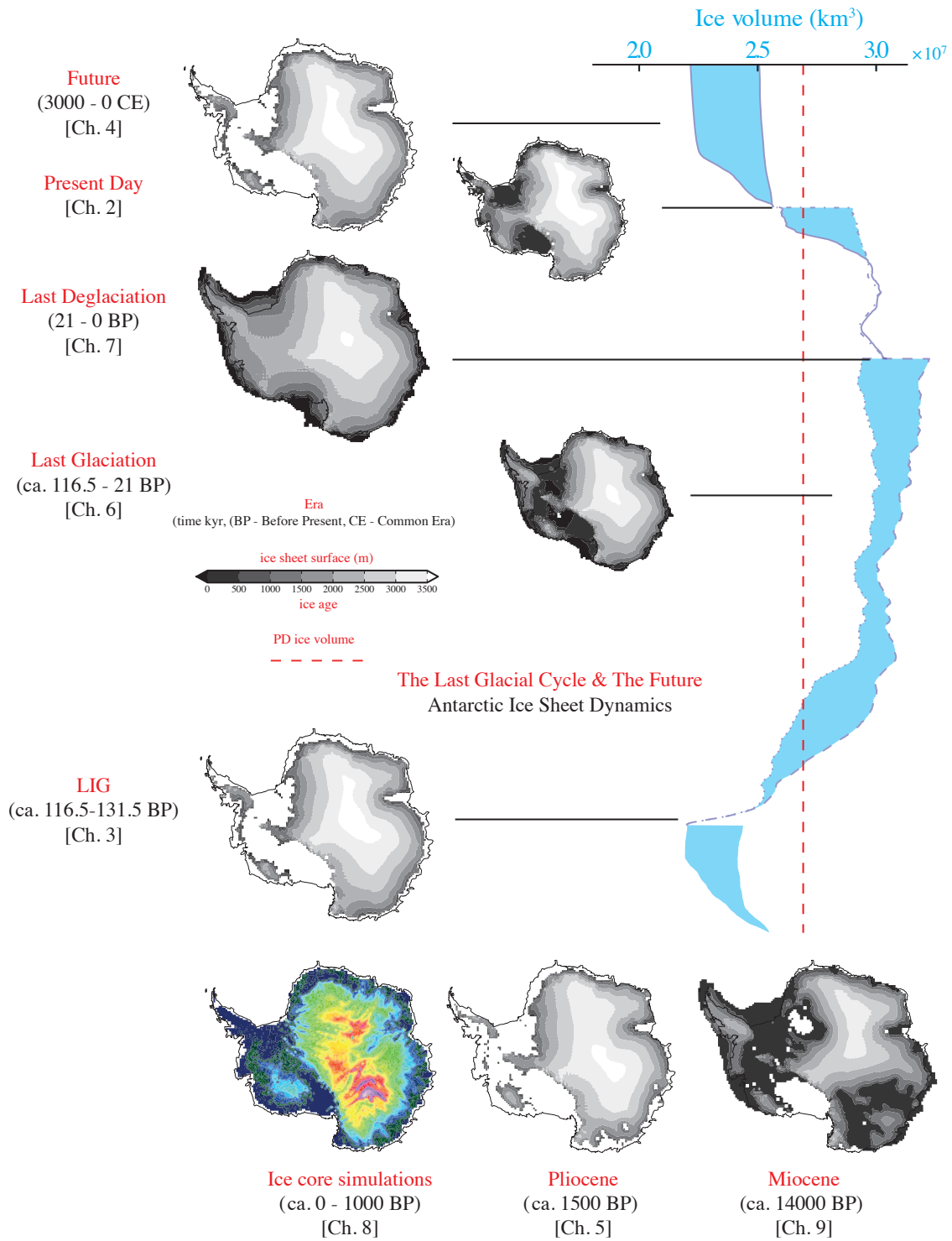


Figure 1.3: A graphical depiction of Antarctic Ice Sheet evolution through the past. Each chapter of this thesis is highlighted with an illustration of the Antarctic Ice Sheet and the climate time slice discussed in the respective chapter. The vertical graph on the right shows the evolution of the Antarctic Ice Sheet in the last glacial cycle (the range of volumes is derived from sensitivity studies presented in this thesis).

both past and future AIS evolution. Figure 1.3 illustrates the framework of this thesis.

In this thesis the dynamic evolution of the AIS during the last glacial-interglacial cycle (chapters 3, 6, 7) is investigated, under consideration of the role of ocean warming or cooling and surface mass balance on the coupled ice sheet-shelf and grounding line dynamics. Special focus lies on an ice sheet modeling assessment of Antarctica's potential contribution to global sea level rise during the LIG (chapter 3). In simulating the glacial-interglacial cycle, water stable isotopes are advected through the ice to create an artificial ice core archive which can be compared to the isotopic composition and depth-age relationship in the AIS. In a first step this procedure serves to validate the model's performance and in a second step it supports the interpretation of ice cores from an ice dynamics perspective (see chapters 2.5 and 8). Further, a range of modeling efforts are presented, simulating the future evolution of the AIS in simplified, unabated greenhouse gas emission scenarios (see chapter 4), which assesses the potential Antarctic sea level contribution in the next centuries and millennia. Finally, two additional paleo-environments, the Pliocene (chapter 5) and the Miocene (chapter 9), are illuminated from an AIS perspective. The Pliocene AIS, as an example of a warm climate south polar ice sheet, and the Mid Miocene Climate Transition (MMCT), in which an AIS with present day dimensions formed [Wilson et al., 2013].

Specific questions addressed in this thesis are:

1. Antarctic Ice Sheet dynamics and sea level contribution in the Last Interglacial. The climate in the LIG around 125 kyr BP is considered to be $1 - 2^{\circ}\text{C}$ warmer than most of the Holocene [Otto-Bliesner et al., 2013, Lunt et al., 2013, Bakker et al., 2014]. Despite this moderate warming, it was a time with considerably smaller ice sheets than today, and a surprisingly high sea level (ca. 7 – 9m above the present day sea level e.g. [Dutton and Lambeck, 2012, Kopp et al., 2013, Dutton et al., 2015]). Therefore the question after whereabouts of such water masses poses itself. In chapter 3 the dynamic evolution of the AIS in the LIG is investigated with a 3D ice sheet model (ISM [Thoma et al., 2014]) and a fully coupled atmosphere-ocean general circulation model (COSMOS [Stepanek and Lohmann, 2012, Pfeiffer and Lohmann, 2015]).

Climate models [Lunt et al., 2013, Pfeiffer and Lohmann, 2015] and proxy data [Capron et al., 2014] still exhibit large discrepancies in sea surface temperatures (SST) and surface air temperatures (SAT) especially in the high northern and southern latitudes. While the sea level contribution of Greenland (ca. 2m [Dahl-Jensen et al., 2013]), ocean thermal expansion [McKay et al., 2011] and land based glaciers [Marzeion et al., 2012] (both 0.5m) seems to be well constrained. Here, for the first time, the role of the remaining protagonist, the Antarctic Ice Sheet, is investigated in an ice sheet modeling effort incorporating both AOGCM forcings as well as proxy data (e.g. [Sutter et al., 2015a]). A destabilization of the WAIS by means of the Marine Ice Sheet Instability (MISI [Mercer, 1978, Schoof, 2007]) in the LIG would have contributed over 3m sea level rise [Bamber et al., 2009], thereby filling the sea level gap which the other main contributors leave.

In chapter 3 the potential mechanisms triggering the MISI are discussed, and the transient evolution of the AIS in the LIG is examined. The crucial role of Southern Ocean temperature and the ice-ocean interaction underneath the Antarctic ice shelves is identified as the main driver behind a collapse of the WAIS, while a precipitation or surface temperature driven retreat is found to be implausible. It

is shown that the climate forcing delivered by the general circulation model applied (COSMOS [Lunt et al., 2013, Pfeiffer and Lohmann, 2015]) does not suffice to destabilize the WAIS. A Southern Ocean temperature anomaly threshold of $2 - 3^\circ$ is required to tip the WAIS into an unstable configuration, triggering runaway retreat and leading to a AIS sea level contribution during the LIG of ca. 3 – 4m.

These results support the hypothesis that the WAIS played a substantial role in LIG sea level evolution. Further, an underestimation of Southern Ocean temperatures in COSMOS is identified which seems to be a common misrepresentation in general circulation models. Thus the results call for a better representation of polar ocean circulation processes and especially the inclusion of ice ocean interaction and feedbacks into coupled climate models in order to realistically simulate high latitude interglacial climate dynamics.

2. The stability of the WAIS in the next centuries and millennia. Future climate evolution and AIS dynamics could unfold in similar patterns as in past interglacials such as the Eemian. However, large uncertainties still exist in predictions of both future climate and sea level changes, which are mainly rooted in the limited understanding of ice sheet dynamics and the regional manifestation of global climate change in the Southern Hemisphere. Recently, a range of studies dedicated to estimating future Antarctic contributions to sea level change have been published [Golledge et al., 2015, Winkelmann et al., 2015, Ritz et al., 2015, Sutter et al., 2015a], applying different modeling approaches and time horizons. The main question driving these investigations is whether the marine ice sheets in Antarctica might eventually turn into a rapid retreat mode, a process which has been suggested to have already started for the glaciers in the Amundsen Sea embayment [Rignot et al., 2014, Joughin et al., 2014].

In chapter 4 simulations of future AIS evolution over the next centuries and millennia are discussed, with the aim of identifying critical thresholds beyond which the WAIS becomes unstable. The main difference between future and LIG climate change is the pace and maybe the amplitude of warming (which strongly depends on the behavior of societies worldwide, and is therefore a major source of uncertainty). To discuss a range of scenarios, several warming trajectories are applied as a climate forcing in the 3D ISM for the next 5000 years. The results show that the future evolution of the AIS strongly depends on the emission of greenhouse gases over the next decades. Depending on the scenario, effects range from small increases in ice volume, to a lock-in of irreversible collapse of the WAIS unfolding gradually over the next millennia and raising sea level by ca. 3m.

A more extreme forcing which would lead to the large scale disintegration of the major Antarctic ice shelves within this century¹⁴, would lead to the collapse of the WAIS within a few centuries. Under such conditions, the AIS contributes ~ 0.5 m to sea level rise until the end of this century. These extreme estimates of future Antarctic contributions to sea level rise highlight the urgency of improving the understanding of the physical processes underpinning WAIS collapse.

3. Constraining the size of the AIS in the late Pliocene warm period. The late Pliocene warm period (also known as the PRISM interval 3.264 to 3.025 million years before present), is another potential analogue to future climate change [de Boer et al., 2015]) which serves as an example of a relatively warm climate¹⁵. The sensitivity of the AIS to such a warm climate can serve as an indicator of

¹⁴Due to melting and calving events.

¹⁵Exceeding the warming in the LIG [Lunt et al., 2013, Pfeiffer and Lohmann, 2015].

potential future dynamics on the continent. However, the available ice core record from Antarctica only covers the last eight glacial cycles (ca. 740.000 years [Jouzel et al., 2007]) and circumantarctic marine sediment cores, providing hints of past ice sheet extent, only exhibit ice sheet growth and retreat during the last glacial cycle. Further a comprehensive ice sheet modeling study constraining the AIS evolution in the Pliocene is still missing, thus limiting the knowledge of Pliocene AIS size, shape and evolution. The Pliocene Antarctic Ice Sheet volume and extent remains unknown. In chapter 5 the efforts of the first ice sheet modeling intercomparison project staged in the Pliocene [de Boer et al., 2015] are presented. While the different ice sheet models applied in the study show consistent results in simulations of the present day AIS, model spread for the Pliocene is substantial and prohibits a meaningful conclusion on Antarctic Ice Sheet extent and volume in the PRISM interval. This calls for more homogenized ISM parameterizations and further ice sheet model intercomparison efforts, not only limited to the Pliocene, but also for the better understood periods like the LIG, LGM or PD.

4. Glacial advance of the AIS into the LGM and pacing of post-glacial retreat. Knowledge about the AIS' evolution during the last glacial cycle is largely constrained to the post-LGM retreat [Bentley et al., 2014]. Marine paleoproxy information previous to that period is largely overridden by the retreat of the grounded LGM ice sheets, thus pre-LGM information is mostly limited to the interpretation of cosmic radio-isotopes (Beryllium) in rocky outcrops (Nunataks) protruding the ice sheet. So far only a handful modeling studies are available on the timing and the underlying dynamics of the AIS' glacial advance after the LIG. Some discuss the advance only in scope of a long-term multi-glacial cycle analysis with coarse parameterizations of both atmospheric and ocean forcing [Huybrechts, 2002, Pollard and DeConto, 2009], others implement more sophisticated approaches, comparable to those used in this thesis, but specifically address the sensitivity to changing basal conditions and less so to oceanic forcing [Maris et al., 2014]). A third kind of modeling approach applies extensive tuning and high spatial resolutions in multi-ensemble simulations to approach a realistic LGM AIS [Golledge et al., 2013] compared to proxy reconstructions [Bentley et al., 2014]. After all, there are large differences between model studies and scope. Consequently, estimations of LGM extent and volume changes vary widely from ca 5-18m [Huybrechts, 2002, Bentley, 1999, Golledge et al., 2013] sea level equivalent. Further the pace and variability of the AIS' growth following the LIG is largely unknown, since variations of global sea level were mostly dominated by the waxing and waning of the large northern hemisphere ice sheets. All studies seem to focus mostly on bedrock properties by varying sliding parameterizations, mostly ignoring the impact of different ice shelf melt scenarios.

In chapters 6-7 the full glaciation and deglaciation after the LGM is simulated with a 3D ISM, forced by the climate output from COSMOS [Stepanek and Lohmann, 2012]). Results indicate that either the Antarctic circumpolar current and deep water is simulated slightly too warm in COSMOS or that surface accumulation is too low to allow for substantial grounding line advance into the LGM. Nevertheless, tuning of the basal shelf melt rates show that a wide range of LGM AIS configurations can be simulated (4 – 12m sea level equivalent) within a reasonable parameter space. The ISM results in concert with paleo proxy constraints show that the AIS glacial advance was probably a slow process culminating in an LGM ice sheet, lowering global sea level by about 3 – 7m compared to the present day. The LGM ice sheet mostly extended to the continental shelf break in the Weddell Sea while the simulations show multiple potential LGM grounding line positions in the Ross Sea. The interior AIS was slightly thinner

than present day due to a general weakening of the hydrological cycle during the glacial. The WAIS appears to have been slightly thinner than present day as well, with a vast flat ice sheet covering the present ice shelves in both the Ross and the Weddell Sea. The results strongly depend on the distribution and strength of basal melting underneath the ice shelves, especially the Filchner-Ronne Ice Shelf (FRIS) and Ross Shelf (RS). Small variations in ocean temperatures underneath the FRIS and RS can tip the scale in favor of glaciation or against.

The post-LGM deglaciation dynamics depend heavily on the maximal extent and volume of the LGM ice sheet, and the applied ocean forcing. The results show that only strong melt pulses during the first millennia of deglaciation could have destabilized the marine LGM ice sheets which extended into the Weddell and Ross Sea. A bifurcation in the post-LGM ice volume evolution depending on the basal shelf melt rate indicates a tipping point upon which the marine ice sheet instability is triggered in these ocean sectors. Continuous high shelf melt rates ($\sim 20 - 30 \frac{\text{m}}{\text{a}}$) lead to a collapse of the Weddell Sea ice sheet within 1.000 years. Since deglacial AIS retreat occurred in several stages [Bentley et al., 2014, Weber et al., 2014] recurring cold spells [Vazquez Riveiros et al., 2010] presumably prolonged the lifetime of the Weddell and Ross Sea ice sheets.

The results uncover several systematic characteristics of AIS LGM extent and volume as well as for deglacial dynamics which call for the inclusion of more observational proxy data, and improved detailed climate simulations from GCMs for the Southern Hemisphere, to better constrain the parameter space and the climate forcing during the last glacial cycle. Further higher spatial model resolutions and a better understanding of the basal properties specifically of the marine bedrock are needed to further pin down regional patterns of pre- and post-LGM AIS evolution.

5. Unlocking the Antarctic climate archive. Antarctic ice cores serve as invaluable climate archives which are encrypted by the complex formation and origin of past precipitation over the ice sheet [Dansgaard, 1964, Jouzel et al., 1997]. Deciphering these archives requires in depth knowledge of the present isotope temperature relation at the respective sites, as well as information of past changes in ice sheet elevation, seasonality of precipitation and moisture source. Paleoclimate proxies conserved in geologic formations such as ice cores and marine sediment cores are scarce (in both time and spatial dimension). Thus, the interpretation of past climate evolution derived from observational evidence must go hand in hand with a careful interpretation of model simulations. Ice sheet chronologies, and to a limited extent isotopic distributions are a valuable constraint on ice sheet model simulations. Despite efforts of simulating Greenland [Clarke and Marshall, 2002, Lhomme et al., 2005] and Antarctic [Huybrechts et al., 2007] ice cores and isotope distributions, such an ISM benchmark test against ice core data has not been attempted yet. As both GCMs and ISMs improve their depiction of past, present and future climate evolution, ice core simulations can be used to improve the interpretation of proxy data conserved in the Antarctic and Greenland ice sheets. In chapter 8 first attempts to simulate the isotopic composition and age depth relationship of the AIS in a holistic model environment, including an AOGCM and a 3D ISM, are presented. This work combines the results from the previous chapters (6-7) with a passive tracer advection algorithm (chapter 2) to simulate the isotopic information stored in the AIS during the full last glacial cycle (ca. 130.000 years) and strives for a comparison between simulated and real Antarctic ice cores (chapter 8).

6. The mid-Miocene AIS. Identifying the main driving forces of ice sheet growth and extent in the Miocene cold reversal. The topic of the mid-Miocene climate transition (MMCT [Shevenell et al., 2004, Knorr and Lohmann, 2014] concludes this thesis. It marks the first formation of a modern AIS extension [Zachos et al., 2001, Billups and Schrag, 2002, Shevenell et al., 2004] during a transition to a colder Miocene climate. This cooling was probably caused by a combination of a decrease of atmospheric $p\text{CO}_2$ [Zachos et al., 2001, Foster et al., 2012, Badger et al., 2013] and changes in oceanic circulation triggered by tectonic events [Hamon et al., 2013]. This cooling allowed for an expansion of the AIS to a size comparable to the magnitude of today's ice sheet. Nevertheless, the actual configuration of the mid-Miocene AIS is still an open question. In chapter 9 the processes and drivers behind the mid-Miocene AIS advance are discussed by means of equilibrium ice sheet simulations under a variety of climate and bedrock boundary conditions. The results suggest that not the south polar climate conditions, but the available land area above sea level at the time, holds major control on final equilibrium ice sheet extent. Though different climate forcing derived from COSMOS lead to significantly different ice volumes, the effects of changes in the initial bedrock configurations on ice volume dwarf the climatic drivers. A large dynamic range of mid-Miocene AIS size, given different climate forcings and bedrock initializations, is simulated corresponding to an ice volume spread of $\sim 35\text{m}$ sea level equivalent. These results highlight the importance of well constrained initial boundary conditions for ice sheet models, especially in deeper geological history.

Methods

2.1 The Ice Sheet Model

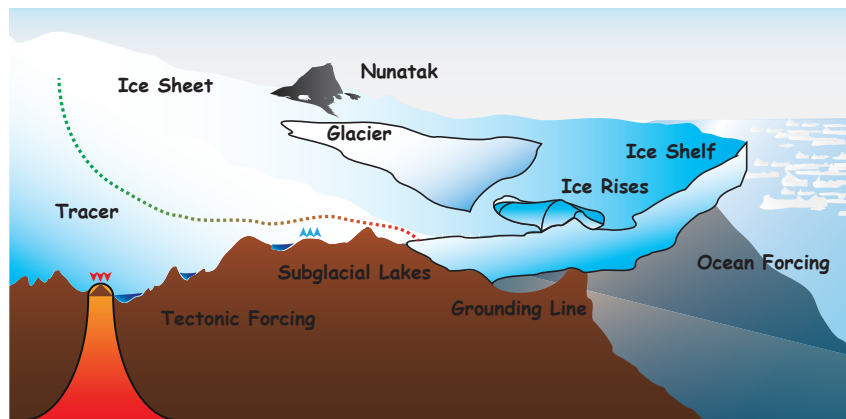


Figure 2.1: Physical components of RIMBAY. The 3D ice sheet model RIMBAY, used in this study, represents all major physical components of Antarctica, such as ice shelves, subglacial hydrology, ice streams as well as including external forcings such as sea level and ocean temperatures. Topographic and hydrologic features like nunataks and subglacial lakes are also accounted for.

¹The 3D ISM RIMBAY [Thoma et al., 2014], the work horse of this thesis is a "multi physics" higher order ice sheet model [Pattyn, 2003, Thoma et al., 2014]. The model includes all major features of the polar ice sheets (ice shelves, nunataks, fast flowing glaciers, basal hydrology etc. (see Figure 2.1)). All simulations presented in this thesis are carried out on a 40x40 kilometer regular grid with 41 vertical sigma layers, covering the whole Antarctic Ice Sheet. The coarse resolution was chosen to allow for extensive exploration of the parameter space spanned by the basal friction and shelf melt rate coefficient (see equations 2.1 & 2.3) and other parameters. The model complexity was reduced to the shallow-ice and shallow-shelf approximation of the Navier-Stokes equation, with no higher order terms included, due to the long computation time of the paleo-simulations. The shallow-ice approximation neglects all stresses except for the vertical stress term. Ice flow is governed by the overburden pressure of the ice as well as the surface and bedrock slope. Equation (2.2) highlights the equation for the lateral velocity according to the SIA.

¹This chapter mainly consists of the publication "*Integration of passive tracers in a three-dimensional ice sheet model*" [Sutter et al., 2015b].

$$\tau_b = \beta^2 \cdot u \quad (2.1)$$

$$\vec{u}(z) = -2(\rho g)^n |\nabla|^{n-1} \nabla s \int_b^z A(\theta^*) (s-z)^n dz + \vec{u}_b \quad (2.2)$$

Where τ_b is the basal shear stress, β the basal friction coefficient and u the velocity², n is the exponent found in the Glen flow law [Cuffey and Paterson, 2010] set to the empirical value of 3³, $A(\theta^*)$ is a temperature dependent flow rate factor and \vec{u}_b the basal velocity, ρ and g are density of ice (910kgm⁻³) and gravitational force constant (9.81ms⁻²). The integral is evaluated from the bedrock (b) underneath the ice to ice surface (s). This approximation is valid for ice sheets with a small depth-to-width relationship, which applies to the interior of Greenland and Antarctica but not to the margins, where ice dynamics are governed by ice shelves and fast flowing ice streams. In the shallow-shelf approximation basal friction is omitted while lateral velocities are assumed to be constant throughout the depth of the shelf ($\frac{\partial u}{\partial z}, \frac{\partial v}{\partial z} = 0$). Figure 2.2 illustrates the different stress field domains within the model domain.

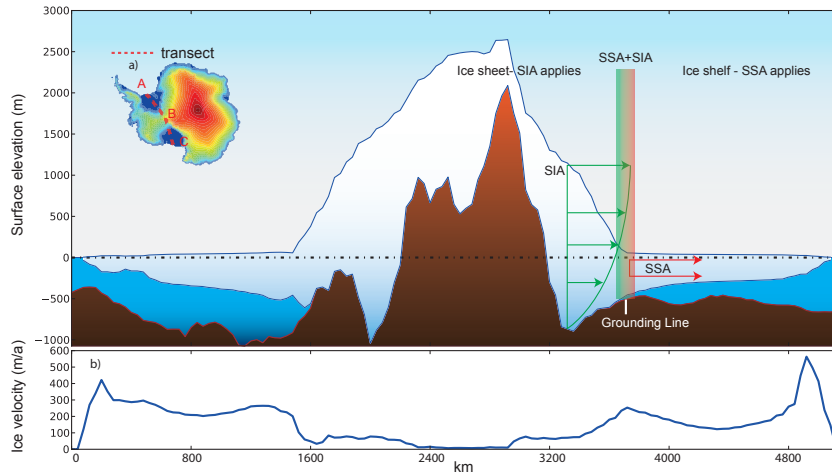


Figure 2.2: Transition between the shallow shelf (SSH) and shallow ice (SIA) approximations. Where ice is grounded the SIA applies and ice flow is governed by the overburden pressure, surface slope and bedrock topography. The floating shelf ice is governed by the SSH. There, basal friction is set to zero and ice flow is governed by longitudinal stress. The area close to the grounding line is represented by a combined SSH+SIA term (depicted by the shaded coloring). Inlet a) illustrates the transect through the present day topography/bathymetry starting from Larsen Shelf through Filchner-Ronne and Ross Shelf (A-B-C). b) Velocities along the transect (A-B-C).

Since RIMBAY does not yet resolve subgrid grounding line positions explicitly⁴, model sensitivity to the applied climate forcing was validated by testing RIMBAY in a model setting adapting the methodology applied in Pollard & DeConto (2009) [Pollard and DeConto, 2009] and simulating comparable grounding line migration. This gives confidence that sheet-shelf dynamics are sufficiently resolved on long time scales, coarse resolution and lack of explicit grounding line treatment notwithstanding.

²Here for simplicity the one dimensional case is chosen.

³Some ice sheet models use n as a variable parameter for tuning purposes. For the sake of simplicity, here the empirical value is chosen.

⁴A simple linear interpolation of basal friction is applied to guarantee a smooth transition between grounded and floating ice.

2.2 Ice Shelf Mass Balance

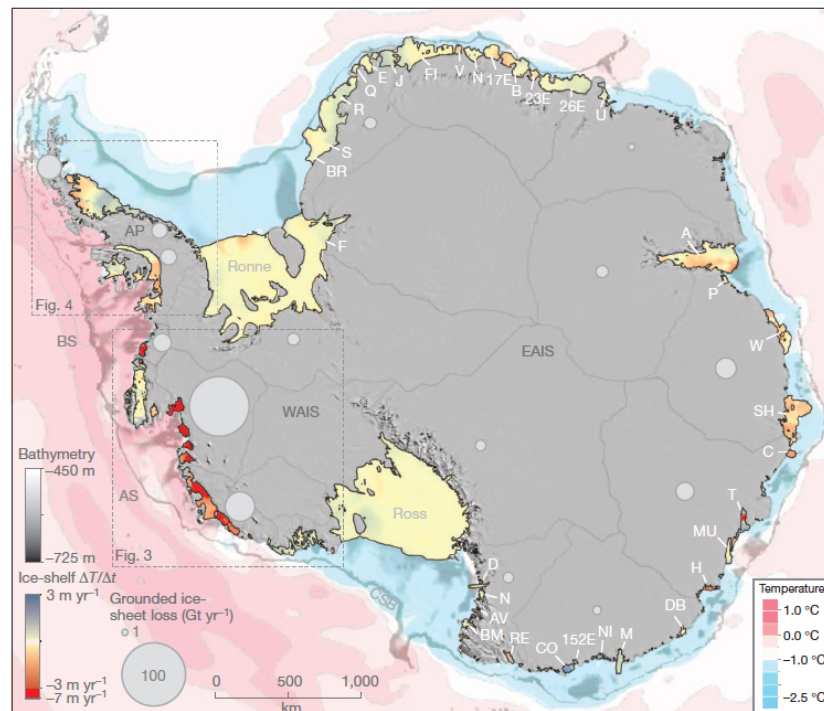


Figure 2.3: Thickness change rates of Antarctic ice shelves (from [Pritchard et al., 2012].)

The mass balance of the AIS is mainly controlled by snowfall and sub-shelf melting plus calving under and along the fringes of the circum-antarctic ice shelves. While the surface accumulation is simply derived from the external climate forcing, things get complicated if it comes to the mass balance of the Antarctic ice shelves (see Figure 2.3 for an overview of present day Antarctic shelf thickness change rates). Melting underneath the ice shelves is controlled by the heat transport into the ice cavities driven by ocean currents (see Figure 2.4). The salinity of the water masses and the depth of the ice-ocean boundary layer ultimately controls the freezing temperature of the ocean water. If the water is above this freezing temperature, the surplus energy can be used to melt the ice shelf. At present day the combined ice shelf mass loss due to calving and basal melting amounts to ca. 2.766 Gt [Depoorter et al., 2013] or ca. 2.414 [Rignot et al., 2013] (see Figure 11.2 in chapter 11), of which a little over half is due to melting (the other half being lost via calving).

It proves difficult to accurately represent ice shelf melting in climate models [Nakayama et al., 2014], and so far only high resolution ocean models resolve the sub ice shelf circulation patterns in a more detailed manner [Hellmer et al., 2012]. The necessary high resolution required to resolve transport processes⁵ and a realistic bathymetry, poses large challenges for paleoclimate modeling due to the associated long simulation times. Moreover, the dynamic evolution of the shelf cavity geometry would require a regridding of the land sea mask in simulations on long time scales. So far, there is no high resolution, adaptive grid ice-ocean model available which could simulate basal melt rates over the course of glacial interglacial cycles. For the purpose of this thesis, a simple basal melt rate parametrization scheme is adapted based

⁵So called eddy allowing or eddy resolving ocean models [Thompson, 2008, Thompson et al., 2014, Langlais et al., 2015].

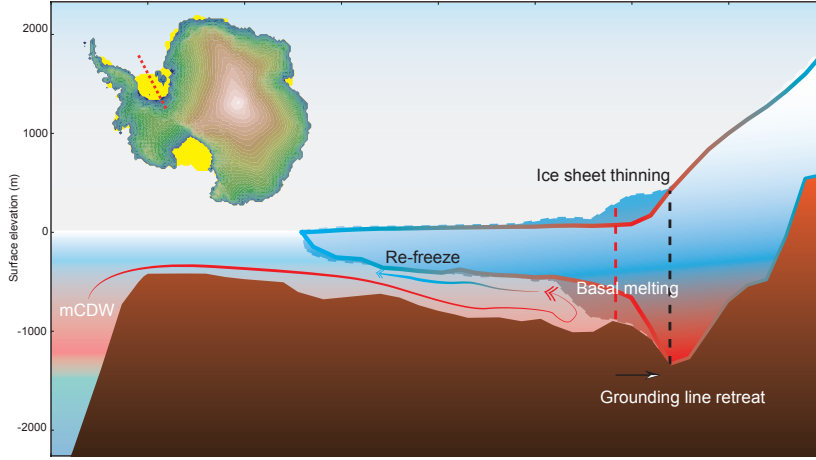


Figure 2.4: A simplified schematic of ice ocean interactions underneath the Antarctic ice shelves. Warm water (e.g. modified circumpolar deep water, mCDW) intrudes an ice shelf cavity and causes melting close to the grounding line. The melt rate mainly depends on water temperatures and the depth of the cavity (pressure melting point). As heat is exchanged between water and ice, driving the melt process, the water cools down and exits the cavity, while potentially refreezing along the way. If melt rates at the grounding line exceed the mass flow coming from the interior of the ice sheet, the ice thins and eventually begins to float. This causes a retreat of the grounding line until a new equilibrium is reached.

on the approach by Beckmann & Goosse [Beckmann and Goosse, 2003]. The equation for the basal shelf melting is constituted by the following terms

$$M(T_f, T_O, z) = \frac{\beta_{bg} \cdot \rho_w \cdot c_{pw} \cdot \gamma_T (T_O - T_f(z))}{\rho_i L_i} \quad (2.3)$$

$$T_f = 0.0939^\circ C - 0.057^\circ C \cdot S_O + \frac{7.64e^{-4^\circ C}}{m} \cdot z; \quad (2.4)$$

where T_f is the freezing point temperature, T_O the ocean temperature at the ice ocean boundary, ρ_w the ocean water density, c_{pw} ocean heat capacity, γ_T heat transfer coefficient, S_O the salinity, and z the depth of the ice ocean boundary. β_{bg} is the only tunable parameter in equation 2.3 and is chosen to represent the best fit compared to present day observed melt rates (Figure 11.2). Further details about melt rate tuning and their effect on ice dynamics are given in the Appendix. For calculation of the melt rates, the melt parametrization requires an ocean temperature at any given point underneath the shelves. Since observations inside Antarctic ice shelf cavities are sparse and COSMOS only simulates the ocean temperatures up to the ice shelf edge (or the sea ice edge, whichever constitutes the demarcation line between land and ocean) the temperature field is extrapolated from the shelf edge into the cavity. Such an approach does not capture the actual circulation patterns. Nevertheless, it yields acceptable results compared to present day melt rates for the purpose of paleoclimate simulations. If the ice sheet retreats, new ocean nodes are formed into which the ocean temperature from the adjacent points is extrapolated.

Relatively fast dynamic ice sheet changes such as in glacial-interglacial transitions call for the simulation of more sophisticated, fully coupled ice-ocean interactions. This is not feasible yet, due to computational limitations. For this reason, a second best implementation of shelf melt rates is chosen here. Additional uncertainties are introduced by the ocean forcing fields used to drive the ISM. A simple comparison between the mean ocean temperatures from the World Ocean Atlas (WOA) for the years (2005-2012) ([Locarnini et al., 2013]) and the WOA 2009 [Locarnini et al., 2010]⁶, illustrates that the choice of the present day forcing will greatly affect the ice sheet simulations.

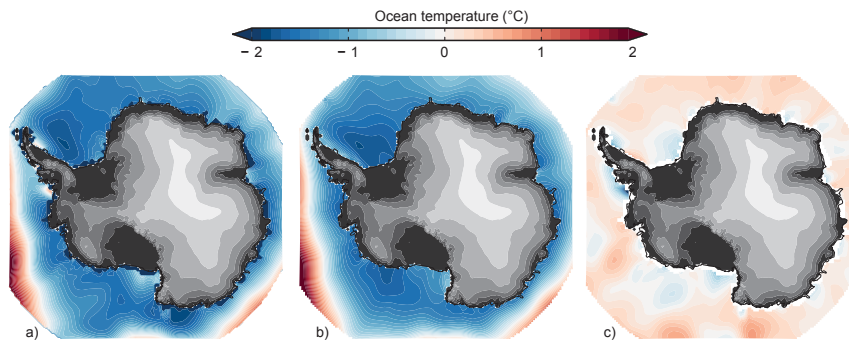


Figure 2.5: Sea surface temperatures from the World Ocean Atlas 2013 [Locarnini et al., 2013] (a) and 2009 [Locarnini et al., 2010] (b) and their difference WOA09 - WOA13 (c).

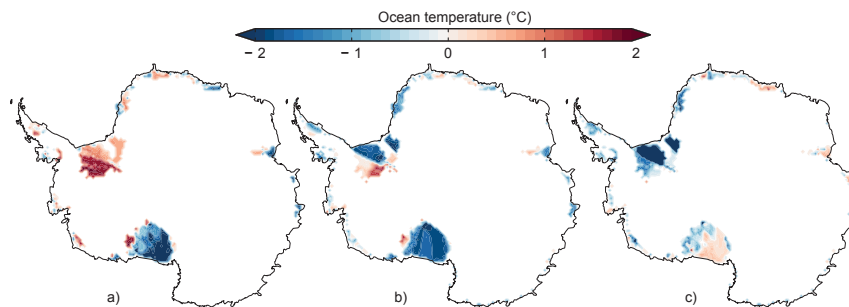


Figure 2.6: Ocean temperatures underneath the ice shelves after linear extrapolation from the ice edge. (a) WOA13 [Locarnini et al., 2013], (b) WOA09 [Locarnini et al., 2010], (c) WOA09 - WOA13.

⁶Which is a compilation of mean fields averaged over the years 1955-2006.

2.3 Present Day Control Run

Due to its long characteristic time scales, flow velocity ranges over several orders of magnitude (from $\frac{\text{cm}}{\text{a}}$ to $\frac{\text{km}}{\text{a}}$), unknown basal properties and ice temperature regime, it is notoriously difficult to create a model spinup which provides a reasonable representation of the transient state of the present day Antarctic Ice Sheet. While the surface velocities [Rignot et al., 2011] and the geometry [Fretwell et al., 2013] of the PD AIS are well known, proxy constraints for past ice sheet configuration are sparse and observations of basal properties and topography [Sun et al., 2014b, Gasson et al., 2015] still suffer from large uncertainties. To find a reasonable set of parameters for the simulations presented within this thesis, ensemble simulations are carried out with present day climate forcing (see chapter 11), aiming at an optimized representation of PD Antarctic geometry and surface velocities. The AIS, as observed per remote sensing and measurements on the ground, is in a transient state. Provided with only a rough idea of this initial transient state, it is impossible to create a control run for ice sheet modeling studies which recreates the present day ice sheet convincingly.

The general approach in the ISM community is to simulate an AIS with a fixed surface geometry only allowing temperatures and velocities to equilibrate. Taking this as a "pivot" ice sheet, the control simulation then freely evolves the latter under the applied climate conditions. Here, the reference simulation forced by present day climate (see Figure 11.4) is presented. It constitutes the PD control simulation for all experiments carried out in the scope of this thesis. After equilibrating temperature and velocities for 50000 years, the model evolves freely for 15000 years. The equilibrated ice sheet with a fixed present day topography is used as the initial ice sheet for the simulations presented in chapters 3, 4 and 5. Figure 2.7 shows the results from the PD control simulation.

It is evident, that the AIS after 15kyrs of simulation does not resemble the PD ice sheet perfectly. However, the general geometry of the ice sheet with ice shelves and grounded ice fits reasonably well (Figure 2.7 B). All ice shelves are resolved except for small ice tongues fringing Wilkes Land in East Antarctica. This is due to the coarse resolution which does not capture small scale features (smaller than 40 km that is). The shapes of the FRIS and the RS are well captured, as well as the ice shelves of

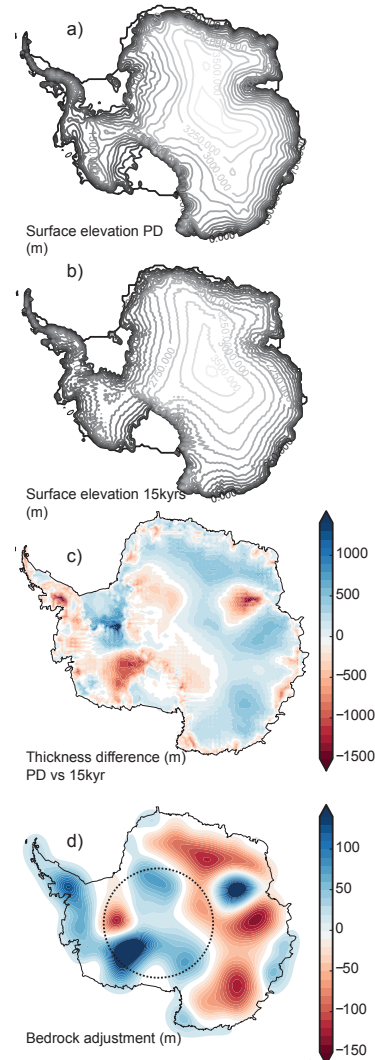


Figure 2.7: Results of the present day control run. a) surface contours BEDMAP1, b) after 15kyrs of simulation, c) thickness mismatch, d) bedrock adjustment.

the Amundsen and Bellinghausen Sea. The Amery Shelf is somewhat deformed, this is again rooted in the coarse resolution which does not resolve the tributary glaciers feeding into the shelves in fine enough detail. In this thesis a revised form of the somewhat older BEDMAP1 topography is implemented which is known to be problematic in some regions. However the overall representation of geometry, ice flow pattern and ice volume fits the present day AIS reasonably well.

2.4 COSMOS

The climate forcings utilized in this thesis mainly derive from the AOGCM COSMOS (see Figure 2.8). It consists of the atmospheric model ECHAM5 [Roeckner et al., 2003], which is employed at a resolution of T31 (1.5x1.5 degrees) and 19 vertical levels, the ocean model MPIOM [Marsland et al., 2003], which includes a sea ice component, as well as the land surface model JSBACH [Brovkin et al., 2009]. MPIOM is run with a resolution of GR30, consisting of 40 unevenly spaced vertical layers, with an approximate lateral resolution of 1.5x3 degrees, with significantly higher resolution at the model's poles, situated over Greenland and Antarctica. At the poles, resolutions can reach $\sim 20 - 40$ km. COSMOS is tested in benchmark experiments such as for the Pliocene and LIG [Stepanek and Lohmann, 2012, Lunt et al., 2013, Pfeiffer and Lohmann, 2015] yielding results in the range of a suite of models. In this thesis, COSMOS simulations staged in the LIG [Pfeiffer and Lohmann, 2015], LGM and Miocene [Knorr et al., 2011, Knorr and Lohmann, 2014] are utilized. The COSMOS climates used in the different applications presented in this thesis are highlighted at the beginning of each chapter and in the Appendix.

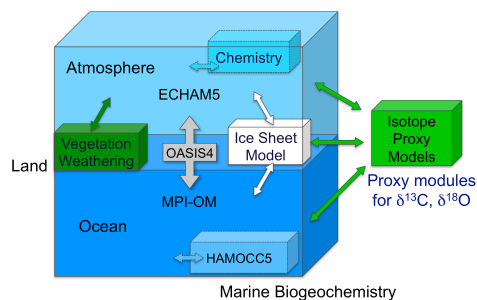


Figure 2.8: Conceptual illustration of the COSMOS [Stepanek and Lohmann, 2012] components and their coupling scheme. In this thesis, the fully coupled atmosphere-ocean version is utilized. Ice sheets are prescribed and do not change over time.

2.5 Passive Tracer Modeling

Components of the climate system, such as ice sheets and marine sediments serve as invaluable archives, which can be tapped into, to reconstruct paleoclimate conditions. The relative abundance of hydrogen and oxygen isotopes in ice cores is a proxy for past local temperature evolution. However the translation of these proxies into temperature is not straightforward. Complex interdependencies in the climate system can hide or override the local climate signal at which the ice core was drilled. Using 3D ice sheet modeling in concert with passive tracer advection, one can simulate the isotopic distribution in ice sheets and compare them to ice core data. Combining this method with a coupled climate model environment, containing atmosphere and ocean components, one can theoretically simulate the isotopic cycle from the source to the actual ice record. Such an approach would greatly support the interpretation of proxy data whilst constraining the output of 3D ice sheet models (ISMs). Here, the implementation of passive tracer

advection in the 3D ISM RIMBAY [Thoma et al., 2014] is presented and the potential of the method to reproduce chronologies of the polar ice sheets assessed.

2.5.1 A Paleothermometer

The polar ice sheets contain information on past climate conditions conserved in the form of relative abundances of hydrogen and oxygen isotopes. This information can be tapped by drilling ice cores. Snow precipitating on the surface of an ice sheet contains a distinct isotopic signature which depends on the respective temperature during condensation [Dansgaard, 1964]. The present day temperature-isotope relationship can be estimated, by measuring the isotope content in snow and fitting it to the observed temperatures at site [Dansgaard, 1964], [Jouzel et al., 1997]. This relationship can then be used to reconstruct past temperature variations. To put this reconstruction into perspective, it is necessary to establish a timeline for the ice core's isotope variations, which can be derived from annual layer counting in the upper part of the ice core or via mass spectrometry of the deep parts of the latter. Close to the bedrock it is often impossible to decipher a meaningful chronology due to complicated flow patterns of the ice which fold and heavily compress the local stratigraphy. Many processes apart from the condensation at site can influence the relative isotope concentration of precipitation. Temperature variations at the source or even a change in the source area might significantly change isotope concentrations [Jouzel et al., 1997]. Circulation pathways might undergo dynamic changes as well, which complicates the relationship between temperature and isotope concentrations.

3D ice sheet modeling combined with tracer advection can provide a modeled stratigraphy for Antarctica and Greenland, which can then be compared to the available proxy data [Goelles et al., 2014, Clarke and Marshall, 2002, Lhomme et al., 2005]. In this thesis, a passive tracer module for the 3D ISM RIMBAY (RIMTRACE) was developed to reproduce the stratigraphy and isotope distribution of Greenland and Antarctica. RIMTRACE was first tested in simplified model environments based on the EISMINT geometry [Huybrechts and Payne, 1996] and further validated against the analytical Nye-Haefeli age-depth relation [Nye, 1963, Haefeli, 1963].

2.5.2 Passive Tracer Advection

There are two widely used methods of transporting passive tracers in numerical simulations both implemented in the tracer advection model discussed below. The Lagrangian advection assumes the particle-perspective, which means that the particle is followed along its trajectory through the model grid. In contrast to the Lagrangian approach the Eulerian tracer advection solves the advection equation

$$\nabla_t A = \partial_t A + u\partial_x A + v\partial_y A + w\partial_z A = 0 \quad (2.5)$$

at every grid point covering the whole model domain. This has the advantage of producing information at every grid point. A is the advected property with absolute and partial derivatives with respect to time and space (∇_t, ∂_{xyz}). The drawback of the Euler approach lies within the numerical diffusion arising

from solving the advection equation in a finite differences environment. Furthermore, it is impossible to trace back trajectories of single tracers from their origin. This is a valuable feature of the Lagrangian transport, allowing detailed transport studies of any passive tracer object. The disadvantage of the Lagrangian transport lies in the sparse coverage of the model domain, which might be even more reduced by dispersive flow, as is the case in the lower parts of an ice sheet.

Validation of Tracer Modules

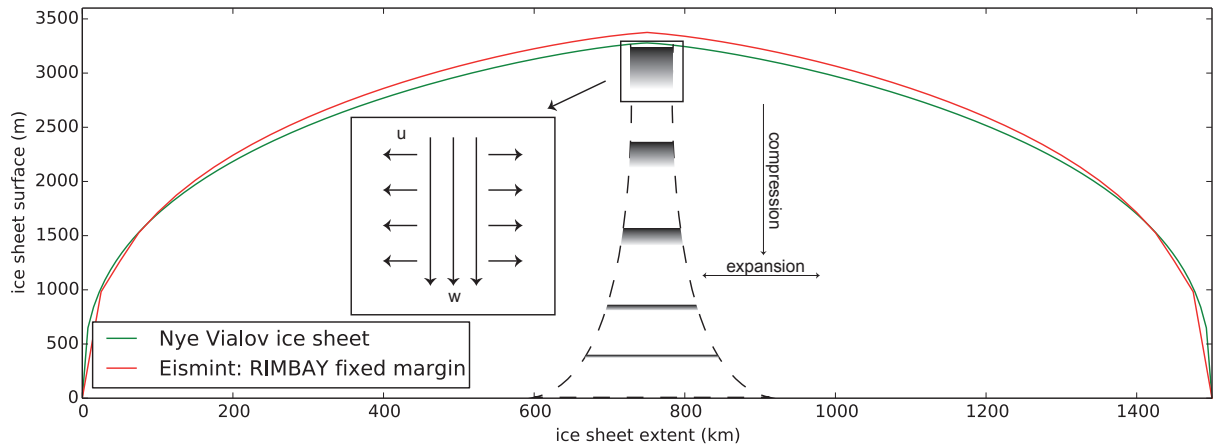


Figure 2.9: Ice sheet equilibrium topography of the EISMINT Fixed Margin experiment compared to the analytical description of the Nye-Vialov ice sheet. The shaded areas illustrate the combined effect of compression and layer thinning (not to scale). The box depicts constant horizontal velocities along the vertical axis and constant vertical velocities along the horizontal axis close to the ice divide.

Tracer tests are carried out in controlled model environments in order to ensure the capability of the tracer modules of reproducing realistic transport processes. The EISMINT project provides the perfect testing ground for this purpose. Both Lagrangian and Euler transport schemes are applied to simulations of spherical ice domes with radial accumulation pattern on flat bedrock. The ice sheet is run into equilibrium and subsequently the transport module is activated. The simulated age-depth relationship at the ice divide of both transport schemes is compared. Additionally both transport schemes are compared to the analytical age-depth distribution for a Nye-Vialov ice sheet, which is characterized as a radially symmetric ice dome with relatively steep flanks (see Figure 2.9).

Analytical Comparison to the Nye-Vialov Solution

The Nye-Vialov solution [Rybak and Huybrechts, 2003] for an idealized ice sheet (eq. 2.6) was used to compare the performance of the Lagrangian and Eulerian tracer advection approach (see Figure 2.10). Utilizing the analytical age-depth relationship for an ice sheet without basal melting, no horizontal advection, and constant vertical strain rate we can directly compare both advection methods to a pre-defined age-depth relationship (eq. 2.7):

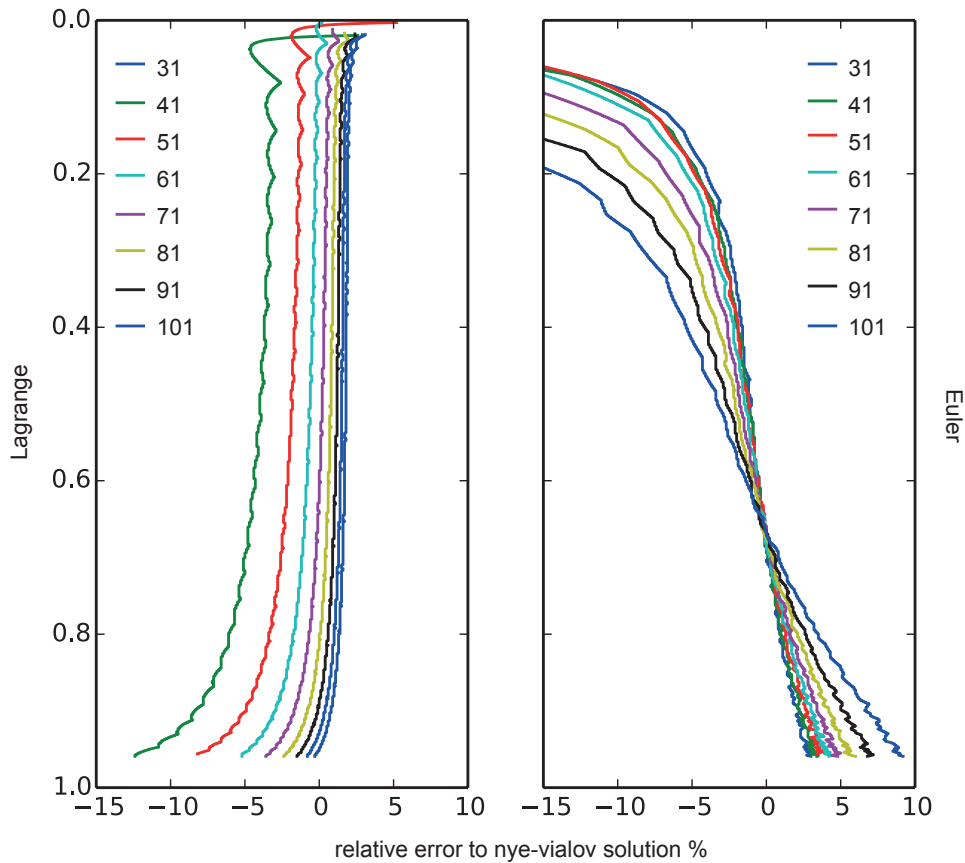


Figure 2.10: Sensitivity of the age depth relationship in an idealized Nye-Vialov ice sheet environment. Ice ages were calculated at the ice divide where an analytical solution to the age-depth problem exists. The figure compares two model runs with 31 and 101 sigma levels. Especially the Eulerian tracer method is highly sensitive to the number of sigma levels. The large error of both methods at the ice sheet surface, where the ice age should be zero is due to the very coarse resolution of the surface layers. This leads to an erroneous representation of velocities and thus to large discrepancies between the Eulerian and Nye-Vialov solution. Furthermore, Eulerian advection is a diffusive scheme leading to an age spread in the deep layers of the ice sheet.

$$H_0 = \left(\frac{20M}{A} \right)^{\frac{1}{2(n+1)}} \left(\frac{1}{\rho g} \right)^{\frac{1}{2(n+1)}} L^{\frac{1}{2}} \quad (2.6)$$

$$A = \frac{H_0}{G} \ln \left(\frac{z}{H_0} \right) \quad (2.7)$$

where H_0 is the ice sheet thickness at the divide, M the mass balance ($\frac{m}{a}$), A is the time (in years) it would take to get from the surface (divide position) to the location z within the ice sheet, g is gravitational force (9.81ms^{-2}) and ρ ice density (910kgm^{-3}), L denotes the characteristic length of the ice sheet, G is surface accumulation and z the depth inside the ice sheet. The basic assumption behind the Nye-Vialov solution is that ice inside glaciers or ice caps undergoes compression by overburden pressure (compaction) and, increasing with depth, layer thinning due to lateral extension. The horizontal velocity is assumed to be constant through any vertical transect through the ice sheet while the vertical velocity is constant along any horizontal line (strip shaped ice sheet). In the standard configuration of 50km lateral resolution and 41 vertical sigma layers (terrain following coordinates) the difference between both advection methods to the analytical solution is negligible in the upper domain of the ice divide. However, the solutions diverge in the lower part of the ice sheet close to the bedrock. This is due to the interpolation error accumulated along the trajectory in case of the Lagrangian approach and due to the increasing impact of numerical diffusion in the Eulerian solution. Low vertical resolutions result in considerable deviations of the Eulerian age-depth relation from the analytical solution, whilst the Lagrangian advection is less affected. Increasing the amount of sigma levels (finer vertical resolution), the performance of both advection methods can be instantly improved, reducing the discrepancy close to bedrock significantly. This approach is applicable in an idealized resource-friendly model-setup (such as the EISMINT environment, without ice shelves or complicated geometries as opposed to full scale simulations of the AIS), however full scale simulations of large ice sheets limit the computationally feasible degree of resolution to around 50-100 sigma levels.

2.6 Feasibility of Tracer Studies

The aim of this study was to assess the capability of the 3D ISM RIMBAY to reproduce ice sheet chronologies. To this end model validations against an analytical age-depth scale were carried out to test the accuracy of the implemented advective transport schemes. Both schemes exhibit excellent accuracy down to $\approx 85\%$ depth of the ice sheet. Below this depth high vertical resolutions are required to maintain a chronology deviating by less than 5% from the analytical solution. Computational cost is the main concern limiting the available number of vertical layers ($n \leq 100$). Taking into account the various unknowns in climate forcings when it comes to transient simulations of the Antarctic or Greenland ice sheet, a tracer age accuracy of 95% relative to the analytical solution throughout the ice sheet in an idealized setup should be more than sufficient. To compare simulated chronologies to ice core data, transient simulations of ice sheet dynamics are necessary to reproduce realistic ice flow patterns.

In a first step, tracers are tested in sensitivity studies of the AIS in which crucial flow parameters and boundary conditions are tuned to yield an equilibrium ice sheet comparable to the present day

configuration. First results (see chapter 8) show a strong dependence of ice ages on basal shelf dynamics, sea level and surface mass balance. Following the validation of the tracer routine RIMTRACE, the next steps include the transient simulation of ice core chronologies in glacial-interglacial model runs. Comparing the results acquired in this fashion to ice core data, will provide an important constraint to the ISM model results. Fitting the ISM output to match the observed ice core chronologies will hopefully help in assessing past ice sheet geometries. The results from test runs of the Eulerian and Lagrangian advection methods, show that the Lagrangian scheme yields more accurate results and includes the advantage of backtracking tracers to their point of origin. However both schemes will be further improved. An additional implementation and comparison to the Semi-Lagrangian tracer scheme, as discussed in [Goelles et al., 2014] would complement the efforts to shed light on the polar climate archives. The last step in the puzzle will be the implementation of the RIMBAY-TRACE ISM into the coupled climate model COSMOS [Stepanek and Lohmann, 2012] including a complete isotope cycle which would provide the first fully coupled model assessment of the isotope and age distribution of the polar ice sheets (see discussion in chapter 8).

Last Interglacial Antarctic Ice Sheet Dynamics

3.1 Last Interglacial West Antarctic Ice Sheet Collapse

¹The WAIS is considered the major contributor to global sea level rise in the LIG. Proxy data from exposed fossil reef terraces suggest sea levels in excess of 7m in the last warm era, of which not much more than 2m are considered to originate from melting of the Greenland Ice Sheet. The results presented here mark the first time a comprehensive data-driven modeling study has reproduced a sea level contribution required to fill this gap. The evolution of the AIS is simulated during the LIG with a continental scale 3D thermomechanical ice sheet model forced by COSMOS (see chapter 2 and 11). The results show that high LIG sea levels, as derived from proxy data, cannot be reproduced with the atmosphere-ocean forcing delivered by COSMOS. Sensitivity studies show that a Southern Ocean temperature anomaly threshold for total WAIS collapse of 2 – 3°C is found, accounting for a sea level rise of 3 – 4m during the LIG, while the EAIS remains mostly stable. A nonlinear two-stage WAIS retreat imprinted in two distinctive peaks of sea level rise during the interglacial is evident in the simulations. Furthermore, the findings indicate that spatial variations in surface mass balance anomalies strongly modulate AIS dynamics and can both accelerate or prevent WAIS collapse.

3.1.1 Setting the Stage

The LIG climate at about 125kyrs BP is considered to be warmer than most of the Holocene and a time with considerably smaller ice sheets than today. Proxy evidence suggests global sea levels about 7m higher than present day [Kopp et al., 2013, Dutton et al., 2015] of which only ca. 3m are covered by contributions from ocean thermal expansion [McKay et al., 2011], land-based glaciers (both 0.5m) [Marzeion et al., 2012] and melting of the Greenland Ice Sheet (2m) [Dahl-Jensen et al., 2013]. The remaining 4m missing in the sea level rise budget must therefore derive from a mass loss from the AIS. Observations and modeling studies of the EAIS present a mixed picture of potential growth [Harig and Simons, 2015] or partial collapse unfolding over several millennia [Mengel and Levermann, 2014]. The

¹This chapter is partly based on the Publication *Ocean temperature thresholds for Last Interglacial West Antarctic Ice Sheet collapse* [Sutter et al., 2015a] by **Sutter, J.**, Gierz P., Grosfeld, K., Thoma, M., and Lohmann, G..

marine sections of the WAIS have the potential to raise global sea level by more than 3m [Bamber et al., 2009] and are the likely suspects for LIG sea level contribution. They are prone to the MISI [Schoof, 2007] potentially triggered by warming of surface [Mercer, 1978] and ocean temperatures [Joughin and Alley, 2011]. It has been pointed out that WAIS collapse could be initiated by increased melting at the base of the ice shelves, which buttress their tributary glaciers and exert a backpressure force on the ice streams and outlet glaciers of the hinterland [Scambos et al., 2004]. A reduction of this buttressing effect caused by ice shelf retreat would lead to an acceleration of the glaciers, draining more and more ice into the ocean. Further a grounding line situated on inland downward sloping bedrock is inherently unstable [Schoof, 2007], thus an initial grounding line retreat, caused by increased basal melting underneath the ice shelves, could push the WAIS into a configuration where a runaway retreat due to the MISI is triggered. Recent observations indicate that such processes are already underway in the Amundsen Sea sector [Rignot et al., 2014, Joughin et al., 2014]. Observations and modeling studies show melt rates in excess of several tens of meters per year underneath the ice shelves in this region during the last decades [Jacobs et al., 2011]. In addition, analyses of boreholes drilled through Whillans Ice Stream (Ice Stream B) at the Siple Coast (see chapter 11 Figure 11.8) have found marine diatoms indicative of an open marine environment in the Ross embayment in the late Pleistocene [Scherer et al., 1998] (probably during marine isotope stage 11 (MIS11)). Warming of Southern Ocean temperatures could have lead to a complete or partial WAIS collapse during the LIG as well, which would explain the high sea levels found in reconstructions.

3.2 Experimental Setup

In this study, the dynamic behavior of the AIS is simulated in transient model simulations, spanning the LIG utilizing a continental scale 3-Dimensional ISM (RIMBAY [Thoma et al., 2014]). All simulations are carried out on a 40x40km regular grid with 41 vertical sigma layers, covering the whole AIS. The coarse resolution was chosen to allow for extensive exploration of the parameter space spanned by the basal friction and shelf melt rate coefficient. Since subgrid grounding line positions are resolved with a simple interpolation scheme, sufficient model sensitivity to the applied climate forcing is validated by a "control" simulation. This is done, adopting the basal melt rate parameterization applied in Pollard & DeConto (2009) [Pollard and DeConto, 2009]. In this test comparable grounding line migration in an "extreme interglacial" setting are simulated (see chapter 11 Figure 11.9). This gives confidence that sheet-shelf dynamics are comparably resolved on long time scales, coarse resolution and lack of a more sophisticated grounding line treatment notwithstanding. Basal melt rates underneath the shelf are simulated based on the method described by Beckmann & Goosse [Beckmann and Goosse, 2003] and match the total Antarctic shelf melt rate for present day conditions [Depoorter et al., 2013]. To capture the complex interactions and nonlinearities in the climate system the ISM is forced with climate time slice output of an AOGCM (COSMOS [Lunt et al., 2013, Pfeiffer and Lohmann, 2015] for the LIG (for a more detailed overview of the methods see chapters 2 & 11). Transient forcing is realized by interpolating between the LIG climate time slice and present day climate with the glacial index method where the glacial index is derived from Dome C deuterium depletion [Jouzel et al., 2007, Stenni et al., 2010] (Figure 3.1 and chapter 11 Figure 11.7). Deuterium depletion measured in ice cores is widely used as a proxy for local

past temperature changes [Jouzel et al., 1997]. The temperature variations recorded in an ice core can be used to reconstruct the long-term climate variations in the region. The climate forcing at any given time during the simulations is calculated (here shown with surface temperature) as

$$T_{surf}^{i,j}(t) = T_{surf}^{i,j}(LIG) \cdot \frac{\delta(t) - \delta_{PD}}{1 - \delta_{PD}} + T_{surf}^{i,j}(PD) \cdot \frac{1 - \delta(t)}{1 - \delta_{PD}} \quad (3.1)$$

where $T^{i,j}$ denotes the temperature at node i, j ; $\delta(t)$ the normalized Deuterium value at time t ; and $\delta_{(PD)}$ the normalized present day mean Deuterium value. Experiments E and Eg (see Appendix) depict the two different LIG climatologies simulated with COSMOS which exhibit significant differences in accumulation (E slight reduction, Eg 20% increase) and Southern Ocean subsurface temperatures (E slight cooling, Eg $\sim 0.5^\circ\text{C}$ warming, see Figures 11.5 and 11.6). Using this forcing, transient RIMBAY simulations from 131.5 to 118kyrs BP are carried out. Antarctic sea level contribution is calculated by accounting for the water equivalent volume above floatation for marine ice sheets and the volume changes of the ice sheets grounded above sea level via the formula

$$\frac{V_{afb}^0 - V_{afb}^f}{A_O} = SLE \text{ (m)} \quad (3.2)$$

where V_{afb}^0 is the initial and V_{afb}^f is the final volume above floatation, while A_O is the global ocean area. The effect of bedrock relaxation due to reduced ice loads is accounted for.

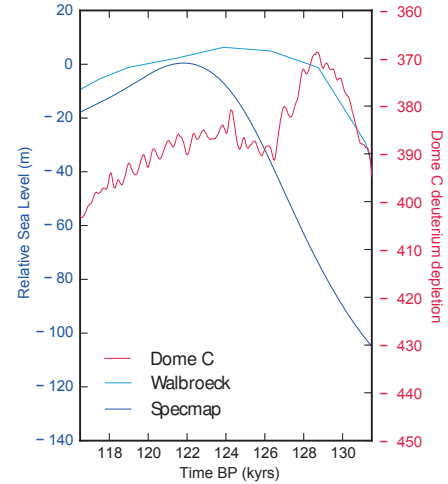


Figure 3.1: Dome C Deuterium depletion and sea level reconstructions for the LIG. The sea level forcing used in this thesis is based on [Walbroeck et al., 2002].

3.3 Stable West Antarctic Ice Sheet under COSMOS Forcing

In the associated transient experiments (denoted as E0 and Eg0), the ice dynamics and mass balance are not significantly affected compared to the control run (Figure 3.2, blue and green lines). While the subsurface Southern Ocean warming is considerable in Eg, which might be caused by a weakened Atlantic Meridional Overturning Circulation (AMOC) due to freshwater perturbations from Greenland meltwater [Gierz et al., 2015] and a subsequent warming of the Southern Ocean by means of the bipolar seesaw effect [Barker et al., 2011], it is not sufficient to trigger any destabilization of WAIS. An increased surface mass balance in Eg even leads to an overall increase of Antarctic ice volume and a sea level drop by about 0.5m at mid-interglacial (Figure 3.2 b). Comparison to proxy data [Capron et al., 2014, Rosenthal et al., 2013] of LIG ocean temperature anomalies indicates that the AOGCM underestimates Southern Ocean temperature anomalies by several degrees. Proxy and climate modeling evidence suggests

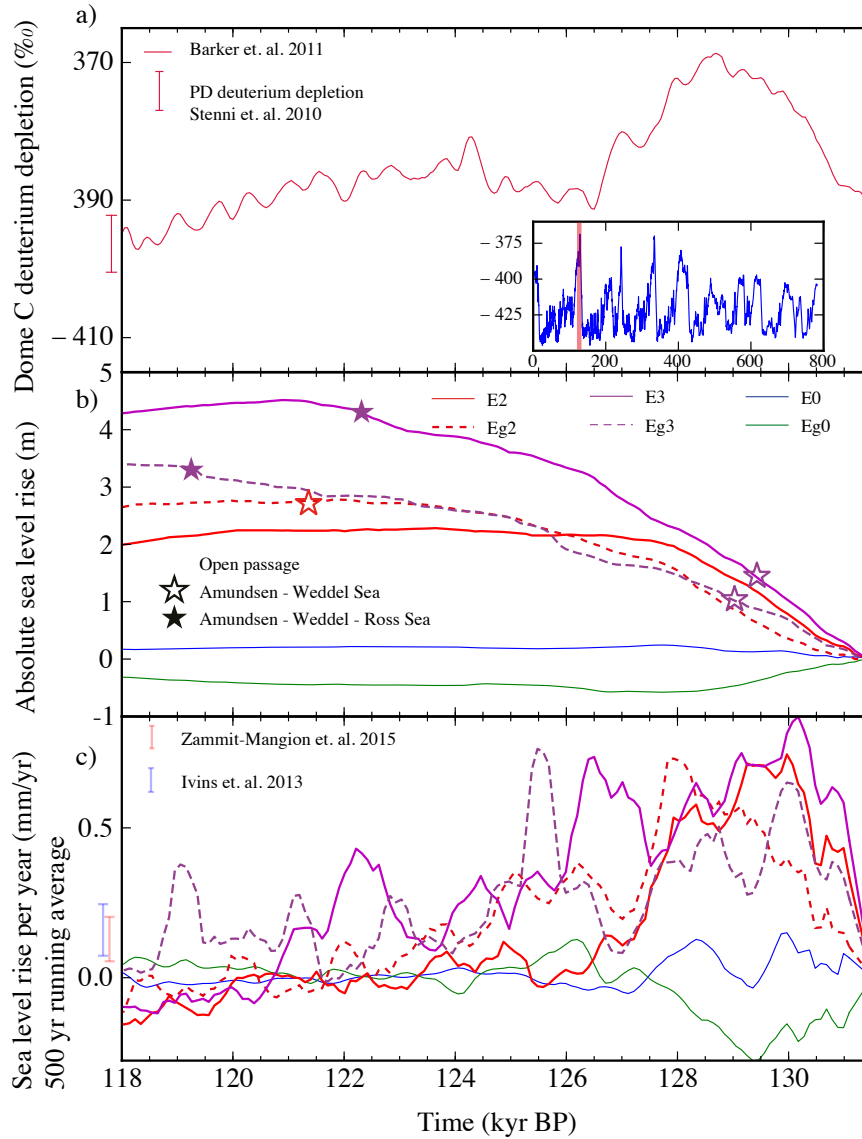


Figure 3.2: a) Shows Deuterium depletion from Dome C ice core [Jouzel et al., 2007]. The inlay shows the complete record (with the highlighted section marking the LIG, time axis in kyr). The present day mean deuterium depletion at the ice core site [Stenni et al., 2010] is depicted by the red bar next to the graph. Please note that the time axis runs from right (past) to left (present). b) Simulated Antarctic contribution to sea level rise. Simulations with 2 and 3 °C Southern Ocean temperature anomalies are shown (results for 1°C not shown here, see chapter 11, Figure 11.10 and 11.13). The stars indicate the points in time at which partial (open) or complete (filled) WAIS collapse is reached. c) shows the corresponding sea level rise rates in mm/yr (500 year running mean). The two bars next to the graph depict observed present day Antarctic sea level contributions. Complete collapse is modelled in E3 and Eg3. Partial collapse is already reached at 2 °C ocean warming for scenario Eg2.

an intensification of the hydrological cycle accompanying climate warming, carrying more humidity to the AIS [Frieler et al., 2015], hence increasing the snowfall over the continent. Such an intensification (resembled in experiment Eg) would increase the ice volume and lower the sea level. The moderate increases in surface temperatures preclude a major effect of surface melting or fabric softening of the ice matrix which would lead to faster ice flow and discharge into the ocean. This line of reasoning leaves only Southern Ocean warming as the most probable candidate for triggering the MISI in the LIG.

3.4 Ocean Temperature Thresholds for West Antarctic Ice Sheet Collapse

In order to analyze the full sensitivity range of the WAIS during the LIG, uniform ocean temperature anomalies of $1 - 3^{\circ}\text{C}$ (compared to present day observations) are applied, combined with the surface climate of E and Eg. The corresponding transient experiments are denoted as E1, E2, E3, Eg1, Eg2, Eg3 and are shown in Figure 3.2b, c. The results suggest a temperature threshold for a complete decay of the WAIS between $2 - 3^{\circ}\text{C}$, which is within a conceivable range of estimated Southern Ocean temperature anomalies derived from proxy data [Capron et al., 2014, Rosenthal et al., 2013]. WAIS collapse manifests in a nonlinear fashion, initialized by a complete melt of the major ice shelves in the Ross and Weddell Seas (taking about 500 years, see e.g. Figures 11.11–11.15 in chapter 11). Due to the loss of buttressing and sustained melting close to the grounding line, the ice shelves tributary glaciers draining central West Antarctica accelerate and discharge increasing amounts of grounded ice into the sea. Thinning of the coastal ice sheet leads to floatation and subsequent grounding line retreat (Figure 3.3a). This results in rates of sea level rise in excess of $\frac{1\text{mm}}{\text{a}}$ averaged over 100 years (Figure 3.2c), a multifold increase compared with present day contributions of the AIS [Zammit-Mangion et al., 2015, Ivins et al., 2013]. This high sea level rise is sustained until ca. 129kyrs BP (E3 and Eg3) (Figure 3.2c) and is followed by a slowdown of ice loss-rate, owing to the large remaining ice dome centered at the WAIS divide. At this point, an open sea passage between the Weddell Sea and Amundsen Sea has been established (Figure 3.3a and 11.12-11.15). Driven by large surface topography gradients, surface velocities of the remaining ice dome increase, leading to thinning and the conversion of grounded ice into ice shelves. As the grounding line retreats towards the steep reverse bedrock slopes of the Byrd subglacial basin (Figure 3.3a and 11.8), the ice sheet approaches yet another unstable configuration. Warm waters entering from the Amundsen Sea intrude into the opening ocean gateway, melting the newly formed ice shelf, thereby accelerating the second phase of ice loss and grounding line retreat which again culminates in sea level rise of up to $\frac{1\text{mm}}{\text{a}}$ in E3 and Eg3 around 126.5 and 125.5kyrs BP respectively (Figure 3.2c).

3.4.1 Twin Peak Sea Level Rise

The characteristic evolution of WAIS surface elevation in the LIG, controlled by a combination of the MISI, warm sub-surface ocean temperatures and variations in surface accumulation, leads to a distinctive double peak in sea level rise contribution of the WAIS (Figure 3.2c). A potential subsurface ocean-temperature-cooling episode flanked by increases in the surface mass balance, might lead to some recovery

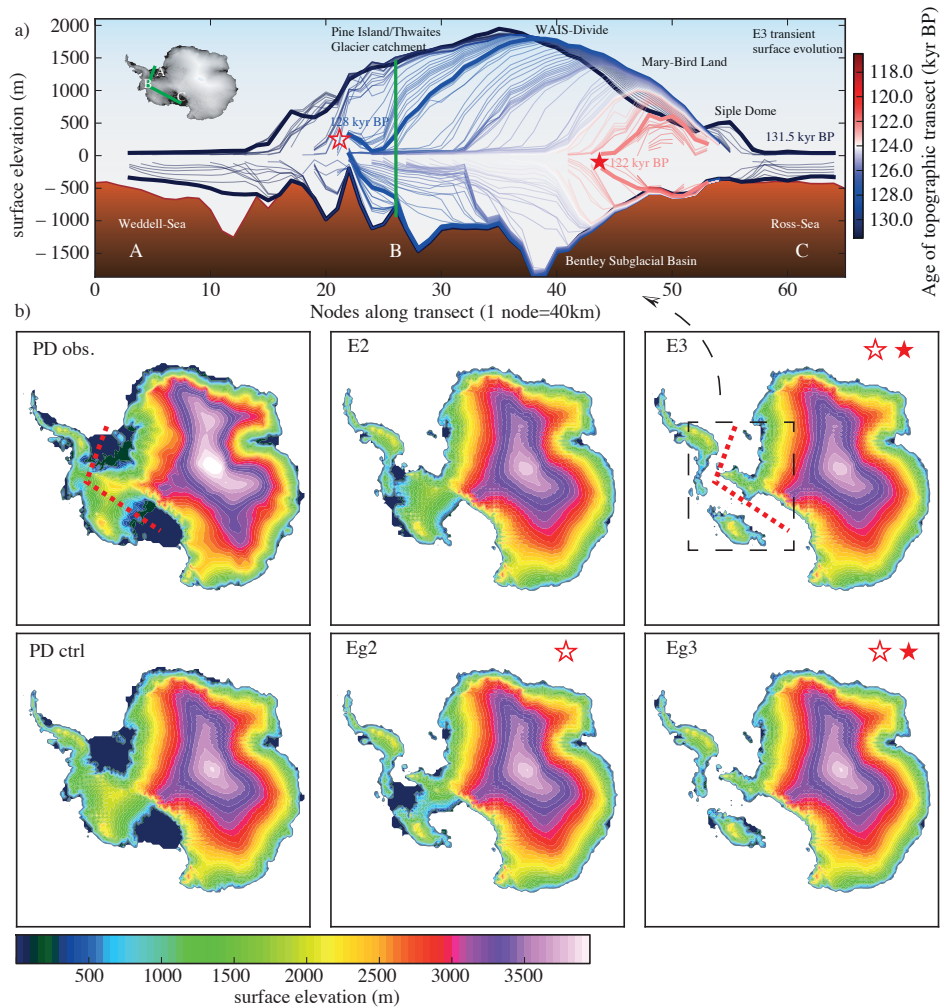


Figure 3.3: Transect across the West Antarctic Ice Sheet (WAIS) showing the transient evolution of the surface topography during the simulation E3. Each transect line illustrates a snapshot during the LIG (one snapshot every 100 years). Several semi-stable grounding line positions are visible around inland ascending bedrock slopes. Thick transect lines depict the time at which partial or complete collapse of WAIS is reached, defined by the opening of ocean gateways between the Weddell and Amundsen Sea and subsequently the Ross Sea (identified as in Figure 3.2 b) by stars). Inlay shows transect location from the Weddell Sea (a) to the Ross Sea (b). b) Surface topographies at the end of each simulation (PD observations, E2 ocean anomaly, E3, PD ctrl, Eg2, Eg3). Dark blue areas depict ice shelves. The transect from (a) is again depicted by the red dashed line in the first and third surface topography box (PD observations and E3).

in ice volume between the two stages of collapse shown in the simulations. This process could have played a role in the previously suggested double peak in LIG sea level high stand [Kopp et al., 2013] (Northern Hemisphere ice sheet evolution might exacerbate this effect).

3.4.2 Further Climatological Driving Forces

Driven by ocean temperature warming, the collapse of WAIS is strongly modulated by the surface mass balance. This is reflected in differences of sea level rise of more than 1m between simulations E3 and Eg3 (Figure 3.2b). The higher surface mass balance in Eg3 leads to a reduction of sea level rise. On the other hand, the increased accumulation in Eg can lead to higher surface gradients, favoring faster ice discharge [Winkelmann et al., 2012]. In the case of Eg2, this leads to a partial collapse of the WAIS and 0.5m higher sea level compared with E2. A retreat of the WAIS as simulated in this study, leads to the opening of large open areas of water which would increase ocean surface temperatures due to absorption of solar radiation. Atmospheric cooling due to changes in the cyclonic circulation [Steig et al., 2015] could dampen this warming. Additionally, the seasonal cycle of sea ice in the newly formed West Antarctic ocean ranges would influence ocean circulation. However, such atmospheric and ocean feedback effects induced by dramatic changes in the ice geometry cannot be captured as yet. Fully coupled Atmosphere-Ice-Ocean GCMs are not available at this stage.

3.5 Reconciling LIG Sea Level Highstand

In summary, our simulations show that in the LIG as well as in the future, strong sub-surface Southern Ocean warming is the critical parameter leading to destabilization of the WAIS. Melting at the base of Antarctic ice shelves is largely driven by intrusion of modified circumpolar deep water, which enters the shelf cavity along deep bathymetric channels [Schmidtko et al., 2014]: a process just recently simulated in high-resolution ocean models [Hellmer et al., 2012]. Our results call for the representation of these bathymetric warm water pathways in future large-scale AGCM climate models coupled to ice sheet dynamics. This study shows, that a Southern Ocean temperature regime corresponding to the extreme end of paleo-reconstructions in the LIG could have pushed the WAIS into a configuration, where the MISI instability and runaway retreat is triggered, reconciling a LIG sea-level highstand of around 7m, in consequence of the melting of ice masses in Greenland and Antarctica.

Future Antarctic Dynamics

¹A prominent difference between the climate in the LIG and projected future warming is the faster projected warming rate of the ocean and atmosphere. To assess the future evolution of the AIS the methodology applied in the LIG case is now employed in idealized future scenarios based on the warming projections of the IPCC ([Stocker et al., 2013], similar to [Golledge et al., 2015]). A simple warming ramp peaking at a uniform 2 or 3°C warming of the Southern Ocean within 200 years is assumed. This is accompanied by an atmospheric surface temperature warming of 6°C, together with an increase in accumulation between 10 and 40%. This corresponds to the range covering estimates of future precipitation changes shown in Figure 4.1 [Frieler et al., 2015]) relative to the present day. A rapid warming on this scale triggers an accelerated retreat of the WAIS, gradually raising eustatic sea level up to 1 and 2m within 3000 years and up to 4m within the next 5000 years (Figure 4.3). This sea level rise surpasses the potential contribution of WAIS, and implicates an increased discharge from central Antarctica. In the first couple of centuries, the Antarctic ice shelves would disintegrate, paving the way for a large scale retreat of the WAIS, which would gain momentum by ca. 2400 CE. The initial acceleration of sea level rise stabilizes at a constant contribution of ca. 1 – 1.5mm/yr (10 – 15 cm/century) over the next millennia (Figure 4.3). To investigate the stability of the WAIS in a hypothetical extreme warming scenario in which the Antarctic ice shelves collapse within a century, the FRIS and RS are subjected to a strong negative mass balance (prescribed by a melting rate underneath the shelves of ca. $40\frac{\text{m}}{\text{a}}$), thereby mimicking the modeling set-up applied by [Pollard et al., 2015] or the extreme forcings prescribed in [Winkelmann et al., 2015]. This setting culminates in ice shelf disintegration within several decades and leads to the total collapse of the WAIS within this millennium. In consequence, a sea level rise in excess of 0,5m per century leading to a long-term rise of sea level of larger than 6m accompanies the antarctic contribution in such scenario (Figure 4.3).

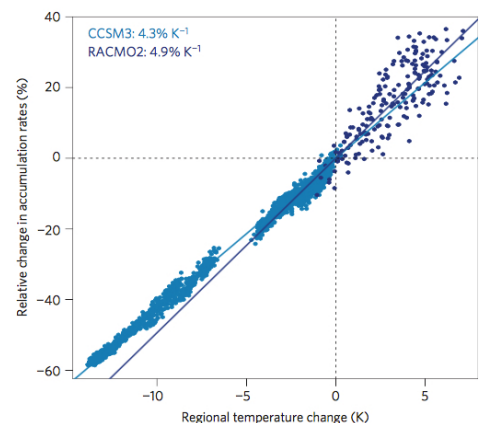


Figure 4.1: Projected future precipitation changes with temperature derived from regional climate simulations (CCSM3 and RACMO2). The precipitation-temperature relationship derived from ice cores is slightly larger (from [Frieler et al., 2015]).

¹This chapter is partly based on the Publication *Ocean temperature thresholds for Last Interglacial West Antarctic Ice Sheet collapse* [Sutter et al., 2015a] by **Sutter, J.**, Gierz P., Grosfeld, K., Thoma, M., and Lohmann, G..

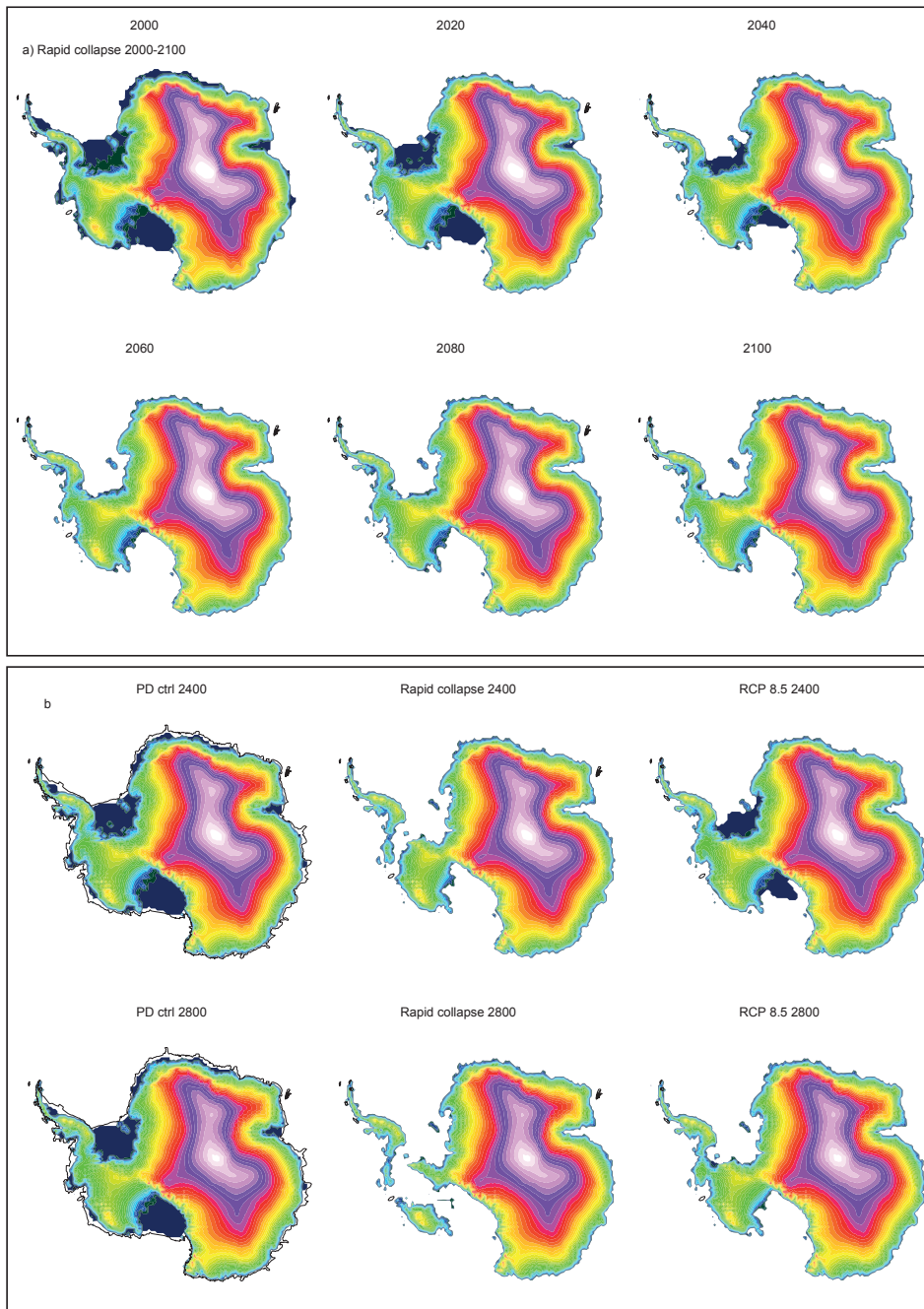


Figure 4.2: Surface elevation of the Antarctic Ice sheet in different scenarios in the year 2400 and 2800. a) Disintegration of the Antarctic ice shelves within this century in an extreme scenario. b) snapshots of the Antarctic surface elevation in the years 2400 and 2800 for the extreme warming and "RCP-8.5-like" 3°_10% scenarios. The PD control run is included for comparison.

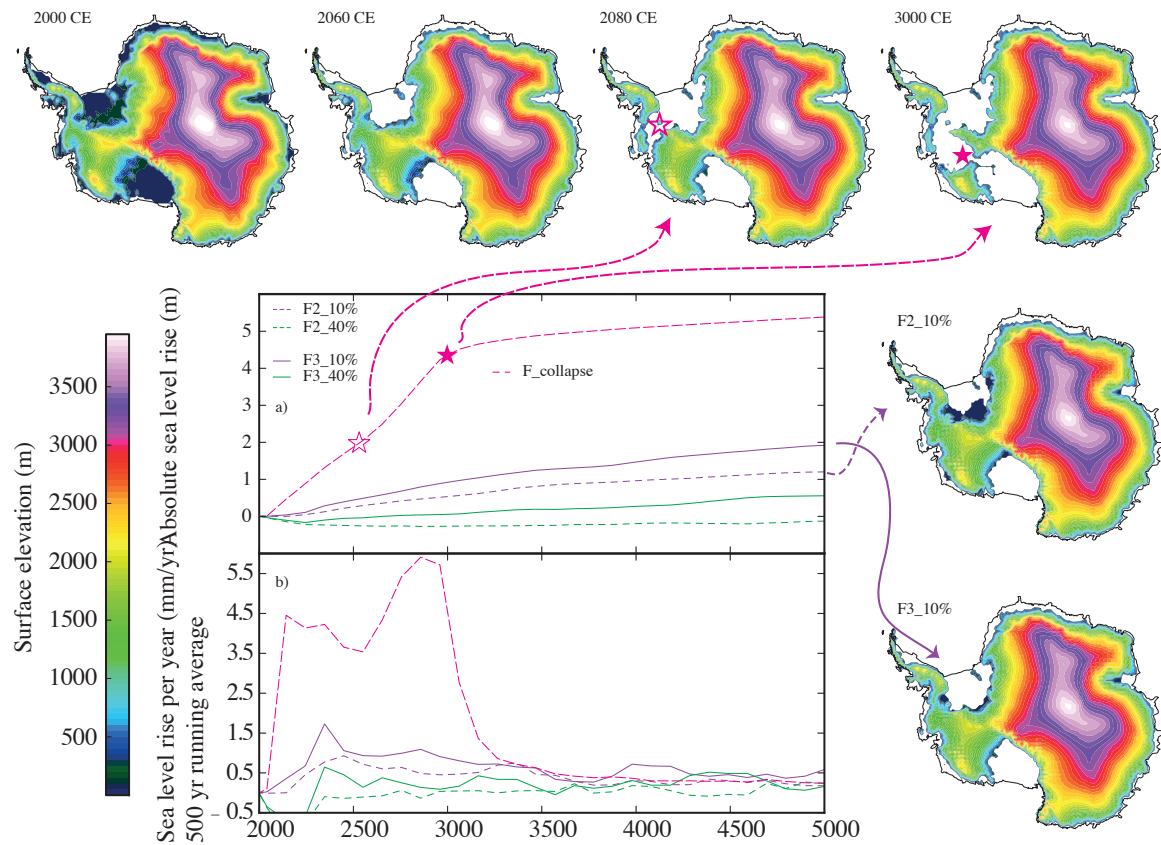


Figure 4.3: WAIS evolution in our idealized future warming scenarios. All simulations follow a 200 years warming ramp initiated in the year 2000 (a). Peak warming is reached in the year 2200 (e.g. $+2^\circ$ ocean warming, $+6^\circ\text{C}$ SAT and 10 % precipitation increase (denoted by $2^\circ_{10\%}$). In the simulation F_{collapse} high melt rates are prescribed, in order to disintegrate all ice shelves within the next century (the stars identify the timing of partial and complete WAIS collapse. b) Corresponding sea level rise per year for above simulations. The upper horizontal row depicts the evolution of the surface topography for the rapid ice shelf collapse scenario. The vertical row maps the ice sheet topography after 1kyr for Experiments $2^\circ_{10\%}$ and $3^\circ_{10\%}$. The black line in the surface elevation maps approximates the present day extent of the AIS.

The coarse resolution applied in our modeling setup prevents an adequate representation of the Marine Ice Sheet in Wilkes Land (East Antarctica)², which has been shown to be prone to the MISI triggered by sustained ice shelf melting in previous studies [Fogwill et al., 2014, Mengel and Levermann, 2014] and would raise global sea level by an additional 3 – 4m if completely collapsed. The vision of a rapid WAIS collapse within this millennium is at the far end of conceivable future WAIS dynamics, being only triggered in drastic warming scenarios, e.g. a mean 10°C surface warming would be required to lift mean annual surface temperatures at the FRIS and RS above the viability limit for ice shelves [Vaughan and Doake, 1996]). The relatively slow retreat of the AIS shown in the "IPCC"-based simulations presented here (2°_10% to 3°_40%) shows a gradual grounding line retreat in West Antarctica rather than a rapid collapse as also proposed by the study of[Ritz et al., 2015] (see Figure 4.4).

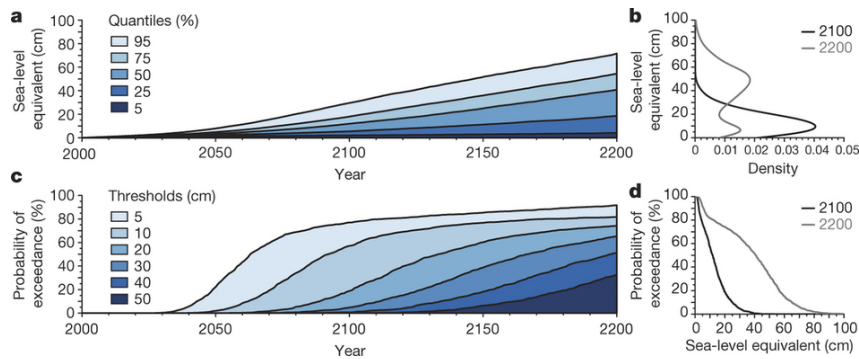


Figure 4.4: Probabilistic estimates of future Antarctic Ice Sheet sea level contribution until the year 2200 (from [Ritz et al., 2015]).

Nonetheless, [Golledge et al., 2015] show a much faster collapse of the WAIS, potentially unfolding during the next centuries (upper limit in Figure 4.5), using higher spatial resolutions of 10 – 20km versus 40km in this study. This allows for better resolved small outlet glaciers and marine-based ice sheets, such as in the Wilkes Basin (EAIS), which explains the overall higher sea levels. Unfortunately, melt rates are not given in their publication, thus, a straight comparison of the shelf mass balances is not possible. Further, the ISM used by [Golledge et al., 2015] is known to have a shelf melt parameterization which is more sensitive to ocean temperature changes [de Boer et al., 2015]. Figure 4.5 shows the estimates of future Antarctic sea level contribution from [Golledge et al., 2015].

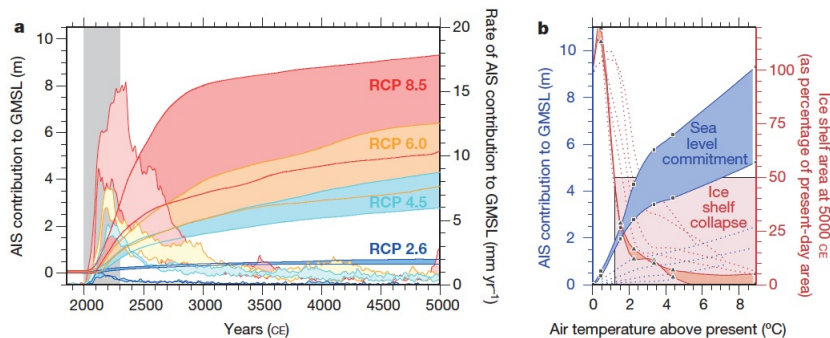


Figure 4.5: Projections of future Antarctic Ice Sheet sea level contribution depending on "ICPP-like" scenarios (from [Golledge et al., 2015]).

²The ice shelf cavities fringing the Wilkes Land are too small to be accurately resolved with a 40km spatial resolution.

The suite of recent ISM studies [Ritz et al., 2015, Golledge et al., 2015, Winkelmann et al., 2015, Sutter et al., 2015a, Feldmann and Levermann, 2015] and current observational evidence [Rignot et al., 2014, Joughin et al., 2014] provide ample evidence that the WAIS will be, or already is destabilized by the prevailing warming trend affecting Antarctica. However, both, observational data and modeling studies still contain considerable uncertainties. Mass balance observations for the AIS partly contradict each other depending on the applied methodology [Zwally et al., 2015]. Further, bedrock properties are largely unknown and ice shelf processes poorly resolved in ISMs, limiting the accuracy of AIS dynamics in ISM projections. The future evolution of the AIS hinges on both, the amplitude and the rate of ocean and surface warming, thereby leaving a large event horizon between rapid collapse and moderate retreat [Ritz et al., 2015, Winkelmann et al., 2015, Golledge et al., 2015, Sutter et al., 2015a].

Constraining Antarctic Ice Sheet Volume in the Late-Pliocene

¹The Pliocene warm period approximately 3 million year ago is yet another potential analogue for future global climate evolution. In this chapter the main findings of the Pliocene Ice Sheet Modeling Intercomparison Project, or short PLISMIP, are summarized. As laid out in chapter 3 (WAIS collapse in the LIG) the future evolution and potential instability of the AIS might have analogues in the past. There, the implications from ice sheet modeling results centered in the LIG as well as in the future are discussed. Here, the main findings of an international ice sheet model intercomparison project [de Boer et al., 2015] are presented. A suite of modeling efforts and proxy based climate reconstructions estimates a mean global temperature increase in the Mid-Pliocene at around 2 – 4°C ([Haywood et al., 2011, Dowsett et al., 2011, Dowsett et al., 2013, Haywood et al., 2013, Salzmann et al., 2013]), similar to the warming which is expected until the end of the 21st century. Sea level was about 10 – 30m above PD levels ([Raymo et al., 2011, Rohling et al., 2014]) with a maximum Greenland Ice Sheet contribution of around 7m. This puts the AIS contribution at 3 – 23m, a staggering range. Assuming the lower limit, the sea level could have solely originated from the Antarctic soft spot, the WAIS (see chapter 3). A larger contribution to sea level is only possible if the EAIS significantly retreated from its present day configuration. The collection of sea level proxy reconstructions (if conclusive) point to a definite collapse of the WAIS and probably a considerable retreat of parts of the EAIS, e.g. the marine ice sheets of Wilkes Land ([Mengel and Levermann, 2014]).

5.1 Experimental Boundary Conditions and Participating Ice Sheet Models

The PlioMIP model results ([Haywood et al., 2013], see middle column in Figure 5.1) differ substantially but all seem to largely agree that a significant polar amplification occurred over the Antarctic region in the Pliocene ([de Boer et al., 2015]). For the setup used in this study the AOGCM climate forcing

¹This chapter is based on the Publication *Simulating the Antarctic ice sheet in the late-Pliocene warm period: PLISMIP-ANT, an ice-sheet model intercomparison project* [de Boer et al., 2015] by de Boer, B., Dolan, A. M., Bernales, J., Gasson, E., Goelzer, H., Golleger, N. R., **Sutter, J.**, Huybrechts, P., Lohmann, G., Rogozhina, I., Abe-Ouchi, A., Saito, F., van de Wal, R. S. W..

Table 5.1: Overview of the PLISMIP-ANT experiments following [Dolan et al., 2012]. The simulations are structured in two phases, phase one consisting of the present day control experiments using the climatology from HadCM3 and ERA-40. The Pliocene experiments are derived from HadCM3 with PRISM3 boundary conditions (from [de Boer et al., 2015]).

Phase	Climate input		Initial ice sheet
	Atmosphere	Ocean	
Control _{HadCM3}	PI HadCM3	PI HadCM3	Bedmap1 or 2
Control _{Obs}	ERA-40	WOD-09	Bedmap1 or 2
Pliocene _{Ice-PD}	Plioc. HadCM3	Plioc. HadCM3	Bedmap1 or 2
Pliocene _{Ice-PRISM3}	Plioc. HadCM3	Plioc. HadCM3	PRISM3
Pliocene _{PD-Ant}	Plioc. HadAM3 with modern Ant.	Plioc HadCM3	Control _{HadCM3}

from PlioMIP (HadCM3) was employed. It has been used extensively within Pliocene climate modeling [Haywood and Valdes, 2004] and shows average climate conditions which range in the mean of a large model ensemble. For comparison the AOGCM used in the other studies presented within this thesis exhibits comparable, but slightly warmer late Pliocene climate conditions [Stepanek and Lohmann, 2012].

As in the PD control simulations presented in chapter 2 the applied PD ocean forcing is derived from the World Ocean Database 2009 ([Locarnini et al., 2010]). The atmospheric forcing for the control simulations (observational vs AOGCM forcing) is derived from the mean climatology in ERA-40 [Uppala et al., 2005] and HadCM3 [de Boer et al., 2015, Bragg et al., 2012]. The ERA-40 forcing is warmer (around 4°) over the continent and a bit wetter ($0.2-0.5 \text{ m yr}^{-1}$) over coastal areas. The largest differences occur over the interior of East Antarctica (where ERA-40 shows accumulation up to a factor 5 lower) which is the largest catchment for surface accumulation and therefore has a significant impact on the ISM reconstructions of the AIS.

The Pliocene (HadCM3) simulations utilize the PRISM3 boundary conditions for AIS elevation and a $p\text{CO}_2$ of 405ppm. Figure 5.2 illustrates the climate forcings of the two PD ctrl simulations (HadCM3 and ERA-40) and the Pliocene climate (HadCM3). Primarily due to the lower ice sheet elevation over Antarctica the surface temperature over the continent is about 7°C warmer compared to pre-industrial climate. The region of the Wilkes and Aurora basins are influenced by considerable higher precipitation rates of $0.4 - 0.6 \frac{\text{m}}{\text{a}}$. Subsurface ocean temperatures show a large ocean temperature warming of about $\sim 2.6^\circ\text{C}$ underneath the ice shelves which is in the temperature range triggering a collapse of the WAIS in the LIG for the ice sheet model used in this thesis (see chapter 3). The influence of a reduced AIS in the Pliocene (PRISM3) is investigated by carrying out an additional Pliocene control simulation with present day AIS boundary conditions (Pliocene_{Ice-PD}). The general ice sheet model settings (bedrock, geothermal heat flux, resolution) are the same as discussed in chapter 2, equilibrium simulations are run for 100.000 years (Figure 5.7).

Table 5.2 provides an overview of the technical details of the ISMs applied in this intercomparison project. All ISMs use a combination of the shallow-ice and shallow-shelf approximation. The general features of the ice sheet models are very similar except for the treatment of grounding line dynamics and the calculation

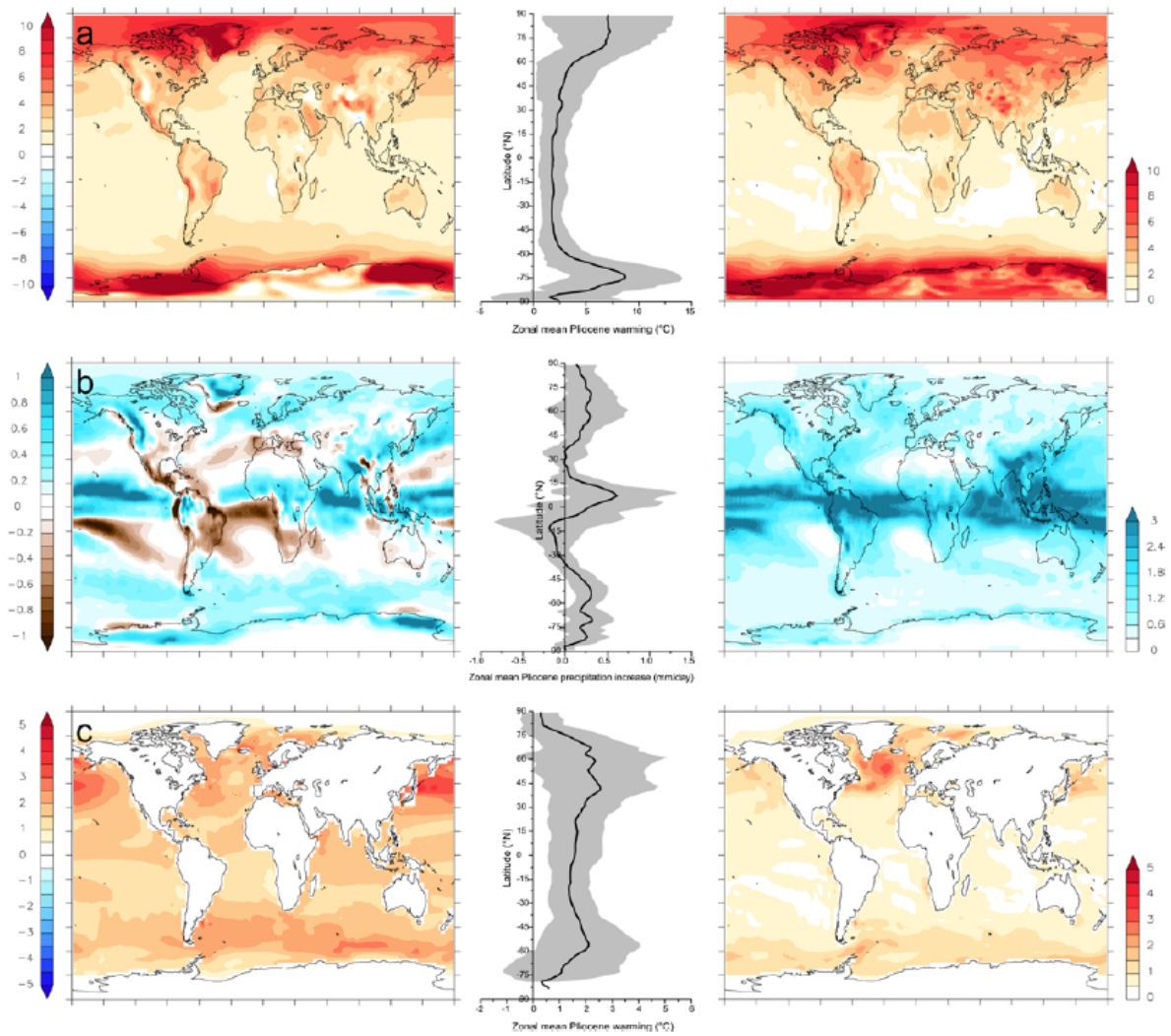


Figure 5.1: Ensemble results from PlioMIP [Haywood et al., 2013] (multi-model means, zonal means and model 2σ from Experiment 2). a) mean annual surface temperature anomaly, b) mean annual precipitation rate, c) mean annual sea surface temperature anomaly (versus pre-industrial). The shading around the zonal mean (middle column) is the model 2σ (from [Haywood et al., 2013]).

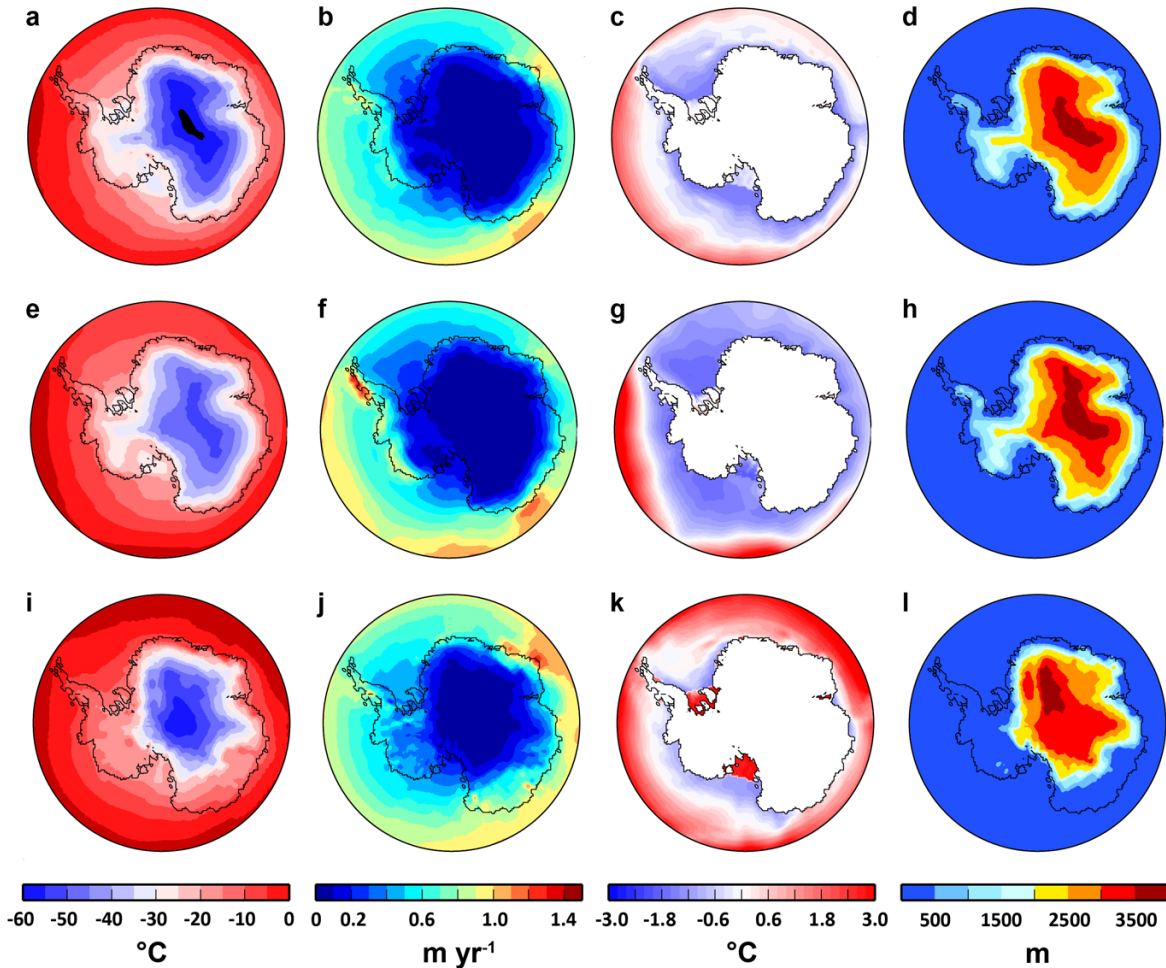


Figure 5.2: Yearly mean climatology of the three different climate forcings used in this study. The top panel shows the results of the pre-industrial Had-CM3 simulation, the middle panel represents the ERA-40 reanalysis data [Uppala et al., 2005] and Southern Ocean temperatures from the WOD-09 [Locarnini et al., 2010]. The bottom panel highlights the Pliocene Had-CM3 simulation with full PRISM-3 boundary conditions [Haywood et al., 2011]. From left to right, surface-air temperature in $^{\circ}\text{C}$, precipitation in $\frac{\text{m}}{\text{a}}$ water equivalent, sea surface temperatures at the bottom of ice shelves in $^{\circ}\text{C}$ and surface topography in the climate model in m. The black line in all panels represents the Bedmpa1 outline of the grounding line (from [de Boer et al., 2015]).

Table 5.2: Overview of the ISMs applied in this study (from [de Boer et al., 2015]).

Characteristics	Model name					
	AISM-VUB	ANICE	PISM	PSU-ISM	RIMBAY	SICOPOLIS
Numerical methods	3-D thermo-mechanic, fd SIA, SSA.	3-D thermo-mechanic, fd SIA + SSA for floating ice and sliding velocity.	3-D thermo-mechanic, fd SIA + SSA for floating ice and sliding velocity.	3-D thermo-mechanic, fd SIA, SSA	3-D thermo-mechanic, fd SIA, SSA.	3-D thermo-mechanic, fd SIA, SSA.
Treatment of the grounding line	no additional parameterisation.	no additional parameterisation.	subgrid interpolation and one-sided surface gradients.	grounding line flux boundary condition of Schoof (2007).	smoothing gradient over two grid boxes.	no additional parameterisation.
Enh. factors	$E_{SIA} = 2, E_{SSA} = 0.9$	$E_{SIA} = 5, E_{SSA} = 1$	$E_{SIA} = 2.85, E_{SSA} = 0.7$	$E_{SIA} = 1, E_{SSA} = 0.3$	$E_{SIA} = 1, E_{SSA} = 1$	$E_{SIA} = 1$ for interglacial ice and 5 for glacial ice, $E_{SSA} = 1$
Time step	1 year for SMB and Hi 20 years for Ti and Hb	Adaptive, about 0.5–2 years for SIA and Hi, 1 month for SMB, 5 years for SSA and temperature.	Adaptive, about 1–20 years for Hi, SIA and temperature	Adaptive, 2–5 years for Hi and calving, 50 years for Ti and Hb 50–100 years for SMB	3 years for Hi, velocities and temperature	1 year for SIA, SSA and Hi, 5 years for water content, age and temperature.
SMB	PDD + refreezing, PDD factors: 8 mm (C° day) ⁻¹ for ice melt 3 mm (C° day) ⁻¹ for snow melt	ITM model + refreezing. GCM precipitation field is adjusted as function of temp.	PDD 8 mm (C° day) ⁻¹ for ice melt 3 mm (C° day) ⁻¹ for snow melt	PDD 8 mm (C° day) ⁻¹ for ice melt 3 mm (C° day) ⁻¹ for snow melt	PDD 8 mm (C° day) ⁻¹ for ice melt 3 mm (C° day) ⁻¹ for snow melt	PDD + refreezing, PDD factors: 8 mm (C° day) ⁻¹ for ice melt 3 mm (C° day) ⁻¹ for snow melt
Shelf melting	BG03 heat flux as function of T_0 , vertically interpolated to ice-shelf bottom $F_{melt} = 5.2 \times 10^{-3} \text{ m s}^{-1}$ for protected and $21.8 \times 10^{-3} \text{ m s}^{-1}$ for exposed shelves.	BG03 heat flux as function of T_0 , vertically interpolated to ice-shelf bottom $F_{melt} = 2 \times 10^{-3} \text{ m s}^{-1}$, plus exposed shelf melt of 3 m yr^{-1} and open ocean melt rate of 5 m yr^{-1} .	Quadratic relationship from Holland et al. (2008) with T_{oc} at 600 m depth.	BG03 heat flux with quadratic function of T_{oc} , vertically interpolated to ice-shelf bottom $F_{melt} = 5 \times 10^{-3} \text{ m s}^{-1}$ with additional factor $K = 3$	BG03 heat flux as function of T_{oc} , vertically interpolated to ice-shelf bottom. $F_{melt} = 11 \times 10^{-3} \text{ m s}^{-1}$.	BG03 heat flux as function of T_0 , vertically interpolated to ice-shelf bottom. $F_{melt} = 5 \times 10^{-3} \text{ m s}^{-1}$ for protected, $5 \times 10^{-2} \text{ m s}^{-1}$ for exposed and $5 \times 10^{-1} \text{ m s}^{-1}$ for open ocean shelves.
Basal sliding	Weertman sliding	Mohr–Coulomb plastic law with basal stress included in SSA.	Mohr–Coulomb plastic law with basal stress included in SSA.	Weertman sliding sliding condition tuned.	Weertman sliding	Weertman sliding with sub-melt sliding.
References	Huybrechts (1990, 2002) Furst (2013)	de Boer et al. (2013)	Golledge et al. (2012) Winkelmann et al. (2011)	Pollard and DeConto (2012a) Pollard and DeConto (2012b)	Thoma et al. (2014)	Sato and Greve (2012)

of melt rates underneath the ice shelves. It has to be pointed out, that these ultimately are the main drivers of ocean induced changes in the ice sheet evolution specifically in a warming climate. This is probably the main reason for the model spread in the simulations, especially in the Pliocene simulations.

5.2 The Present Day Control Simulations

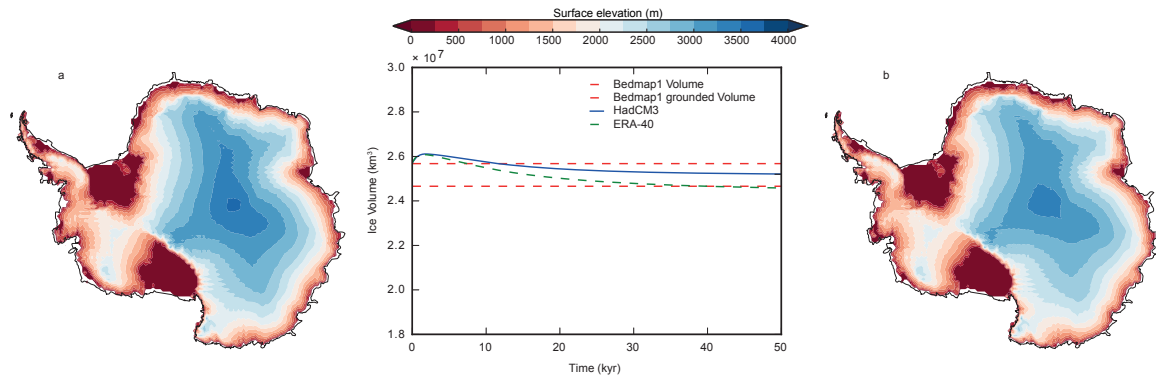


Figure 5.3: Equilibrium surface elevation in the RIMBAY Control_{HadCM3} (a) and Control_{Obs} (b) simulations. The central plot shows the volume evolution, the dashed horizontal lines depict the present day total and grounded ice volume according to Bedmap1.

Comparing the different ice sheet models, a wide spread of equilibrium ice sheet volumes is evident from the results of the present day control simulations. This is largely due to the differing initial temperature regimes and treatment of basal boundary conditions underneath the ice shelves and the grounded ice. RIMBAY, the model used in this thesis, shows the best match with the present day ice sheet volume (Figures 5.3 & 5.7). The thickness anomalies of all ice sheet models share misrepresentations compared to observations, which are common in all shallow-shelf-shallow-ice models. The EAIS is simulated slightly

lower than present day surface elevation. This is due to the coarse resolution, insufficient representation of the bedrock topography and the shallow ice approximation. The lower accumulation in Era-40 over the EAIS [Uppala et al., 2005] is imprinted in a shallower ice divide throughout East Antarctica and consequently a slightly smaller overall ice volume. Further, the different parameterizations of the basal friction are evident from the extent of surface lowering in the models. All models except for PISM exhibit an initial increase in ice volume gradually leveling off into a steady state. The origin of the different PISM behavior seems to be its specific tuning of basal friction. Figure 5.4 shows the equilibrium ice sheet elevations for the HadCM3 forced present day control run and Figure 5.5 the comparison to the reference volume derived from present day observations.

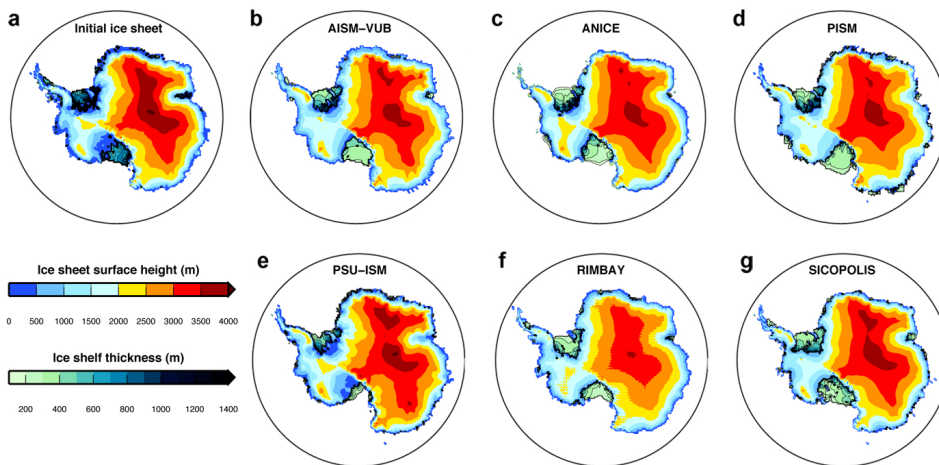


Figure 5.4: Results of the present day equilibrium control simulations for the different ISMs (from [de Boer et al., 2015]).

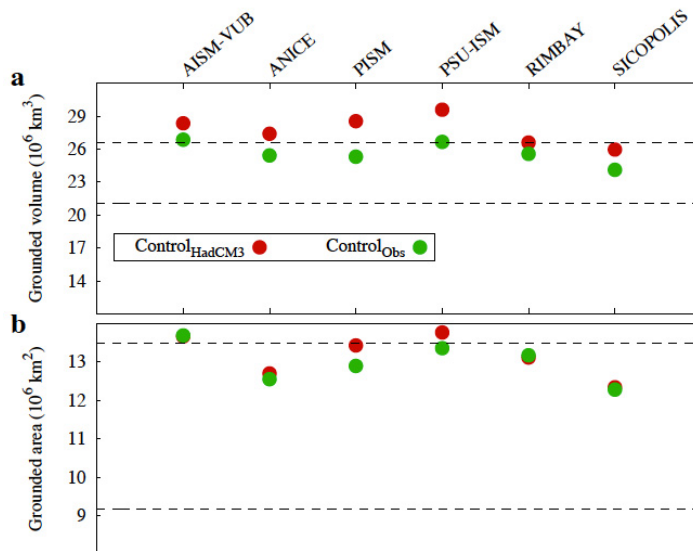


Figure 5.5: Comparison of grounded volume (relevant for the Antarctic contribution to sea level changes) and area for the different ISMs in the control simulations. The horizontal lines depicts the present day and Pliocene grounded ice volume and area of the initial ice sheet configurations (from [de Boer et al., 2015]).

5.3 Pliocene Antarctic Ice Sheet Equilibrium Simulations

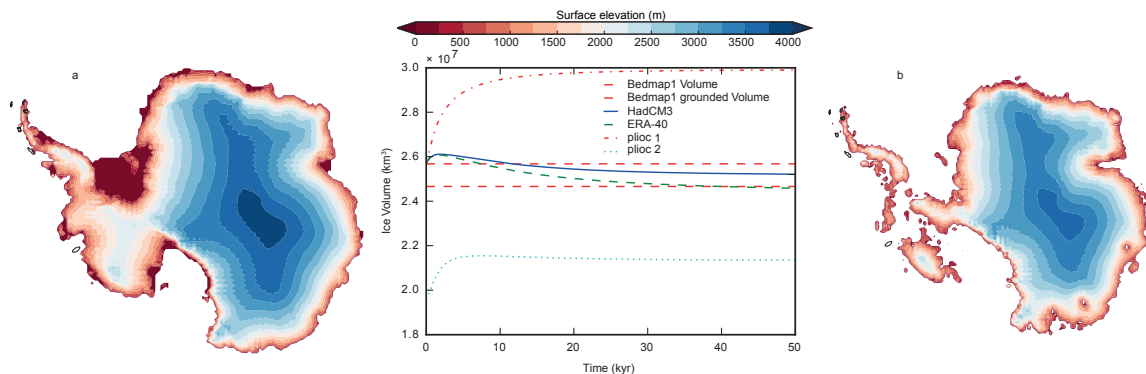


Figure 5.6: Equilibrium surface elevation in the RIMBAY Pliocene_{ICE-PD} (a) and Pliocene_{ICE-PRISM3} (b) simulations. The central plot shows the volume evolution, the dashed horizontal lines depict the present day total and grounded ice volume according to Bedmap1.

As expected from the PD control simulations all ISMs show significant variations in equilibrium ice volume for the Pliocene simulations as well. For the Pliocene control simulation (Pliocene climate with an initial present day ice cover) only RIMBAY and PSU-ISM show an increase in ice volume while the other models show a partly or complete collapse of the WAIS in the Pliocene if initializing the simulation with a present day ice sheet². A collapse could be delayed or prevented by the considerable increase in Pliocene precipitation over the AIS. Figure 5.7 shows the equilibrium surface elevations attained by the different ice sheet models in the Pliocene control simulation.

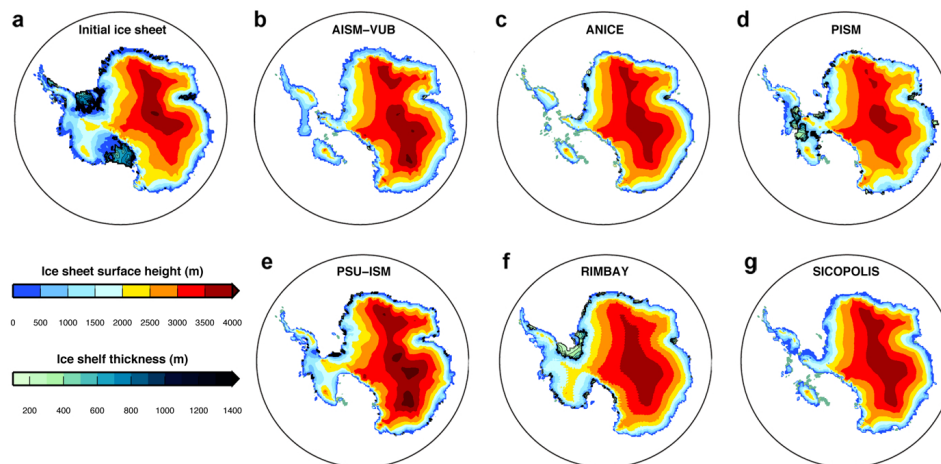


Figure 5.7: Results of the Pliocene control simulations, initialized from the present day AIS (from [de Boer et al., 2015]).

Also, for the Pliocene simulations forced with the AOGCM climate including the PRISM3 AIS reconstruction there is considerable model spread. Nonetheless, no ice sheet model simulates an advance of

²A collapse of WAIS for the updated version of RIMBAY used in the other chapters of this thesis might be triggered, since the southern ocean temperature anomalies applied in the Pliocene control run fall into the range which triggers a collapse of WAIS in the LIG simulations (for details please refer to chapter 3).

the WAIS into the marine bedrock sectors due to the warm ocean temperatures surrounding the land based small ice caps. It is remarkable, that only the ice sheet modeled by ANICE is largely confined to the PRISM3 ice boundaries (except for some regions such as the Wilkes and Aurora basins) which is due to its use of a insulation temperature melt model (ITM), while all other models use the positive degree day method (PDD). All other ice models are quite similar in their results considering the extent of ice caps in the WAIS sector. This extent is ultimately constraint by the limited bedrock area above sea level and the warm ocean temperatures preventing large scale ice shelf formation.

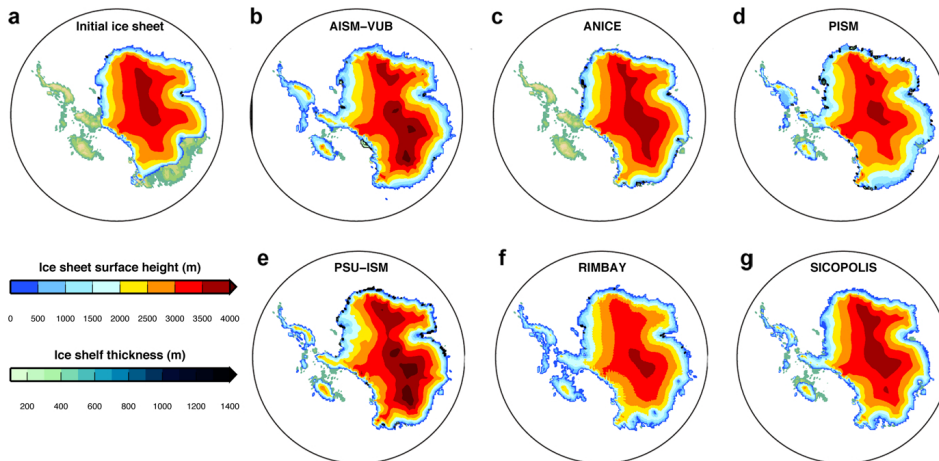


Figure 5.8: Results for the Pliocene equilibrium simulations driven by Had-CM3 Pliocene climate and the full PRISM-3 boundary conditions (from [de Boer et al., 2015]).

5.4 Contribution to Late-Pliocene Sea Level

Just as in the control experiments the different ice sheet models simulate a wide range of equilibrium Pliocene ice sheets. These differences are aggravated by the more extreme warming scenario, forcing the ice sheet into a new equilibrium surface elevation compared to the present day topography. The sea level equivalent ice sheet elevation changes in the PD control experiments showed that RIMBAY achieved the best match compared to the present day ice sheet configuration for the BEDMAP 1 boundary conditions (for which it is tuned) and ranges amongst the best performing models for the newer BEDMAP 2 topography. It is worth mentioning that the comparison of an equilibrium ice sheet simulation to the present day AIS is not necessarily proving a good model performance since the present day AIS is not in equilibrium with the climate forcing. Nevertheless, it is the best benchmark available for evaluation of large scale 3D ice sheet models at this stage.

The full sea level spread for the PD control experiments is $-3.23 \pm 2.93\text{m}$ s.l.e. (meter sea level equivalent) for the $\text{Control}_{\text{HadCM3}}$ simulations with the Bedmap1 topography. Model spread for the Bedmap2 environment is $1.11 \pm 3.02\text{m}$ s.l.e. resembling a shift to smaller ice sheets. Looking at the simulated ice sheet volumes, it is evident that current ice sheet models still require improvements and constraints on key parameters. The spread of simulated sea level rise or fall for the Pliocene control experiments is a staggering 20m in between models (for both BEDMAP 1 and 2). In the $\text{Pliocene}_{\text{Ice-PRISM3}}$ simulation

Table 5.3: Summary of the Antarctic contributions to sea level in the different simulations and for each ISM. The RIMBAY results are highlighted with a box (adopted from [de Boer et al., 2015]).

ISM	Ctrl _{HadCM3}	Ctrl _{Obs}	Pliocene _{Ice-PD}		Pliocene _{Ice-PRISM3}		Pliocene _{PD-Ant}	
AISM (B1)	-4.91	-1.06	-3.45	(1.47)	0.25	(5.16)	-5.17	(-0.25)
ANICE (B1)	-2.85	1.79	0.54	(3.39)	6.05	(8.89)	-8.78	(-5.94)
PISM (B1)	-5.12	2.38	3.00	(8.12)	8.02	(13.14)	NA	
PSU-ISM (B1)	-7.26	-0.46	-7.97	(-0.71)	0.35	(7.62)	-12.36	(-5.10)
RIMBAY (B1)	-0.80	2.08	-12.61	(-11.82)	6.06	(6.86)	-6.13	(-5.34)
SICOPOLIS (B1)	1.54	6.08	0.82	(-0.72)	5.29	(3.75)	-0.39	(-1.93)
AISM (B2)	-0.73	4.19	-2.45	(-1.72)	7.69	(8.42)	-1.15	(-0.42)
ANICE (B2)	3.86	9.00	6.01	(2.15)	11.51	(7.66)	0.54	(-3.32)
PISM (B2)	5.66	9.96	8.55	(2.90)	15.37	(9.71)	NA	
PSU-ISM (B2)	-3.44	2.04	-6.85	(-3.41)	4.52	(7.96)	-5.95	(-2.51)
RIMBAY (B2)	1.62	3.81	-10.18	(-11.80)	12.67	(11.05)	NA	
SICOPOLIS (B2)	-0.30	3.84	0.22	(0.52)	13.48	(13.79)	0.05	(0.35)

model spread is ca. 0 – 16m s.l.e., clearly a range to large to draw detailed conclusions about Pliocene AIS volume. This is mainly attributable to the different parameterizations of ice shelf mass balance and bedrock condition (specifically the basal shelf melt and refreeze, as well as the representation of grounding line migration).

5.5 PLISMIP Inconclusive

The results of the PLISMIP efforts captured in this chapter clearly show, that there is still room for considerable improvements regarding parameterizations and implementation of ice physics in the ice sheet modeling domain. While the control simulations yield reasonable results for the present day ice sheet (for which they are explicitly tuned) the model spread is still considerable (ca. 5m s.l.e. which corresponds to a WAIS collapsed and more). Switching from the Bedmap1 to the Bedmap2 topography results in considerably smaller ice sheets (ca. 4m s.l.e.), however the model spread stays the same. Ultimately, most of the differences between models can be ascribed to the different approaches in the parameterization of basal shelf melt and ice flux over the grounding line which where the main free parameterizations distinguishing the ice sheet models. Ice shelf mass balance and grounding line migration exert the largest influence on ice sheet dynamics on the coastal area of the AIS. Simulated equilibrium ice sheet volume differences in the Pliocene simulations are thus large. This prevents a model based reconstruction and constraint on Late-Pliocene AIS volume, and calls for a homogenization of spin up procedures and a limited parameter space in which 3D ISMs are initialized and can operate. Unless such a standardization of boundary conditions for ISMs for certain applications is not realized, interpretability of isolated ISM simulations will remain limited. It has been shown, that ice sheet dynamics in the Pliocene are highly sensitive to different climate forcings [Dolan et al., 2015]. Further improvements of proxy and model

based understanding of late-Pliocene climate conditions are needed to constrain the applied forcing in ice sheet modeling studies. Unfortunately, at this stage both the spread in climate forcings derived from AOGCMs, as well as the differing ice sheet dynamics derived from ISMs prohibit a conclusive model based statement on late-Pliocene AIS volume and extent.

Glaciation and the Last Glacial Maximum

Large ice sheets blanketed the high latitudes of the Northern and Southern Hemisphere in the LGM (ca. 21kyrs BP¹. Northern Europe and the northern territories of America were engulfed by gigantic ice masses (the Laurentide, Fennoscandian and Greenland Ice Sheets) and the AIS extended its reach up to the continental shelf breaks. The expansion of the global cryosphere lowered the sea level by about 120m [Waelbroeck et al., 2002, Imbrie et al., 1989]. Clues about the spatial extension of the various ice sheets are recorded in proxy archives from numerous sources such as glacial lineations for land-based ice sheets and glaciers, or grounding line wedges in circumpolar marine sediments. Despite all proxy reconstruction efforts (see e.g. the Review of [Bentley et al., 2014] or [Hillenbrand et al., 2012]) of LGM ice sheet spatial extent and volumes, glacial and deglacial Antarctic history remain poorly constrained. Early modeling efforts estimate a LGM Antarctic ice volume increase of 14 – 18m [Huybrechts, 2002] sea level equivalent (SLE). Later proxy compilations combined with glacial modeling constrain this ice budget to 6–13m SLE [Bentley, 1999]. Recent modeling and reconstruction efforts however estimate an AIS expansion corresponding to ~ 6 m SLE [Golledge et al., 2013]. LGM proxy reconstructions indicate that glacial advance did not unfold uniformly but affected the sectors of the AIS in different ways ([Bentley et al., 2014] and Figure 6.12). The large cold water ice shelves FRIS and RS are assumed to have been covered with grounded ice by a flat ice sheet [Bentley et al., 2014, Bentley et al., 2010, Golledge et al., 2013] (see Figure 6.12). While there was substantial thickening of ice at the fringes of the EAIS, central East Antarctica surface elevation might have been slightly lower (-100m) due to a reduced hydrological cycle carrying less humidity to the continent. The Antarctic Peninsula ice sheet probably thickened substantially while large parts of WAIS might have thinned a little. The Amundsen Sea sector witnessed considerable grounding line advances resulting in a raised ice sheet surface elevation

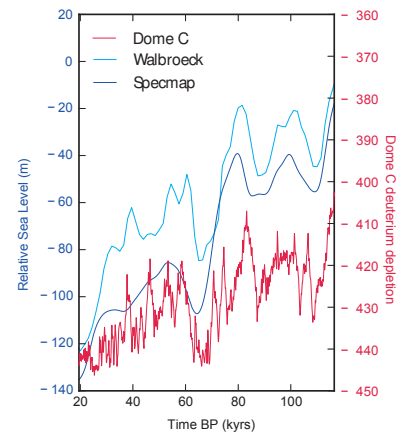


Figure 6.1: Dome C Deuterium depletion [Jouzel et al., 2007] and sea level [Waelbroeck et al., 2002, Imbrie et al., 1989] reconstructions during the last glaciation.

¹The peak glacial in the Southern Hemisphere was somewhat delayed compared to the northern glaciation. The AIS might have conserved its maximum extent in some regions as late as 15kyrs BP [Bentley et al., 2014].

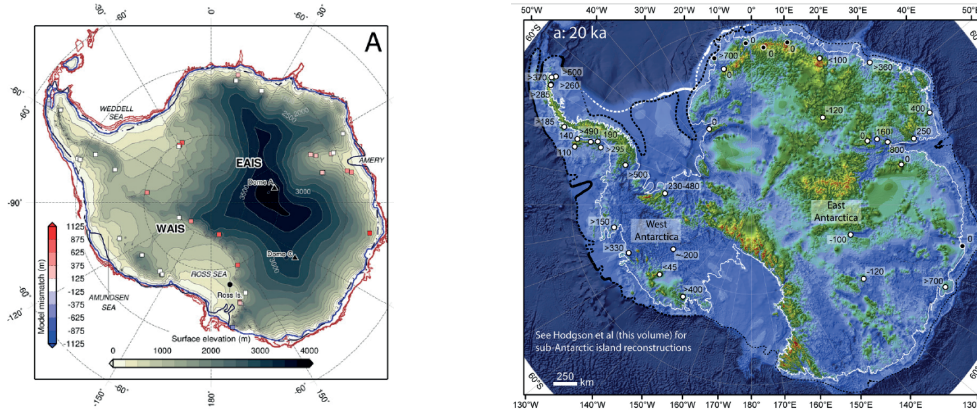


Figure 6.2: LGM grounding line reconstruction from ice sheet modeling (from [Golledge et al., 2013]) and proxies (from [Bentley et al., 2014]).

along the coastline. Despite the recent intensification in modeling and reconstruction efforts the glaciation and shape of the AIS in the LGM remains nebulous. In this chapter, simulations of the advance patterns of the AIS beginning at the onset of the last deglaciation and ending at the LGM ca. 21kyr BP are presented, discussing the role of Southern Ocean cooling, precipitation changes and surface temperatures.

6.1 Antarctic Ice Sheet Advance Following the Last Interglacial

In the final stages of the LIG the WAIS was presumably largely collapsed (see chapter 3), leaving large swathes of open ocean with plenty of heat storage at the front of the outlet glaciers draining the ice sheet. Initial re-advance of the ice sheet was thus most likely a slow process, due to relatively high melt rates close to the grounding line and the slow growth of thick ice shelves which buttress their tributary glaciers, thereby slowing down ice discharge into the ocean. The main climatological drivers of the re-advance of

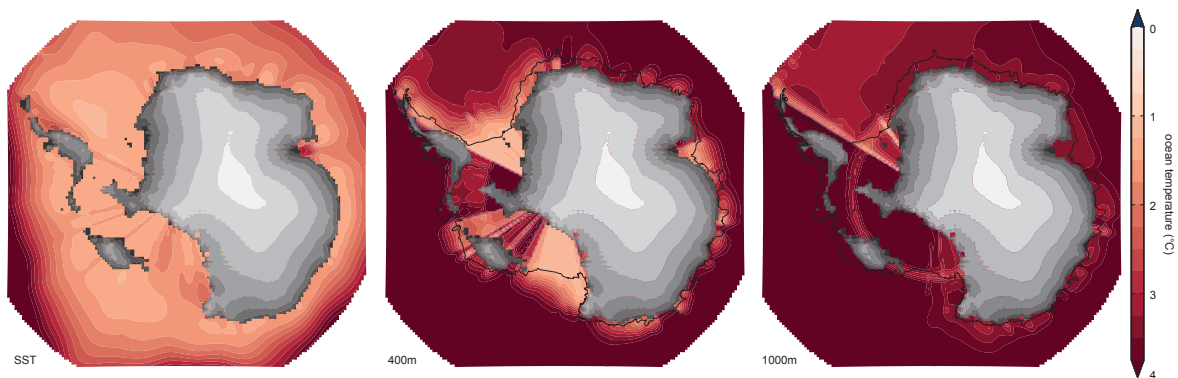


Figure 6.3: Surface elevation and Southern Ocean temperatures of the AIS in the final stages of the LIG (corresponding to simulation LIG3 in chapter 3). Southern Ocean temperatures, SST, 400m and 1000m are shown.

the AIS were cooling surface and ocean temperatures, whilst the hydrological cycle generally weakened transporting less moisture and thus less precipitation to the continent. Ocean cooling allowed for a re-

advance of the large ice shelves especially the FRIS and RS which buttressed their tributary glaciers leading to increasing surface elevations and subsequent grounding of ice, hence advancing the grounding line. The newly formed shelves and ice sheets would thereby compensate for the weakening precipitation such that the overall ice volume increased despite of reduced surface accumulation during the glacial.

6.2 Glacial COSMOS Forcing

As a LGM boundary condition for the glacial-interglacial cycle simulations, a COSMOS time slice at 21,000 years BP is applied (see chapters 2 and 11 for details about the COSMOS model setup). While the circumpolar sea surface temperature is similar to present day, the Southern Ocean cooled considerably in depths of 400m (ca. 1.13°C) to 1000m (ca. 1.95°C) (Figure 6.4). This generally favored ice shelf growth, and subsequently the advance of the grounding line. However, cooling at the front of the ice

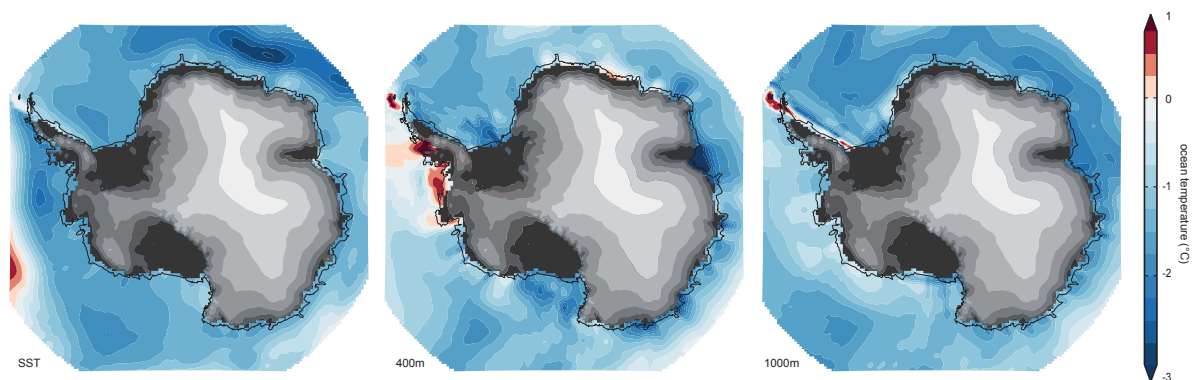


Figure 6.4: LGM forcing from the AOGCM COSMOS. Southern Ocean temperatures sea surface, 400m and 1000m depth overlain by the present day ice sheet topography for reference are shown.

shelves (or respectively the sea ice edge) is moderate, resulting in a small cooling signal underneath the ice shelves, since the ocean temperatures are extrapolated into the ice shelves' cavities. This suggests that the simulated Southern Ocean temperature changes in the LGM are only a moderate driver in the simulations, as basal melt rates are only slightly lower than present day. The main driver of grounding line advance is ultimately the fall of sea level forced by the build up of Northern Hemisphere ice sheets, promoting a grounding of ice shelves. This effect, in concert with low surface air temperatures slowing down the ice flow by stiffening the ice fabric, overcompensates the reduced surface accumulation (which is ca. -45% lower than at PD).

While the transient forcing on the road to the LGM increases the Antarctic ice volume in a reasonable manner, it is crucial to review the simulated final LGM ice sheet configuration on the basis of proxy reconstructions. If the WAIS accumulates too much ice, it is impossible to simulate a realistic deglacial retreat into the holocene without massively increasing ice shelf melt rates. If the basal friction in East Antarctica is too high, the ice sheet grows to thick; if it is too low the ice sheet "smears out". In the following, the effects of different scalings of shelf melting and basal friction on ice volume and LGM ice sheet configuration are presented and discussed.

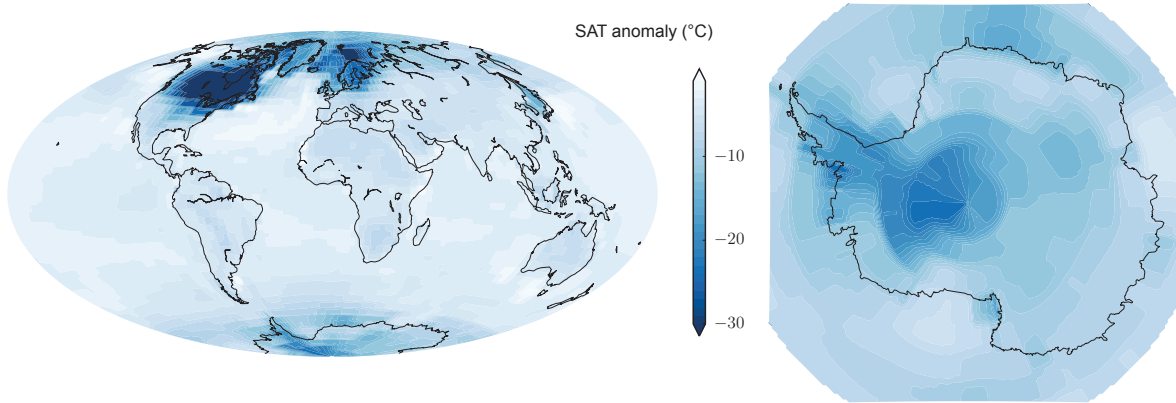


Figure 6.5: LGM forcing from the AOGCM COSMOS. Surface air temperature anomalies globally and for the Antarctic Ice Sheet.

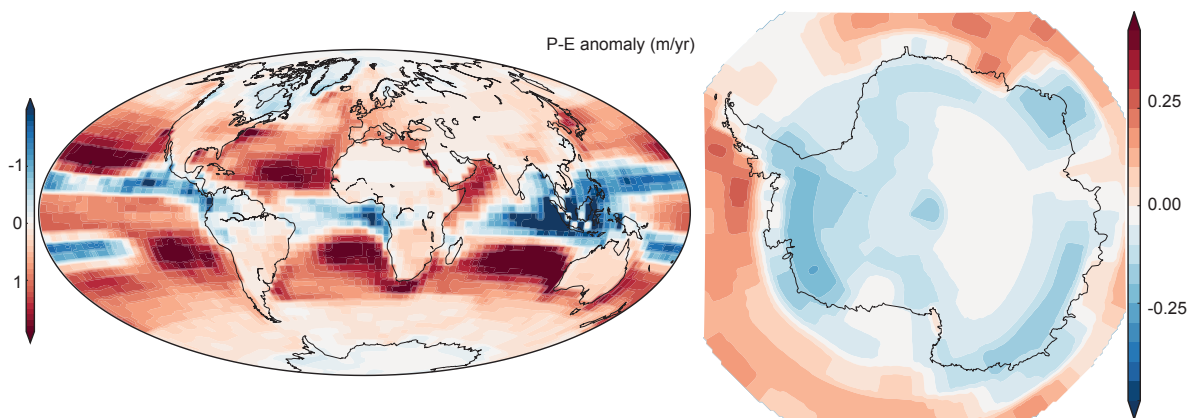


Figure 6.6: LGM forcing from the AOGCM COSMOS. Precipitation anomalies globally and for the Antarctic Ice Sheet.

6.3 The Role of Parametrizations and their Implication on Sea Level Evolution

From a modeling perspective two parameters, the basal friction and the ice shelf basal melting coefficient, are influencing the ice flow regime and mass balance decisively. The ice shelf melting parameter scales the temperature dependent melt rates underneath the floating ice, whilst the basal properties, controlled by the basal friction coefficient, control the flow speed over the bed. Figure 6.7 and 6.8 illustrate the effect of the ice shelf melt parameter on the Antarctic ice volume. The basal melt rate parameter in the sensitivity experiments is scaled from the PD value (0.011) to 10% of the PD value (0.0011). Figure 6.8 depicts simulations where the shelf melt rate parameter for the Ross Sea is reduced to 10%. This is motivated by the warm ocean temperatures transported from the Amundsen Sea into the Ross cavity by the extrapolation routine, resulting in unrealistically warm waters in the Ross sea. Figure 6.7 shows the volume effect for a uniform shelf melt rate parameter.

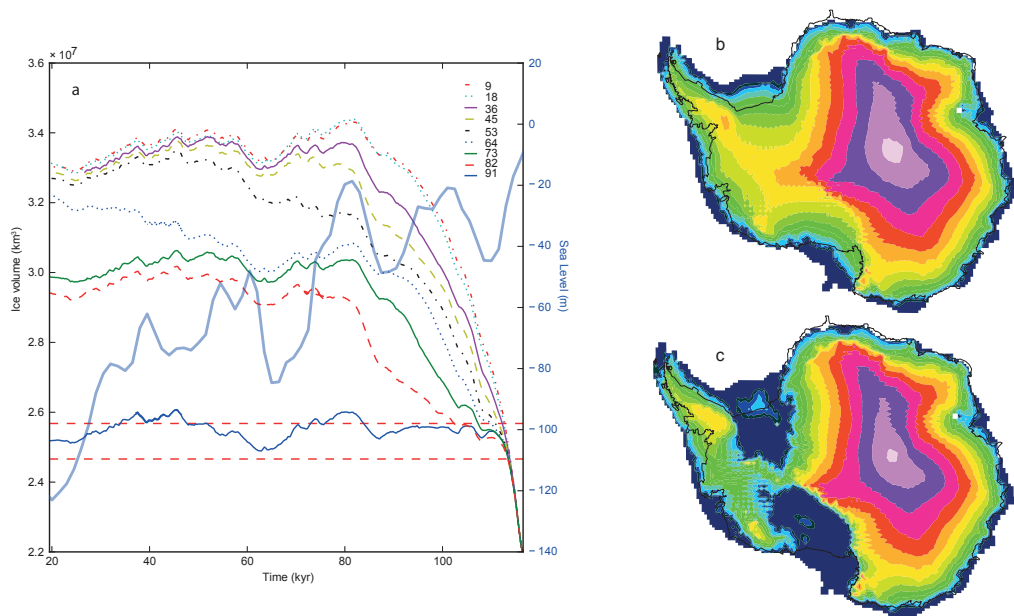


Figure 6.7: Antarctica's last glaciation depending on melt rates. The scaling factor in the shelf melt parameterization [Beckmann and Goosse, 2003] is varied between 10% of the present day value to 100%. The numbers on the right side of the figure denote the scaling of the melt parameter, e.g. 91 → 91% of present day parameter.

The corresponding AIS LGM configurations are shown in Figure 6.7b) and 6.8b). It is evident that the choice of parameters has a large impact on the final LGM ice sheet, the Antarctic sea level contribution and the subsequent deglaciation. Changes in the ice shelf melt rate are the main driver of the AIS advance during the last glaciation next to the fall of global sea level caused by the growth of northern hemisphere ice sheets. Reducing the melt rate scaling parameter in the ice sheet model by only 10 % can lead to differences in sea level at the LGM of several meters (see Figure 6.7), emphasizing the strong sensitivity of the AIS to the shelf mass balance in glacial as well as interglacials. Transient simulations with the PD control parametrization (as carried out for the LIG), result in an only slightly larger AIS compared to recent modeling efforts (e.g. [Golledge et al., 2013]). However, the results are within the overall range

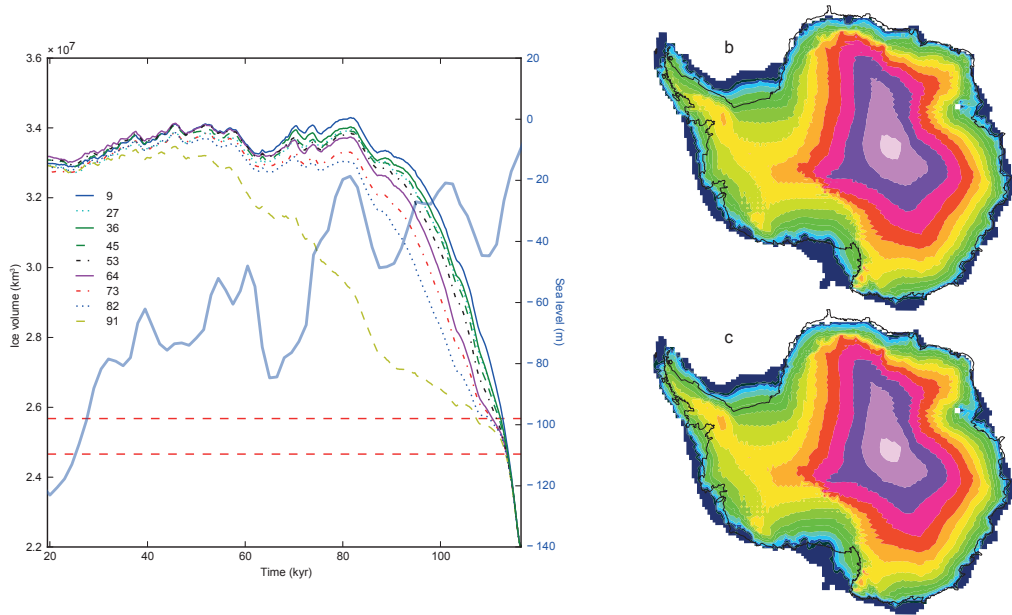


Figure 6.8: Antarctica's last glaciation depending on melt rates. Same as in the figure above, except for low melt rates in the Ross sea leading to full glaciation. The numbers on the right side of the figure denote the scaling of the melt parameter of the Filchner-Ronne Shelf in percent of the present day value.

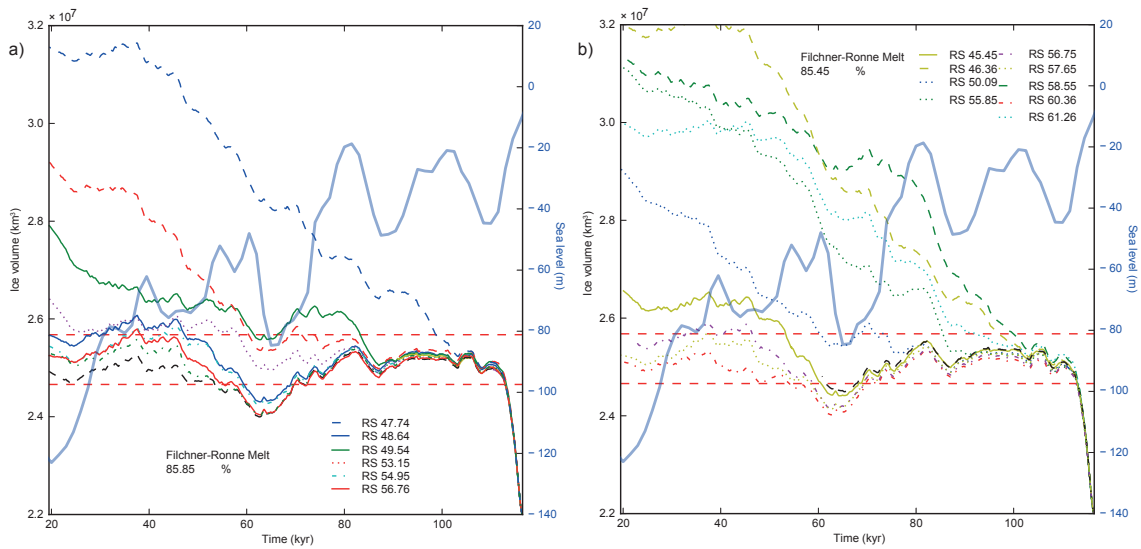


Figure 6.9: Antarctica's last glaciation depending on melt rates underneath the Filchner-Ronne and Ross shelf. a) Filchner-Ronne melt coefficient at 85.85% of the present day value, b) at 85.45%. The numbers in the legends show the melt coefficient for the Ross-Sea in percent of the present day value.

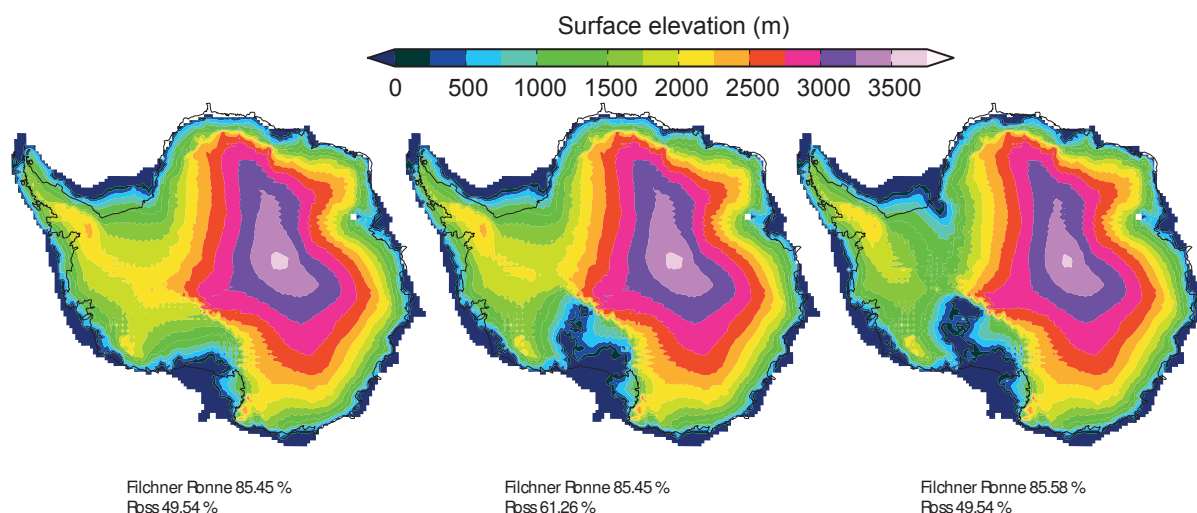


Figure 6.10: Last Glacial Maximum Antarctic surface elevations with a parameter set, reconstructing an Antarctic Ice Sheet close to proxy reconstructions. Numbers denote the scaling of the basal shelf melting parameter for the Filchner-Ronne and the Ross Shelf (e.g. 85.45% of present day parameter).

of estimated ice volumes [Bentley, 1999, Bentley et al., 2014, Golledge et al., 2013, Maris et al., 2014] and well below the ICE5/6G reconstruction which seems to generally overestimate AIS volume. While the lower limit for LGM ice shelf melting is zero melt, the ice sheet model prohibits a higher shelf melt rate coefficient than used in the PD control simulations (see chapter 2). In such cases thick ice shelves cannot form, and the grounding line only advances marginally during the glaciation.

6.4 A Wide Range of Potential Last Glacial Maximum Ice Sheet Configurations

Limitation to only one COSMOS climate time slice for the last glacial has the disadvantage of overly simplifying the Southern Hemisphere paleoclimate dynamics. This pertains specifically to the Southern Ocean heat budget and circulation changes. The simulated melting underneath the ice shelves can only be validated against observations in the present-day control-run since there are simply no proxy data for this variable. To be methodologically consistent, the PD parametrization should be kept fixed for the full transient simulation of the last glacial cycle. Neither is this approach feasible due to the limited accuracy of the applied boundary conditions (e.g. the initial configuration of the ice sheet and bedrock topography or the transient climate forcing) nor has it been done in any contemporary work in the field. Nevertheless, by observing the behavior of the ISM through the glacial and comparing it with proxy constraints, valuable conclusions can be drawn about possible misrepresentations of mass balance, dynamics and applied climate forcing. This is evident in figure 6.7 which depicts the sensitivity of the AIS dynamics in different cooling scenarios during the glaciation period, expressed in total ice volume of grounded and floating ice.

As already discussed in chapter 3, the applied COSMOS climate forcing does not reproduce an evolution of the AIS which corresponds with proxy reconstructions of sea level evolution (which is so far the only main constraint on AIS volume in the LIG). The same holds for the advance of the AIS into the glacial. Applying the PD parametrization, the transient climate forcing derived from the glacial index method and the COSMOS time slices does not result in ice sheet advance since basal melt rates close to the grounding line are not low enough to overcompensate the reduced accumulation. Only reducing the basal shelf melt parameter and thus the melting further by 10 – 20% results in whole-scale advance and a LGM AIS volume and extent in the range of proxy reconstructions. This might be either due to too high AOGCM ocean temperatures in the LGM or a misrepresentation of basal melting in the ice sheet model. Additionally, the extrapolation routine creates an "inflow" of warm water from the Amundsen Sea into the Ross and Weddell Sea which is not realistic as soon as the respective ocean basins are covered by ice again, thus blocking the ocean circulation. As an additional factor, the bedrock topography and slipperiness is not specifically investigated here, but is shown to have an important effect on ice dynamics (e.g. [Golledge et al., 2013, Maris et al., 2014]).

6.5 Drivers of Antarctic Ice Sheet Glaciation

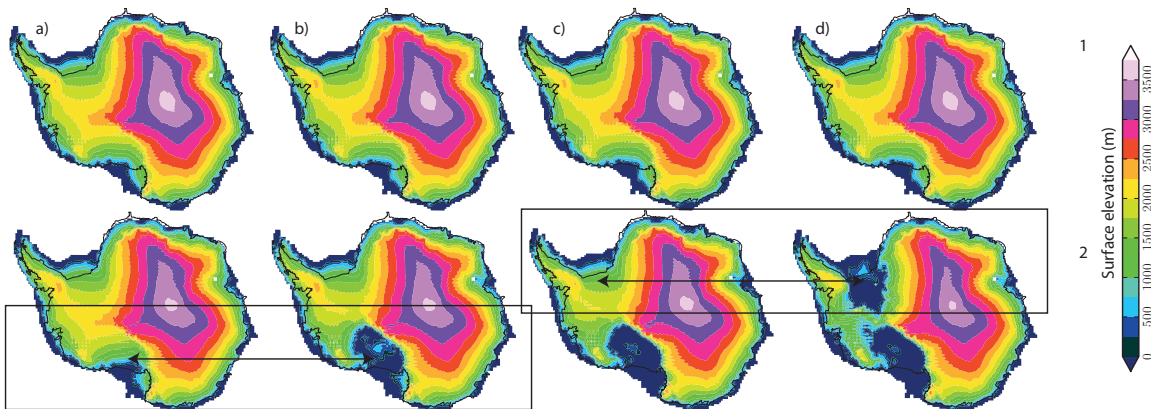


Figure 6.11: Antarctic surface elevation at 21 kyr BP for different melt rate scaling factors. Uniform scaling of the melt rate coefficient. 1 : a) 9.00 b) 18.18 c) 36.36 d) 45.45. 2 : a) 54.54 b) 63.63, c) 72.72 d) 90.9. The black squares highlight the transition from a glaciated ocean basin to a basin free of grounded ice.

The results show that the extent of glaciation and grounded ice thickness in the Ross and Filchner-Ronne sector of the WAIS are the determining factors of the maximum ice sheet volume in the LGM. The results presented above show a clear clustering between two LGM ice sheet configurations depending on the glaciation dynamics in the Ross and Weddell Sea sector. If basal melt rates in the Ross Sea are low, melting in the Weddell Sea sector does not play a big role as long as it allows for the formation of thick ice shelves and subsequent grounding line advance. If low melt rates in the Ross Sea allow for a fast glaciation within the first ca. 20.000 years of glaciation, there is no basal melting scenario with melt rates below or at present day level in the Weddell Sea which does result in a smaller ice sheet than ca. 33 millions km³ (or ca. 10 – 11m sea level depression). The reverse case, an early glaciation of the Weddell Sea seeding a subsequent glaciation of the Ross Sea, has not been tested here. Ice shelf melt processes in one ocean

basin, allowing, delaying or preventing ice advance dynamics in another, seemingly detached basin, have not been discussed in the literature yet, but might be an important factor in large scale glaciations of Antarctica in the past. When applying an uniform basal shelf melt scaling, a scaling above ca. 97% of the PD value (0.011 see Methods) in the Filchner-Ronne Sector prevents the formation of a grounded ice sheet in the Weddell Sea. A scaling above ca. 73% of the PD value prevents the formation of a Ross Sea grounded ice sheet. Both the Ross and Weddell Sea sectors were at least partly glaciated in the LGM according to proxy records (one has to bear in mind, that the extent of glaciation is poorly constrained). Figure 6.11 shows the final LGM ice sheets for different basal shelf melt scenarios. A melt rate tuning for the Weddell and Ross Sea sectors allowing for a full glaciation of the two ocean basins while keeping the newly formed grounded ice sheet as flat as possible was achieved with scaling factors for the Ross Sea of $bg_{RS} \sim 0.0075$ (PD value being 0.011) and for the Weddell Sea $bg_{WS} \sim 0.0095$. Such a parametrization leads to an AIS LGM volume corresponding to a sea level lowering of ca. 6 – 8m compared to today representing a volume of about $\sim 30 \cdot 10^7 \text{ km}^3$.

6.6 Proxy and Modeling Constraints on the Last Glacial Maximum Antarctic Ice Sheet

The final extent of the AIS, and more importantly the thickness of the WAIS [Larter et al., 2014] is crucial for the deglaciation behavior and timing². The AIS during the LMG must have been in a configuration, in which the WAIS divide was not much thicker - or even slightly thinner than at present (see discussion in previous section).

Evidence from marine sediments suggest that both Weddell and Ross Sea were at least partly glaciated [Hillenbrand et al., 2012, Hillenbrand et al., 2014, Bentley et al., 2014]. The ice sheet covering the area occupied by today's FRIS was probably flat and shallow [Golledge et al., 2012] with a surface elevation of around 1000m, otherwise a complete retreat of the grounding line towards the 21st century location would have been highly unlikely from an ISM perspective. This puts a constraint on both thickness and extent of the Weddell Sea ice sheet during the LGM. While the Weddell Sea completely glaciates as soon as ocean temperatures are low enough, it seems that there are multiple potential LGM grounding line positions in the Ross Sea ranging from a semi-glaciated state up to complete glaciation towards the shelf edge. Both minimum and maximum glaciations can be achieved within a reasonable set of parameters given the AOGCM climate forcing used in this study. However, an advance of the grounding line to the shelf edge only occurs, when basal melting underneath the Ross Shelf is significantly reduced. Otherwise there is a continuum of grounding line configurations, partly covering the Ross Sea with a grounded ice sheet (see Figure 6.12 and 11.16 in chapter 11). This suggests that the Ross Sea may not have been completely glaciated in the LGM, at least not up to the continental shelf break. While the coarse resolution prevents in depth studies of LGM grounding lines in the smaller ocean basins such as in the Amundsen- and Bellinghousen-Sea there are significant differences depending on the applied forcings. Comparing the modeled LGM grounding lines in the smaller as well as larger ocean basins to marine proxy data (e.g. grounding line wedges) would provide further insight into the AIS' LGM advance. The

²As well as for the Antarctic contribution to sea level changes in the LGM.

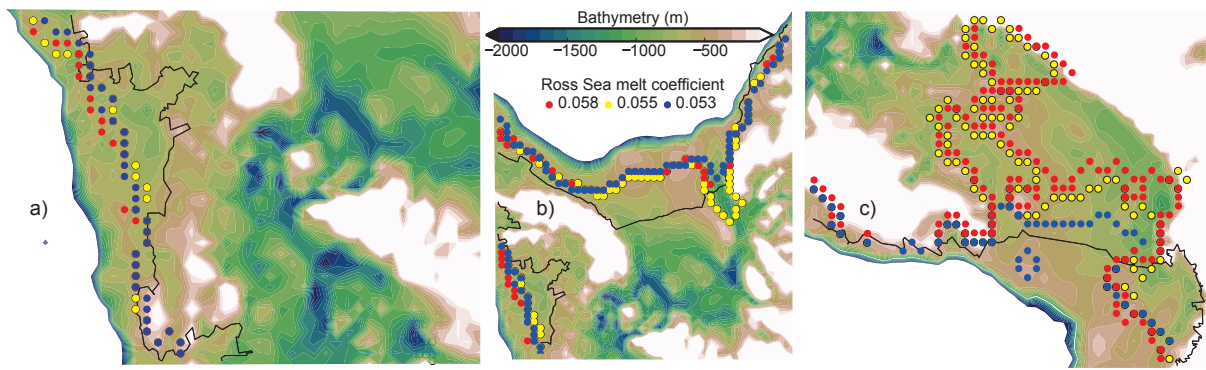


Figure 6.12: Antarctic LGM grounding line positions in the year 19.500 BP simulated in experiments LGM1, LGM2 & LGM3. a) Amundsen Sea, b) Weddell Sea, c) Ross Sea. Only one color is given where grounding lines overlap.

results of this study show a relatively wide range of sea level changes depending on the climate forcing. Reducing the degree of uncertainty in the LGM and transient climate forcing would put the ISM based interpretation of LGM AIS advance on a more solid fundament.

Post-Glacial Retreat of the Antarctic Ice Sheet

The post-glacial and Holocene retreat of the AIS was an inhomogeneous process varying greatly in timing and extent in the different Antarctic sectors [Bentley et al., 2014, Weber et al., 2014]. The timing of the AIS retreat is constraint by proxy reconstructions from marine sediments and dating of land masses uncovered by the ice sheet [Heroy and Anderson, 2007, Hillenbrand et al., 2014]. A recent study identifies multiple retreat episodes marked by peaks in ice rafted debris (IRD) between 20.000 and 19.000 years ago, and episodes between 17.000 and 9.000 years ago [Weber et al., 2014]. [Golledge et al., 2014] investigated Antarctic deglacial dynamics and contributions to melt water pulse 1A with an ISM and relatively high spatial resolutions. However, the simulations are heavily constraining ice dynamics by proxy reconstructions, using the ice shelf mass balance and parameterizations of bedrock properties to reproduce proxy horizons as accurately as possible. Here a different approach is chosen. Similar to the previous chapter, ensemble simulations are run to explore the range of potential Antarctic deglacial ice sheet evolution.

Three vantage points of initial LGM AIS configuration are chosen from which the AIS is freely evolved until the present day. Relatively low volume AISs, which reproduce a range of proxy reconstructions for LGM [Bentley et al., 2014], are chosen for this purpose. Transient forcing is achieved in the same manner as in chapters 3 and 6. It is evident from Figure 7.2, that a straightforward application of the COSMOS and present day forcing does not reproduce a realistic deglacial retreat of the AIS, but actually leads to further ice sheet growth, spurred by the intensifying hydrological cycle. The Southern Ocean warming assumed in the standard experimental setting is too weak to destabilize the ice shelves fringing the grounded ice sheets of the Weddell and Ross Sea. However, such an ocean forced destabilization is the

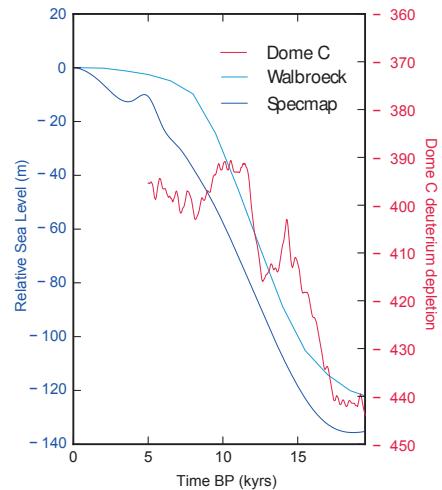


Figure 7.1: Dome C Deuterium depletion and sea level reconstructions for the deglaciation. The sea level forcing used in this thesis is based on [Waelbroeck et al., 2002].

Table 7.1: LGM experiments

Table 7.2: Overview of the three LGM configurations chosen for the deglaciation simulations. The third column shows the Antarctic contribution to sea level depression, and the third column the mean shelf melt rate. Column four and five denote the scaling parameter in the basal shelf melt equation for the Filchner-Ronne and Ross shelves.

Exp	Volume (10^7 km^3)	s.l.e (m)	M_a^m	FRIS	Ross
LGM 1	2.79	-1.145	1.522	0.0095	0.0055
LGM 2	2.92	-3.58	1.515	0.0095	0.0058
LGM 3	3.155	-7.74	1.475	0.0095	0.0053

only viable mechanism of ice sheet retreat, as the accumulation increases in a warming climate [Frieler et al., 2015]. Sea level rise (Figure 7.1), fueled by the waning of Northern Hemisphere ice sheets, is not sufficient to push the grounded LGM ice sheets into large scale retreat (Figure 7.2).

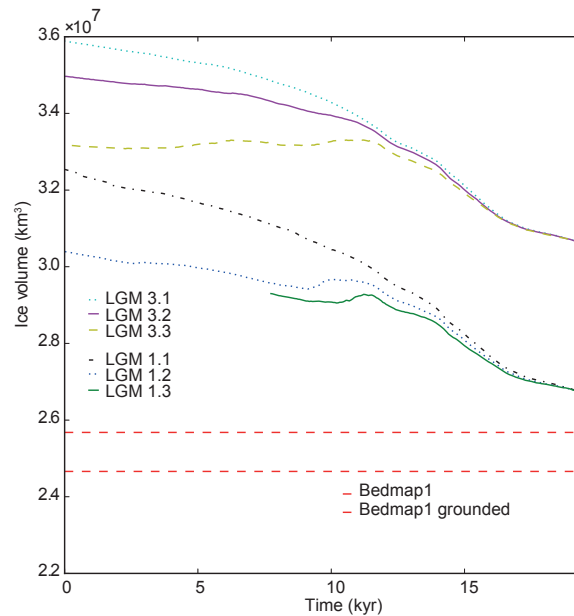


Figure 7.2: Antarctic Ice Sheet volume during the deglaciation, forced in the standard setting with the original COSMOS forcing fields. LGM1-3 denote the three initial Last Glacial Maximum Antarctic Ice Sheet configuration. Three different ice shelf melt scaling values are chosen for every simulation (e.g. LGM 3.1-3.3).

Figure 7.3 shows the final surface elevation after deglaciation for experiments LGM 1.1, 1.3 and 3.1, 3.3 (x.1 being the present day melt coefficient, x.3 present day melt coefficient multiplied by 3). While the Ross Sea LGM ice sheet fully retreats in scenario LGM 1.3, only partial retreat is achieved in LGM 3.3 (due to the larger initial ice volume). The Weddell Sea stays glaciated with almost identical grounding line advances in both scenarios. The position of the WAIS divide in the LGM (at 19.500 years BP) is comparable to its present day location. In the course of the deglacial simulations however, the divide migrates northwards, due to the large Weddell Sea ice sheet affecting the ice flow. The present day location of the ice divide in the EAIS is surprisingly well reproduced. This is indicative of a strong bedrock and precipitation influence on EAIS flow patterns and partial decoupling from WAIS dynamics.

Melt rates in both scenarios are rather low, around one $1\frac{\text{m}}{\text{a}}$ in the Weddell and Ross Sea and $3\frac{\text{m}}{\text{a}}$ in the Amundsen Sea. Such low melt rates are not sufficient to destabilize the ice shelves fringing the large grounded ice sheets resting on marine basins. The ice shelf buttressing stays intact, while the shallow marine ice sheets accommodate the additional accumulation, leading to an overall growth of the AIS. A large scale destabilization of the LGM ice shelves must have been triggered in the first millennia after the LGM via large increases in ice shelf melting and - or big calving events. As RIMBAY does not include a calving parameterization, intensified melting and calving is investigated via scaling up the melt rate coefficient. This does not resemble calving processes physically and prevents a separation of calving effects from shelf melt. However, it allows a quantification of necessary shelf mass balances to destabilize the marine LGM ice sheets.

7.1 Ice Shelf Dynamics Key to Antarctic Ice Sheet Retreat

In the following, thresholds in the ice shelf mass balance leading to a destabilization of the LGM marine ice sheets of the Weddell and Ross Sea are investigated. In a first approach a Southern Ocean warming pulse of 2°C at the beginning of the deglaciation is applied uniformly throughout the water column. The warming pulse starts at 19.500 years BP and is maintained up to 5.000 years, in 500 year steps. The timing of the pulse is chosen to coincide with main retreat events as suggested by [Weber et al., 2014] and [Bentley et al., 2014]. Figure 7.4 shows the effect of such a warming pulse on the AIS deglacial evolution. While an initial retreat driven by thinning ice shelves is clearly visible, it is reversed even before the end of the melt pulse. This means that the increasing precipitation over the ice sheets overcompensates the shelf loss.

Triggering the melt pulse later (at 17.5000 years BP) leads to an overall larger ice sheet. Interestingly, applying the melt pulse for 3000 years between 17.5000 and 14.5000 years BP results in the same ice sheet volume as when starting it 2000 years earlier. This might be interpreted as an ice shelf dynamics memory effect on the grounded ice sheet. The same observation holds for 2000 and 1000 years melt pulses shifted in their initial year. Figure 7.5 shows the present day AIS surface elevation for a 4.000 (b) and 500 (c) years melt pulse starting at 19.500 years BP. The initial topography at the LGM is depicted in Figure 7.5 a).

While a short melt pulse is sufficient to create a Ross Sea free of an ice sheet, the Weddell Sea stays glaciated even for the 5000 year pulse. As in the experiments shown in the previous section, the ice divide in West Antarctica is shifted northwards due to the remaining Weddell ice sheet. The shape and position of the ice divide in East Antarctica is surprisingly well reconstructed, indicative of a distinctive separation of ice dynamics in the WAIS and EAIS. A 2°C melt pulse results in shelf melt rates up to $10\frac{\text{m}}{\text{a}}$, which is still not sufficient to destabilize the marine ice sheet covering the Weddell Sea. In the next section the effect of still higher melt rates at the onset of deglaciation is investigated.

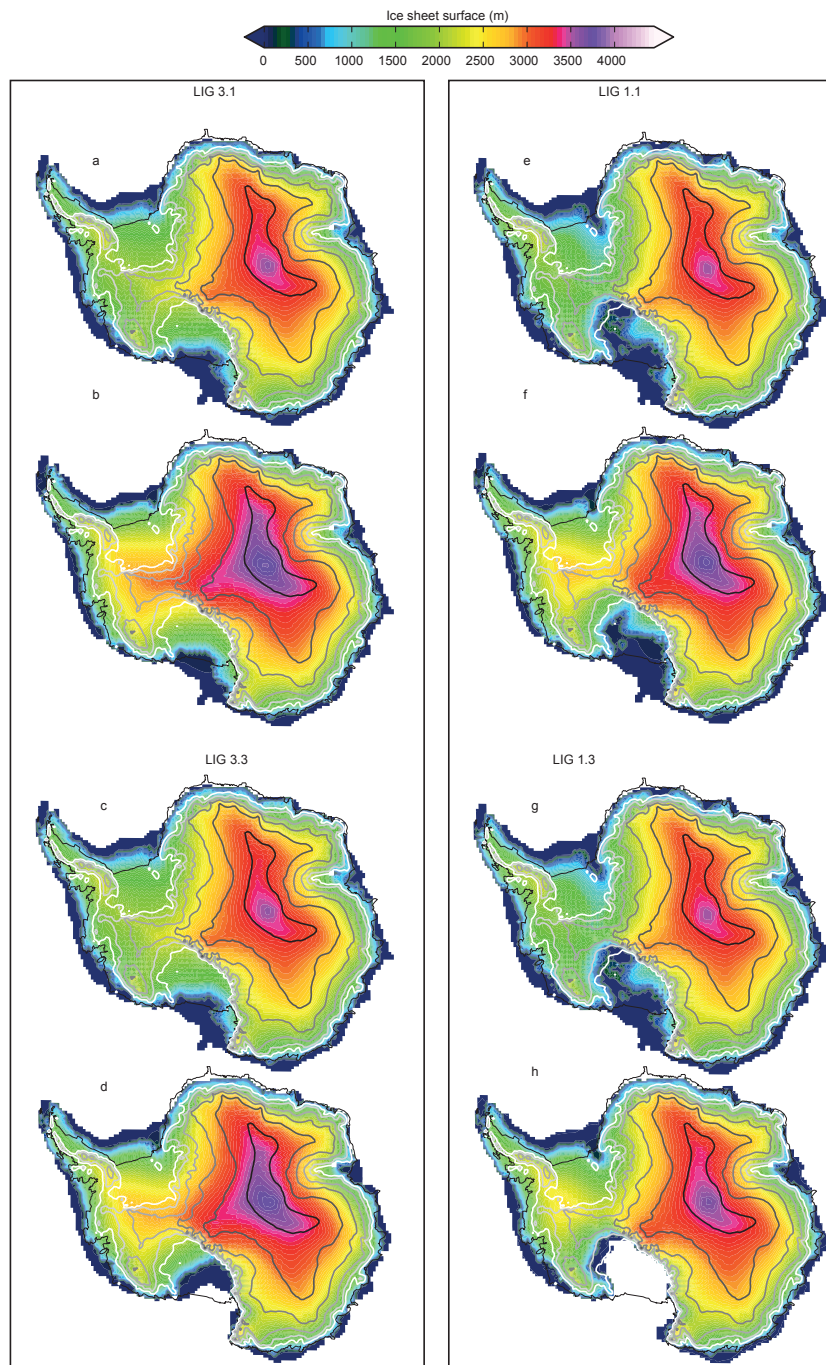


Figure 7.3: Antarctic Ice Sheet volume after the deglaciation, forced in the standard setting with the original COSMOS forcing fields. a) initial surface topography at the LGM (19,500 years BP) for experiment LGM 3.1 (-7.74m sea level equivalent), b) final surface topography at present day, c)-d) same for LGM 3.3; e)-f) same as a)-b) but for LGM1.1 (-1.15m sea level equivalent), g)-h) same as c)-d) but for LGM 1.3.

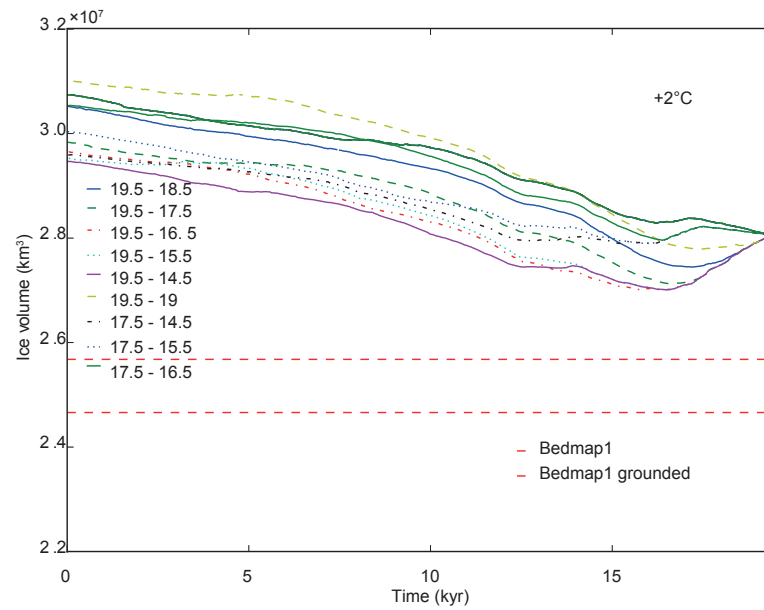


Figure 7.4: Antarctic Ice Sheet volume evolution during the last deglaciation, forced in the standard setting with COSMOS forcing fields and additional 2°C Southern Ocean warming pulse for a limited duration (e.g. from 19.500 years until 15.500 years BP).

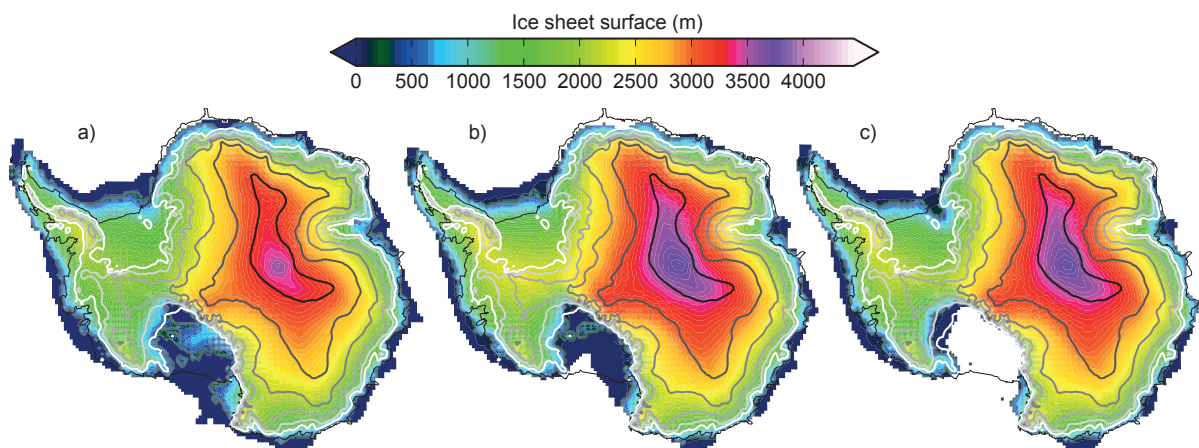


Figure 7.5: Antarctic Ice Sheet volume after the deglaciation, forced in the standard setting with the original COSMOS forcing fields, but with a melt 2°C melt pulse of 500 to 5000 years duration. a.1) initial surface topography at the LGM (19.500 years BP) for experiment LGM 2 (-3.35m sea level equivalent), b) and c) show the final ice sheet at present day for a 500 and 5000 year melt pulse.

7.2 The Effects of Fast Ice Shelf Collapse and Bathymetry

In the following the effect of fast collapsing ice shelves are discussed. For this purpose the shelf mass balance is strongly tuned by means of the melt rate scaling coefficient (see chapter 2). Melt rates are multiplied up to a yearly melting of $20 - 30 \frac{m}{a}$. Comparable melt rates are found presently close to the grounding line in the Amundsen Sea sector. Such negative mass balances could have been caused either by an increase in heat supply underneath the ice shelves, e.g. due to a shift in the circumantarctic Southern Ocean circulation, or due to increased calving or a combination of the two. In any case such high ice shelf melt rates cannot be excluded and could be the decisive factor tipping the WAIS into large scale retreat.

Figure 7.6 shows the ice volume during the last deglaciation for drastically increased melt rates applied from 19.500 years BP onwards (again in 500 year steps). The MISI is triggered in the Weddell Sea eventually between 17.000 and 15.000 years BP depending on melt rates. The violent collapse of the marine ice sheet unfolds within little more than one millennium raising sea level by almost 3m. In this scenario, a complete retreat of the Weddell Sea ice sheet by the year 15.000 BP has taken place, preceding the reconstructed retreat in [Bentley et al., 2014] (Weddell Scenario A) by a few millennia. This however is not surprising, as extreme melt rates sustained over a long time interval are assumed in the scenario presented here. Different ISM tuning choices can lead to a "better" reproduction of the retreat patterns suggested by geologic reconstructions (see [Golledge et al., 2014]). The modeling results

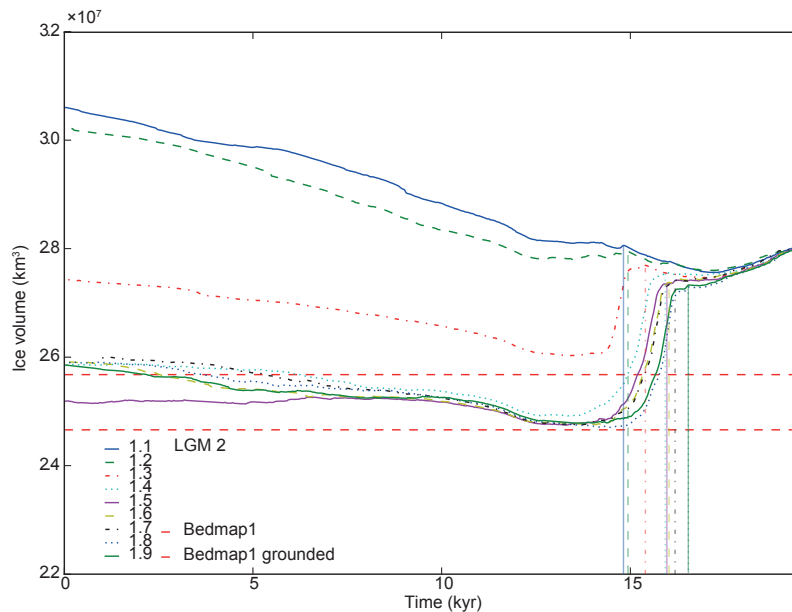


Figure 7.6: Antarctic Ice Sheet volume evolution during the last deglaciation, forced in the standard setting with COSMOS forcing fields and additional scaling of the basal shelf melting.

suggest that there is an intrinsic time scale (ca. 1.000 years) for the collapse of the Weddell Sea ice sheet assuming prevailing high shelf melt rates. In reality, high shelf melt rates over several thousand years are improbable, as natural variabilities characteristic for shelf-ocean-sea ice feedbacks¹ would prohibit

¹E.g. the modification of deep water formation via brine rejection.

a constant forcing as assumed for this scenario. Re-occurring cold spells (e.g. as suggested by South Atlantic proxy data [Vazquez Riveiros et al., 2010]), and centennial changes of the ocean circulation [Chen et al., 2015] could slow down the retreat of the marine LGM ice sheets.

Nevertheless, idealized scenarios (like the present one) inform about intrinsic dynamics underpinning ice sheet retreat or advance. The crucial threshold for the collapse of the Weddell Sea ice sheet is the bedrock topography. Two deep topographic throughs act as facilitators of the MISI. The Thiel-Through [Hein et al., 2011] in the eastern Weddell Sea seems to play the key role for the post-LGM MISI. A Shallow bathymetry of ca. 500m depth is situated northwards of the deep Weddell Sea valleys, stabilizing the ice sheet as long as these regions are covered by grounded ice (see Figure 7.8). These dynamics illustrate the importance of bedrock topography and LGM ice sheet advance for AIS deglaciation and timing.

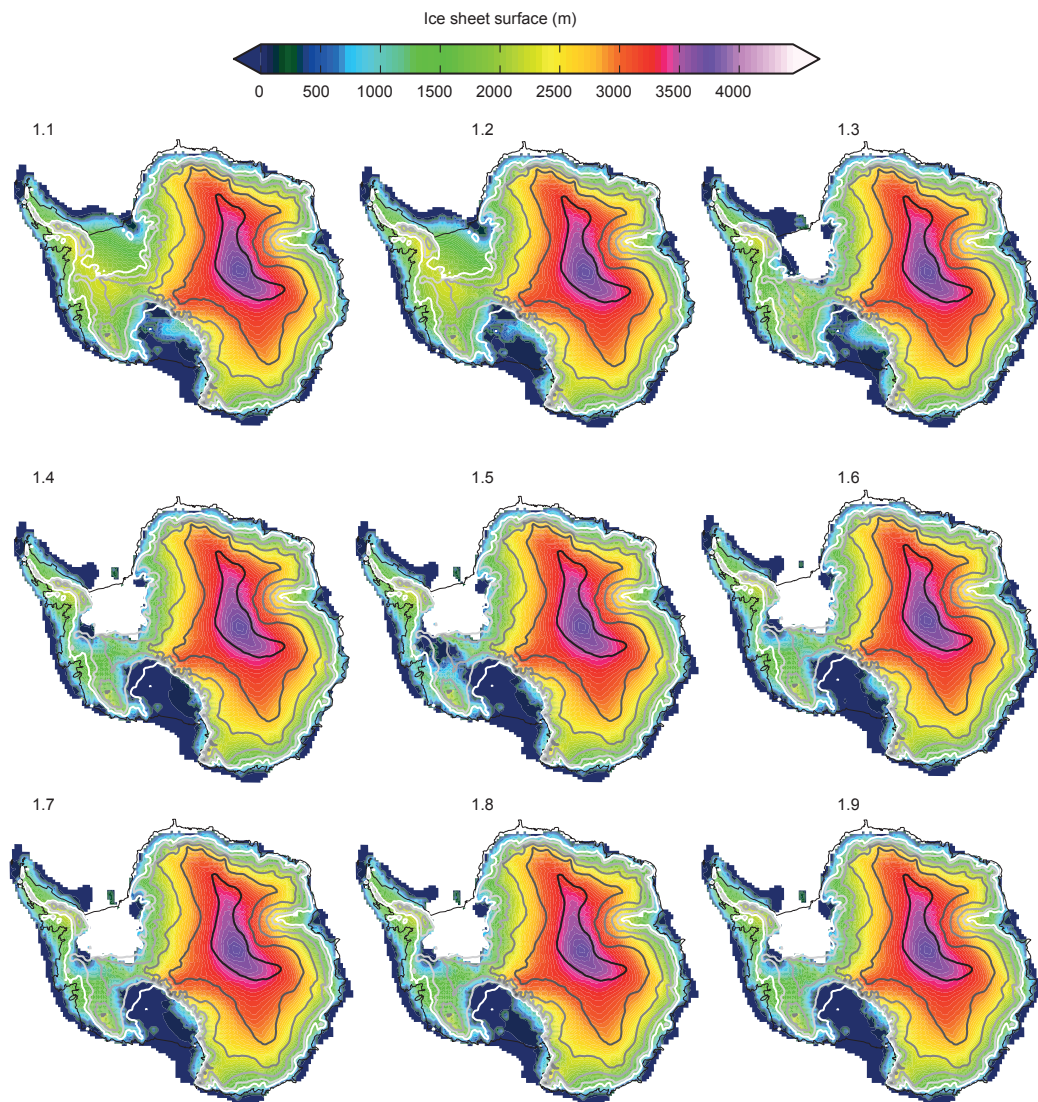


Figure 7.7: Antarctic Ice Sheet surface elevation at present day after deglaciation. The Antarctic Ice Sheet topographies relate to the volume plotted in Figure 7.6, numbers above the individual ice sheet depictions show the scaling factor used in the basal shelf melt equation.

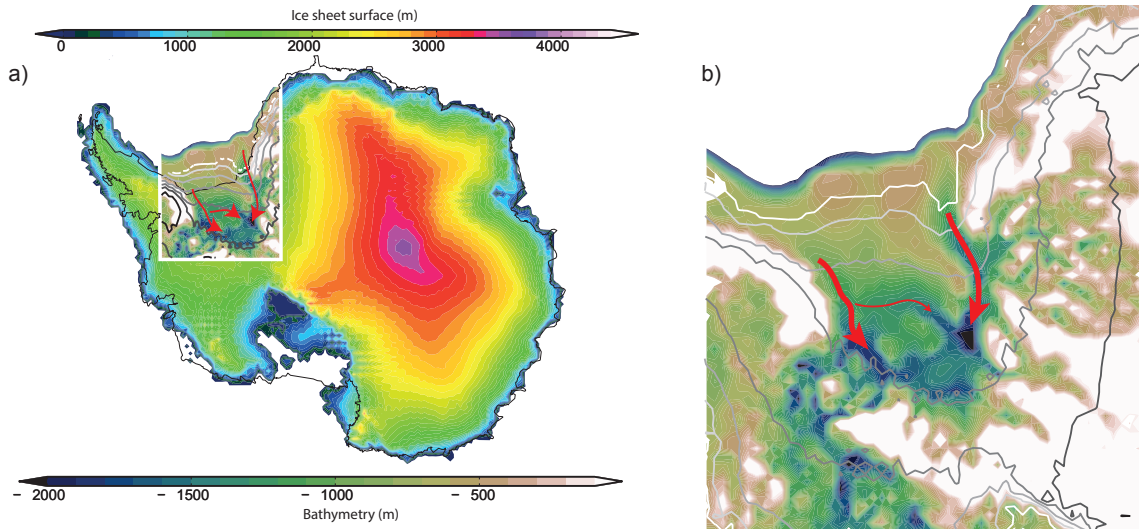


Figure 7.8: b) Ross Sea bathymetry overlain by the Last Glacial Maximum surface contour (simulation LGM3). a) Surface elevation of the Last Glacial Maximum Antarctic Ice Sheet is given as a reference. Boxed region is shown magnified in b).

7.3 The Deglaciation Puzzle

In this chapter, exemplary deglaciation scenarios focussing on the effects of ice shelf mass balance are discussed. A bifurcation in the ice volume evolution depending on ice shelf melting is found. This bifurcation is caused by the thresholds determining whether the MISI in the Weddell Sea is triggered or not. The determining factors behind these thresholds are the initial LGM AIS configuration, ice shelf dynamics and bedrock properties (the latter not being discussed here). Sustained high shelf melt rates in the Weddell Sea unravel an intrinsic timescale of ~ 1000 years for complete collapse of the Weddell Sea ice sheet. Proxy reconstructions suggest that deglaciation in this sector took place over several millennia. This is indicative of recurring cold spells in the Weddell Sea, slowing down the collapse. The ice dynamics in the Weddell Sea are but one piece in the post LGM deglaciation puzzle of the AIS. Processes occurring in the Amundsen Sea and the EAIS are beyond the scope of this discussion. An extended cross-examination of the influence of different climate forcings and bedrock properties should be carried out to further explore the processes underpinning post-glacial AIS retreat.

Three main conclusions can be drawn from the results of the deglaciation climate sensitivity simulations presented in the previous chapter.

Firstly, the final shape and flow regime of the AIS in the LGM (ca. 19.500 years BP) predefines the initial dynamics of deglaciation to a large degree. Sizable marine ice sheets in the Weddell and Ross Sea slow down ice retreat and influence the marine bathymetry via the inundation of Earth's mantle. Such variations in Antarctic bathymetry in turn influence the timing of ice sheet retreat and the necessary ocean forcing for triggering the MISI.

Secondly, the magnitude and timing of sub-ice shelf melting events and widespread calving crucially depends on the choice of ocean forcing which is poorly constrained by proxy data.

Thirdly, the basal properties underneath the marine ice sheets of the Weddell and Ross Sea determine the speed of ice sheet collapse, as they influence the slipperiness of the bed, and hence the ice flow.

Unraveling the Past: a Model-Data Intercomparison of Ice Cores

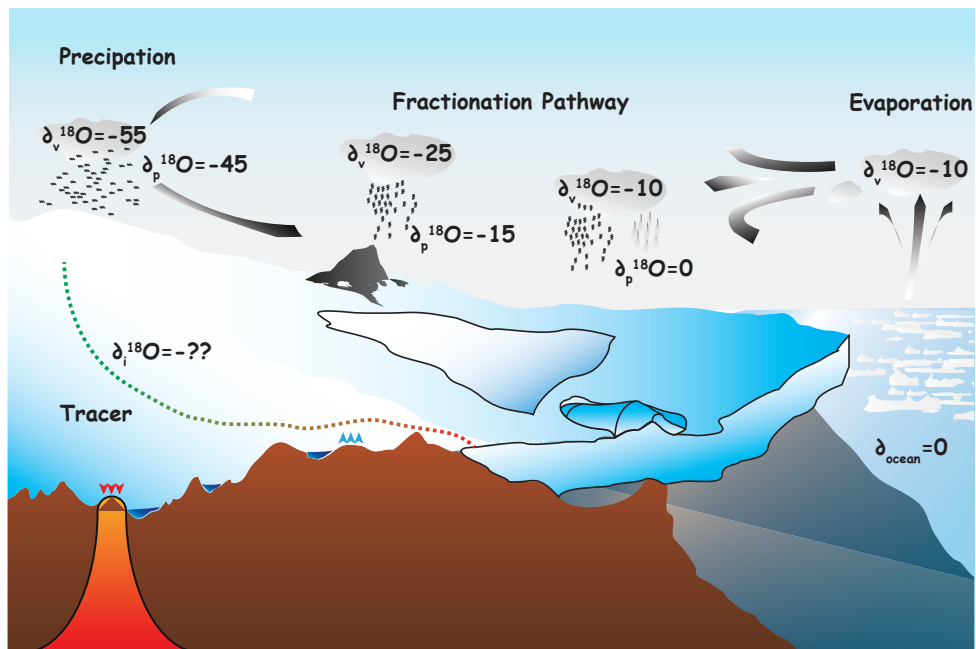


Figure 8.1: Schematic illustration of fractionation pathways over Antarctica. Water evaporates in mid to high latitudes (carrying a fingerprint of local temperature) and is advected toward the ice sheet where further fractionation via condensation occurs (depletion of heavy oxygen and hydrogen isotopes).

The principles of the physical processes forming the isotopic archive in ice cores have been briefly sketched in the Methods chapter as well, but shall be reviewed again here. The largest reservoir of water on Earth, the ocean, feeds the AIS with a steady supply of snow, which then becomes part of the ice matrix flowing back to its source, the ocean. In this cycle, the concentration of water stable isotopes changes with every phase transition occurring during precipitation, evaporation or condensation. The present day precipitation over Antarctica carries a distinctive climatic fingerprint which is related to the temperatures at the source, i.e. the evaporation in the middle and high latitudes, the pathway (condensation), and its final destination over the ice sheet. This mostly consistent relationship [Jouzel et al., 1997, Jouzel and Masson-Delmotte, 2007] can be used to create a paleothermometer unraveling past variations in surface temperatures and has been used to reconstruct the past eight glacial cycles from Antarctic and Greenland

ice cores (e.g. [Jouzel et al., 2007, Dahl-Jensen et al., 2013]). If the accumulation above the ice core location is high enough to form distinctive snow layers it is possible to count those layers up to a certain depth. Thereby a chronology of past climate fluctuations is established and reconstructions from other ice cores and marine or land based geologic recorder systems can be related to them. Numerous informations can be drawn from the structure of an ice core. The thickness of the layers is an indication for the amount of precipitation in the past, melt layers bare witness of past melt events, and the relative abundance of hydrogen and oxygen isotopes is a measure of past temperatures. However, several factors influence the ice cores isotopic distribution, such as changes in the source region or temperature, circulation or changes in surface temperature¹ at the ice core's location. Useful interpretation of ice core data therefore relies on a meaningful differentiation of those effects which is a demanding task. Therefore, climate models simulating the hydrological cycle in concert with ice sheet modeling are useful tools to decipher the climatic events leading to the variations in the isotope composition in ice cores.

8.1 Caveats of Ice Core Modeling

Would climate models accurately simulate the past hydrological cycle and ice sheet models exactly reproduce the waxing and waning of ice sheets, simulated ice cores would be identical to observations. This would make the interpretation of past climate evolution straightforward. However, as "all models are wrong", mismatches in model-data intercomparisons are always abundant. This paragraph will focus on the limitations of ice core simulations from an ice sheet modeling point of view. Contemporary ice sheet models suffer from three major limitations. Firstly, the initial state of the ice sheet at the beginning of a simulation will always be erroneous as long as information on bedrock topography, ice temperature and ice flow in the real world is limited. This means that every simulation of an ice sheet will be initialized from constraints which are disparate from the ones in reality in turn affecting the trajectory and final state of the simulated ice sheet. Secondly, the external forcings, i.e. the surface mass balance, ocean temperatures, geothermal heat flux, wind stress, sea level etc. will deviate somewhat from the actual climate state, thus driving the ice sheet away from its real world counterpart as the simulation unfolds. Thirdly the physical processes governing the flow of ice are only approximated in every ice sheet model. All these factors limit the interpretability of ice core simulations and ice sheet modeling results in general.

That being said, it is still worthwhile to carry out these simulations. Combined with an abundant proxy archive, the results of climate simulations are the only way to reconstruct the dynamic changes Earth's climate underwent in the past. In recent years, several studies tackled the field of ice core reconstructions via ice sheet modeling using 3D ice sheet models in concert with passive tracer advection routines. However they were mostly limited to proof of concept studies (Figure 8.2, Figure 8.3 and [Goelles et al., 2014, Rybak and Huybrechts, 2003]) or simple parameterizations of the climate forcing and ice dynamics for the Greenland ice sheet (e.g. [Clarke and Marshall, 2002, Lhomme et al., 2005]). One study set out to simulate an Antarctic ice core, the EPICA Dronning Maud Land (EDML) core, with sophisticated assumptions of climatic drivers and a complex ice sheet model [Huybrechts et al., 2007] to support the interpretation of the EDML ice core data. However, a more holistic approach aspired in this thesis

¹E.g. caused by atmospheric or ice sheet elevation changes.

including a general circulation model simulating the hydrological cycle and a 3D ice sheet model, aims at the reconstruction of the Antarctic Ice Sheet's isotopic distribution through the last glacial cycle. In the following sections, first results from equilibrium Antarctic ice core simulations are presented.

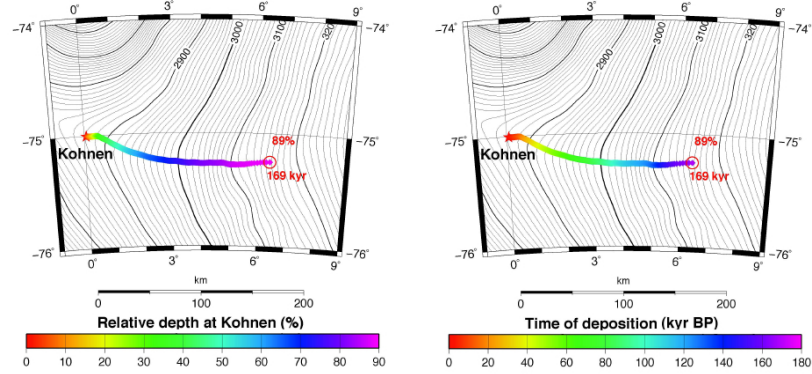


Figure 8.2: EDML ice core modelling results (from [Huybrechts et al., 2007]). The ice core is traced back to its origin in a multi-cycle ice sheet modeling approach. The left panel shows the relative depth at Kohnen up to a depth of 89%. The right panel depicts the relative age (time of deposition) at the ice core.

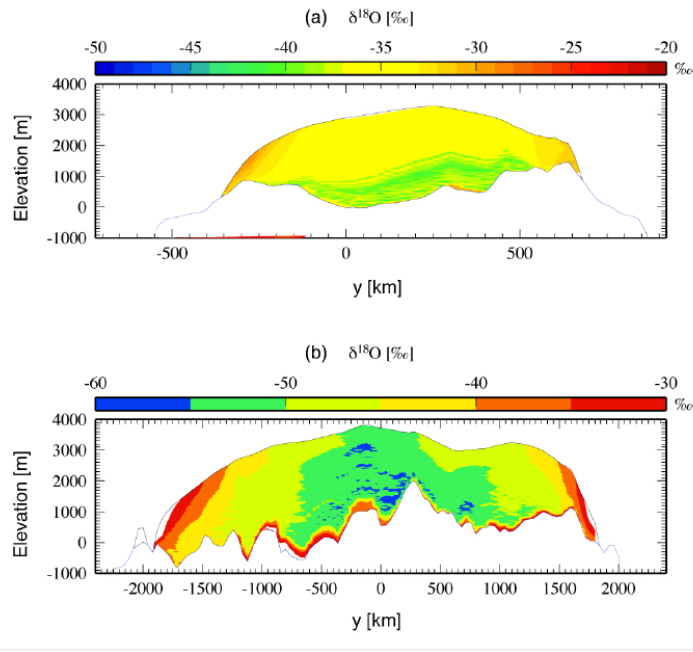


Figure 8.3: Modeled isotope distributions along two transects crossing the a) GRIP core, Greenland and b) Vostok core, Antarctica (from [Goelles et al., 2014]).

8.2 Experimental Setup

Both Lagrangian and Eulerian tracer advection have been implemented in the ISM in the scope of this work (see chapter 2). The results have shown that the Lagrangian approach is more suitable for actual

ice core simulations, due to its superior accuracy (no diffusion) and the possibility to backtrack individual ice pockets to their origin at the surface (a valuable piece of information, especially if looking at ice cores which have been drilled downslope of an ice divide). Figure 8.5 illustrates the general principle of tracer simulations in the Lagrangian approach. Tracers² are initialized at defined time steps³ and density⁴ at the surface where they become part of the ice matrix and are advected with the flowing ice (velocities are calculated via trilinear interpolation). At the surface they are identified by their coordinates, the surface temperature, isotopic concentration (if available) and surface elevation. Whenever a tracer hits bedrock, it is deactivated and lost. Basal freeze on or advection via basal melt water is not accounted for in the model. Along its trajectory the depositional properties (e.g. location, surface temperature, isotopic composition) of each tracer can be retrieved at any given moment.

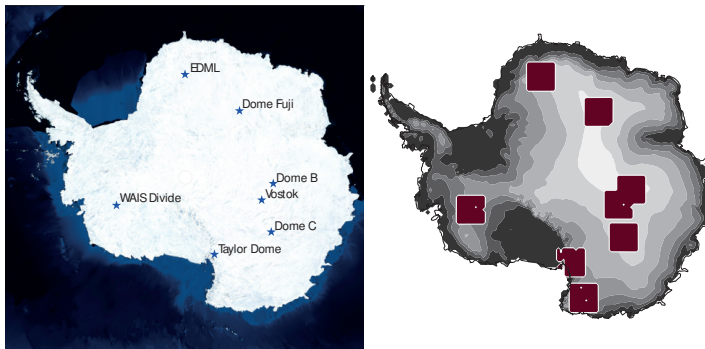


Figure 8.4: Locations of deep ice cores simulated in this study.

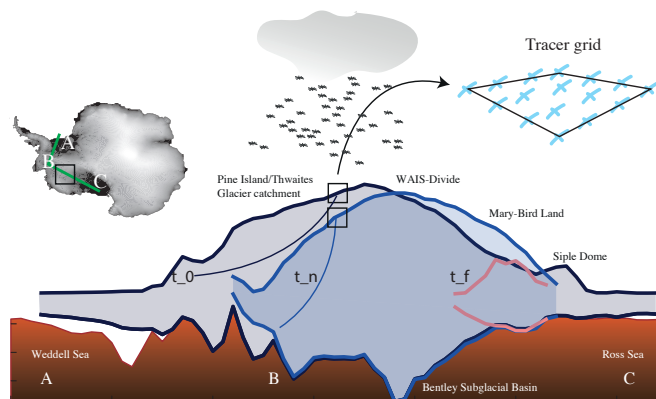


Figure 8.5: Schematic of Lagrangian forward modeling studies. Tracers are initialized at the surface (depicted by the black boxes) with a pre-defined density (tracer grid) at defined time intervals and advected through the ice sheet. The tracer area covers the ice cores of interest. Three transects are depicted illustrating the shape of the Antarctic Ice Sheet along a flight path defined by the points (A-B-C) at specific time slices (t_0, t_n, t_f) in a transient simulation.

²Snow precipitating on the surface of the ice sheet.

³E.g. every 50 years.

⁴Tracers per grid cell.

8.3 Present Day Equilibrium Results

To illustrate the feasibility of the tracer approach to simulate Antarctic ice cores, Lagrangian tracers are advected through the ice sheet in a present day equilibrium run (see chapter 2). For this purpose, every 1000 years tracers are initialized at the surface (16 tracers per grid box, one tracer every 10 km) and advected through the model domain. Figure 8.6 & 8.9 show the results of a 300.000 years equilibrium simulation along two transects crossing the present day coordinates of the Vostok and Dome Fuji core. Figure 8.6 shows ice ages at different sigma layers (15, 25, 35 of 41 layers) after 300.000 model years forced by present day climate. It is evident that only the EAIS and specific areas of the WAIS harbor ice older than 50.000 years. Regions of oldest Antarctic ice are characterized by large ice thicknesses, cold conditions, slow ice flow, low geothermal heat flux and bedrock conditions favoring low ice velocities (see e.g. [Van Liefferinge and Pattyn, 2013]).

The coarse resolution of the model and the simplified climate forcing generate an AIS evolution and ultimately an equilibrium ice sheet distinctively different from the PD ice sheet configuration. The ice divides have shifted, the EAIS is thinner and the coastal fringes of Antarctic thicker than the present day ice sheet. It is evident that both at Vostok and Dome Fuji simulated ice ages are much lower than their real life counterparts (see Figure 8.9 b)). This is to be expected by the design of the experiment. Present day equilibrium simulations of the AIS, generally underestimate the age of the ice as flow velocities are too fast and the ice fabric too warm, due to the constantly applied present day climate (no memory effect from the last glacial is imprinted in the ice sheet). Further precipitation is generally high and relatively fast outlet glacier drain the hinterland. Those glaciers were either slower during the last glaciation or replaced by low lying, slow flowing grounded ice sheets (see chapter 6). Finally, gaps in the tracer coverage are visible especially in the regions of the EAIS covered by thick ice. These "blind" spots in the ice fabric are caused by the divergent nature of the ice flow, which might advect tracers away from ice divides. A higher density of tracers initiated at the surface can mitigate this divergence, but increases the computational costs, which might limit high densities for long term paleo studies depending on the computation resources available (since the ISM in

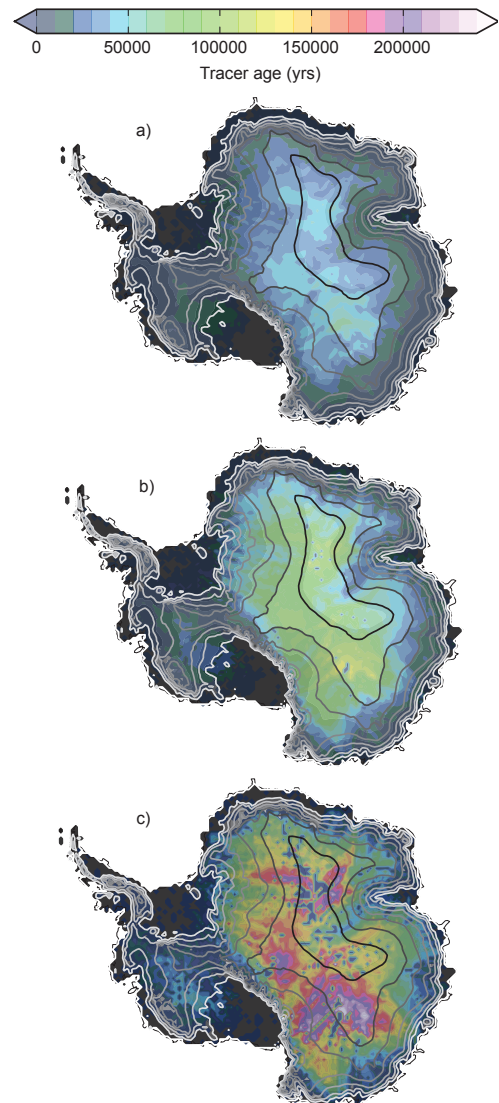


Figure 8.6: Ice ages in different depths of the Antarctic Ice Sheet at the end of a present day equilibrium simulation along terrain following coordinates (sigma layers). The contour lines depict the surface topography for the present day ice sheet in 500m steps (maximum elevation 4000m.). a) depth level 15, b) depth level 25, c) depth level 35) of 41 levels.

this study is not parallelized, this can become a serious limitation).

Seven deep ice cores are selected for analysis in the PD control simulation, one of them situated in the WAIS. The WAIS divide core oldest age is surprisingly similar to the actual age measured in the real core, despite the large changes WAIS underwent in the last glacial cycle. The reason for this agreement is unclear, but might be accidental and rooted in a combination of misrepresentations in the model (e.g. bedrock topography, accumulation, ice flow, ocean forcing etc.) generating the PD age-depth relationship. The misrepresentations in the simulation crystalize dramatically in the Taylor Dome, Dome C and Vostok cores. Taylor Dome is a core at the fringes of the ice sheet located in a complicated ice-bedrock topography, which can not be resolved realistically in the present model setting. The Dome C and Vostok core have ice ages too young throughout the ice core. In future studies, more realistic transient ice sheet simulations of the full last glacial cycle and beyond will be the basis for ice core simulations of the main deep Antarctic ice cores drilled so far. These studies will be expanded by advection of isotopes delivered by an AOGCM. This will allow for a reconstruction of the AIS' isotopic signature throughout the last glacial-interglacial climate cycles, closing the water stable isotope budget and allowing for a more informed interpretation of climate data derived from marine sediment cores (ice sheet elevation correction on $\delta^{18}O$ values).

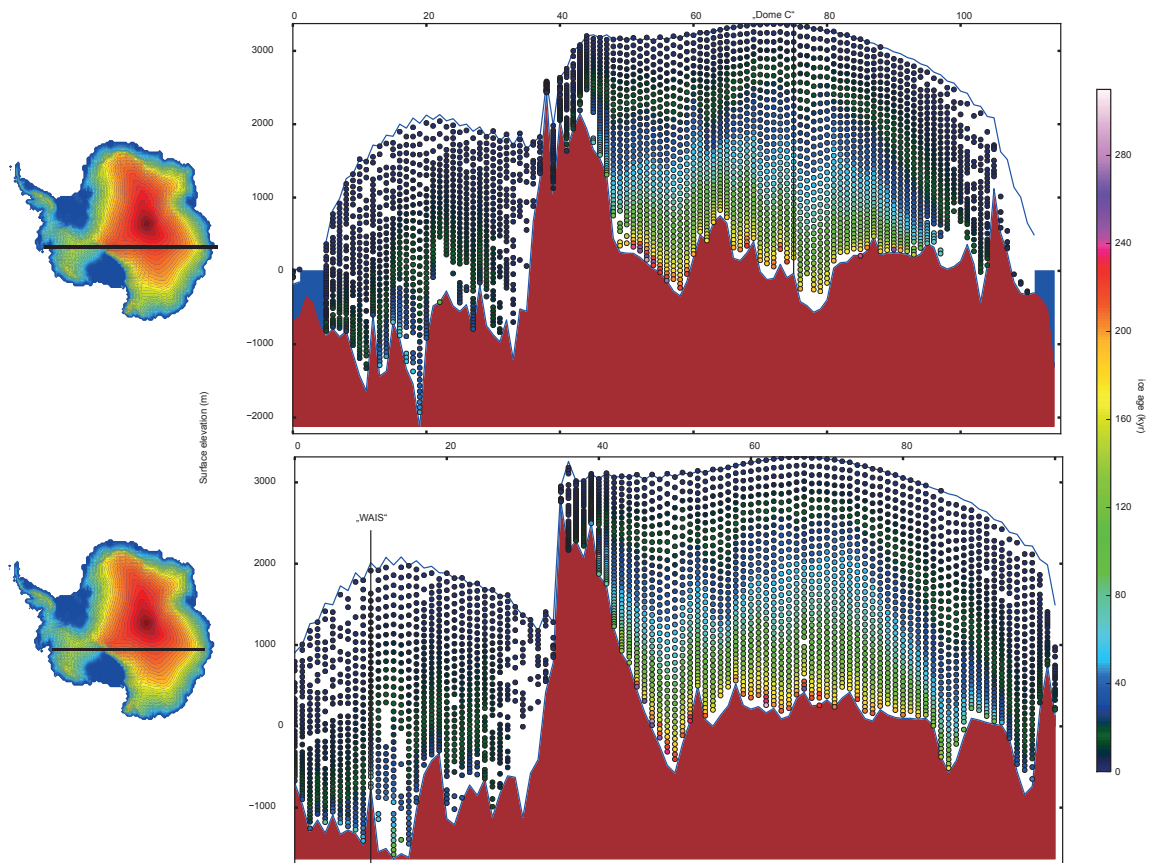


Figure 8.7: Transect through the Antarctic Ice Sheet along the position of the Dome C and WAIS ice core at the end of a 300,000 year equilibrium simulation forced by present day climate. Ice ages at every grid node are depicted by color coded dots. The position of the transect with respect to the Antarctic Ice Sheet is highlighted next to each transect. Vertical bars depict the coordinates of the real ice cores.

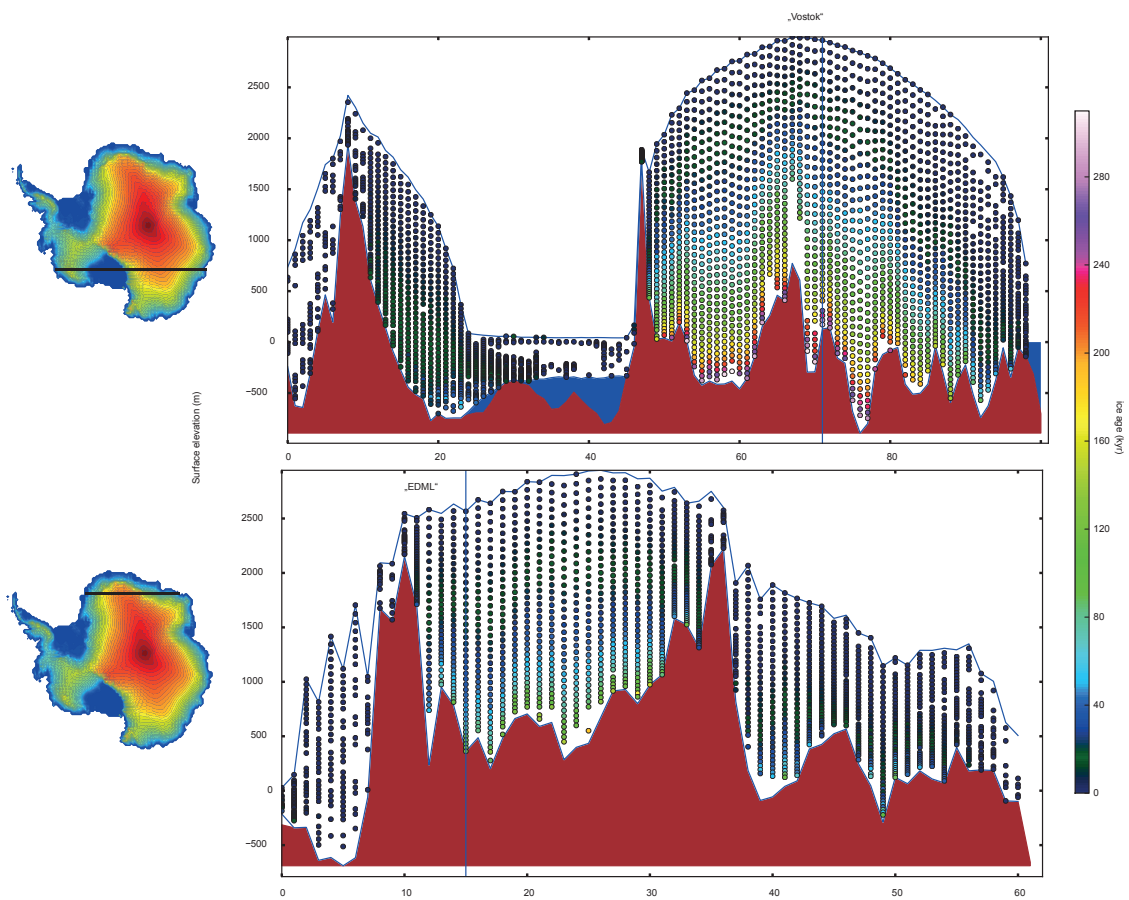


Figure 8.8: Transect through the EDML and Vostok ice core.

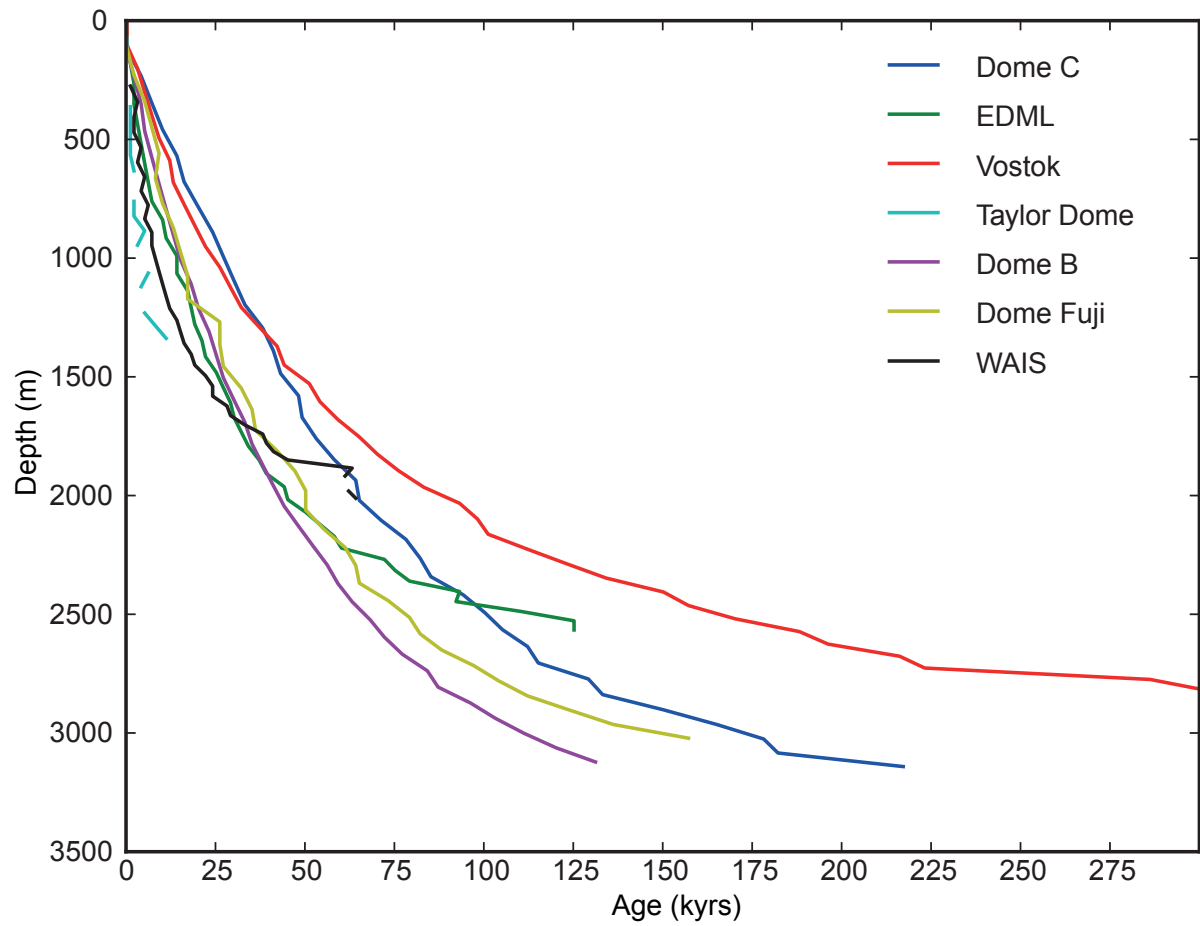


Figure 8.9: Age-depth relationship for the deep tracers simulated in the present day equilibrium simulation.

Antarctic Ice Sheet Evolution in the Miocene

The middle Miocene climate transition (MMCT) ca. 14.2 to 13.8 million years ago [Shevenell et al., 2004] marks a substantial cooling of Cenozoic climate and the growth of an Antarctic Ice Sheet (AIS) to present day dimensions [Zachos et al., 2001, Billups and Schrag, 2002, Shevenell et al., 2004, Mudelsee et al., 2014]. While the causes for the cooling and growth of the AIS are still under debate, a combination of $p\text{CO}_2$ drawdown [Zachos et al., 2001, Foster et al., 2012, Badger et al., 2013], insolation [Holbourn et al., 2005, Holbourn et al., 2013, DeConto et al., 2007], and major changes in the global ocean circulation are identified as key drivers. The systemic effects of mid-Miocene AIS growth, i.e. its feedbacks on atmospheric and oceanic circulation, are investigated both for the MMCT [Knorr and Lohmann, 2014] and the Eocene-Oligocene Transition (EOT ca. 33 ml. years BP) [Goldner et al., 2014] and show a substantial influence of the AIS on Southern Hemisphere climate. Further processes affecting Southern Hemisphere cooling could be tectonic changes in the Tethys [Hamon et al., 2013] and Drake gateways. While the effects of different AIS configurations and south polar ice sheet advance have been studied with fully coupled AOGCMs (e.g. [Knorr and Lohmann, 2014]), a dynamic coupled ice sheet element is still missing in the analysis. In this chapter 3D ISM sensitivity experiments, investigating the role of different Miocene climate boundary conditions and bedrock reconstructions on the dynamics of the mid-Miocene AIS evolution, are presented. The results suggest that the main control on AIS advance is the available bedrock surface above sea level and the moisture transport towards the continent, while temperature changes play only a minor role. This relationship holds as long as temperatures are low enough to allow for an initial ice sheet.

9.1 Experimental Design

The growth of the AIS under a suite of mid-Miocene boundary conditions is investigated. Three different mid-Miocene climates simulated by COSMOS [Knorr and Lohmann, 2014, Knorr et al., 2011] are used as climate forcing (in the following denoted as MI, MII, MIII Figures 9.1 and 9.2). To investigate the effect of both Southern Hemisphere climate and the range of potential Antarctic topographic configurations, the initial bedrock condition is varied for all climate scenarios (PD, PDr, Wmin, Wmax see Figure 9.3). The bedrock topographies used here are the present day topography (PD) [Brocq et al., 2010], a

relaxed present day bedrock configuration after removing the ice load (PDr), and two Miocene bedrock reconstructions (W_{min} , W_{max}) [Wilson et al., 2012]. This bedrock setup is identical to [Wilson et al., 2013] but extended by the present day bedrock configuration. MI is forced with a pCO_2 of 450 ppm and an AIS with a quarter of the mean present day ice sheet surface. MII uses a pCO_2 of 450 ppm as well, but a present day AIS, while MIII uses the present day ice sheet with a pCO_2 of 278 ppm.

Exp	AIS	pCO_2	Spin up (kyr)	Mean (yr)
M I	$PD_{\frac{1}{4}}$	450	2	100
M II	PD	450	2	100
M III	PD	278	2	100

Table 9.1: Overview over the three Miocene COSMOS simulations. The second column denotes the topographic Antarctic boundary conditions, PD being the present day ice sheet, $PD_{\frac{1}{4}}$ an Antarctic Ice Sheet with a quarter of the present day ice sheet surface elevation. Third column denotes atmospheric pCO_2 concentration. Column four is the integration time for the simulation spin up, while column five is the mean climatology used as forcing in the ISM simulations.

Southern Ocean temperatures (Figure 9.1), precipitation (Figure 9.2) and the number of days per year with surface temperatures above zero (which are essential for the occurrence of surface melt events) vary considerably between the climate scenarios. The reduced surface elevation in MI (25% of the present day surface elevation) has drastic effects on sea surface temperatures, surface air temperatures and precipitation. The increase in surface elevation in MII leads to a cooling of air temperatures in central Antarctica, while circumantarctic temperatures generally increase. The cooling over the ice sheet in MII is reflected in lower precipitation above the AIS (Figure 9.2), while circumantarctic temperatures increase in MII leading to a significantly warmer SST (see Figure 9.1 a)). The larger AIS in MII does not effect sub-surface Southern Ocean temperatures, which are very similar both in MI and MII. However, in MII the ocean temperature close to the FRIS and RS warms due to warmer surface temperatures. As the water temperature in the West Antarctic ocean basins is the determinant for the formation of a marine ice sheet-shelf in this region (see chapters 3 and 6), ice-ocean interactions in the MMCT could be the decisive factor controlling WAIS dimensions. It will be shown later, that the concomitant high pCO_2 concentration and AIS surface elevation in MII have a major influence on Weddell Sea ice shelf formation.

MIII is the coldest of the three climate scenarios, which is expressed in Southern Ocean temperatures generally 1 – 2°C cooler than MI and MII throughout the water column (Figure 9.1). Large scale precipitation above Antarctica is greatly reduced in MIII compared to the MII and MI, but still generally twice or triple the present day surface mass balance (resembling the precipitation-temperature relationship for Antarctica [Frieler et al., 2015]). Both pCO_2 and growth of the AIS have a large impact on the global and Southern Hemisphere climate. The feedbacks of AIS changes on ocean and atmospheric circulation are not fully represented in the COSMOS simulations, as only ice sheet surface but not extent (hence albedo) have been changed between MI and MII. This means that the main effect influencing surface temperatures is due to a more pronounced lapse rate cooling in MII and MIII. An initially ice-free Weddell-Sea for example would intensify the differences between MI and MII. Further, dynamic changes of ice sheet elevation, extend and especially ice-ocean feedbacks in the ice shelf cavities are not yet accessible in global climate simulations and thus not included here.

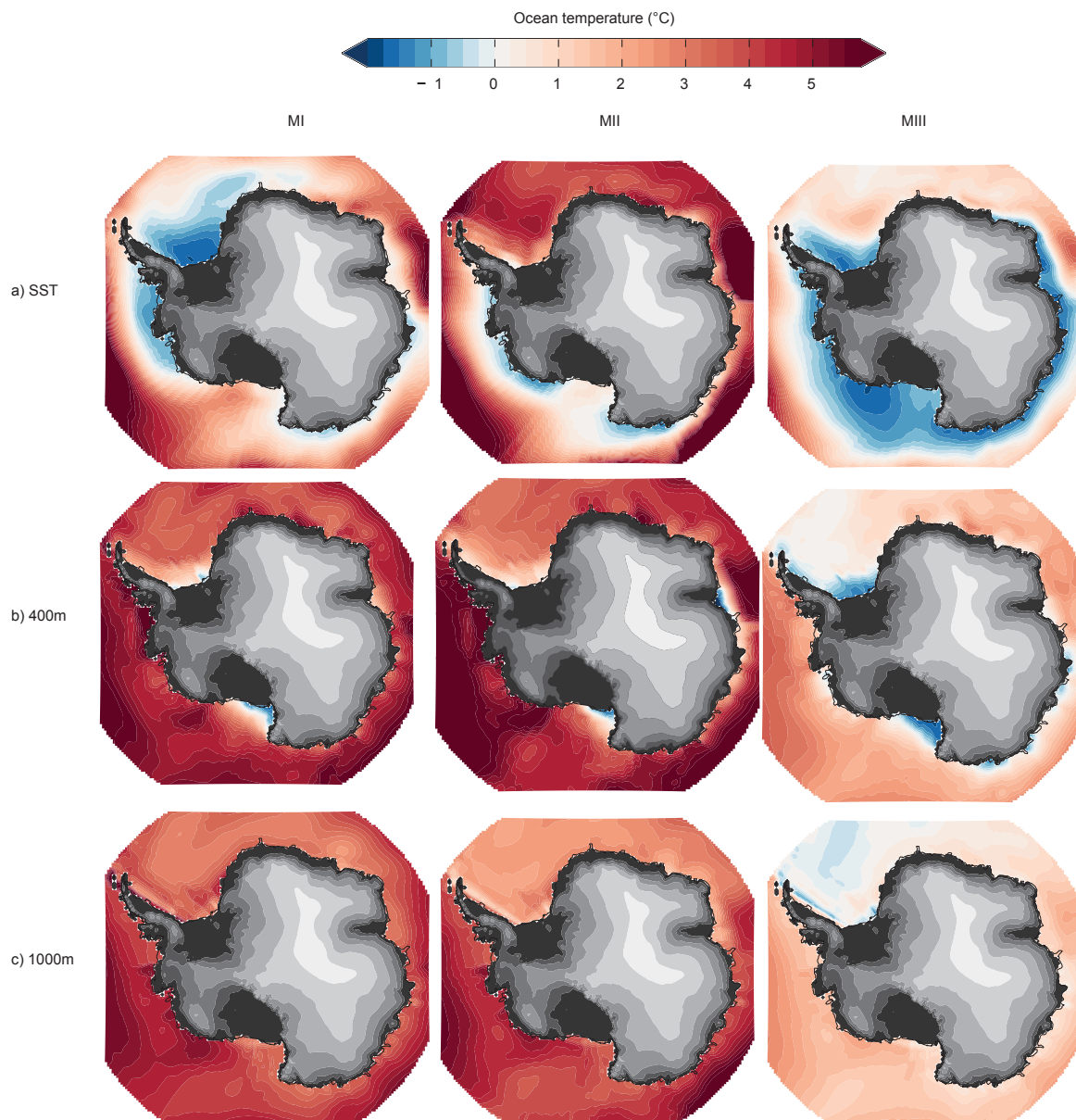


Figure 9.1: Miocene Southern Ocean temperatures simulated by COSMOS [Knorr and Lohmann, 2014] (SST, 400m, 1000m). MI (25% Antarctic surface thickness, $p\text{CO}_2$ 450 ppm), MII (present day Antarctic Ice Sheet thickness, $p\text{CO}_2$ 450 ppm), MIII (present day Antarctic Ice Sheet surface thickness, $p\text{CO}_2$ 278 ppm).

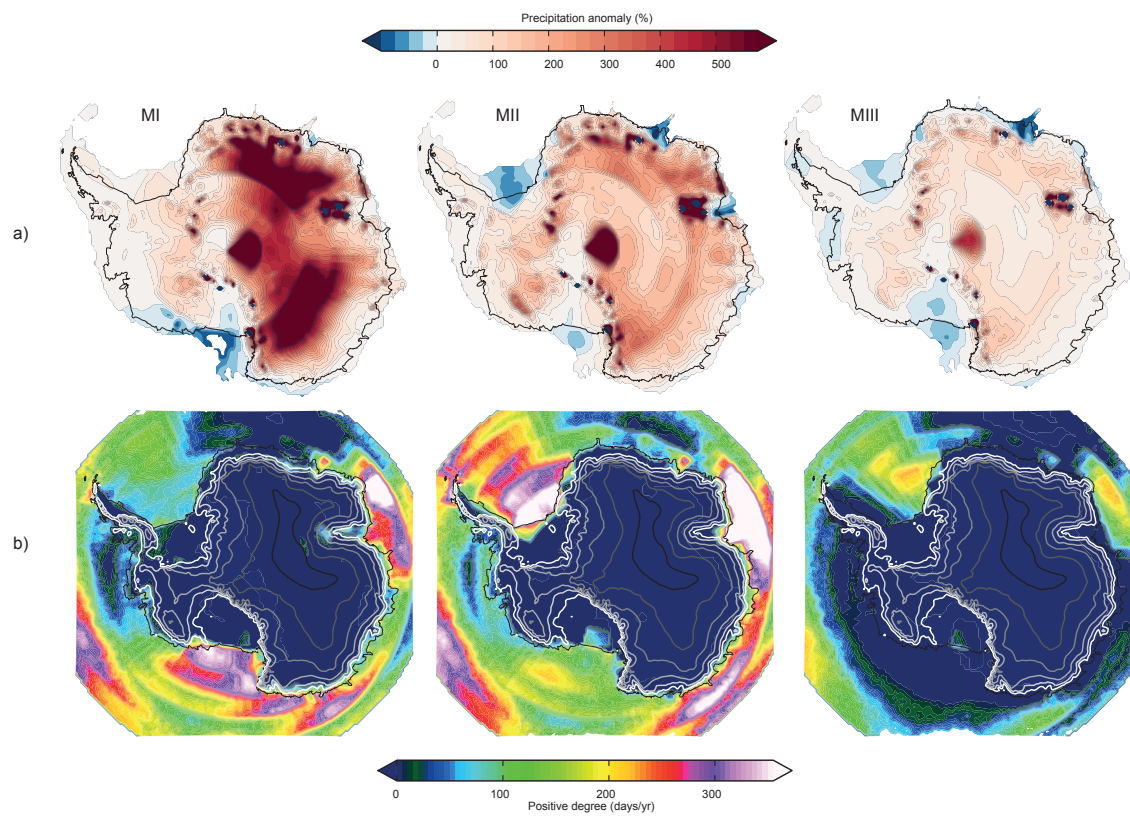


Figure 9.2: a) Miocene precipitation anomalies. b) Miocene positive degree days. MI (25% Antarctic surface height, $p\text{CO}_2$ 450 ppm), MII (present day Antarctic Ice Sheet volume, $p\text{CO}_2$ 450 ppm), MIII (present day Antarctic Ice Sheet volume, $p\text{CO}_2$ 278 ppm).

The second factor which affects mid-Miocene AIS growth considerably is the available bedrock area above sea level. As temperatures in the MMCT cool down sufficiently to allow a large ice sheet on the Antarctic continent, while ocean temperatures are still warm (i.e. more than 2°C above the present day temperature distribution, the approximate viability limit for a West Antarctic Ice Sheet extending into the marine bedrock regions (see chapter 3)), the available bedrock area above sea level is the decisive variable limiting the AIS Miocene advance. Since high ocean temperatures confine the grounded ice sheet to land above sea level the choice of initial bedrock conditions will greatly affect the final equilibrium mid Miocene ice sheet size.

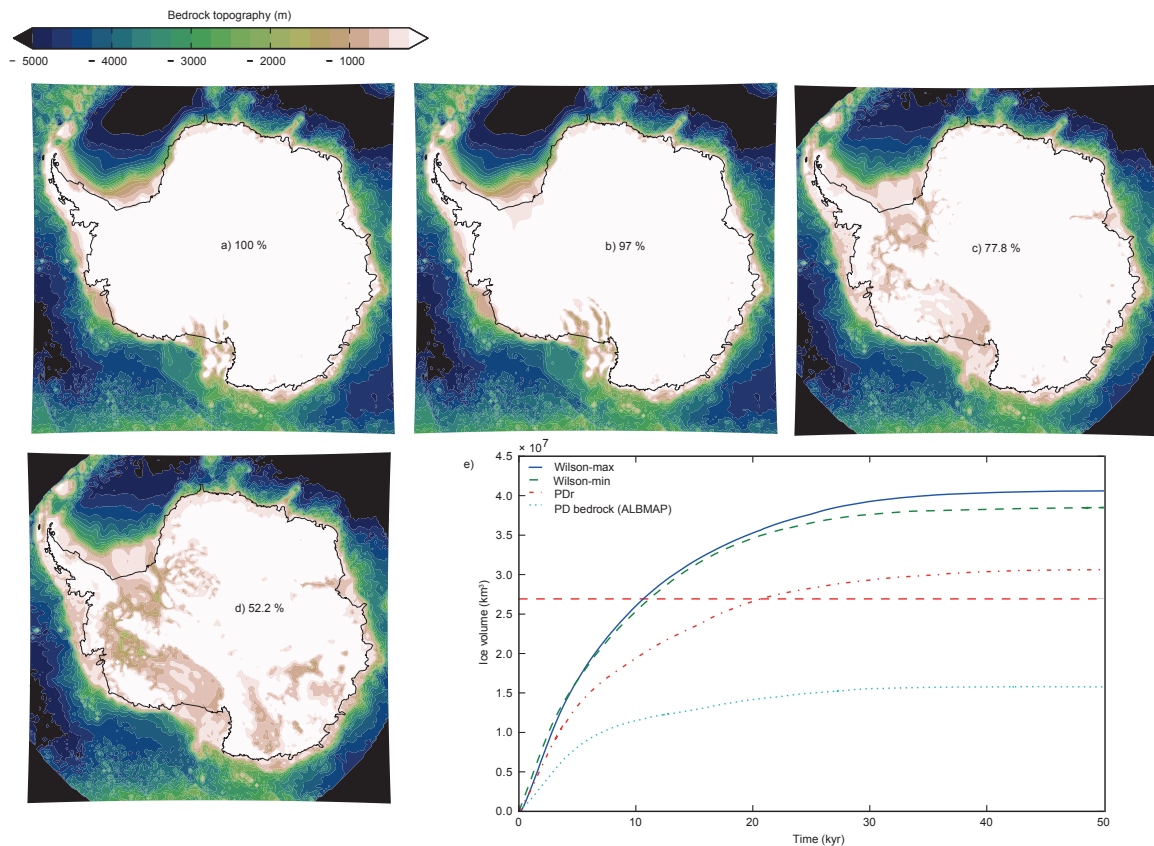


Figure 9.3: This figure illustrates the effect of the choice of initial bedrock topography on Antarctic Ice Sheet extent and volume in the mid-Miocene. Four different topographies are used, the bedrock reconstructions of Wilson et.al [Wilson et al., 2012] (max and min), a relaxed present day bedrock (after removal of the present day AIS), and the present day bedrock (ALBMAPv1 [Brocq et al., 2010]). The numbers in the figures denote the available land above sea level area relative to the Wilson-max reconstruction. e) shows the AIS volume evolution in the equilibrium simulations based on the climate forcing from MII for the different bedrock reconstructions a)-d).

9.2 Bedrock vs. Climate

As soon as the summer surface temperature viability limit for an ice sheet is crossed, the advance of the AIS in the Miocene ultimately depends on three factors : the Southern Ocean temperature, the humidity transported onto the continent and finally the available land above sea level. The first factor, the ocean

temperatures, function as a switch that either allow for grounding line migration into the marine basins of West and East Antarctica or not, greatly affecting the lateral extent of the ice sheet. The COSMOS climate used in this study yields ocean temperatures which confines the AIS to the available land above sea level (see Figure 9.5). While large ice shelves develop¹, a marine ice sheet in West- and East Antarctica can not evolve. Therefore surface mass balance and bedrock configuration are the controlling factors of AIS size (see Figure 9.5). Surface mass balance is dependent on the amount of water vapor transported towards the continent, which increases with rising temperatures [Frieler et al., 2015], resulting in larger ice sheets in warmer climates, which sounds counterintuitive at first glance, but makes sense as long as the summer surface temperatures stay below a critical limit which prevents extensive surface melt events. The available spread in climate conditions provided by the three COSMOS simulations used here, allows for a range of Antarctic equilibrium ice sheet volumes lowering sea level by $\approx 28 - 40\text{m}$ compared to PD (in the Wilson max case). This already considerable spread of ca. 12m. is somewhat dwarfed by the effect of the choice of initial bedrock conditions, which accounts for ca 50m difference in sea level (see Figures 9.6, 9.4 and 9.7). These results clearly illustrate the importance of well constrained initial boundary conditions for paleo ice sheet modeling in general and specifically for the MMCT and Antarctic inception.

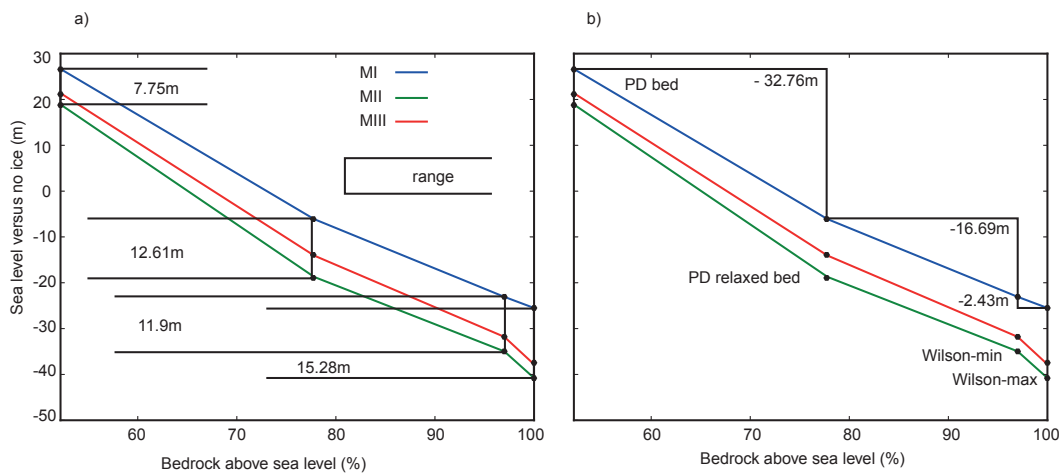


Figure 9.4: This figure illustrates the effect of the choice of initial bedrock topography and climate forcing on Antarctic Ice Sheet volume (expressed in meter sea level equivalent) in the mid Miocene. Four different topographies are used, the bedrock reconstructions of Wilson et.al [Wilson et al., 2012] (Wmax and Wmin) representing 100% land above sea level (the reference land area) and 97%, a relaxed present day bedrock with 77.8% (after removal of the present day AIS), and the present day bedrock [Brocq et al., 2010] with 52.2% i.e. roughly half of the land area above sea level compared to Wmax. The numbers in graph a) denote the changes in sea level between the climate forcings MI and MIII. Numbers in b) depict the changes in sea level under the same climate forcing but for the different topographic boundary conditions.

¹In contrast to the simulations in [Wilson et al., 2013], which are focused on the EOT, resulting in higher ocean and surface temperatures.

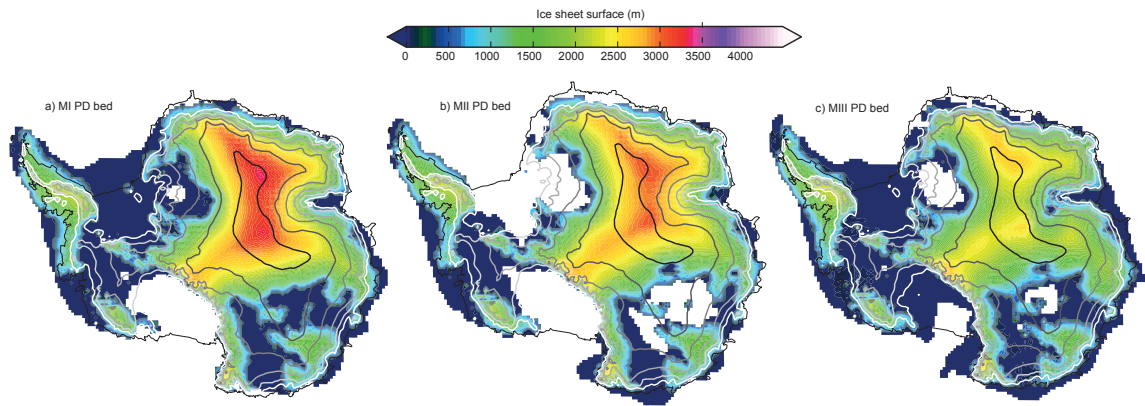


Figure 9.5: Sensitivity of the equilibrium Antarctic Ice Sheet volume to different climate conditions (MI,MII,MIII) for present day relaxed bedrock conditions.

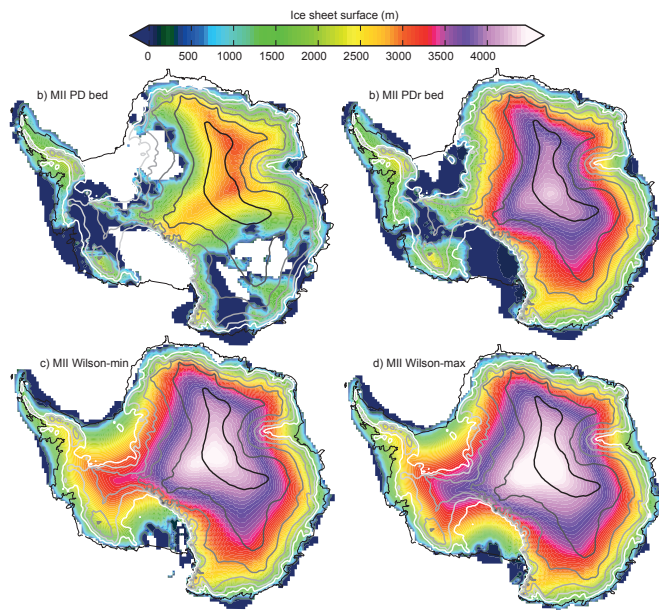


Figure 9.6: Sensitivity of the equilibrium Antarctic Ice Sheet volume to different bedrock reconstructions (PD, PD relaxed, Wilson-min,Wilson-max) under MII climate conditions.

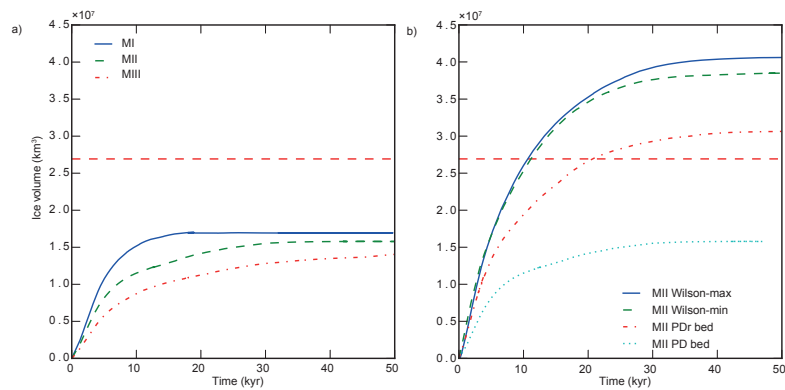


Figure 9.7: Sensitivity of the equilibrium Antarctic Ice Sheet volume to different climate (a) and bedrock (b) conditions. Present day bedrock in a), MII forcing in b).

9.3 Mid-Miocene AIS Dynamics Driven by Bedrock Configuration and Precipitation

The results of this study suggest that accelerated growth of the AIS in the MMCT was largely controlled by the available land above sea level and the containment of the ice sheet to the latter due to a warm Southern Ocean preventing the formation of a marine ice sheet in East and West Antarctica. Under those conditions, the mid-Miocene AIS growth and final volume mainly depends on the accumulation pattern and distribution. It is intuitive that the inception of the AIS in the EOT [Wilson et al., 2013, Goldner et al., 2014] was triggered by a cooling atmosphere, reducing the summer melt to coastal areas and allowing for the growth of a substantial ice sheet in the interior of the continent. A growing ice sheet would then further cool the atmosphere via the albedo and lapse rate effect fueling its own growth and further influence Southern Ocean circulation [Knorr and Lohmann, 2014, Goldner et al., 2014]. For the MMCT discussed here, provided that surface temperatures were below zero for most of the year and throughout the continent, the warmer the climate the higher the Antarctic surface mass balance². This leads to the largest ice sheets under the warmest AOGCM forcing. However, for the inception of an AIS ultimately atmospheric cooling and subsequently the cessation of significant surface melting are the determining factors. The experiments carried out in this study are forced by COSMOS climate using present day AIS with smaller surface elevations. This means that surface temperatures and especially summer surface temperatures might be underestimated, or rather correspond to a mid-Miocene climate, where an ice sheet with an extent similar to today's ice sheet has already formed. In a next step the effects of a continent bare of ice on the MMCT and EOT climate shall be investigated. The forcing attained in this way will then be used to carry out the same sensitivity experiments as laid out above, investigating the effects of bedrock topography and climate on the EOT Antarctic inception and MMCT AIS growth with a more realistic pre-present day AIS mid-Miocene climate forcing. This study shows that within the range of uncertainties considering bedrock reconstructions there is a wide realm of possible mid-Miocene Antarctic Ice Sheet configurations (corresponding to differences in sea level of about 50m). The difference in sea level equivalent ice volume corresponding to the three climate forcings applied here are up to five times lower (ca 10m). Compared to the EOT equilibrium ice sheets simulated in [Wilson et al., 2013], the MMCT AIS is generally large in this study. This is due to the lower $p\text{CO}_2$ values used here (278 & 450 compared to two times pre-industrial levels, $\sim 520 - 560$ in [Wilson et al., 2013]), the initial AIS boundary conditions and the different representation of ocean dynamics in this study.

²Due to an intensification of the hydrological cycle.

Conclusions

This thesis provides an in-depth ice sheet modeling perspective on Antarctic Ice Sheet (AIS) dynamics under various climate conditions, ranging from glacial to extreme warm times. Recurring themes, characteristic of the unique geography of Antarctica, dominate AIS dynamics throughout geologic time scales. The marine setting of the West Antarctic Ice Sheet (WAIS) is a determining factor of AIS growth and retreat. While surface temperatures and precipitation control the long term shape of the ice sheet, its interactions with the Southern Ocean can cause dramatic changes within centuries. The paleo-climate dynamics of the AIS bear witness of potential future developments in the high southern latitudes which could affect the shape of the planet for millennia to come.

This thesis has shown, that the WAIS has undergone tremendous changes during the last glacial cycle, lowering and raising sea level by up to ca. $\sim 17\text{m}^1$, with growth and retreat rates far exceeding the ones measured during the recent decades. The WAIS played and will play a key role in these dynamics, thus it is crucial to promote both, the current model understanding of ice sheet dynamics, as well as the proxy based understanding of past climate variations in the region.

Deeper in the past, in the Pliocene and Miocene, AIS dynamics are much less understood than in the Quaternary. Moreover, a conclusive model based constraint on AIS volume during this period is not possible at this stage. Of interest however, are results attained in this thesis which show a much stronger influence of bedrock topography on AIS evolution during the Mid-Miocene Climate Transition (MMCT) than in the Quaternary. Further ice sheet-climate interactions must be incorporated in the model based analysis of such dramatic climate transitions to access the full range of feedback processes. The results for the Pliocene AIS dynamics are inconclusive at this point and strongly depend on the initial conditions of the ice sheet model (ISM). Here, more proxy based regional climate reconstructions are needed to further constrain the ISM forcing.

The following sections summarize the main findings of the research questions outlined in the introduction.

¹ $\sim 3 - 5\text{m}$ Last Interglacial (LIG) sea level rise versus $1 - 12\text{m}$ neagtive contribution in the Last Glacial Maximum (LGM).

10.1 Antarctic Ice Sheet Dynamics and Sea Level Contribution in the Last Interglacial

The first question posed in this thesis, was addressed at the potential collapse of the WAIS in the LIG and its underpinning processes and drivers [Sutter et al., 2015a]. While the LIG is a well studied climate interval [Lunt et al., 2013, Otto-Bliesner et al., 2013, Bakker et al., 2014], the Antarctic contribution to the high sea level at the time is still largely unknown. Global sea level was up to 7 – 9m above present day levels [Kopp et al., 2013, Dutton et al., 2015], though mean surface air temperatures only increased by 1 – 2°C [Otto-Bliesner et al., 2013]. The combined contributions of the Greenland ice sheet, ocean thermal expansion and land based glaciers probably did not exceed 4m [Dahl-Jensen et al., 2013, McKay et al., 2011, Marzeion et al., 2012]. The disparity between these contributions and sea level proxy reconstructions could have only been closed by substantial retreat of the AIS². Understanding the dynamic evolution of the AIS in the LIG is invaluable in for the outlook on future climate change, which may far exceed the last warm time. So how did the AIS change during the LIG?

This question was addressed by a combination of 3D ice sheet modeling and a transient climate forcing generated from COSMOS simulations ([Stepanek and Lohmann, 2012, Pfeiffer and Lohmann, 2015]), extrapolated in time via an ice core based glacial index. Employing this method, current model based understanding of LIG climate was used to force the ISM. The time frame chosen covers the onset of the last interglacial³ at 131.5 kyr before present (BP) and ends at the year 116.5 kyr BP. While two different COSMOS outputs using different boundary conditions have been used, both did not force the WAIS into a configuration in which the Marine Ice Sheet Instability [Schoof, 2007] (MISI) can be triggered. The choice of the Greenland ice sheet surface elevation in COSMOS seems to affect the Southern Hemisphere climate considerably, with significant increases in both ocean temperature (ca. 0.5°C throughout the water column) and precipitation (ca. +20%). While surface temperatures are higher as well, they never exceed or get close to zero degree for most of the continent. This excludes surface melting as one of the reasons for WAIS collapse.

The processes behind the influence of the Greenland topography on the Southern Hemisphere climate are not clear yet. The COSMOS simulations do not include an interactively coupled ice sheet component, which would allow for changes in freshwater flux, albedo or lapse rate effects influencing e.g. the Atlantic Meridional Overturning Circulation (AMOC) strength and therefore the Southern Hemisphere via the bipolar seesaw [Barker et al., 2011]. In the model setting used in this thesis, only the initial surface temperature via the lapse rate effect and wind patterns are dynamically affected due to the lower Greenland elevation. It is further worth mentioning that the differences in Southern Ocean temperatures between the two climate time slices are smaller than the differences between some Atmosphere-Ocean General Circulation Models (AOGCMs) for the PD. This illustrates that there is still need for improvements of AOGCMs.

It is evident that surface mass balance changes in the LIG could not have caused a collapse of WAIS. The

²A collapse of the WAIS can raise global sea level by more than 3m [Bamber et al., 2009].

³Defined as the time at which the Deuterium isotope concentrations at Dome C [Jouzel et al., 2007] reached present day values after the pen-ultimate glacial.

increased precipitation above the continent due to atmospheric warming [Frieler et al., 2015, Thomas et al., 2015] actually would have had the opposite effect, namely stabilizing the WAIS. Increased ice shelf melting due to a warming Southern Ocean is the remaining candidate for tipping WAIS into an unstable configuration, leading to runaway grounding line retreat via the MISI. Indeed a Southern Ocean warming threshold of 2 – 3°C was found to be sufficient to thin ice shelves sufficiently to trigger the MISI in the catchment areas of the Filchner Ronne Ice Shelf and the Glaciers draining into the shelves of the Amundsen Embayment⁴. The resulting runaway retreat raises sea level by 3 – 4m, strengthening the hypothesis that the AIS played a major role in LIG sea level rise.

Another interesting result from this study is the intrinsic dynamics of LIG WAIS collapse, which unfolds in two distinctive decay phases. Southern Ocean warming, bedrock topography and ice sheet elevations are the key factors, modulated by changes in precipitation, which lead to a double peak in Antarctic LIG sea level contribution. A twin peak LIG sea level has been proposed in a recent proxy based study [Kopp et al., 2013]. Such a sea level variation might have been at least partly caused by the WAIS collapse dynamics found in this study. Here it is shown that LIG WAIS collapse could have been triggered by Southern Ocean warming within the range of proxy reconstructions [Capron et al., 2014]. Future Southern Ocean warming [Stocker et al., 2013] probably reaches the threshold warming for large scale WAIS collapse during the next century.

The discrepancies between the LIG COSMOS simulations [Pfeiffer and Lohmann, 2015] and proxy data [Otto-Bliesner et al., 2013, Capron et al., 2014] and the range of AIS evolution depending on the LIG forcing applied in the ISM [Sutter et al., 2015a] illustrate the limitations of current proxy and model understanding. While this study provides Southern Hemisphere warming thresholds for WAIS collapse in the LIG, they need to be corroborated by further studies based on more accurate reconstructions of LIG climate as well as an improved ISM framework. From a climate modeling perspective further refinement of polar ocean circulation and its interactions with a dynamic ice sheet component are needed. This goes beyond increasing the spatial resolution of AOGCMs. A coupled ice sheet component is a prerequisite to accurately simulate high latitude climate change such as the LIG warming⁵. From an ISM point of view, a more realistic process based representation of ice shelf-ocean interaction must be aspired. Ice sheet models suffer from lack of sufficient data coverage of ocean temperatures and heat transport inside the Antarctic ice shelf cavities. Simulated, parameterized or prescribed ice shelf melt rates vary by up to one or two orders of magnitude, precluding a serious intercomparison between models. Standard climate forcing fields for representative time slices, first and foremost for the present day climate, should be made available, on which basis the fitness of ISMs shall be benchmarked. In such standardized simulations, the simulated ice shelf mass balances and bedrock properties should be objected to special scrutiny and compared to proxy or instrumental observations if possible. Such an approach would reveal shortcomings as well as common interpretable features of state of the art ISMs.

⁴Recent studies suggest, that this region has already been destabilized by 20th century warming [Rignot et al., 2014, Joughin et al., 2014].

⁵Coupling in this context goes beyond the inclusion of surface elevation changes, but must allow for large changes of the marine ice sheets of West and East Antarctica.

10.2 Future Antarctic Sea Level Contribution

The waxing and waning of the large polar ice sheets in past interglacials are often discussed as potential analogues for future changes of the AIS and GIS. In the LIG, moderate global warming correlated with relatively large changes in eustatic sea levels (7–9m [Kopp et al., 2013, Dutton et al., 2015]). Above, the role of the AIS in the LIG sea level rise is discussed (see chapter 3). How will the AIS respond to future warming? Will the current trend of accelerating glaciers and thinning ice sheets in the WAIS [Rignot et al., 2014, Joughin et al., 2014] persist in future decades? Will the mass gain of the EAIS offset the losses in West Antarctica [Zwally et al., 2015], or will the marine ice sheets in the Wilkes and Aurora Basins be destabilized as well [Mengel and Levermann, 2014, Fogwill et al., 2014, Greenbaum et al., 2015]? Can increases in precipitation in a warming world [Frieler et al., 2015] stabilize the WAIS?

In chapter 4 future AIS dynamics under a suite of warming scenarios based on the 5th Assessment Report of the IPCC [Stocker et al., 2013] are investigated [Sutter et al., 2015a]. Simple linear warming ramps of the Southern Ocean peaking at warming between 1 and 3°C, accompanied by uniform surface air temperature warming of 6°C and increases in precipitation of 10–40% until the year 2200 are applied (denoted by 2°_10%–3°_40%). This range is similar to the upper limit of IPCC warming scenarios. An additional scenario captures extreme warming going beyond the IPCC projections. In this scenario the Antarctic ice shelves quickly collapse (e.g. driven by enhanced calving and surface-subsurface melting) within the next decades.

The predictions of future AIS dynamics under the IPCC-like scenarios suggest a partial collapse of the WAIS unfolding over several millennia, raising sea level by up to 2m (peak yearly Antarctic contributions to sea level rise reach $\sim 2\text{mm} \cdot \text{yr}^{-1}$ i.e. $20 \frac{\text{cm}}{\text{century}}$). However, the scenarios assuming strong increases in precipitation show a negative Antarctic contribution to sea level during the next one or two centuries. Later, the increased coastal thinning of the ice sheet due to warm ocean currents overcomes the volume increase caused by increases in precipitation. The initial sea level lowering is quite small and would not offset the projected contributions from the Greenland Ice Sheet. These results suggest minor contributions to sea level rise during the next centuries compared to the expected contribution by melting of the Greenland ice sheet.

Should the Antarctic ice shelves indeed quickly melt and break off within decades⁶, the ISM results indicate a dramatic collapse of the WAIS within a few centuries, with dire consequences for coastal communities worldwide. AIS annual sea level contribution would catapult to several millimeter per year, surpassing the combined annual contributions of Greenland, Glaciers, thermal expansion and Antarctica during the last decade, culminating in meter sea level rise during the next millennia. The results of this study mostly agree with predictions from similar ISMs [Winkelmann et al., 2015, Ritz et al., 2015] for the extreme scenario and moderate scenario. However, lower AIS sensitivities to Southern Ocean warming than in [Golledge et al., 2015] are calculated here, which is probably due to the more extensive tuning of basal properties in the Parallel Ice Sheet Model (PISM e.g. [Golledge et al., 2013]), the higher

⁶Caused e.g. by a combination of hydrofracturing and subsequent calving and increased surface-subsurface shelf melt as suggested in [Pollard et al., 2015].

resolution (10km versus 40km used in this study) and differences in the treatment of the grounding line⁷. Sub-shelf melt rates are often not shown in ISM studies predicting future AIS dynamics [Winkelmann et al., 2015, Ritz et al., 2015, Golledge et al., 2015], impeding comparisons between studies. This is bad practice as [de Boer et al., 2015] have shown that ISM intercomparison studies can unravel drastic differences between ice sheet models (see the last section of this chapter for a more detailed discussion of current ice sheet models). No conclusive ISM based statement about future behavior of the AIS under global warming can be made at this point, as too many processes e.g. of ice-ocean interactions and grounding line migration are not sufficiently incorporated in both ISMs and AOGCMs.

Yet, most models suggest a lock-in of a large scale WAIS collapse [Sutter et al., 2015a, Winkelmann et al., 2015, Golledge et al., 2015, Ritz et al., 2015, Feldmann and Levermann, 2015] in case of failing mitigation strategies reducing greenhouse gas emissions. The timing of this collapse differs widely in between scenarios and ISMs applied, ranging from a century to several millennia. Further improvements of process based understanding, especially of ice-ocean interactions and grounding line dynamics, is needed as well as homogenized scenario designs (with respect to the applied climate forcings) and parameterizations. ISM development must remain unconstrained and in a state of constructive competition, while standardized scenario designs should provide the basis for periodic reviews of ice sheet model fitness.

10.3 The Antarctic Ice Sheet in the Pliocene

Constraining the size of the AIS in the late Pliocene warm period is a difficult endeavor, as proxy data on AIS extent is virtually non existent and only indirect conclusions can be drawn from marine sediment data. However, the period between 3.264 to 3.025 million years BP, also known as the PRISM interval [Dowsett et al., 2010], is well studied by both climate models [Dolan et al., 2011, Haywood et al., 2013] and data [Salzmann et al., 2013, Dowsett et al., 2013], estimating global temperatures between 1.83 and 3.60°C warmer than pre-industrial levels. This makes the PRISM interval an excellent candidate for studying a climate in the past with similar climatic conditions as those to be expected in the future.

Late Pliocene sea level is estimated at 10 – 30m above present day [Raymo et al., 2011, Rovere et al., 2014, Rohling et al., 2014]. These estimates are uncertain, e.g. due to unknown tectonic processes and glacial isostatic adjustment [Rowley et al., 2013]. Nevertheless, large contributions from the GIS and AIS are required to reach the sea levels suggested by proxy data. The Pliocene Ice Sheet Modeling Intercomparison Project (PLISMIP) sets out to constrain AIS dimensions in the late Pliocene to improve the interpretation of Pliocene sea level data from an ice sheet modeling vantage point. Six numerical ice sheet models were employed in this study. The experimental setup includes five different scenarios, two of which are present day control runs (forced by HadCM3 and ERA40 re-analysis data), the other three are staged in the Pliocene. While all ISM could reproduce an AIS similar to the present day shape in the control runs, relatively large discrepancies are evident in the ice sheet volume. The spread results in sea level contributions between the models for the present day climate forcings (HadCM3 and ERA40)

⁷Further Golledge et. al. employ a different basal shelf melting scheme [Holland and Jenkins, 1999], based on Southern Ocean temperatures derived from a coarse resolution ocean model while not mentioning the method with which sub-shelf ocean temperatures are retrieved (the ocean model only calculates ocean temperatures up to the fringes of the Antarctic sea ice coverage).

of $0.00 \pm 6.1\text{m}$ s.e. for Bedmap1 and $-1.9 \pm 4.9\text{m}$ s.e for Bedmap2.

The Pliocene equilibrium simulation with an initial present day ice sheet yields sea level equivalent volume changes of -3.7 ± 2.2 (Bedmap1) and -1.5 ± 1.5 (Bedmap2). Here, the sensitivity of the shelf melt parameterizations and grounding line migration schemes in the different ice sheet models becomes apparent. The model spread under *identical* climate forcing is as large as $\sim 18\text{m}$. PISM and RIMBAY are farthest apart, probably resembling the higher shelf melt rates, more slippery bedrock and different grounding line treatment employed in PISM. Positive sea level contributions are simulated in all Pliocene simulations with an initial Pliocene AIS (resembling a small ice dome in East Antarctica, PRISM3 reconstruction [Dowsett et al., 2010]). However, the smaller ice sheets simulated for this Pliocene simulation are largely caused by a warm Southern Ocean preventing expansion of the AIS into the Antarctic ocean basins in the Weddell and Ross Sea. Thus the final equilibrium ice sheet volume strongly depends on the initial configuration of the AIS.

Specific conclusions about Pliocene AIS extent and volume can not be drawn from PLISMIP as the spread between the ISMs is simply too large. The PLISMIP study [de Boer et al., 2015] calls for further ice sheet model intercomparisons, with refined experimental design which has to identify uncertainties deriving from different AOGCM forcings and distinguish them from uncertainties deriving from parameterizations of basal shelf melting and grounding line migration. Using the same sub shelf melting and surface mass balance schemes in all ISMs (at least in intercomparison studies) would allow for identification of ice sheet dynamic effects [de Boer et al., 2015].

10.4 The Antarctic Ice Sheet in the Last Glacial Maximum

The last glacial cycle (ca. 130.000 until ca. 10.000 years BP) is the best constrained climate interval, with a relatively large coverage of well dated proxy data from ice cores [Jouzel et al., 2007], marine sediment data [Capron et al., 2014, Bentley et al., 2014], tree rings, speleothems and other. However there are considerable knowledge gaps especially considering the timing and extent of the AIS's glaciation and the driving mechanisms behind the deglaciation [Bentley et al., 2014]. How fast did the AIS re-advance after the LIG? What was the antarctic contribution to LGM sea level depression⁸?

This study investigates both glaciation and deglaciation based on ice sheet modeling using COSMOS climate forcing [Stepanek and Lohmann, 2012, Pfeiffer and Lohmann, 2015] and ice core data [Jouzel et al., 2007]. A special focus lies on marine ice sheet dynamics driven by Southern Ocean circulation and temperature changes. Further effects of different sliding mechanisms on the glaciation of the marine sectors of the AIS are analyzed.

It is found that glaciation of the AIS is largely controlled by the advance of grounded ice sheets into the Weddell and Ross sea sectors. This advance is ultimately driven by the glacial cooling of the Southern Ocean. Since glacial climate is generally dryer than during warm periods, less humidity is advected onto

⁸Global sea level has been ca. 120m lower than present day, mostly due to the build up of large northern hemisphere ice sheets.

the AIS, reducing precipitation. However the large fall of sea level, rooted in the formation of vast ice sheets in the northern hemisphere, grounds previously floating ice shelves. Simultaneously the cooling of the Southern Ocean favors the formation of thick ice shelves which buttress their tributary glaciers. This ice shelf thickening slows down the ice flow in the hinterland, in turn leading to the growth of the grounded ice sheet. While precipitation decreases as the climate cools, the ocean and sea level induced ice sheet thickening leads to a slow advance of the AIS towards the continental shelf edge. Ocean temperatures act as a lever controlling the advance of the ice sheet into the marine basins previously covered by ice shelves. The dynamics of the different ice shelves are interlocked to a certain degree, as the grounding line migration in the Weddell Sea influences the ice dynamics in the Ross Sea several hundred kilometers away. A reduced glaciation of the Ross Sea can push the ocean temperature limit for ice sheet formation in the Weddell Sea to lower temperatures.

A combined assessment of proxy reconstructions [Bentley et al., 2014], other model studies [Golledge et al., 2013, Maris et al., 2014] and the simulations carried out in this study suggest a slow glaciation of the AIS culminating in a slightly larger ice sheet covering the Weddell Sea sector, which at least partly extends to the continental shelf break. The ISM results indicate a partial glaciation of the Ross Sea while it is difficult to constrain the dynamics in the ocean sectors along the smaller ice shelves (e.g. in the Amundsen Sea sector) due to the coarse resolution of the ISM. Sea level depression due to AIS growth is simulated to be between $\sim 1 - 2\text{m}$ with a more probable range of $3 - 7\text{m}$.

The results roughly agree with the findings of other model studies (e.g. [Golledge et al., 2013, Maris et al., 2014]), however further ISM studies with higher spatial resolutions, improved climate forcing and better representation of ice shelf and grounding line dynamics are needed to improve the interpretability of these results.

10.5 Antarctic Deglaciation: Towards a Holocene Antarctic Ice Sheet

How did the AIS retreat as the climate approached the current interglacial? Proxy reconstructions identify major post-LGM retreats of the AIS between 19.000 years and 9.000 years BP [Bentley et al., 2014, Weber et al., 2014]. However the processes underpinning these retreat events are unclear, as is the exact timing.

During this thesis, sensitivity studies investigating the influence of ocean warming and ice shelf dynamics on post-LGM AIS retreat were carried out. It is found that average shelf thinning rates of up to $20 - 30 \frac{\text{m}}{\text{a}}$ are necessary to trigger the MISI in the Weddell and Ross Sea. Only a fast destabilization of the ice shelves fringing the LGM West Antarctic marine ice sheets can trigger a retreat of the latter into the present day configuration. The choice of the initial LGM AIS volume and shape considerably influences the post-glacial ice sheet evolution in the ice sheet model simulations. The thickness of the LGM ice sheet extending into the Weddell-Sea is a major control factor on timing and extent of deglaciation. Generally the ice shelf melt rates calculated in the ISM do not suffice to destabilize the fringing Weddell Sea ice

shelves, thus preventing large scale ice sheet retreat. Employing high shelf melt rates, maintained for several millennia beginning at 19.000 year BP, eventually triggers a violent collapse of the Weddell-Sea ice sheet within 1.000 years. Retreat to present day grounding line positions is finished \sim 15.000 years BP, several millennia earlier than suggested by proxy reconstructions. This is indicative of re-occurring cold spells (e.g. as suggested by South Atlantic proxy data [Vazquez Riveiros et al., 2010]) slowing down the retreat of the marine LGM ice sheets.

Sensitivity studies employing higher spatial resolutions and an additional focus on basal properties (e.g. the slipperiness of the marine bed) are required to further improve the model based understanding of post-glacial AIS retreat.

10.6 Unlocking the Antarctic Climate Archive: Ice Core Simulations

Deciphering climate proxies from the past has been a revolutionary step for the field of climate science. The small changes in concentration of heavy hydrogen and oxygen isotopes measured in ice cores and marine sediments bear witness of past temperature, sea level and ice sheet changes. Due to the complex interactions, nonlinear processes and circulation patterns in the climate system continuously changing over time, holistic interpretation of the global proxy archives is a monumental task involving all kinds of scientific disciplines. In Antarctica multiple deep ice cores, extending the accessible frozen climate archive to almost 800.000 years into the past [Jouzel et al., 2007] have been drilled, expanding our knowledge about glacial-interglacial cycles [Petit et al., 1997], rapid climate change [Buizert et al., 2015], as well as the interhemispheric seesaw [Barbante et al., 2006]. Key uncertainties in the interpretation of ice core data remain however. These derive from incomplete knowledge of the depth-age and isotope-temperature relationships (the paleothermometer [Jouzel et al., 1997]) as well as topographic ice sheet changes and the dynamic nature of the hydrological cycle.

Here, an ice sheet modeling based tool is presented, allowing for the simulation of artificial ice cores [Sutter et al., 2015b]. The ice sheet model used in this study incorporates all major features of ice sheet physics, thereby simulated ice cores implicitly include the effects of transient ice dynamics (e.g. the position of the ice divide or elevation changes). When driven by variable climate forcing delivered by an AOGCM the simulated ice cores contain information on circulation changes as well. The comparison of the proxy archive attained in such simulations with real ice cores thus gives ample insights into previously unidentified processes of ice core formation. The simulations carried out in this thesis are limited to proof of concept studies, using present day equilibrium runs to establish the age-depth relationship of the AIS. The results of these simulations show the potential of the method to improve understanding of ice core records, but are not yet sufficient to draw any conclusions on the proxy data. More elaborate experimental settings, including the major climate drivers during the last glacial-interglacial cycles are required for a meaningful comparison between simulated and real ice cores. These simulations are the next step towards a realistic simulation of Antarctic ice cores, but the larger computational resources required by tracer simulations in multi-glacial cycle studies call for the employment of a parallel ISM (the ISM used in this

study [Thoma et al., 2014] is not parallelized). Application of the methods and results attained in this study on ice core simulations will improve both the benchmarking of the ISM as well as the interpretation of the Antarctic ice core archive.

10.7 The Mid-Miocene Antarctic Ice Sheet

The mid-Miocene Climate Transition (MMCT) ca 14.2 to 13.8 million years ago [Shevenell et al., 2004] spurred AIS growth, which in turn lead to additional cooling of the high southern latitudes [Knorr and Lohmann, 2014]. A general cooling of global and especially Southern Hemisphere temperatures favored the formation of a large ice sheet on the Antarctic continent. The reasons behind the MMCT Southern Hemisphere cooling are debated, but a combination of $p\text{CO}_2$ drawdown [Zachos et al., 2001, Foster et al., 2012, Badger et al., 2013], insolation [Holbourn et al., 2005, Holbourn et al., 2013, DeConto et al., 2007], tectonic changes [Hamon et al., 2013] and ice-ocean interaction triggered by a growing ice sheet [Knorr and Lohmann, 2014, Goldner et al., 2014], were the probable drivers of AIS growth [Wilson et al., 2013]. Similar processes are suggested for the Eocene-Oligocene Transition [Goldner et al., 2014]. The effects of AIS growth on MMCT climate have been studied with COSMOS [Knorr et al., 2011, Knorr and Lohmann, 2014].

Here the main drivers of ice sheet growth and extent in the Miocene cold reversal are identified by forcing an ISM with the MMCT climate conditions attained in those studies. The effect of different initial bedrock conditions [Wilson et al., 2012] and different climate forcings are investigated in equilibrium runs. This provides a quantitative measure of the climatic and topographic imprint on the mid-Miocene AIS volume and extent. The study shows a dominating bedrock topography influence on AIS growth, while the fingerprint of different climate forcings is evident but considerably smaller. Four different bedrock topographies are applied varying in the land fraction above sea level. The largest initial topography is taken from [Wilson et al., 2012], with twice the land area above sea level compared to present day conditions. Applying the same climate in these two scenarios results in a difference of almost 30 million km^3 ice volume or a sea level equivalent of $\sim 52\text{m}$ (ca. 22m sea level rise with present day bedrock conditions, and ca 34m sea level drop for the maximum bedrock elevation from [Wilson et al., 2012]). The variation for the different Miocene climate forcings employed is much smaller, amounting to maximal 15.28m which is still a substantial range.

As Southern Ocean temperatures in the mid-Miocene are still high compared to present day values, the AIS is largely constrained to the land fraction above sea level, while extending its reach in the form of large ice shelves. The warm Southern Ocean keeps the grounded ice sheet at bay, therefore the volume of the terrestrial ice sheet is controlled by precipitation and evaporation, the latter being negligible due to sub-zero temperatures almost all over the ice sheet (which is due to the choice of initial ice sheet conditions, being identical to the present day ice sheet extent in the COSMOS simulations). The modeling results highlight the importance of constraining boundary conditions in paleoclimate simulations in order to draw meaningful conclusions on past ice sheet coverage. As in the Pliocene study, described in the previous section, different climate forcings for the same time slice and different topographic boundary conditions can alter equilibrium ice sheet volumes simulated by ISMs substantially. Also, large climatic changes

such as in the EOT or MMCT, which drive enormous shifts in ice sheet volumes, call for a fully coupled representation of the climate system, including a dynamic ice sheet component with sufficiently resolved ice-ocean interactions.

In a forthcoming study the effect of reduced Antarctic ice cover and $p\text{CO}_2$ on mid- and early Miocene climate and AIS dynamics are investigated. This will provide a more holistic view on the complex interactions of ice, ocean and atmosphere in the Miocene.

10.8 Using Ice Sheet Models to Reconstruct Past and Predict Future Ice Sheet Dynamics, a Cautionary Tale

While more and more physical processes and climate feedbacks are incorporated in state of the art ISMs, all still suffer from limitations with respect to both applicability to different timescales and the interpretability of the model results. The choice of an ISM depends on the application, as there is no "one size fits all" ISM yet. The physical processes underpinning ice sheet dynamics never change. More so the requirements on ISMs meant to simulate ice sheet changes on geological timescales which differ from the ones applied to e.g. multi-decadal projections.

Current ISMs, suitable for paleoclimate simulations, must be computationally⁹ efficient, while including as many physical processes as possible. Generally, multi-ensemble simulations, e.g. in parameter sensitivity studies are necessary to cover a wide spectrum of paleoclimate reconstructions, and ice sheet as well as bedrock properties. Such an approach mandates parallelized ISMs even at coarse resolutions ($\sim 40\text{km}$). Higher spatial resolutions (5 – 10km) are needed to resolve dynamics on smaller scales, e.g. the ice flow of narrow Greenland and Antarctic outlet glaciers. On the other end of the spectrum lie short term predictions of future ice sheet behavior, e.g. during the next centuries. Here resolutions of 5km are too coarse to realistically simulate ice dynamics at the ice-ocean boundary (e.g. grounding line migration or marine terminating outlet glaciers).

A whole zoo of ISMs designed either to simulate long term or short term ice sheet evolution is available, yet computational restrictions and limited understanding of marine ice and shelf dynamics still prohibit the development of an "allrounder" ISM. In the following several ISMs¹⁰ and their applications are discussed on the basis of the available literature and the experiences with the ISM used in this study.

Here, a model hierarchy based on spatial and temporal dimensions is used to discuss the models' applicability and fitness with respect to paleo ice sheet simulations. All models included here perform on two levels within this hierarchy, while none has been successfully applied at all three levels so far. In the following a list of selected publications is highlighted for each hierarchy level.

Level 1 Usually Short timescales (years to decades), sub-annual resolution, local to regional processes (e.g. specific ice shelf-glacier systems). Full Stokes models or shallow-shelf-shallow ice (SSA-SIA)

⁹In principle all ISMs should be.

¹⁰This list provides an overview of the most frequently used and a selection of currently developed models.

models. Ice Sheet System Model (ISSM) [Favier et al., 2012, Favier et al., 2014]; Elmer/Ice [Drews, 2015, Krug et al., 2015, Sun et al., 2014a]. On this level most currently known ice dynamics are represented in the model based on physical processes. Major current developments include the simulation of ice shelf-ocean interactions, sensitivity of small to large outlet glaciers, ice shelf calving parameterizations, as well as grounding line migration and local mesh refinement. The focus lies on projections of local to regional future ice dynamics [Favier et al., 2014].

Level 2 Intermediate timescales (decades to centuries), sub-annual to annual resolution, regional to continental processes (e.g. whole ice sheet catchment areas). SSA-SIA models. Bisicles [Cornford et al., 2015]; Parallel ice sheet model (PISM(-PIK)) [Mengel et al., 2015]. Projections of 21st and 22nd century ice dynamics are the major application of Level 2 ISMs, which utilize high spatial resolutions (on the scale of a few hundred meters to several kilometers) and parameterizations of ice ocean interactions such as basal shelf melting, grounding line migration and bedrock properties. These models are usually forced by regional climate models and re-analysis data and use local mesh refinement to resolve small scale processes close to the grounding line.

Level 3 Long time scales (centuries to geologic time scales); regional to continental processes (e.g. glacial-interglacial ice sheet dynamics). PISM [Pattyn et al., 2013, Golledge et al., 2013, Golledge et al., 2014, Mengel and Levermann, 2014, Golledge et al., 2015, Winkelmann et al., 2015, de Boer et al., 2015]; RIMBAY [Pattyn et al., 2013, Sutter et al., 2015a, de Boer et al., 2015]; [Pollard and DeConto, 2009, Pollard and DeConto, 2012, Pollard et al., 2015]. The models listed under Level 3 are mid ($\sim 10\text{km}$) to coarse resolution ($\sim 40\text{km}$) SSA-SIA models which parameterize most processes such as grounding line migration, ice-ocean interactions, bedrock conditions and ice properties. They are well suited for multi-ensemble simulations due to their low computational requirements and used for multi-millennial hind or forecasts of ice sheet dynamics. Since some physical processes are not explicitly calculated in Level 3 ISMs they rely heavily on parameterizations, thus requiring specific tuning. There are only few comparisons between such models for identical climate forcings [Pattyn et al., 2013, de Boer et al., 2015], and they show considerable discrepancies owing to the different tuning and parameterization approaches. However, at the current stage they are the only ISMs which can simulate multi-glacial cycles and cope with a vast range of transient climate scenarios.

At this stage, choosing an ISM for a specific application is always a compromise between computational efficiency and the need for the representation of physical processes. Regarding paleoclimate applications, high resolution ISMs have not yet been successfully applied. The suite of continental SSA-SIA ISMs available, does not differ to much at their core. However, parameterizations of grounding line migration, ice shelf dynamics and basal properties etc. vary widely.

Further, limited communication of ISM specifics (e.g. calculation of basal shelf melt rates, parameterizations of bedrock conditions) in publications lead to misconceptions regarding the interpretability of the model results¹¹. This hampers the exchange between the proxy and modeling community, and thus the interdisciplinary potential of data driven ice sheet modeling studies. As long as there are no ice-ocean models which can simulate the ice shelf mass balance, its feedbacks with the ocean circulation, the ground-

¹¹A mishap not unheard of in other disciplines as well.

ing line migration and the flow regime of the tributary glaciers with sufficient detail, projections of future ice sheet behavior, its effects on global sea level and influence on ocean circulation will remain crude, at least on decadal to centennial timescales. These timescales however are the ones of major interest for society. Thus it remains imperative to improve the applicability of complex high resolution ice sheet models to paleo applications as well as their inclusion in sophisticated coupled climate system models. Applying state of the art 3D ISMs to PD and future Antarctic scenarios continues to be worthwhile and interesting. However, without taking on the crucial, that is the paleoclimate model-data intercomparison, these efforts will fall short of their premise to elucidate past and future ice and climate dynamics.

Appendix

11.1 Ice Sheet Processes

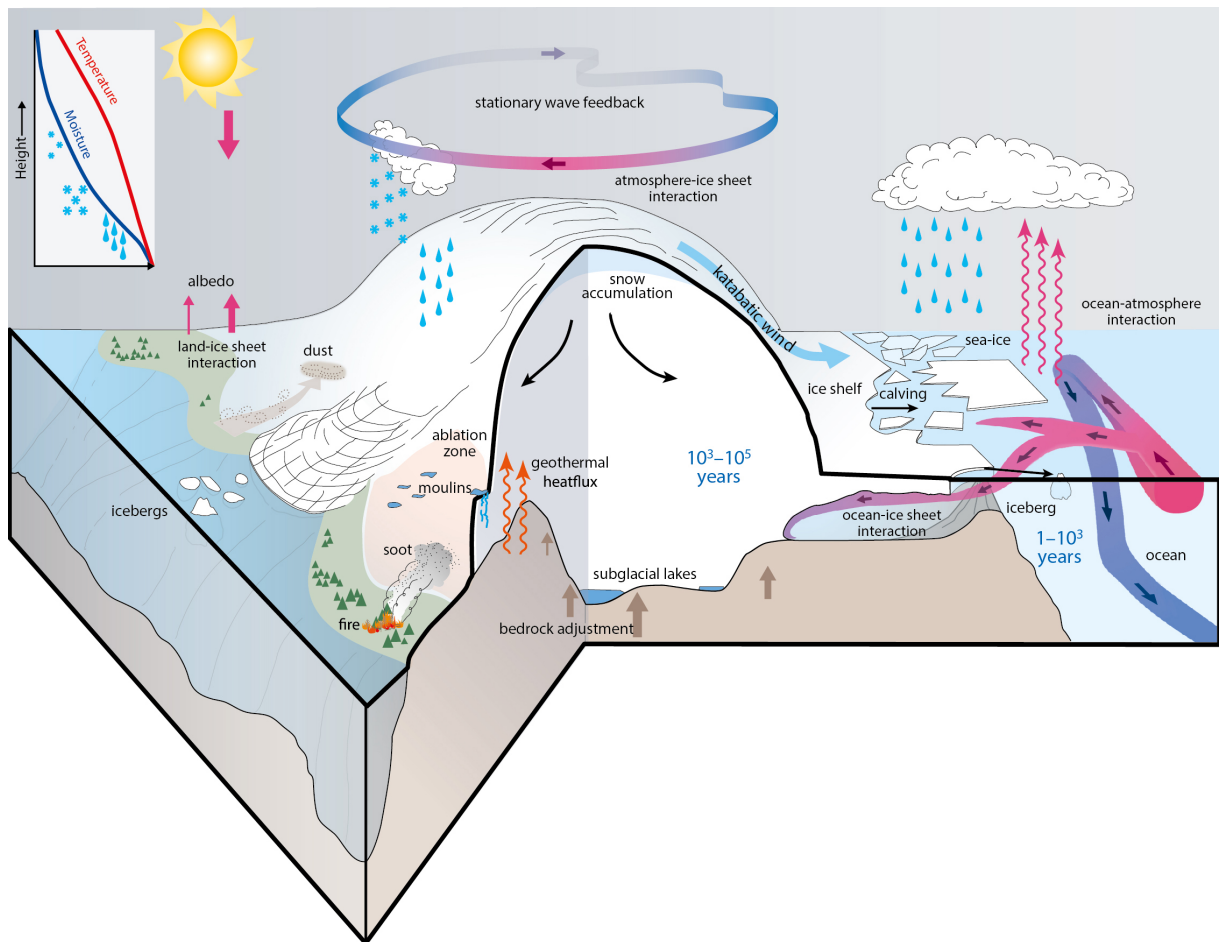


Figure 11.1: Graphical depiction of ice sheet climate interactions based on a generic ice sheet (from [Stocker et al., 2013]).

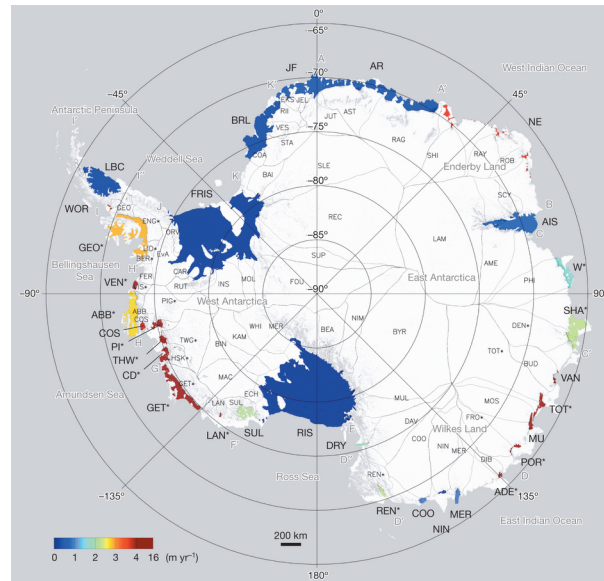


Figure 11.2: Present day mean shelf melt rates (from [Depoorter et al., 2013]).

11.2 Present Day Climate Forcing

Present day climate forcing is compiled from a combination of the ALBMAP [Brocq et al., 2010] data set and the World Ocean Atlas 2009 (see Figures 11.4 and 11.3).

11.3 COSMOS Last Interglacial Climate

Transient coupled climate simulations are realized by utilizing the results from a coupled AOGCM (COSMOS ([Lunt et al., 2013],[Pfeiffer and Lohmann, 2015])) for the LIG and present conditions. The AOGCM is forced by greenhouse gas concentration and orbital parameters for the LIG (125kyr BP) with two different Greenland Ice Sheet configurations. E : present day Greenland topography Eg : modified Greenland topography with a uniform reduction of the Greenland Ice Sheet topography by 1300m ([Pfeiffer and Lohmann, 2015]). Experiments PD, E and Eg were run for 2.000 years where the mean of the last 200 years were taken as input for the transient experiments. COSMOS consists of the atmospheric model ECHAM5 ([Roeckner et al., 2003]), which we employ at a resolution of T31 (1.5x1.5 degrees) and 19 vertical levels, the ocean model MPIOM ([Marsland et al., 2003]), which includes a sea ice component, as well as the land surface model JSBACH ([Brovkin et al., 2009]). MPIOM is employed with a resolution of GR30, consisting of 40 unevenly spaced vertical layers, with an approximate lateral resolution of 1.5x3 degrees, with significantly higher resolution at the model's poles, situated over Greenland and Antarctica.

Both COSMOS and ISM were tested in benchmark experiments for the Pliocene ([de Boer et al., 2015]) and LIG ([Lunt et al., 2013]) climates yielding results in the range of a suite of models for various scenarios.

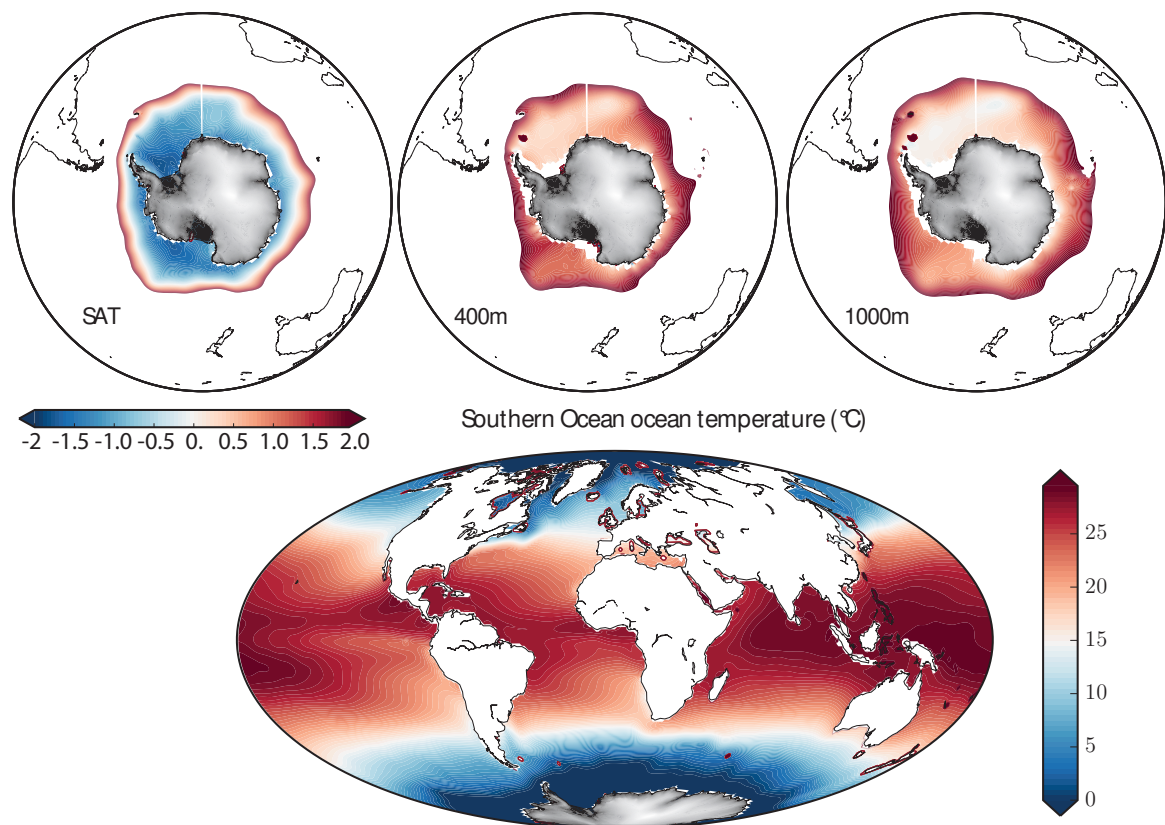


Figure 11.3: Southern ocean temperatures from the World Ocean Atlas 2009 [Locarnini et al., 2010]. Upper row, ocean temperatures at the surface (SST), 400 m depth and 1000 m depth. The lower panel depicts the global temperature distribution.

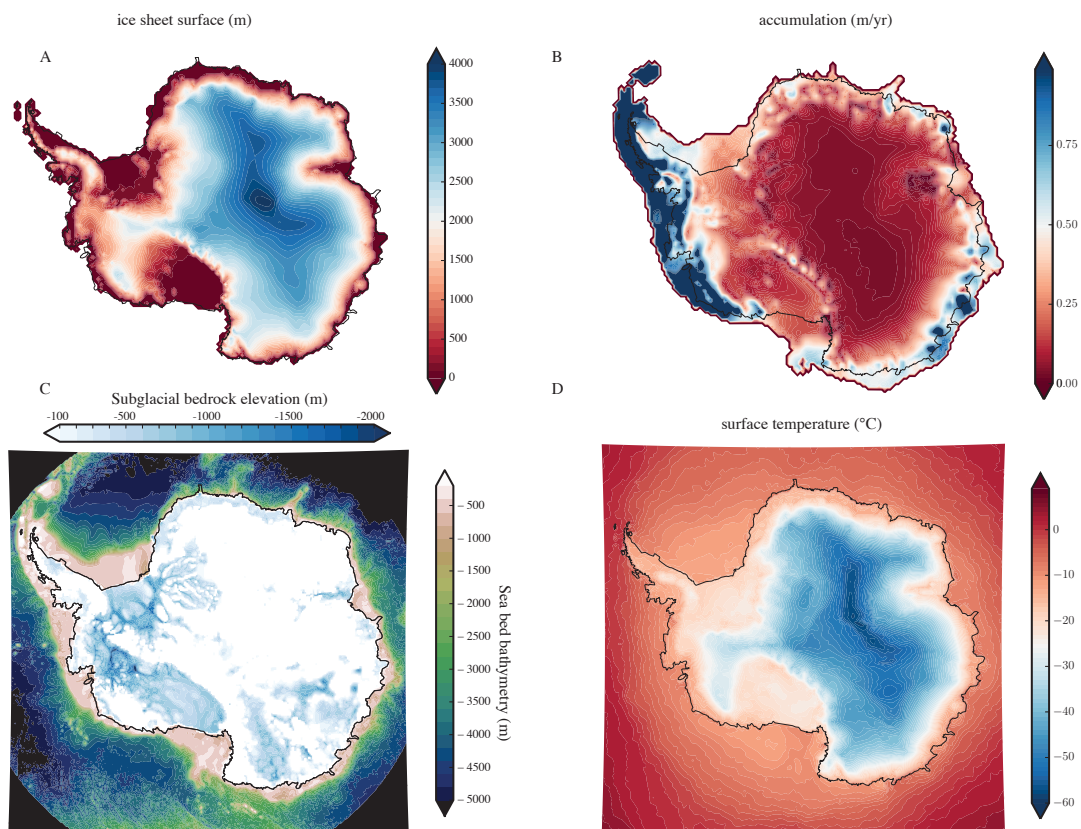


Figure 11.4: Climate forcing derived from ALBMAP v1 [Brocq et al., 2010] data set for ice sheet modeling . A) surface elevation (m) from BEDMAP 1, 40 by 40 km resolution. B) surface accumulation (m/yr) [Arthern et al., 2006]. C) bedrock topography and bathymetry (m) from BEDMAP 1. D) surface temperature ($^{\circ}\text{C}$) [Comiso, 2000].

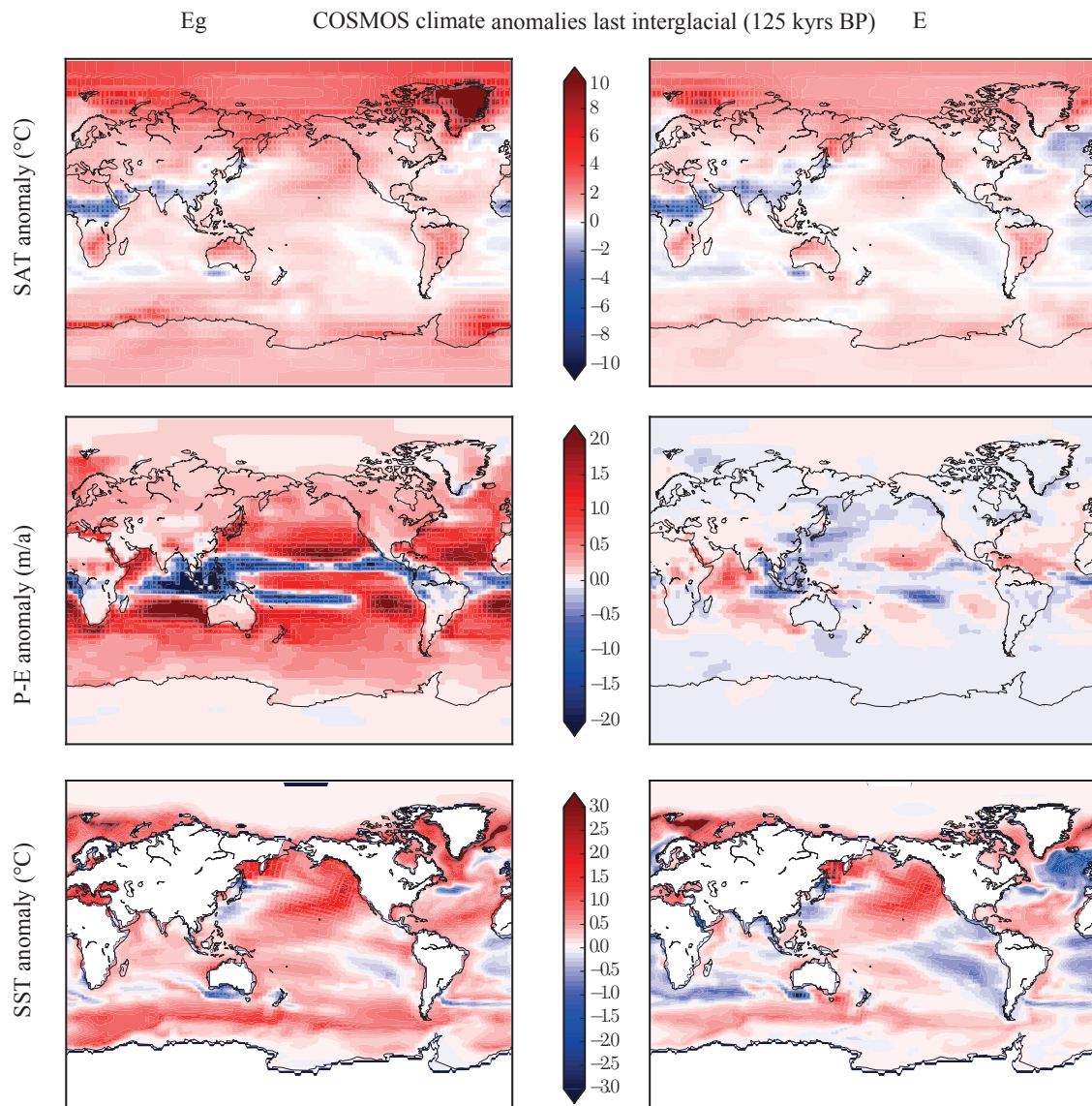


Figure 11.5: Climate anomalies of the two Last Interglacial COSMOS time slice experiments ([Pfeiffer and Lohmann, 2015] and Gierz personal comm.). EmG (modified Greenland Ice Sheet elevation) generally exhibits stronger anomaly amplitudes than E0 while the overall pattern is comparable (except for the P-E anomaly).

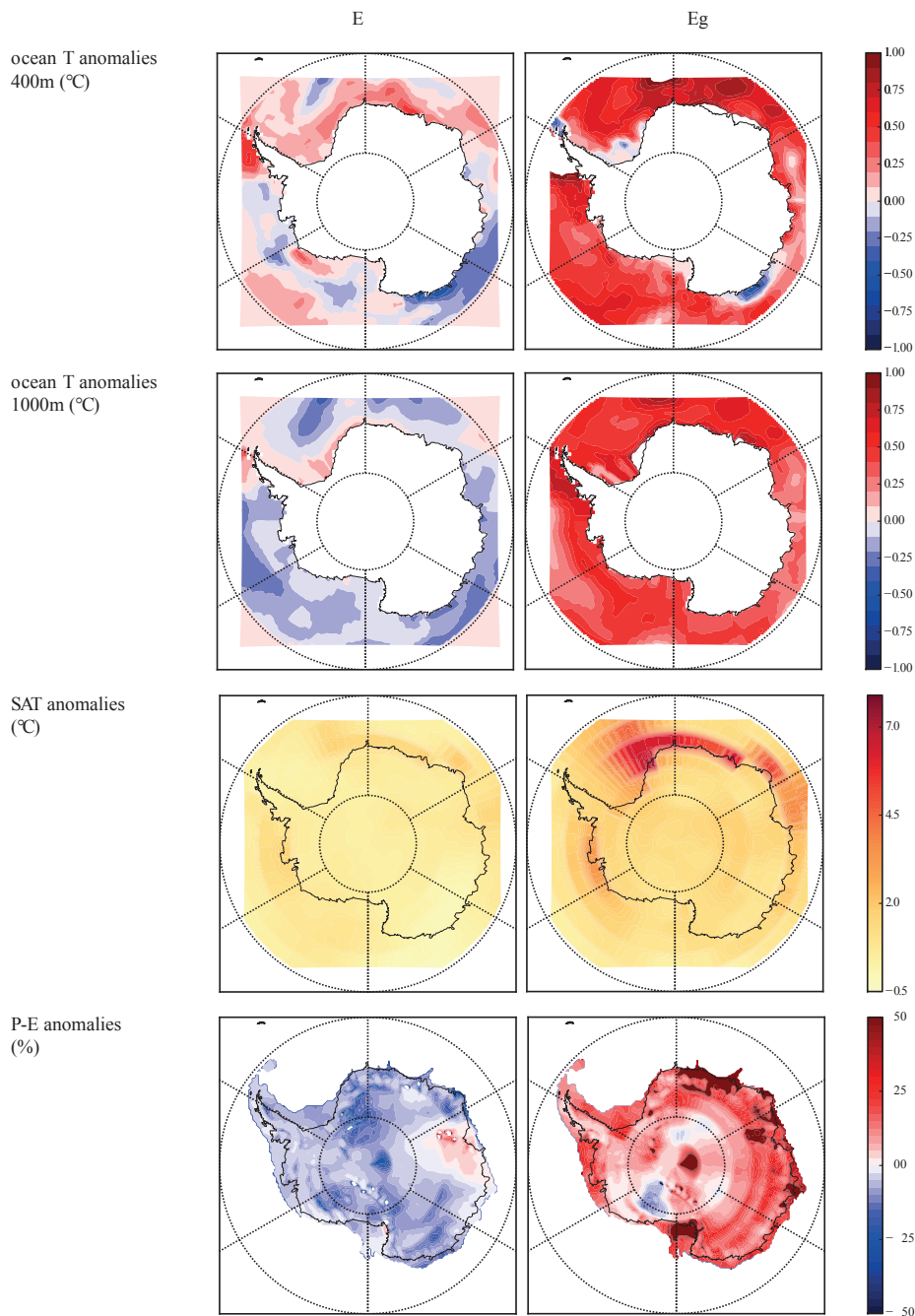


Figure 11.6: Polar climate anomalies (Eg and E). Eg exhibits intermediate and circumpolar deep water warming of about 0.5°C around Antarctica while E shows a slight overall cooling of the Southern Ocean. SAT anomalies are most pronounced in the coastal areas of Antarctica (up to 7°C for Eg) with moderate average warming of ca. 0.75, 1.45° over the continent (E/Eg). Accumulation is slightly reduced by 107 Gigatonnes in E (ca. 8% reduction compared to the present day forcing used in the ctrl simulation) and increased by 274 Gigatonnes (ca. 20%) in Eg.

11.4 Glacial-Interglacial Simulations

Deuterium depletion measured in ice cores is widely used as a proxy for local past temperature changes. The temperature variations recorded in an ice core can be used to derive the long term climate variations in the region. Deuterium depletion data from the Dome C ice core record are used as a glacial index, with which the COSMOS climate forcing is interpolated between present, and LIG climate conditions. The climate forcing at any given time during the simulations is calculated (here shown with surface

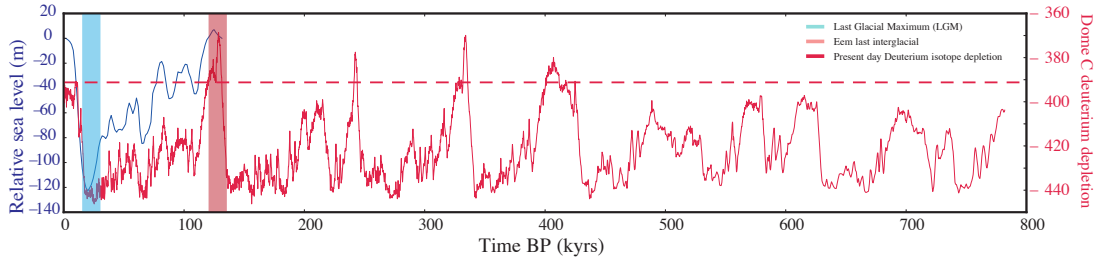


Figure 11.7: Dome C deuterium depletion record (data from [Jouzel et al., 2007]) over the last 800 kyrs in red. The blue line depicts a sea level reconstruction over the last glacial cycle (data from [Waelbroeck et al., 2002]). The dashed red line illustrates the present day deuterium depletion ([Stenni et al., 2010]).

temperature) as

$$T_{surf}^{i,j}(t) = T_{surf}^{i,j}(LIG) \cdot \frac{\delta(t) - \delta_{PD}}{1 - \delta_{PD}} + T_{surf}^{i,j}(PD) \cdot \frac{1 - \delta(t)}{1 - \delta_{PD}} \quad (11.1)$$

where $T^{i,j}$ denotes the temperature at node i, j , $\delta(t)$ the Deuterium value at time t and $\delta(PD)$ the present day mean Deuterium value. The initial year of the LIG simulations is chosen, so that the deuterium depletion value coincides with the mean deuterium depletion measured at Dome C at present day. The final year (118 kyrs BP) marks the time when the deuterium depletion returns to present values (see Figure 3.2). The ISM is started from the present day spin-up at 131.5 kyrs BP.

For the LIG simulations in chapter 3 different scenarios are run. In E and Eg full COSMOS forcing is used, 3D ocean temperatures, surface air temperatures (SAT), precipitation - evaporation (P-E). For the ocean temperature sensitivity runs the COSMOS ocean temperatures are replaced by present day ocean temperatures, modified by constant anomalies of 1° , 2° and 3°C . These anomalies are (synchronously to SAT and P-E) scaled with the Dome C glacial index. In an additional experiment, to benchmark the model results against previous modeling efforts, the basal melt rates parameterization in ([Pollard and DeConto, 2009]) is adopted (see Figure 11.9 for results).

11.5 West Antarctic Ice Sheet Bathymetry

Illustration of the major features of the WAIS bathymetry.

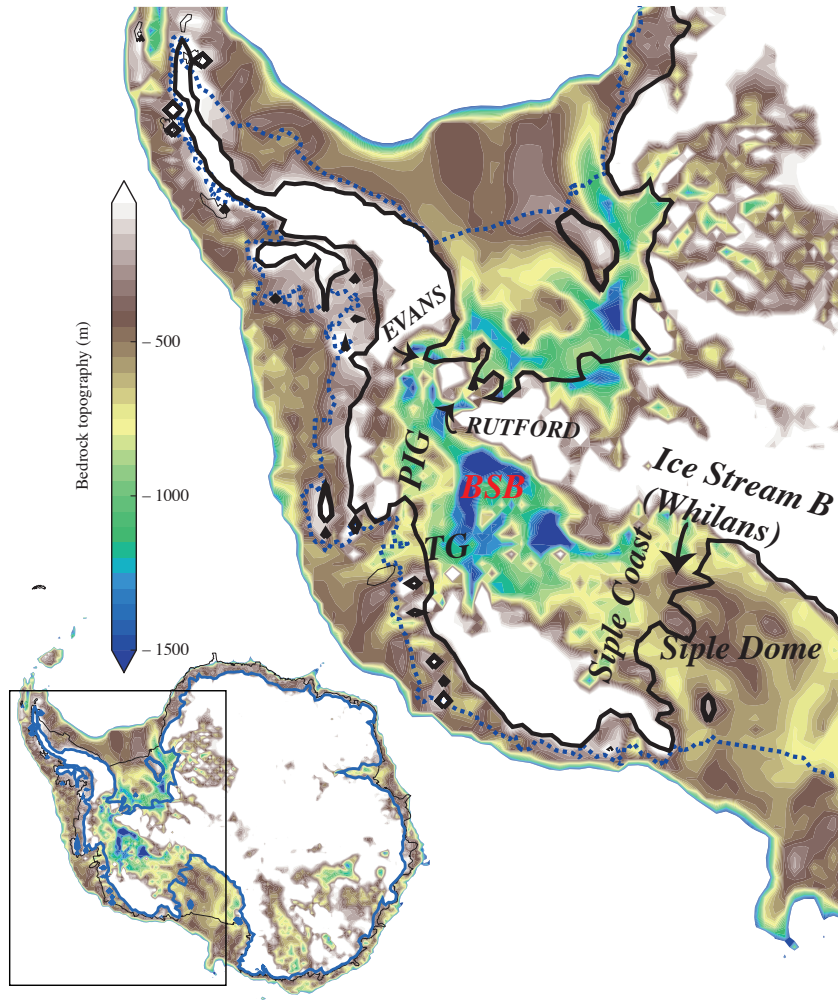


Figure 11.8: Subglacial topography underneath WAIS. The black line approximates the present day grounding line position. PIG: Pine Island Glacier, TG: Thwaites Glacier, BSB: Byrd Subglacial Basin, Evans Ice Stream and Rutford Ice Stream.

11.6 Model Behavior in the "Pollard 2009" Setting

ISM test case for an extreme interglacial employing the parameterization of basal shelf melt rates by [Pollard and DeConto, 2009].

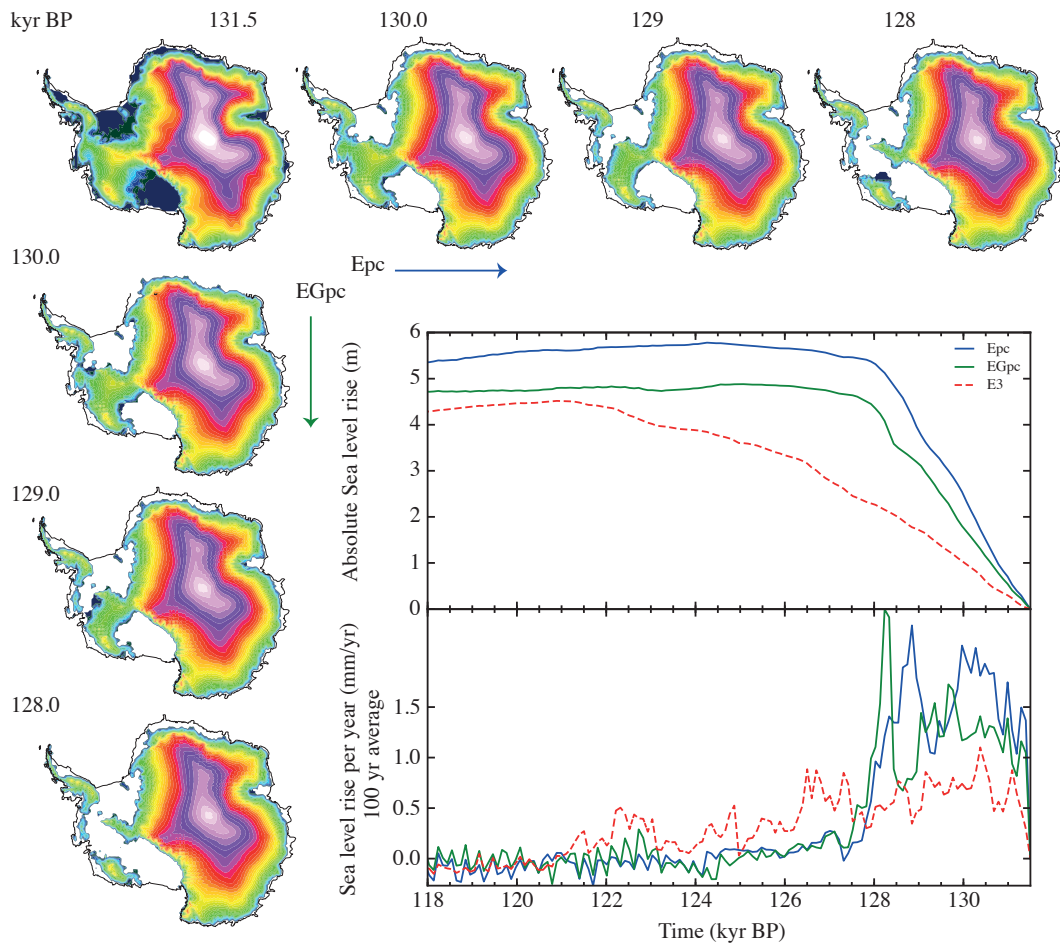


Figure 11.9: Evolution of Antarctic surface topography during the last interglacial with prescribed basal shelf melt rates adapted from [Pollard and DeConto, 2009] for an extreme interglacial (Index 'pc' stands for Pollard and DeConto). Horizontal : surface elevations in experiment E, vertical: surface elevation in experiment Eg. Note the steep increase in sea level in the pc simulations as opposed to the warmest ocean forcing scenario E3 (shown as the dashed red line for comparison).

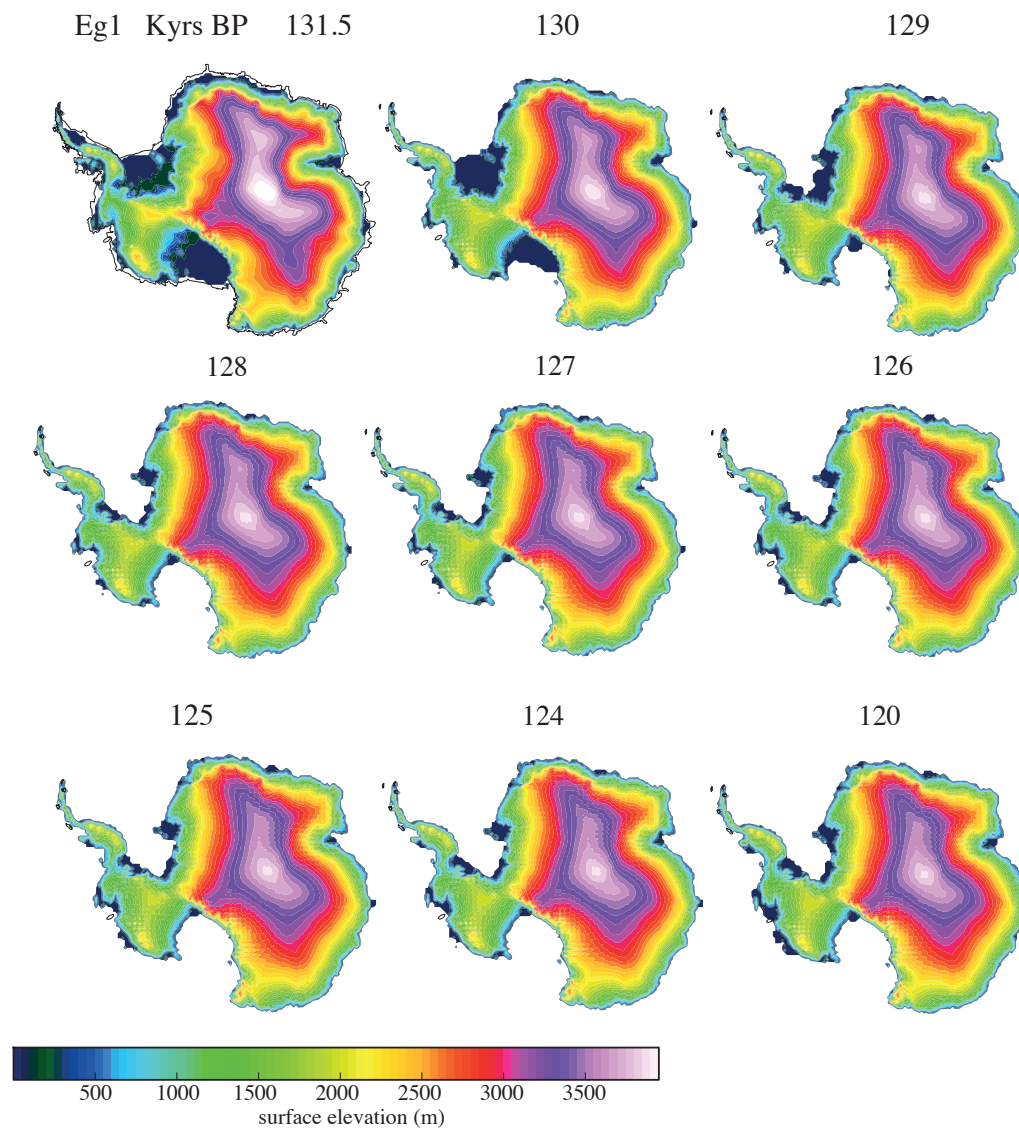


Figure 11.10: Simulation Eg1 for a 1°C Southern Ocean temperature anomaly.

11.7 Transient Evolution of the AIS

In the following the AIS surface evolution in the respective LIG sensitivity simulations (E1, E2, E3, Eg1, Eg2, Eg3) is shown. Every 1.000 years one snapshot is taken.

11.8 LGM Grounding Line Positions

Final grounding line positions in the year 19.500 BP in Antarctic sensitivity studies.

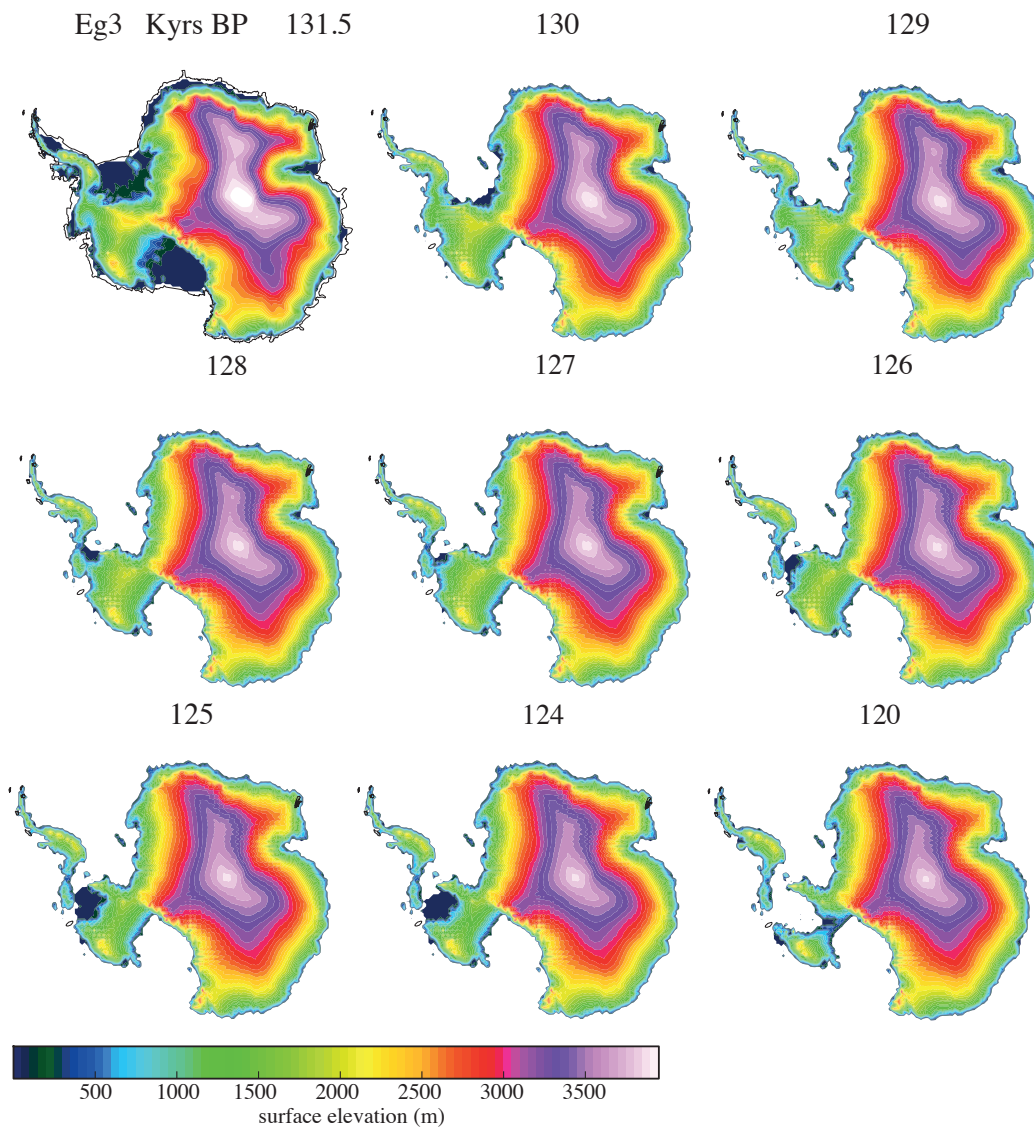


Figure 11.12: Simulation Eg3 (total WAIS collapse) for a 3°C Southern Ocean temperature anomaly. In contrast to E2 vs Eg2 for a 3°C ocean warming, increased accumulation leads to a slight compensation of mass loss in the WAIS and hence to a decelerated retreat and collapse.

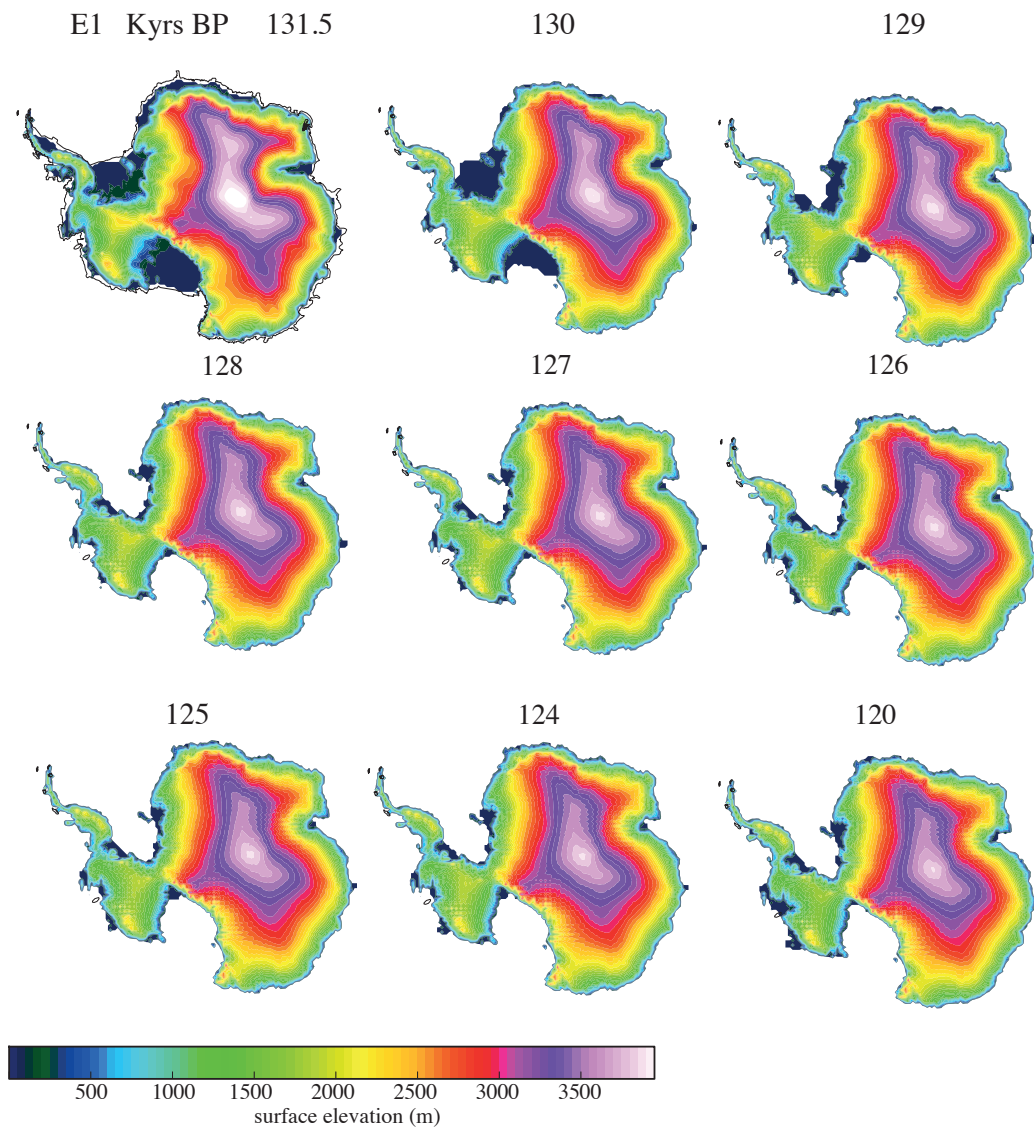


Figure 11.13: Simulation E1 for a 1°C Southern Ocean temperature anomaly.

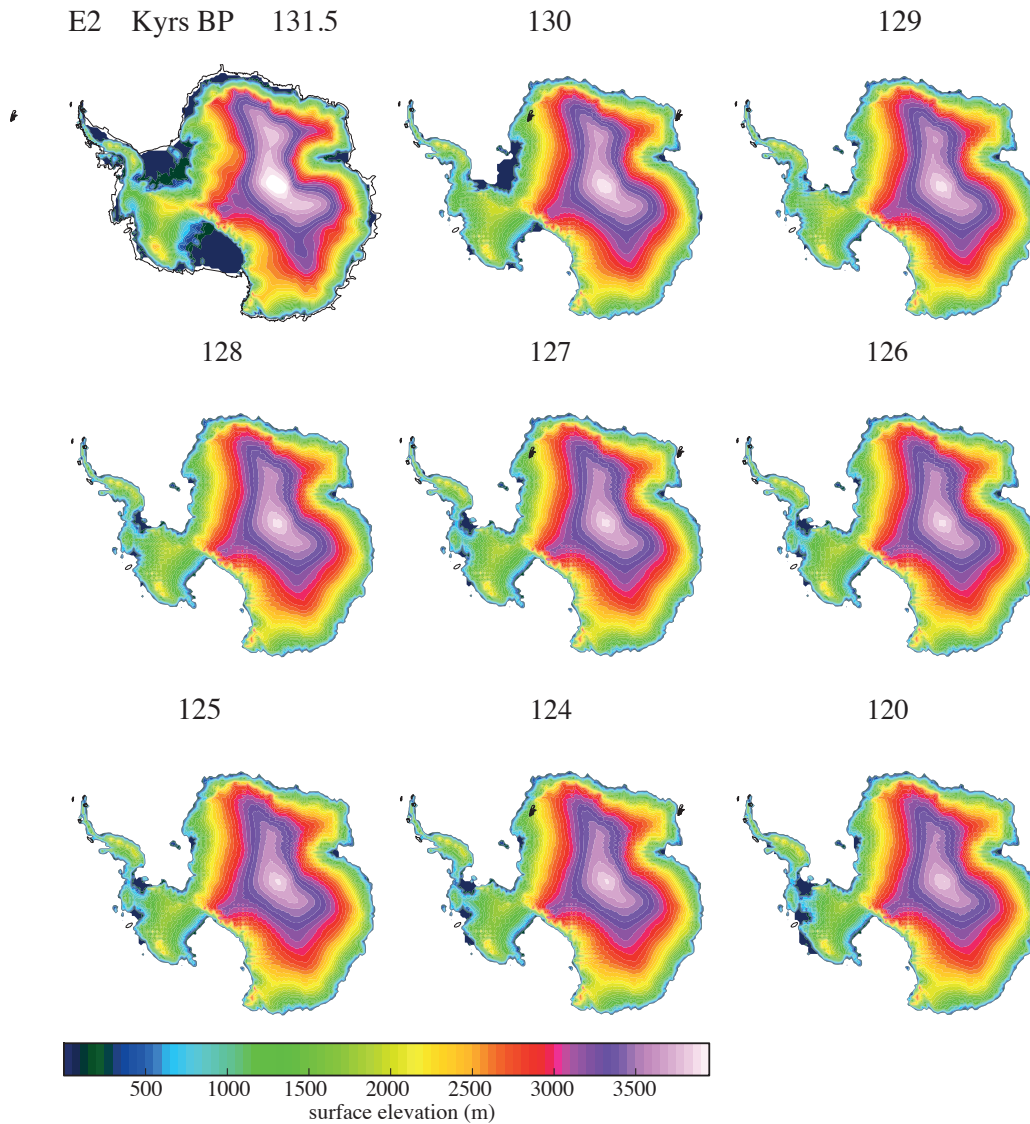


Figure 11.14: Evaluation of surface elevation in simulation E2 (moderate grounding line retreat), for a peak 2°C Southern Ocean temperature anomaly during the interglacial. Grounding line retreat around the West Antarctic Ice Sheet proceeds slowly along the bathymetric valleys underneath the marine ice sheet. Ice sheet retreat mainly proceeds into the basin underneath Thwaites Glacier while Pine Island Glacier remains fairly stable with only moderate grounding line retreat. The other major section along which grounding line retreat unfolds is the basin part of the drainage system into the Ronne-Filchner shelf (underneath Evans and Rutford Ice Streams). For an overview of the WAIS bathymetry see Figure 11.8.

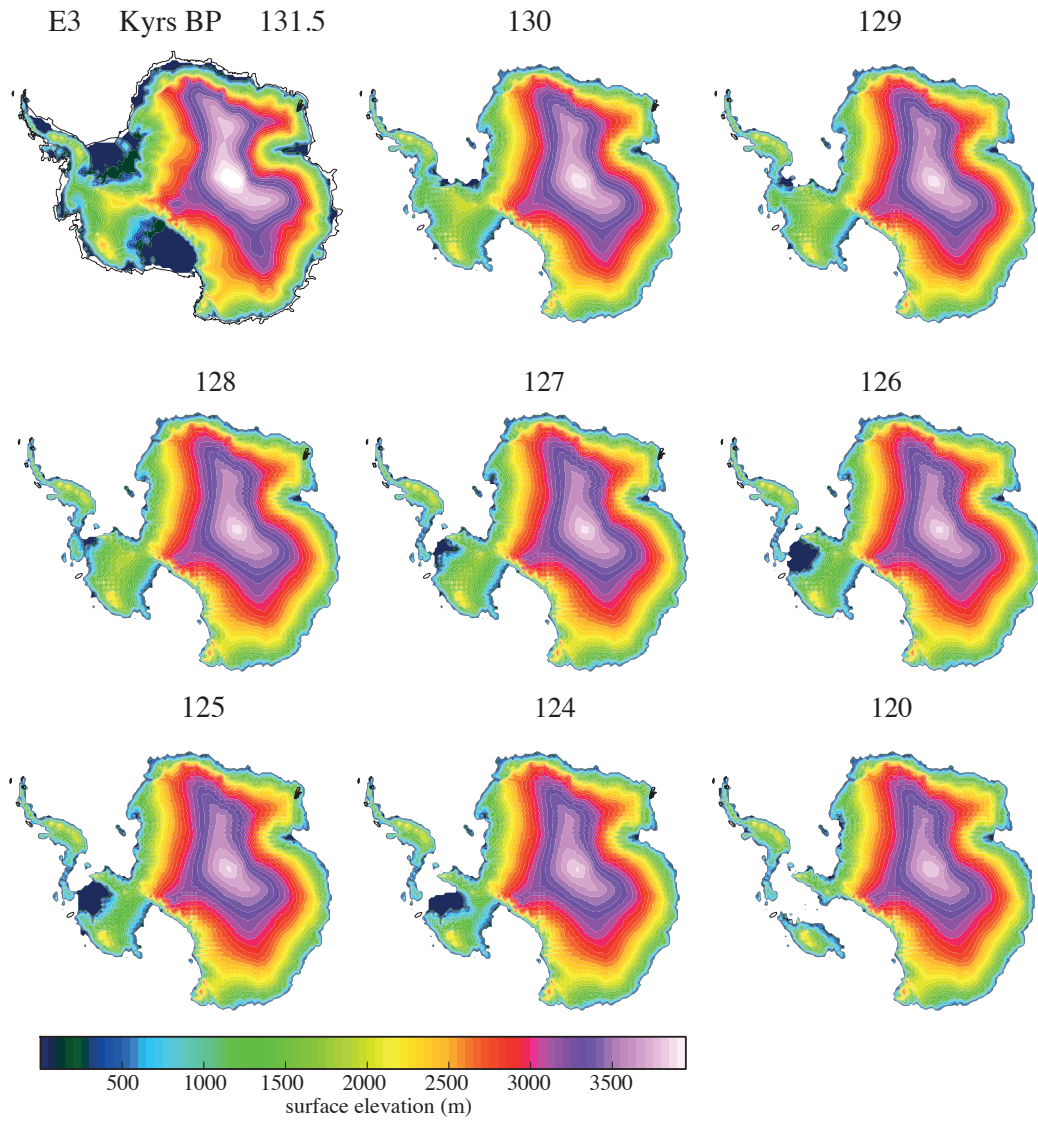


Figure 11.15: Simulation E3 (total WAIS collapse) for a 3°C Southern Ocean temperature anomaly.

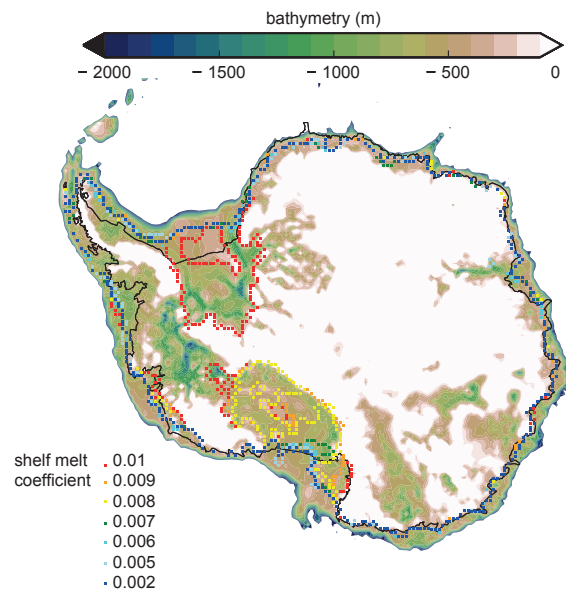


Figure 11.16: Antarctic LGM grounding line positions (19,500 years BP) depending on the shelf melt rate coefficient. Grounding lines partly overlap for different shelf melt rate parameterizations, in such cases the grounding line produced by the lowest shelf melt coefficient is shown.

11.9 List of Publications

de Boer, B., Dolan, A. M., Bernales, J., Gasson, E., Goelzer, H., Golledge, N. R., Sutter, J., Huybrechts, P., Lohmann, G., Rogozhina, I., Abe-Ouchi, A., Saito, F., and van de Wal, R. S. W. (2015b). Simulating the Antarctic Ice Sheet in the late-pliocene warm period: Plismip-ant, an ice-sheet model intercomparison project. *Cryosphere*, 9(3), 881 – 903.

Sutter, J., Thoma, M., and Lohmann, G. (2015a). Integration of passive tracers in a three-dimensional ice sheet model.

Sutter, J., Gierz, P., Grosfeld, K., Thoma, M., and Lohmann, G. (2015b). Ocean Temperature Thresholds for Last Interglacial WAIS collapse. *Geophysical Research Letters*, in Review.

Bibliography

- [Abe-Ouchi et al., 2013] Abe-Ouchi, A., Saito, F., Kawamura, K., Raymo, M. E., Okuno, J., Takahashi, K., and Blatter, H. (2013). Insolation-driven 100,000-year glacial cycles and hysteresis of ice-sheet volume. *Nature*, 500(7461):190–193.
- [Arthern et al., 2006] Arthern, R. J., Winebrenner, D. P., and Vaughan, D. G. (2006). Antarctic snow accumulation mapped using polarization of 4.3-cm wavelength microwave emission. *Journal of Geophysical Research-Atmospheres*, 111(D6).
- [Badger et al., 2013] Badger, M. P. S., Lear, C. H., Pancost, R. D., Foster, G. L., Bailey, T. R., Leng, M. J., and Abels, H. A. (2013). CO₂ drawdown following the middle Miocene expansion of the Antarctic Ice Sheet. *Paleoceanography*, 28(1).
- [Bakker et al., 2014] Bakker, P., Masson-Delmotte, V., Martrat, B., Charbit, S., Renssen, H., Groger, M., Krebs-Kanzow, U., Lohmann, G., Lunt, D. J., Pfeiffer, M., Phipps, S. J., Prange, M., Ritz, S. P., Schulz, M., Stenni, B., Stone, E. J., and Varma, V. (2014). Temperature trends during the present and Last Interglacial periods - a multi-model-data comparison. *Quaternary Science Reviews*, 99:224–243.
- [Bamber et al., 2009] Bamber, J. L., Riva, R. E. M., Vermeersen, B. L. A., and LeBrocq, A. M. (2009). Reassessment of the potential sea-level rise from a collapse of the West Antarctic Ice Sheet. *Science*, 324(5929):901–903.
- [Barbante et al., 2006] Barbante, C., Barnola, J. M., Becagli, S., Beer, J., Bigler, M., Boutron, C., Blunier, T., Castellano, E., Cattani, O., Chappellaz, J., Dahl-Jensen, D., Debret, M., Delmonte, B., Dick, D., Falourd, S., Faria, S., Federer, U., Fischer, H., Freitag, J., Frenzel, A., Fritzsche, D., Fundel, F., Gabrielli, P., Gaspari, V., Gersonde, R., Graf, W., Grigoriev, D., Hamann, I., Hansson, M., Hoffmann, G., Hutterli, M. A., Huybrechts, P., Isaksson, E., Johnsen, S., Jouzel, J., Kaczmarek, M., Karlin, T., Kaufmann, P., Kipfstuhl, S., Kohno, M., Lambert, F., Lambrecht, A., Lambrecht, A., Landais, A., Lawer, G., Leuenberger, M., Littot, G., Loulergue, L., Luthi, D., Maggi, V., Marino, F., Masson-Delmotte, V., Meyer, H., Miller, H., Mulvaney, R., Narcisi, B., Oerlemans, J., Oerter, H., Parrenin, F., Petit, J. R., Raisbeck, G., Raynaud, D., Rothlisberger, R., Ruth, U., Rybak, O., Severi, M., Schmitt, J., Schwander, J., Siegenthaler, U., Siggaard-Andersen, M. L., Spahni, R., Steffensen, J. P., Stenni, B., Stocker, T. F., Tison, J. L., Traversi, R., Udisti, R., Valero-Delgado, F., van den Broeke, M. R., van de Wal, R. S. W., Wagenbach, D., Wegner, A., Weiler, K., Wilhelms, F., Winther, J. G., Wolff, E., and Members, E. C. (2006). One-to-one coupling of glacial climate variability in Greenland and Antarctica. *Nature*, 444(7116):195–198.

- [Barker et al., 2011] Barker, S., Knorr, G., Edwards, R. L., Parrenin, F., Putnam, A. E., Skinner, L. C., Wolff, E., and Ziegler, M. (2011). 800,000 years of abrupt climate variability. *Science*, 334(6054):347–351.
- [Beckmann and Goosse, 2003] Beckmann, A. and Goosse, H. (2003). A parameterization of ice shelf-ocean interaction for climate models. *Ocean Modelling*, 5(2):157–170.
- [Bentley, 1999] Bentley, M. J. (1999). Volume of Antarctic ice at the Last Glacial Maximum, and its impact on global sea level change. *Quaternary Science Reviews*, 18(14):1569–1595.
- [Bentley et al., 2014] Bentley, M. J., Cofaigh, C. O., Anderson, J. B., Conway, H., Davies, B., Graham, A. G. C., Hillenbrand, C. D., Hodgson, D. A., Jamieson, S. S. R., Larter, R. D., Mackintosh, A., Smith, J. A., Verleyen, E., Ackert, R. P., Bart, P. J., Berg, S., Brunstein, D., Canals, M., Colhoun, E. A., Crosta, X., Dickens, W. A., Domack, E., Dowdeswell, J. A., Dunbar, R., Ehrmann, W., Evans, J., Favier, V., Fink, D., Fogwill, C. J., Glasser, N. F., Gohl, K., Golledge, N. R., Goodwin, I., Gore, D. B., Greenwood, S. L., Hall, B. L., Hall, K., Hedding, D. W., Hein, A. S., Hocking, E. P., Jakobsson, M., Johnson, J. S., Jomelli, V., Jones, R. S., Klages, J. P., Kristoffersen, Y., Kuhn, G., Leventer, A., Licht, K., Lilly, K., Lindow, J., Livingstone, S. J., Masse, G., McGlone, M. S., McKay, R. M., Melles, M., Miura, H., Mulvaney, R., Nel, W., Nitsche, F. O., O’Brien, P. E., Post, A. L., Roberts, S. J., Saunders, K. M., Selkirk, P. M., Simms, A. R., Spiegel, C., Stollendorf, T. D., Sugden, D. E., van der Putten, N., van Ommen, T., Verfaillie, D., Vyverman, W., Wagner, B., White, D. A., Witus, A. E., Zwart, D., and Consortium, R. (2014). A community-based geological reconstruction of Antarctic Ice Sheet deglaciation since the Last Glacial Maximum. *Quaternary Science Reviews*, 100:1–9.
- [Bentley et al., 2010] Bentley, M. J., Fogwill, C. J., Le Brocq, A. M., Hubbard, A. L., Sugden, D. E., Dunai, T. J., and Freeman, S. P. H. T. (2010). Deglacial history of the West Antarctic Ice Sheet in the Weddell Sea embayment: Constraints on past ice volume change. *Geology*, 38(5):411–414.
- [Billups and Schrag, 2002] Billups, K. and Schrag, D. P. (2002). Paleotemperatures and ice volume of the past 27 Myr revisited with paired Mg/Ca and $18\text{O}/16\text{O}$ measurements on benthic foraminifera. *Paleoceanography*, 17(1):3–1–3–11.
- [Bragg et al., 2012] Bragg, F. J., Lunt, D. J., and Haywood, A. M. (2012). Mid-Pliocene climate modelled using the UK Hadley Centre Model: PlioMIP experiments 1 and 2. *Geoscientific Model Development*, 5(5):1109–1125.
- [Brocq et al., 2010] Brocq, L., A. M., P., and A. J., V. A. (2010). An improved antarctic dataset for high resolution numerical ice sheet models (albmap v1). *Earth System Science Data*, 2(2):13.
- [Brovkin et al., 2009] Brovkin, V., Raddatz, T., Reick, C. H., Claussen, M., and Gayler, V. (2009). Global biogeophysical interactions between forest and climate. *Geophysical Research Letters*, 36(7):n/a–n/a. L07405.
- [Buizert et al., 2015] Buizert, C., Adrian, B., Ahn, J., Albert, M., Alley, R. B., Baggenstos, D., Bauska, T. K., Bay, R. C., Bencivengo, B. B., Bentley, C. R., Brook, E. J., Chellman, N. J., Clow, G. D., Cole-Dai, J., Conway, H., Cravens, E., Cuffey, K. M., Dunbar, N. W., Edwards, J. S., Fegyveresi, J. M., Ferris, D. G., Fitzpatrick, J. J., Fudge, T. J., Gibson, C. J., Gkinis, V., Goetz, J. J., Gregory, S., Hargreaves, G. M., Iverson, N., Johnson, J. A., Jones, T. R., Kalk, M. L., Kippenhan, M. J., Koffman,
-

- B. G., Kreutz, K., Kuhl, T. W., Lebar, D. A., Lee, J. E., Marcott, S. A., Markle, B. R., Maselli, O. J., McConnell, J. R., McGwire, K. C., Mitchell, L. E., Mortensen, N. B., Neff, P. D., Nishiizumi, K., Nunn, R. M., Orsi, A. J., Pasteris, D. R., Pedro, J. B., Pettit, E. C., Price, P. B., Priscu, J. C., Rhodes, R. H., Rosen, J. L., Schauer, A. J., Schoenemann, S. W., Sendelbach, P. J., Severinghaus, J. P., Shturmakov, A. J., Sigl, M., Slawny, K. R., Souney, J. M., Sowers, T. A., Spencer, M. K., Steig, E. J., Taylor, K. C., Twickler, M. S., Vaughn, B. H., Voigt, D. E., Waddington, E. D., Welten, K. C., Wendricks, A. W., White, J. W. C., Winstrup, M., Wong, G. J., Woodruff, T. E., and Members, W. D. P. (2015). Precise inter-polar phasing of abrupt climate change during the last ice age. *Nature*, 520(7549):661–U169.
- [Capron et al., 2014] Capron, E., Govin, A., Stone, E. J., Masson-Delmotte, V., Mulitza, S., Otto-Bliesner, B., Rasmussen, T. L., Sime, L. C., Waelbroeck, C., and Wolff, E. W. (2014). Temporal and spatial structure of multi-millennial temperature changes at high latitudes during the Last Interglacial. *Quaternary Science Reviews*, 103:116–133.
- [Chen et al., 2015] Chen, T. Y., Robinson, L. F., Burke, A., Southon, J., Spooner, P., Morris, P. J., and Ng, H. C. (2015). Synchronous centennial abrupt events in the ocean and atmosphere during the last deglaciation. *Science*, 349(6255):1537–1541.
- [Clarke and Marshall, 2002] Clarke, G. K. C. and Marshall, S. J. (2002). Isotopic balance of the Greenland Ice Sheet: modelled concentrations of water isotopes from 30,000 bp to present. *Quaternary Science Reviews*, 21(1-3):419–430.
- [Comiso, 2000] Comiso, J. C. (2000). Variability and trends in antarctic surface temperatures from in situ and satellite infrared measurements. *Journal of Climate*, 13(10):1674–1696.
- [Cornford et al., 2015] Cornford, S. L., Martin, D. F., Payne, A. J., Ng, E. G., Le Brocq, A. M., Gladstone, R. M., Edwards, T. L., Shannon, S. R., Agosta, C., van den Broeke, M. R., Hellmer, H. H., Krinner, G., Ligtenberg, S. R. M., Timmermann, R., and Vaughan, D. G. (2015). Century-scale simulations of the response of the west antarctic ice sheet to a warming climate. *The Cryosphere Discussions*, 9(2):1887–1942.
- [Cuffey and Paterson, 2010] Cuffey, K. and Paterson, W. (2010). *The physics of glaciers*. Academic Press. glacier depth average velocity.
- [Dahl-Jensen et al., 2013] Dahl-Jensen, D., Albert, M. R., Aldahan, A., Azuma, N., Balslev-Clausen, D., Baumgartner, M., Berggren, A. M., Bigler, M., Binder, T., Blunier, T., Bourgeois, J. C., Brook, E. J., Buchardt, S. L., Buizert, C., Capron, E., Chappellaz, J., Chung, J., Clausen, H. B., Cvijanovic, I., Davies, S. M., Ditlevsen, P., Eicher, O., Fischer, H., Fisher, D. A., Fleet, L. G., Gfeller, G., Gkinis, V., Gogineni, S., Goto-Azuma, K., Grinsted, A., Gudlaugsdottir, H., Guillevic, M., Hansen, S. B., Hansson, M., Hirabayashi, M., Hong, S., Hur, S. D., Huybrechts, P., Hvidberg, C. S., Iizuka, Y., Jenk, T., Johnsen, S. J., Jones, T. R., Jouzel, J., Karlsson, N. B., Kawamura, K., Keegan, K., Kettner, E., Kipfstuhl, S., Kjaer, H. A., Koutnik, M., Kuramoto, T., Kohler, P., Laepple, T., Landais, A., Langen, P. L., Larsen, L. B., Leuenberger, D., Leuenberger, M., Leuschen, C., Li, J., Lipenkov, V., Martinerie, P., Maselli, O. J., Masson-Delmotte, V., McConnell, J. R., Miller, H., Mini, O., Miyamoto, A., Montagnat-Rentier, M., Mulvaney, R., Muscheler, R., Orsi, A. J., Paden, J., Panton, C., Pattyn, F., Petit, J. R., Pol, K., Popp, T., Possnert, G., Prie, F., Prokopiou, M., Quiquet, A., Rasmussen,
-

- S. O., Raynaud, D., Ren, J., Reutenauer, C., Ritz, C., Rockmann, T., Rosen, J. L., Rubino, M., Rybak, O., Samyn, D., Sapart, C. J., Schilt, A., Schmidt, A. M. Z., Schwander, J., Schupbach, S., Seierstad, I., Severinghaus, J. P., et al. (2013). Eemian interglacial reconstructed from a Greenland folded ice core. *Nature*, 493(7433):489–494.
- [Dansgaard, 1964] Dansgaard, W. (1964). stable isotopes in precipitation. *Tellus B*.
- [de Boer et al., 2015] de Boer, B., Dolan, A. M., Bernales, J., Gasson, E., Goelzer, H., Golledge, N. R., Sutter, J., Huybrechts, P., Lohmann, G., Rogozhina, I., Abe-Ouchi, A., Saito, F., and van de Wal, R. S. W. (2015). Simulating the antarctic ice sheet in the late-Pliocene warm period: Plismip-ant, an ice-sheet model intercomparison project. *Cryosphere*, 9(3):881–903.
- [DeConto et al., 2007] DeConto, R., Pollard, D., and Harwood, D. (2007). Sea ice feedback and Cenozoic evolution of Antarctic climate and ice sheets. *Paleoceanography*, 22(3).
- [Depoorter et al., 2013] Depoorter, M. A., Bamber, J. L., Griggs, J. A., Lenaerts, J. T. M., Ligtenberg, S. R. M., van den Broeke, M. R., and Moholdt, G. (2013). Calving fluxes and basal melt rates of antarctic ice shelves. *Nature*, 502(7469):89–93.
- [Dolan et al., 2011] Dolan, A. M., Haywood, A. M., Hill, D. J., Dowsett, H. J., Hunter, S. J., Lunt, D. J., and Pickering, S. J. (2011). Sensitivity of Pliocene ice sheets to orbital forcing. *Palaeogeography Palaeoclimatology Palaeoecology*, 309(1-2):98–110.
- [Dolan et al., 2015] Dolan, A. M., Hunter, S. J., Hill, D. J., Haywood, A. M., Koenig, S. J., Otto-Bliesner, B. L., Abe-Ouchi, A., Bragg, F., Chan, W. L., Chandler, M. A., Contoux, C., Jost, A., Kamae, Y., Lohmann, G., Lunt, D. J., Ramstein, G., Rosenbloom, N. A., Sohl, L., Stepanek, C., Ueda, H., Yan, Q., and Zhang, Z. (2015). Using results from the PlioMIP ensemble to investigate the Greenland Ice Sheet during the mid-Pliocene Warm Period. *Climate of the Past*, 11(3):403–424.
- [Dolan et al., 2012] Dolan, A. M., Koenig, S. J., Hill, D. J., Haywood, A. M., and DeConto, R. M. (2012). Pliocene Ice Sheet Modelling Intercomparison Project (PLISMIP) - experimental design. *Geoscientific Model Development*, 5(4):963–974.
- [Dowsett et al., 2010] Dowsett, H., Robinson, M., Haywood, A., Salzmann, U., Hill, D., Sohl, L., Chandler, M., Williams, M., Foley, K., and Stoll, D. (2010). The PRISM3D paleoenvironmental reconstruction. *Stratigraphy*, 7(2-3):123–139.
- [Dowsett et al., 2013] Dowsett, H. J., Foley, K. M., Stoll, D. K., Chandler, M. A., Sohl, L. E., Bentsen, M., Otto-Bliesner, B. L., Bragg, F. J., Chan, W. L., Contoux, C., Dolan, A. M., Haywood, A. M., Jonas, J. A., Jost, A., Kamae, Y., Lohmann, G., Lunt, D. J., Nisancioglu, K. H., Abe-Ouchi, A., Ramstein, G., Riesselman, C. R., Robinson, M. M., Rosenbloom, N. A., Salzmann, U., Stepanek, C., Strother, S. L., Ueda, H., Yan, Q., and Zhang, Z. S. (2013). Sea surface temperature of the mid-piacenzian ocean: A data-model comparison. *Scientific Reports*, 3.
- [Dowsett et al., 2011] Dowsett, H. J., Haywood, A. M., Valdes, P. J., Robinson, M. M., Lunt, D. J., Hill, D., Stoll, D. K., and Foley, K. M. (2011). Sea surface temperatures of the mid-Piacenzian Warm Period: A comparison of PRISM3 and HadCM3. *Palaeogeography Palaeoclimatology Palaeoecology*, 309(1-2):83–91.
-

- [Drews, 2015] Drews, R. (2015). Evolution of ice-shelf channels in Antarctic ice shelves. *The Cryosphere*, 9(3):1169–1181.
- [Dutton and Lambeck, 2012] Dutton, A. and Lambeck, K. (2012). Ice volume and sea level during the Last Interglacial. *Science*, 337(6091):216–219.
- [Dutton et al., 2015] Dutton, A., Webster, J. M., Zwartz, D., Lambeck, K., and Wohlfarth, B. (2015). Tropical tales of polar ice: evidence of Last Interglacial polar ice sheet retreat recorded by fossil reefs of the granitic Seychelles islands. *Quaternary Science Reviews*, 107:182–196.
- [Favier et al., 2014] Favier, L., Durand, G., Cornford, S. L., Gudmundsson, G. H., Gagliardini, O., Gillet-Chaulet, F., Zwinger, T., Payne, A. J., and Le Brocq, A. M. (2014). Retreat of Pine Island Glacier controlled by marine ice-sheet instability. *Nature Climate Change*, 4(2):117–121.
- [Favier et al., 2012] Favier, L., Gagliardini, O., Durand, G., and Zwinger, T. (2012). A three-dimensional full Stokes model of the grounding line dynamics: effect of a pinning point beneath the ice shelf. *Cryosphere*, 6(1):101–112.
- [Feldmann and Levermann, 2015] Feldmann, J. and Levermann, A. (2015). Collapse of the West Antarctic Ice Sheet after local destabilization of the Amundsen Basin. *Proceedings of the National Academy of Sciences*, 112(46):14191–14196.
- [Field et al., 2014] Field, C., Barros, V., Dokken, D., Mach, K., Mastrandrea, M., Bilir, T., Chatterjee, M., Ebi, K., Estrada, Y., Genova, R., Girma, B., Kissel, E., Levy, A., MacCracken, S., Mastrandrea, P., and (eds.), L. W. (2014). *Summary for Policymakers*, book section SPM. Cambridge University Press, Cambridge, United Kingdom and New York, NY, USA.
- [Fogwill et al., 2014] Fogwill, C. J., Turney, C. S. M., Meissner, K. J., Golledge, N. R., Spence, P., Roberts, J. L., England, M. H., Jones, R. T., and Carter, L. (2014). Testing the sensitivity of the East Antarctic Ice Sheet to Southern Ocean dynamics: past changes and future implications (vol 29, pg 91, 2014). *Journal of Quaternary Science*, 29(5):508–508.
- [Foster et al., 2012] Foster, G. L., Lear, C. H., and Rae, J. W. (2012). The evolution of pCO₂, ice volume and climate during the middle Miocene. *Earth and Planetary Science Letters*, 341-344:243 – 254.
- [Fretwell et al., 2013] Fretwell, P., Pritchard, H. D., Vaughan, D. G., Bamber, J. L., Barrand, N. E., Bell, R., Bianchi, C., Bingham, R. G., Blankenship, D. D., Casassa, G., Catania, G., Callens, D., Conway, H., Cook, A. J., Corr, H. F. J., Damaske, D., Damm, V., Ferraccioli, F., Forsberg, R., Fujita, S., Gim, Y., Gogineni, P., Griggs, J. A., Hindmarsh, R. C. A., Holmlund, P., Holt, J. W., Jacobel, R. W., Jenkins, A., Jokat, W., Jordan, T., King, E. C., Kohler, J., Krabill, W., Riger-Kusk, M., Langlely, K. A., Leitchenkov, G., Leuschen, C., Luyendyk, B. P., Matsuoka, K., Mouginot, J., Nitsche, F. O., Nogi, Y., Nost, O. A., Popov, S. V., Rignot, E., Rippin, D. M., Rivera, A., Roberts, J., Ross, N., Siegert, M. J., Smith, A. M., Steinhage, D., Studinger, M., Sun, B., Tinto, B. K., Welch, B. C., Wilson, D., Young, D. A., Xiangbin, C., and Zirizzotti, A. (2013). Bedmap2: improved ice bed, surface and thickness datasets for Antarctica. *Cryosphere*, 7(1):375–393.
- [Frieler et al., 2015] Frieler, K., Clark, P. U., He, F., Buizert, C., Reese, R., Ligtenberg, S. R. M., van den Broeke, M. R., Winkelmann, R., and Levermann, A. (2015). Consistent evidence of increasing Antarctic accumulation with warming. *Nature Climate Change*, 5(4):348–352.
-

- [Gasson et al., 2015] Gasson, E., DeConto, R., and Pollard, D. (2015). Antarctic bedrock topography uncertainty and ice sheet stability. *Geophysical Research Letters*, 42(13):5372–5377.
- [Gierz et al., 2015] Gierz, P., Lohmann, G., and Wei, W. (2015). Response of Atlantic overturning to future warming in a coupled atmosphere-ocean-ice sheet model. *Geophysical Research Letters*, 42(16):6811–6818.
- [Goelles et al., 2014] Goelles, T., Grosfeld, K., and Lohmann, G. (2014). Semi-lagrangian transport of oxygen isotopes in polythermal ice sheets: implementation and first results. *Geoscientific Model Development*, 7(4):1395–1408.
- [Goldner et al., 2014] Goldner, A., Herold, N., and Huber, M. (2014). Antarctic glaciation caused ocean circulation changes at the Eocene-Oligocene transition. *Nature*, 511(7511):574–578.
- [Golledge et al., 2012] Golledge, N. R., Fogwill, C. J., Mackintosh, A. N., and Buckley, K. M. (2012). Dynamics of the Last Glacial Maximum Antarctic ice-sheet and its response to ocean forcing. *Proceedings of the National Academy of Sciences of the United States of America*, 109(40):16052–16056.
- [Golledge et al., 2015] Golledge, N. R., Kowalewski, D. E., Naish, T. R., Levy, R. H., Fogwill, C. J., and Gasson, E. G. W. (2015). The multi-millennial Antarctic commitment to future sea-level rise. *Nature*, 526(7573):421–529.
- [Golledge et al., 2013] Golledge, N. R., Levy, R. H., McKay, R. M., Fogwill, C. J., White, D. A., Graham, A. G. C., Smith, J. A., Hillenbrand, C. D., Licht, K. J., Denton, G. H., Ackert, R. P., Maas, S. M., and Hall, B. L. (2013). Glaciology and geological signature of the Last Glacial Maximum Antarctic Ice Sheet. *Quaternary Science Reviews*, 78:225–247.
- [Golledge et al., 2014] Golledge, N. R., Menviel, L., Carter, L., Fogwill, C. J., England, M. H., Cortese, G., and Levy, R. H. (2014). Antarctic contribution to meltwater pulse 1a from reduced southern ocean overturning. *Nature Communications*, 5.
- [Greenbaum et al., 2015] Greenbaum, J. S., Blankenship, D. D., Young, D. A., Richter, T. G., Roberts, J. L., Aitken, A. R. A., Legresy, B., Schroeder, D. M., Warner, R. C., van Ommen, T. D., and Siegert, M. J. (2015). Ocean access to a cavity beneath Totten Glacier in East Antarctica. *Nature Geoscience*, 8(4):294–298.
- [Haefeli, 1963] Haefeli, R. (1963). A numerical and experimental method for determining ice motion in the central parts of ice sheets. *International Association of Scientific Hydrology Publication*, 61(Publication 61 (General Assembly of Berkeley 1963 - Snow and Ice)).
- [Hamon et al., 2013] Hamon, N., Sepulchre, P., Lefebvre, V., and Ramstein, G. (2013). The role of eastern Tethys seaway closure in the Middle Miocene Climatic Transition (ca. 14 Ma). *Climate of the Past*, 9(6):2687–2702.
- [Hanna et al., 2013] Hanna, E., Navarro, F. J., Pattyn, F., Domingues, C. M., Fettweis, X., Ivins, E. R., Nicholls, R. J., Ritz, C., Smith, B., Tulaczyk, S., Whitehouse, P. L., and Zwally, H. J. (2013). Ice-sheet mass balance and climate change. *Nature*, 498(7452):51–59.
-

- [Harig and Simons, 2015] Harig, C. and Simons, F. J. (2015). Accelerated west antarctic ice mass loss continues to outpace east antarctic gains. *Earth and Planetary Science Letters*, 415:134–141.
- [Hattermann et al., 2014] Hattermann, T., Smedsrud, L., NÄst, O., Lilly, J., and Galton-Fenzi, B. (2014). Eddy-resolving simulations of the Fimbul Ice Shelf cavity circulation: Basal melting and exchange with open ocean. *Ocean Modelling*, 82:28 – 44.
- [Haywood et al., 2011] Haywood, A. M., Dowsett, H. J., Robinson, M. M., Stoll, D. K., Dolan, A. M., Lunt, D. J., Otto-Bliesner, B., and Chandler, M. A. (2011). Pliocene Model Intercomparison Project (PlioMIP): experimental design and boundary conditions (Experiment 2). *Geoscientific Model Development*, 4(3):571–577.
- [Haywood et al., 2013] Haywood, A. M., Hill, D. J., Dolan, A. M., Otto-Bliesner, B. L., Bragg, F., Chan, W. L., Chandler, M. A., Contoux, C., Dowsett, H. J., Jost, A., Kamae, Y., Lohmann, G., Lunt, D. J., Abe-Ouchi, A., Pickering, S. J., Ramstein, G., Rosenbloom, N. A., Salzmann, U., Sohl, L., Stepanek, C., Ueda, H., Yan, Q., and Zhang, Z. (2013). Large-scale features of Pliocene climate: results from the Pliocene Model Intercomparison Project. *Climate of the Past*, 9(1):191–209.
- [Haywood and Valdes, 2004] Haywood, A. M. and Valdes, P. J. (2004). Modelling Pliocene warmth: contribution of atmosphere, oceans and cryosphere. *Earth and Planetary Science Letters*, 218(3-4):363–377.
- [Hein et al., 2011] Hein, A. S., Fogwill, C. J., Sugden, D. E., and Xu, S. (2011). Glacial/interglacial ice-stream stability in the Weddell Sea embayment, Antarctica. *Earth and Planetary Science Letters*, 307(1-2):211–221.
- [Hellmer et al., 2012] Hellmer, H. H., Kauker, F., Timmermann, R., Determann, J., and Rae, J. (2012). Twenty-first-century warming of a large antarctic ice-shelf cavity by a redirected coastal current. *Nature*, 485(7397):225–228.
- [Heroy and Anderson, 2007] Heroy, D. C. and Anderson, J. B. (2007). Radiocarbon constraints on Antarctic Peninsula Ice Sheet retreat following the Last Glacial Maximum (LGM). *Quaternary Science Reviews*, 26(25-28):3286–3297.
- [Hillenbrand et al., 2014] Hillenbrand, C. D., Bentley, M. J., Stoll, T. D., Hein, A. S., Kuhn, G., Graham, A. G. C., Fogwill, C. J., Kristoffersen, Y., Smith, J. A., Anderson, J. B., Larter, R. D., Melles, M., Hodgson, D. A., Mulvaney, R., and Sugden, D. E. (2014). Reconstruction of changes in the Weddell Sea sector of the Antarctic Ice Sheet since the Last Glacial Maximum. *Quaternary Science Reviews*, 100:111–136.
- [Hillenbrand et al., 2012] Hillenbrand, C. D., Melles, M., Kuhn, G., and Larter, R. D. (2012). Marine geological constraints for the grounding-line position of the Antarctic Ice Sheet on the southern Weddell Sea shelf at the Last Glacial Maximum. *Quaternary Science Reviews*, 32:25–47.
- [Holbourn et al., 2013] Holbourn, A., Kuhnt, W., Frank, M., and Haley, B. A. (2013). Changes in Pacific Ocean circulation following the Miocene onset of permanent Antarctic ice cover. *Earth and Planetary Science Letters*, 365:38–50.
-

- [Holbourn et al., 2005] Holbourn, A., Kuhnt, W., Schulz, M., and Erlenkeuser, H. (2005). Impacts of orbital forcing and atmospheric carbon dioxide on Miocene ice-sheet expansion. *Nature*, 438(7067):483–487.
- [Holland and Jenkins, 1999] Holland, D. M. and Jenkins, A. (1999). Modeling thermodynamic ice-ocean interactions at the base of an ice shelf. *Journal of Physical Oceanography*, 29(8):1787–1800.
- [Hughes, 1981] Hughes, T. J. (1981). The weak underbelly of the west antarctic ice-sheet. *Journal of Glaciology*, 27(97):518–525.
- [Huybrechts, 2002] Huybrechts, P. (2002). Sea-level changes at the LGM from ice-dynamic reconstructions of the Greenland and Antarctic ice sheets during the glacial cycles. *Quaternary Science Reviews*, 21(1-3):203–231.
- [Huybrechts and Payne, 1996] Huybrechts, P. and Payne, T. A. (1996). The EISMINT benchmarks for testing ice-sheet models. *Annals of Glaciology*, 23.
- [Huybrechts et al., 2007] Huybrechts, P., Rybak, O., Pattyn, F., Ruth, U., and Steinhage, D. (2007). Ice thinning, upstream advection, and non-climatic biases for the upper 89% of the EDML ice core from a nested model of the Antarctic Ice Sheet. *Climate of the Past*, 3(4):577–589.
- [Imbrie et al., 1989] Imbrie, J., McIntyre, A., and Mix, A. (1989). Oceanic response to orbital forcing in the late quaternary: Observational and experimental strategies. In Berger, A., Schneider, S., and Duplessy, J., editors, *Climate and Geo-Sciences*, volume 285 of *NATO ASI Series*, pages 121–164. Springer Netherlands.
- [Ivins et al., 2013] Ivins, E. R., James, T. S., Wahr, J., Schrama, E. J. O., Landerer, F. W., and Simon, K. M. (2013). Antarctic contribution to sea level rise observed by grace with improved gia correction. *Journal of Geophysical Research-Solid Earth*, 118(6):3126–3141.
- [Jacobs et al., 2011] Jacobs, S. S., Jenkins, A., Giulivi, C. F., and Dutrieux, P. (2011). Stronger ocean circulation and increased melting under pine island glacier ice shelf. *Nature Geoscience*, 4(8):519–523.
- [Joughin and Alley, 2011] Joughin, I. and Alley, R. B. (2011). Stability of the West Antarctic Ice Sheet in a warming world. *Nature Geoscience*, 4(8):506–513.
- [Joughin et al., 2014] Joughin, I., Smith, B. E., and Medley, B. (2014). Marine ice sheet collapse potentially under way for the thwaites glacier basin, West Antarctica. *Science*, 344(6185):735–738.
- [Jouzel et al., 1997] Jouzel, J., Alley, R. B., Cuffey, K. M., Dansgaard, W., Grootes, P., Hoffmann, G., Johnsen, S. J., Koster, R. D., Peel, D., Shuman, C. A., Stievenard, M., Stuiver, M., and White, J. (1997). Validity of the temperature reconstruction from water isotopes in ice cores. *Journal of Geophysical Research-Oceans*, 102(C12):26471–26487.
- [Jouzel and Masson-Delmotte, 2007] Jouzel, J. and Masson-Delmotte, V. (2007). {ICE} {CORE} {RECORDS} | Antarctic Stable Isotopes. In Elias, S. A., editor, *Encyclopedia of Quaternary Science*, pages 1242 – 1250. Elsevier, Oxford.
-

- [Jouzel et al., 2007] Jouzel, J., Masson-Delmotte, V., Cattani, O., Dreyfus, G., Falourd, S., Hoffmann, G., Minster, B., Nouet, J., Barnola, J. M., Chappellaz, J., Fischer, H., Gallet, J. C., Johnsen, S., Leuenberger, M., Loulergue, L., Luethi, D., Oerter, H., Parrenin, F., Raisbeck, G., Raynaud, D., Schilt, A., Schwander, J., Selmo, E., Souchez, R., Spahni, R., Stauffer, B., Steffensen, J. P., Stenni, B., Stocker, T. F., Tison, J. L., Werner, M., and Wolff, E. W. (2007). Orbital and millennial antarctic climate variability over the past 800,000 years. *Science*, 317(5839):793–796.
- [Knorr et al., 2011] Knorr, G., Butzin, M., Micheels, A., and Lohmann, G. (2011). A warm Miocene climate at low atmospheric CO₂ levels. *Geophysical Research Letters*, 38.
- [Knorr and Lohmann, 2014] Knorr, G. and Lohmann, G. (2014). Climate warming during Antarctic ice sheet expansion at the Middle Miocene transition. *Nature Geoscience*, 7(5):376–381.
- [Kopp et al., 2013] Kopp, R. E., Simons, F. J., Mitrovica, J. X., Maloof, A. C., and Oppenheimer, M. (2013). A probabilistic assessment of sea level variations within the last interglacial stage. *Geophysical Journal International*, 193(2):711–716.
- [Krug et al., 2015] Krug, J., Durand, G., Gagliardini, O., and Weiss, J. (2015). Modelling the impact of submarine frontal melting and ice melange on glacier dynamics. *The Cryosphere*, 9(3):989–1003.
- [Langlais et al., 2015] Langlais, C. E., Rintoul, S. R., and Zika, J. D. (2015). Sensitivity of Antarctic Circumpolar Current Transport and Eddy Activity to Wind Patterns in the Southern Ocean. *Journal of Physical Oceanography*, 45(4):1051–1067.
- [Larter et al., 2014] Larter, R. D., Anderson, J. B., Graham, A. G. C., Gohl, K., Hillenbrand, C. D., Jakobsson, M., Johnson, J. S., Kuhn, G., Nitsche, F. O., Smith, J. A., Witus, A. E., Bentley, M. J., Dowdeswell, J. A., Ehrmann, W., Klages, J. P., Lindow, J., Cofaigh, C. O., and Spiegel, C. (2014). Reconstruction of changes in the Amundsen Sea and Bellingshausen Sea sector of the West Antarctic Ice Sheet since the Last Glacial Maximum. *Quaternary Science Reviews*, 100:55–86.
- [Lhomme et al., 2005] Lhomme, N., Clarke, G. K. C., and Marshall, S. J. (2005). Tracer transport in the Greenland Ice Sheet: constraints on ice cores and glacial history. *Quaternary Science Reviews*, 24(1-2):173–194.
- [Locarnini et al., 2010] Locarnini, R. A., Mishonov, A. V., Antonov, J. I., Boyer, T. P., Garcia, H. E., Baranova, O. K., Zweng, M. M., and Johnson, D. R. (2010). World Ocean Atlas 2009, volume 1: Temperature. *NOAA Atlas NESDIS 68*, U.S. Government Printing Office.
- [Locarnini et al., 2013] Locarnini, R. A., Mishonov, A. V., Antonov, J. I., Boyer, T. P., Garcia, H. E., Baranova, O. K., Zweng, M. M., and Johnson, D. R. (2013). World Ocean Atlas 2013, volume 1: Temperature. *NOAA Atlas NESDIS 73*, U.S. Government Printing Office, page 40pp.
- [Lunt et al., 2013] Lunt, D. J., Abe-Ouchi, A., Bakker, P., Berger, A., Braconnot, P., Charbit, S., Fischer, N., Herold, N., Jungclaus, J. H., Khon, V. C., Krebs-Kanzow, U., Langebroek, P. M., Lohmann, G., Nisancioglu, K. H., Otto-Bliesner, B. L., Park, W., Pfeiffer, M., Phipps, S. J., Prange, M., Rachmayani, R., Renssen, H., Rosenbloom, N., Schneider, B., Stone, E. J., Takahashi, K., Wei, W., Yin, Q., and Zhang, Z. S. (2013). A multi-model assessment of Last Interglacial temperatures. *Climate of the Past*, 9(2):699–717.
-

- [Maris et al., 2014] Maris, M. N. A., de Boer, B., Ligtenberg, S. R. M., Crucifix, M., van de Berg, W. J., and Oerlemans, J. (2014). Modelling the evolution of the antarctic ice sheet since the last interglacial. *Cryosphere*, 8(4):1347–1360.
- [Marsland et al., 2003] Marsland, S., Haak, H., Jungclaus, J., Latif, M., and RÅ¶lske, F. (2003). The max-planck-institute global ocean/sea ice model with orthogonal curvilinear coordinates. *Ocean Modelling*, 5(2):91 – 127.
- [Marzeion et al., 2012] Marzeion, B., Jarosch, A. H., and Hofer, M. (2012). Past and future sea-level change from the surface mass balance of glaciers. *Cryosphere*, 6(6):1295–1322.
- [McKay et al., 2011] McKay, N. P., Overpeck, J. T., and Otto-Bliesner, B. L. (2011). The role of ocean thermal expansion in Last Interglacial sea level rise. *Geophysical Research Letters*, 38.
- [Mengel et al., 2015] Mengel, M., Feldmann, J., and Levermann, A. (2015). Linear sea-level response to abrupt ocean warming of major west antarctic ice basin. *Nature Climate Change*, advanced online publication.
- [Mengel and Levermann, 2014] Mengel, M. and Levermann, A. (2014). Ice plug prevents irreversible discharge from East Antarctica. *Nature Climate Change*, 4(6):451–455.
- [Mercer, 1978] Mercer, J. H. (1978). West antarctic ice sheet and CO₂ greenhouse effect - threat of disaster. *Nature*, 271(5643):321–325.
- [Mudelsee et al., 2014] Mudelsee, M., Bickert, T., Lear, C. H., and Lohmann, G. (2014). Cenozoic climate changes: A review based on time series analysis of marine benthic d₁₈o records. *Reviews of Geophysics*, 52(3):333–374.
- [Nakayama et al., 2014] Nakayama, Y., Timmermann, R., Schroder, M., and Hellmer, H. H. (2014). On the difficulty of modeling circumpolar deep water intrusions onto the amundsen sea continental shelf. *Ocean Modelling*, 84:26–34.
- [Neumann et al., 2015] Neumann, B., Vafeidis, A. T., Zimmermann, J., and Nicholls, R. J. (2015). Future Coastal Population Growth and Exposure to Sea-Level Rise and Coastal Flooding - A Global Assessment. *Plos One*, 10(3).
- [Nicholls and Cazenave, 2010] Nicholls, R. J. and Cazenave, A. (2010). Sea-Level Rise and Its Impact on Coastal Zones. *Science*, 328(5985):1517–1520.
- [Nye, 1963] Nye, J. (1963). Correction factor for accumulation measured by the thickness of the annual layers in an ice sheet. *Journal of Glaciology*, 4:3.
- [Otto-Bliesner et al., 2013] Otto-Bliesner, B. L., Rosenbloom, N., Stone, E. J., McKay, N. P., Lunt, D. J., Brady, E. C., and Overpeck, J. T. (2013). How warm was the Last Interglacial? new model–data comparisons. *Philosophical Transactions of the Royal Society of London A: Mathematical, Physical and Engineering Sciences*, 371(2001).
- [Pattyn, 2003] Pattyn, F. (2003). A new three-dimensional higher-order thermomechanical ice sheet model: Basic sensitivity, ice stream development, and ice flow across subglacial lakes. *Journal of Geophysical Research-Solid Earth*, 108(B8).
-

- [Pattyn et al., 2013] Pattyn, F., Perichon, L., Durand, G., Favier, L., Gagliardini, O., Hindmarsh, R. C. A., Zwinger, T., Albrecht, T., Cornford, S., Docquier, D., Furst, J. J., Goldberg, D., Gudmundsson, G. H., Humbert, A., Hutten, M., Huybrechts, P., Jouvett, G., Kleiner, T., Larour, E., Martin, D., Morlighem, M., Payne, A. J., Pollard, D., Ruckamp, M., Rybak, O., Seroussi, H., Thoma, M., and Wilkens, N. (2013). Grounding-line migration in plan-view marine ice-sheet models: results of the Ice2Sea MIS2MIP3d intercomparison. *Journal of Glaciology*, 59(215):410–422.
- [Petit et al., 1997] Petit, J. R., Basile, I., Leruyet, A., Raynaud, D., Lorius, C., Jouzel, J., Stievenard, M., Lipenkov, V. Y., Barkov, N. I., Kudryashov, B. B., Davis, M., Saltzman, E., and Kotlyakov, V. (1997). Four climate cycles in Vostok ice core. *Nature*, 387(6631):359–360.
- [Pfeiffer and Lohmann, 2015] Pfeiffer, M. and Lohmann, G. (2015). Greenland Ice Sheet influence on Last Interglacial climate: global sensitivity studies performed with an atmosphere-ocean general circulation model. *Climate of the Past Discussions*, 11(2):933–995.
- [Pollard and DeConto, 2009] Pollard, D. and DeConto, R. M. (2009). Modelling West Antarctic Ice Sheet growth and collapse through the past five million years. *Nature*, 458:329–333.
- [Pollard and DeConto, 2012] Pollard, D. and DeConto, R. M. (2012). Description of a hybrid ice sheet-shelf model, and application to Antarctica. *Geoscientific Model Development*, 5(5):1273–1295.
- [Pollard et al., 2015] Pollard, D., DeConto, R. M., and Alley, R. B. (2015). Potential antarctic ice sheet retreat driven by hydrofracturing and ice cliff failure. *Earth and Planetary Science Letters*, 412:112–121.
- [Pritchard et al., 2012] Pritchard, H. D., Ligtenberg, S. R. M., Fricker, H. A., Vaughan, D. G., van den Broeke, M. R., and Padman, L. (2012). Antarctic ice-sheet loss driven by basal melting of ice shelves. *Nature*, 484(7395):502–505.
- [Raymo et al., 2011] Raymo, M. E., Mitrovica, J. X., O’Leary, M. J., DeConto, R. M., and Hearty, P. L. (2011). Departures from eustasy in Pliocene sea-level records. *Nature Geoscience*, 4(5).
- [Raymo and Ruddiman, 1992] Raymo, M. E. and Ruddiman, W. F. (1992). Tectonic Forcing of Late Cenozoic Climate. *Nature*, 359(6391):117–122.
- [Rignot et al., 2013] Rignot, E., Jacobs, S., Mouginot, J., and Scheuchl, B. (2013). Ice-shelf melting around Antarctica. *Science*, 341(6143):266–270.
- [Rignot et al., 2014] Rignot, E., Mouginot, J., Morlighem, M., Seroussi, H., and Scheuchl, B. (2014). Widespread, rapid grounding line retreat of Pine Island, Thwaites, Smith, and Kohler glaciers, West Antarctica, from 1992 to 2011. *Geophysical Research Letters*, 41(10):3502–3509.
- [Rignot et al., 2011] Rignot, E., Mouginot, J., and Scheuchl, B. (2011). Ice flow of the Antarctic Ice Sheet. *Science*, 333(6048):1427–1430.
- [Ritz et al., 2015] Ritz, C., Edwards, T. L., Durand, G., Payne, A. J., Peyaud, V., and Hindmarsh, R. C. A. (2015). Potential sea-level rise from Antarctic Ice Sheet instability constrained by observations. *Nature*, advance online publication.
-

- [Roeckner et al., 2003] Roeckner, E., Bäuml, G., Bonaventura, L., Brokopf, R., Esch, M., Giorgetta, M., Hagemann, S., Kirchner, I., Kornbluh, L., Manzini, E., Rhodin, A., Schlese, U., Schulzweida, U., and Tompkins, A. (2003). The atmospheric general circulation model ECHAM 5. PART I: Model description. Technical report, MPI für Meteorologie.
- [Rohling et al., 2014] Rohling, E. J., Foster, G. L., Grant, K. M., Marino, G., Roberts, A. P., Tamisiea, M. E., and Williams, F. (2014). Sea-level and deep-sea-temperature variability over the past 5.3 million years (vol 508, pg 477, 2014). *Nature*, 510(7505):432–432.
- [Rosenthal et al., 2013] Rosenthal, Y., Linsley, B. K., and Oppo, D. W. (2013). Pacific ocean heat content during the past 10,000 years. *Science*, 342(6158):617–621.
- [Rovere et al., 2014] Rovere, A., Raymo, M. E., Mitrovica, J. X., Hearty, P. J., O’Leary, M. J., and Inglis, J. D. (2014). The mid-Pliocene sea-level conundrum: Glacial isostasy, eustasy and dynamic topography. *Earth and Planetary Science Letters*, 387:27–33.
- [Rowley et al., 2013] Rowley, D. B., Forte, A. M., Moucha, R., Mitrovica, J. X., Simmons, N. A., and Grand, S. P. (2013). Dynamic topography change of the eastern united states since 3 million years ago. *Science*, 340(6140):1560–1563.
- [Rybak and Huybrechts, 2003] Rybak, O. and Huybrechts, P. (2003). A comparison of Eulerian and Lagrangian methods for dating in numerical ice-sheet models. *Annals of Glaciology, Vol 37*, 37:150–158.
- [Salzmann et al., 2013] Salzmann, U., Dolan, A. M., Haywood, A. M., Chan, W. L., Voss, J., Hill, D. J., Abe-Ouchi, A., Otto-Bliesner, B., Bragg, F. J., Chandler, M. A., Contoux, C., Dowsett, H. J., Jost, A., Kamae, Y., Lohmann, G., Lunt, D. J., Pickering, S. J., Pound, M. J., Ramstein, G., Rosenbloom, N. A., Sohl, L., Stepanek, C., Ueda, H., and Zhang, Z. S. (2013). Challenges in quantifying Pliocene terrestrial warming revealed by data-model discord. *Nature Climate Change*, 3(11):969–974.
- [Scambos et al., 2004] Scambos, T. A., Bohlander, J. A., Shuman, C. A., and Skvarca, P. (2004). Glacier acceleration and thinning after ice shelf collapse in the Larsen B embayment, Antarctica. *Geophysical Research Letters*, 31.
- [Scherer et al., 1998] Scherer, R. P., Aldahan, A., Tulaczyk, S., Possnert, G., Engelhardt, H., and Kamb, B. (1998). Pleistocene collapse of the West Antarctic Ice Sheet. *Science*, 281(5373):82–85.
- [Schmidtke et al., 2014] Schmidtke, S., Heywood, K. J., Thompson, A. F., and Aoki, S. (2014). Multi-decadal warming of antarctic waters. *Science*, 346(6214):1227–1231.
- [Schoof, 2007] Schoof, C. (2007). Ice sheet grounding line dynamics: Steady states, stability, and hysteresis. *Journal of Geophysical Research-Earth Surface*, 112(F3).
- [Shevenell et al., 2004] Shevenell, A. E., Kennett, J. P., and Lea, D. W. (2004). Middle Miocene Southern Ocean cooling and Antarctic cryosphere expansion. *Science*, 305(5691):1766–1770.
- [Steig et al., 2015] Steig, E. J., Huybers, K., Singh, H. A., Steiger, N. J., Ding, Q. H., Frierson, D. M. W., Popp, T., and White, J. W. C. (2015). Influence of West Antarctic Ice Sheet collapse on antarctic surface climate. *Geophysical Research Letters*, 42(12):4862–4868.
-

- [Stenni et al., 2010] Stenni, B., Masson-Delmotte, V., Selmo, E., Oerter, H., Meyer, H., Rothlisberger, R., Jouzel, J., Cattani, O., Falourd, S., Fischer, H., Hoffmann, G., Iacumin, P., Johnsen, S. J., Minster, B., and Udisti, R. (2010). The deuterium excess records of epica dome c and dronning maud land ice cores (East Antarctica). *Quaternary Science Reviews*, 29(1-2):146–159.
- [Stepanek and Lohmann, 2012] Stepanek, C. and Lohmann, G. (2012). Modelling mid-Pliocene climate with COSMOS. *Geoscientific Model Development*, 5(5):1221–1243.
- [Stewart and Thompson, 2015] Stewart, A. L. and Thompson, A. F. (2015). Eddy-mediated transport of warm circumpolar deep water across the antarctic shelf break. *Geophysical Research Letters*, 42(2):432–440. 2014GL062281.
- [Stocker et al., 2013] Stocker, T., Qin, D., Plattner, G.-K., Tignor, M., Allen, S., Boschung, J., Nauels, A., Xia, Y., Bex, V., and (eds.), P. M. (2013). *Technical Summary*, book section TS, page 1535pp. Cambridge University Press, Cambridge, United Kingdom and New York, NY, USA.
- [Sun et al., 2014a] Sun, B., Moore, J. C., Zwinger, T., Zhao, L., Steinhage, D., Tang, X., Zhang, D., Cui, X., and Martín, C. (2014a). How old is the ice beneath Dome A, Antarctica? *The Cryosphere*, 8(3):1121–1128.
- [Sun et al., 2014b] Sun, S., Cornford, S. L., Liu, Y., and Moore, J. C. (2014b). Dynamic response of antarctic ice shelves to bedrock uncertainty. *Cryosphere*, 8(4):1561–1576.
- [Sutter et al., 2015a] Sutter, J., Gierz, P., Grosfeld, K., Thoma, M., and Lohmann, G. (2015a). Ocean Temperature Thresholds for Last Interglacial WAIS collapse. *Geophysical Research Letters*, in Review.
- [Sutter et al., 2015b] Sutter, J., Thoma, M., and Lohmann, G. (2015b). *Integration of Passive Tracers in a Three-Dimensional Ice Sheet Model*, pages 161–170. Springer, Heidelberg.
- [Thoma et al., 2014] Thoma, M., Grosfeld, K., Barbi, D., Determann, J., Goeller, S., Mayer, C., and Pattyn, F. (2014). Rimby - a multi-approximation 3d ice-dynamics model for comprehensive applications: model description and examples. *Geoscientific Model Development*, 7(1):1–21.
- [Thomas et al., 2015] Thomas, E. R., Hosking, J. S., Tuckwell, R. R., Warren, R. A., and Ludlow, E. C. (2015). Twentieth century increase in snowfall in coastal West Antarctica. *Geophysical Research Letters*, 42(21):9387–9393.
- [Thompson, 2008] Thompson, A. F. (2008). The atmospheric ocean: eddies and jets in the Antarctic Circumpolar Current. *Philosophical Transactions of the Royal Society a-Mathematical Physical and Engineering Sciences*, 366(1885):4529–4541.
- [Thompson et al., 2014] Thompson, A. F., Heywood, K. J., Schmidtko, S., and Stewart, A. L. (2014). Eddy transport as a key component of the Antarctic overturning circulation. *Nature Geoscience*, 7(12):879–884.
- [Uppala et al., 2005] Uppala, S. M., Kallberg, P. W., Simmons, A. J., Andrae, U., Bechtold, V. D., Fiorino, M., Gibson, J. K., Haseler, J., Hernandez, A., Kelly, G. A., Li, X., Onogi, K., Saarinen, S., Sokka, N., Allan, R. P., Andersson, E., Arpe, K., Balmaseda, M. A., Beljaars, A. C. M., Van De Berg, L., Bidlot, J., Bormann, N., Caires, S., Chevallier, F., Dethof, A., Dragosavac, M., Fisher, M., Fuentes,
-

- M., Hagemann, S., Holm, E., Hoskins, B. J., Isaksen, L., Janssen, P. A. E. M., Jenne, R., McNally, A. P., Mahfouf, J. F., Morcrette, J. J., Rayner, N. A., Saunders, R. W., Simon, P., Sterl, A., Trenberth, K. E., Untch, A., Vasiljevic, D., Viterbo, P., and Woollen, J. (2005). The era-40 re-analysis. *Quarterly Journal of the Royal Meteorological Society*, 131(612):2961–3012.
- [Van Liefferinge and Pattyn, 2013] Van Liefferinge, B. and Pattyn, F. (2013). Using ice-flow models to evaluate potential sites of million year-old ice in Antarctica. *Climate of the Past*, 9(5).
- [Vaughan and Doake, 1996] Vaughan, D. G. and Doake, C. S. M. (1996). Recent atmospheric warming and retreat of ice shelves on the antarctic peninsula. *Nature*, 379(6563):328–331.
- [Vazquez Riveiros et al., 2010] Vazquez Riveiros, N., Waelbroeck, C., Skinner, L., Roche, D. M., Duplessy, J. C., and Michel, E. (2010). Response of South Atlantic deep waters to deglacial warming during Terminations V and I. *Earth and Planetary Science Letters*, 298(3-4):323–333.
- [Waelbroeck et al., 2002] Waelbroeck, C., Labeyrie, L., Michel, E., Duplessy, J. C., McManus, J. F., Lambeck, K., Balbon, E., and Labracherie, M. (2002). Sea-level and deep water temperature changes derived from benthic foraminifera isotopic records. *Quaternary Science Reviews*, 21(1-3):295–305.
- [Weber et al., 2014] Weber, M. E., Clark, P. U., Kuhn, G., Timmermann, A., Sprenk, D., Gladstone, R., Zhang, X., Lohmann, G., Menviel, L., Chikamoto, M. O., Friedrich, T., and Ohlwein, C. (2014). Millennial-scale variability in Antarctic Ice Sheet discharge during the last deglaciation. *Nature*, 510(7503):134–142.
- [Wilson et al., 2012] Wilson, D. S., Jamieson, S. S. R., Barrett, P. J., Leitchenkov, G., Gohl, K., and Larter, R. D. (2012). Antarctic topography at the Eocene-Oligocene boundary. *Palaeogeography Palaeoclimatology Palaeoecology*, 335:24–34.
- [Wilson et al., 2013] Wilson, D. S., Pollard, D., DeConto, R. M., Jamieson, S. S. R., and Luyendyk, B. P. (2013). Initiation of the West Antarctic Ice Sheet and estimates of total Antarctic ice volume in the earliest Oligocene. *Geophysical Research Letters*, 40(16):4305–4309.
- [Winkelmann et al., 2012] Winkelmann, R., Levermann, A., Martin, M. A., and Frieler, K. (2012). Increased future ice discharge from Antarctica owing to higher snowfall. *Nature*, 492(7428):239–243.
- [Winkelmann et al., 2015] Winkelmann, R., Levermann, A., Ridgwell, A., and Caldeira, K. (2015). Combustion of available fossil fuel resources sufficient to eliminate the Antarctic Ice Sheet. *Science Advances*, 1(8).
- [Zachos et al., 2001] Zachos, J., Pagani, M., Sloan, L., Thomas, E., and Billups, K. (2001). Trends, rhythms, and aberrations in global climate 65 Ma to present. *Science*, 292(5517):686–693.
- [Zammit-Mangion et al., 2015] Zammit-Mangion, A., Rougier, J., Schon, N., Lindgren, F., and Bamber, J. (2015). Multivariate spatio-temporal modelling for assessing antarctica’s present-day contribution to sea-level rise. *Environmetrics*, 26(3):159–177.
- [Zwally et al., 2015] Zwally, H. J., Jun, L., Robins, J. W., Saba, J., Donghui, Y., and Brenner, A. C. (2015). Mass gains of the Antarctic ice sheet exceed losses. *Journal of Glaciology*, in press.
-